Application of Plasma Phenomena

Po-Yu Chang

Institute of Space and Plasma Sciences, National Cheng Kung University

Lecture 10

2024 spring semester

Tuesday 9:10-12:00

Materials:

https://capst.ncku.edu.tw/PGS/index.php/teaching/

Online courses:

https://nckucc.webex.com/nckucc/j.php?MTID=m4082f23c59af0571015416f6e58dd803

2024/5/7 updated

Note!

- No class next Tuesday (5/14) !
- Quiz in class on 5/28!

The magnetic field can be measured by measuring the deflected angle of charged particles

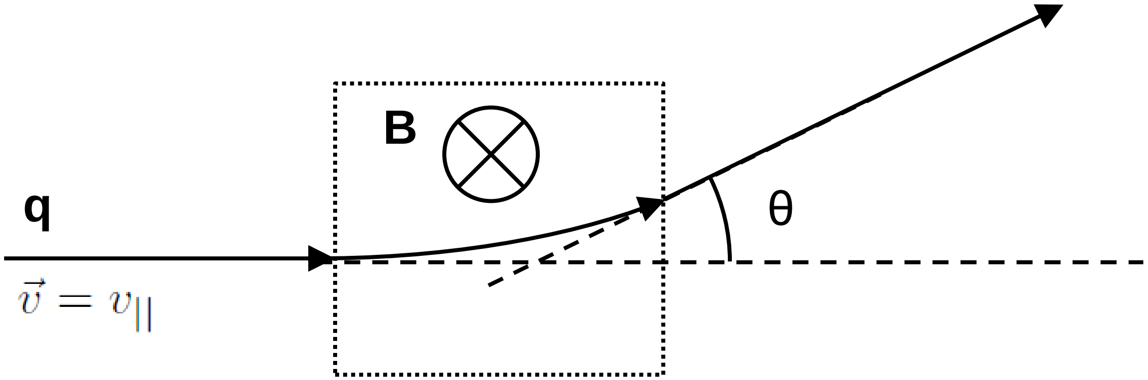

$$F_{\perp} = q\vec{v} \times \vec{B} = qv_{||}B = m\frac{dv_{\perp}}{dt}$$

$$v_{\perp} = \int \frac{qv_{||}B}{m}dt = \frac{qv_{||}}{m}\int Bdt\frac{dx}{dx} = \frac{qv_{||}}{m}\int \frac{B}{v_{||}}dx = \frac{q}{m}\int Bdx$$

$$\tan\theta = \frac{v_{\perp}}{v_{||}} = \frac{q}{mv_{||}}\int Bdx = \frac{q}{\sqrt{2mE}}\int Bdx \qquad \int Bdx = \frac{\sqrt{2mE}}{q}\tan\theta$$

Magnetic field was measured using protons

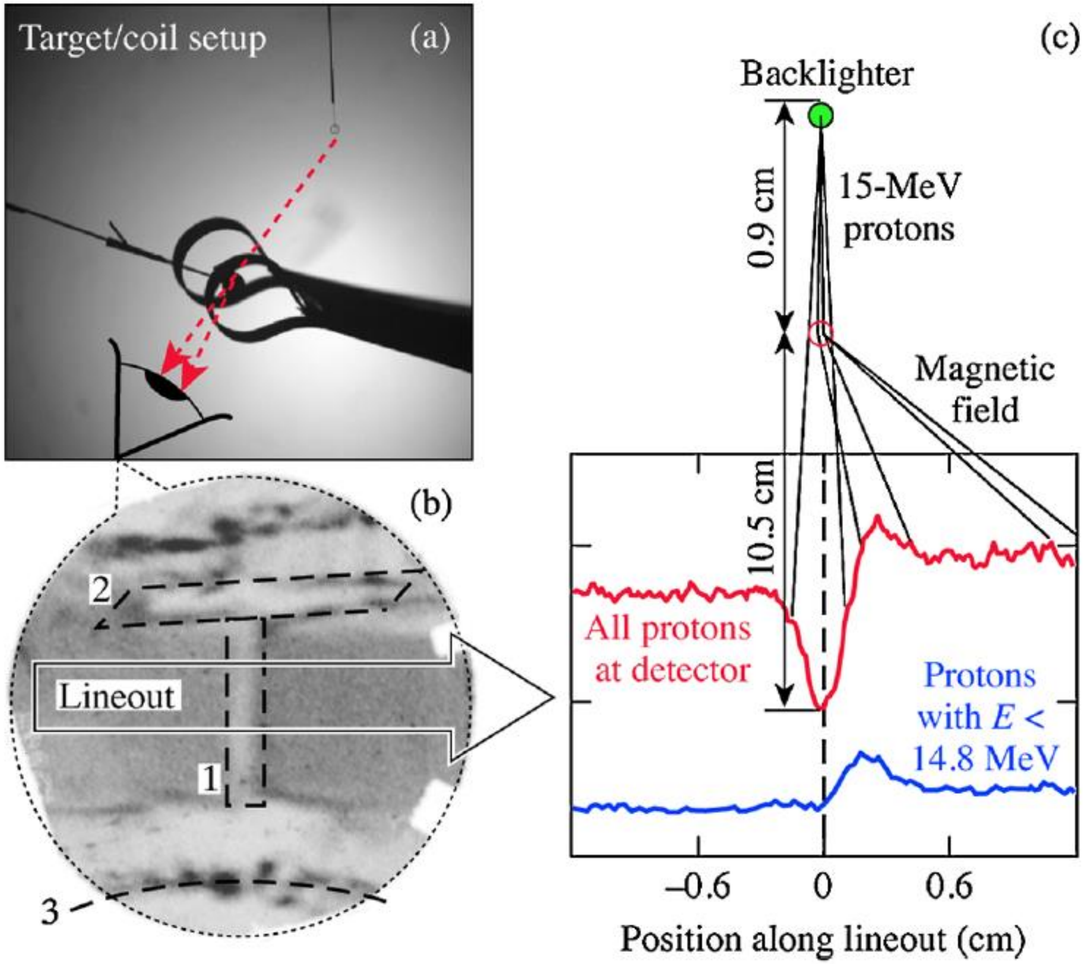

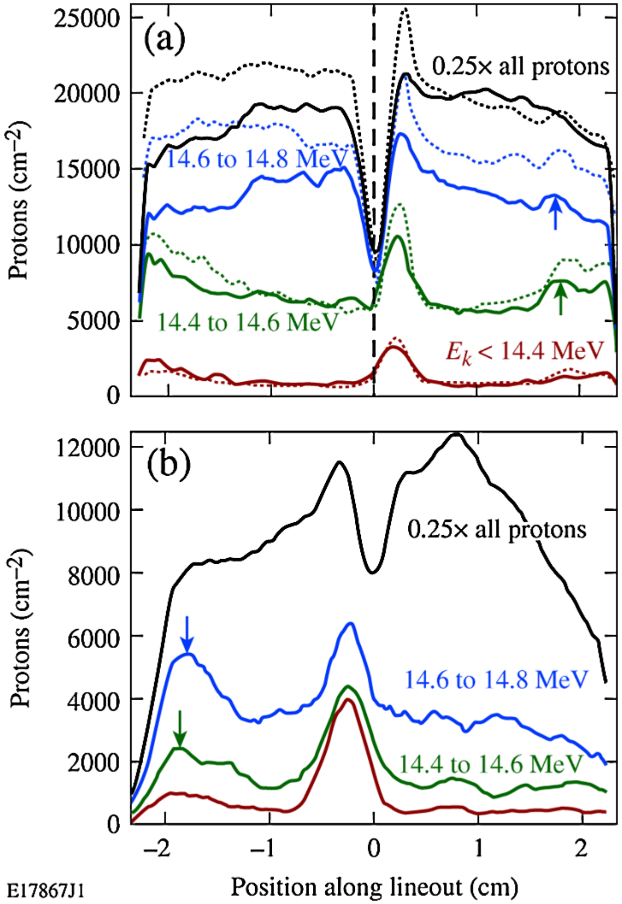

O. V. Gotchev *et al.*, Phys. Rev. Lett. **103**, 215004 (2009)

Protons can be generated from fusion product or copper foil illuminated by short pulse laser

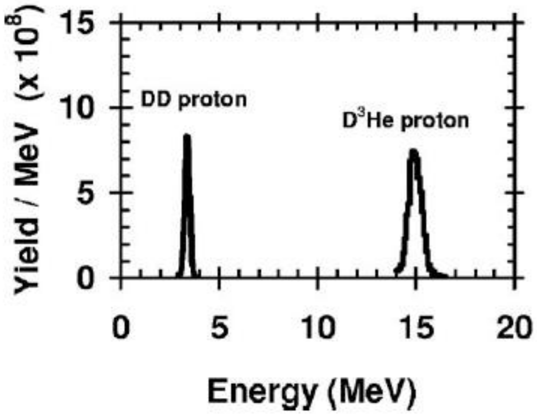

$$D + D \longrightarrow T(1.01\text{MeV}) + p(3.02\text{MeV})$$

$$D + \text{He}^3 \longrightarrow \text{He}^4(3.6\text{MeV}) + p(14.7\text{MeV})$$

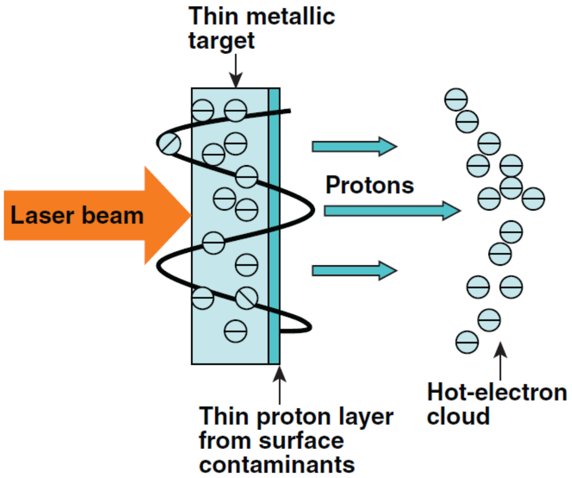
Thin metallic target

Laser beam

Protons

Thin proton layer from surface contaminants

Hot-electron cloud

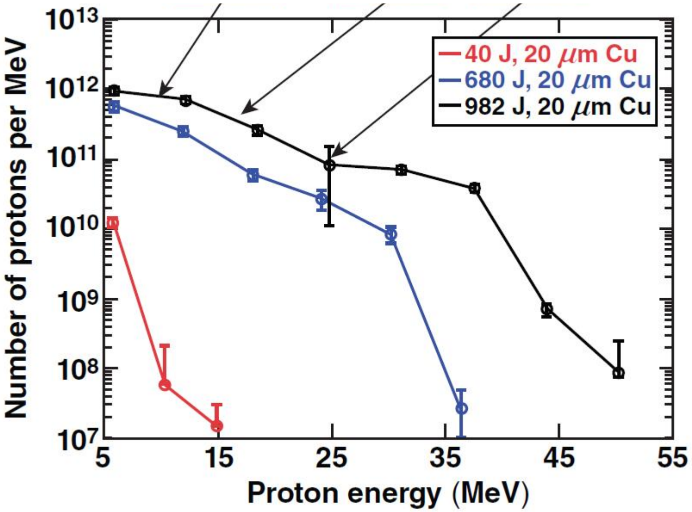

Target normal sheath acceleration (TNSA)

C. K. Li *et al.*, Rev. Sci. Instrum. **77**, 10E725 (2006)
L. Gao, PhD Thesis

Protons can leave tracks on CR39 or film

CR 39

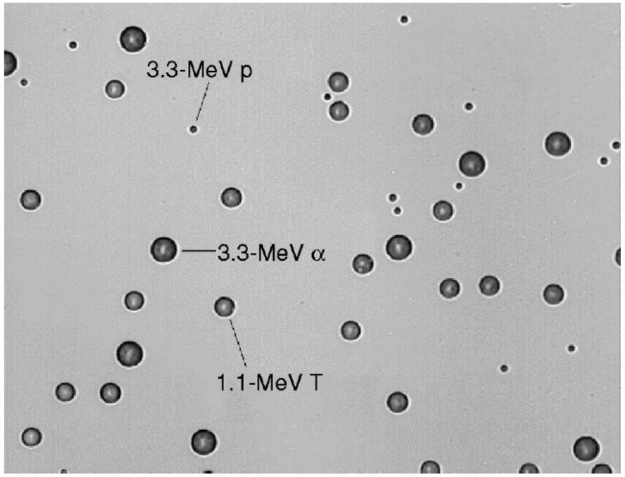

Radiochromic film pack

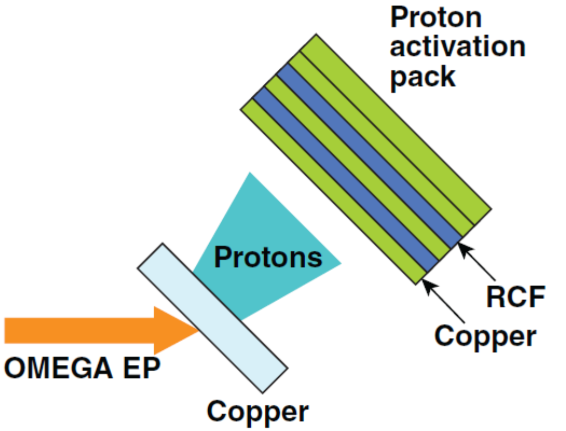

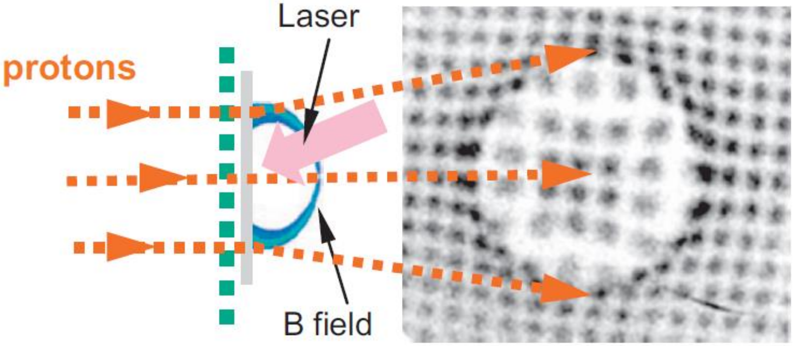

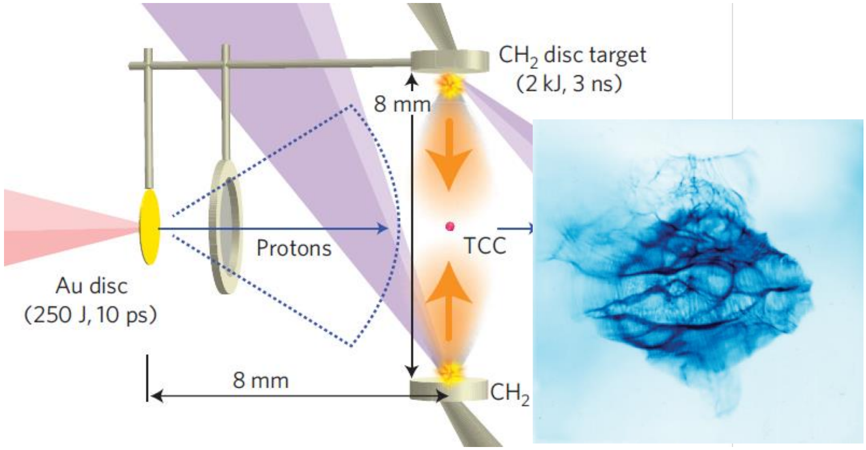

F. H. Seguin *et al.*, Rev. Sci. Instrum. **74**, 975 (2003)
C. K. Li *et al.*, Phys. Plasmas **16**,056304 (2009)
L. Gao, PhD Thesis
N. L. Kugland et al., Nature Phys. B, 809 (2012)

Track diameter on the CR39 is depended on the particle energy that incidents

CR 39

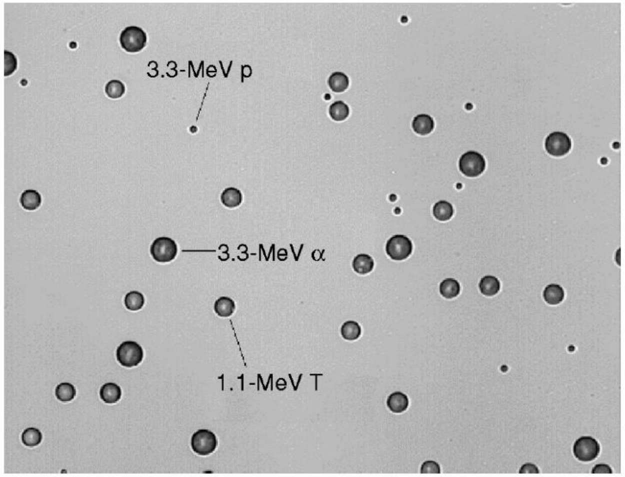

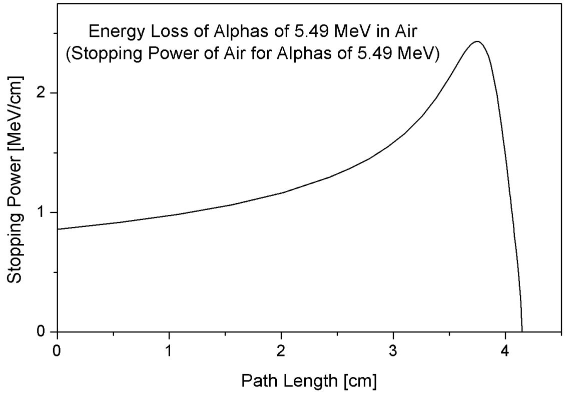

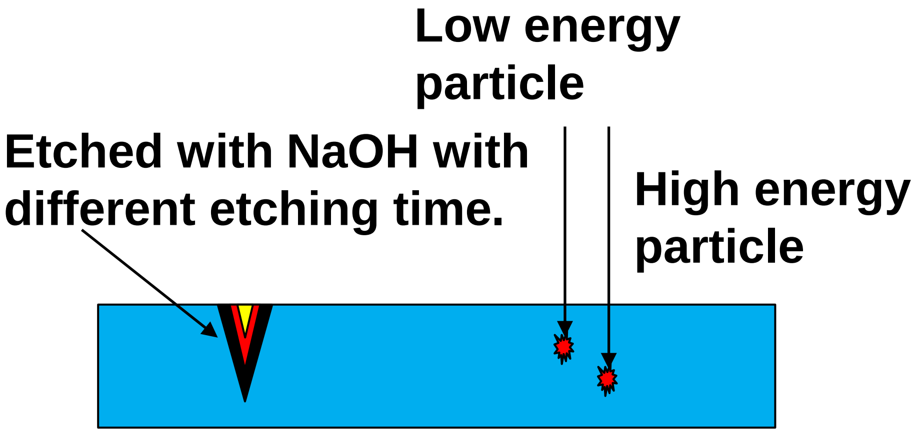

Low energy particle

Etched with NaOH with different etching time.

High energy particle

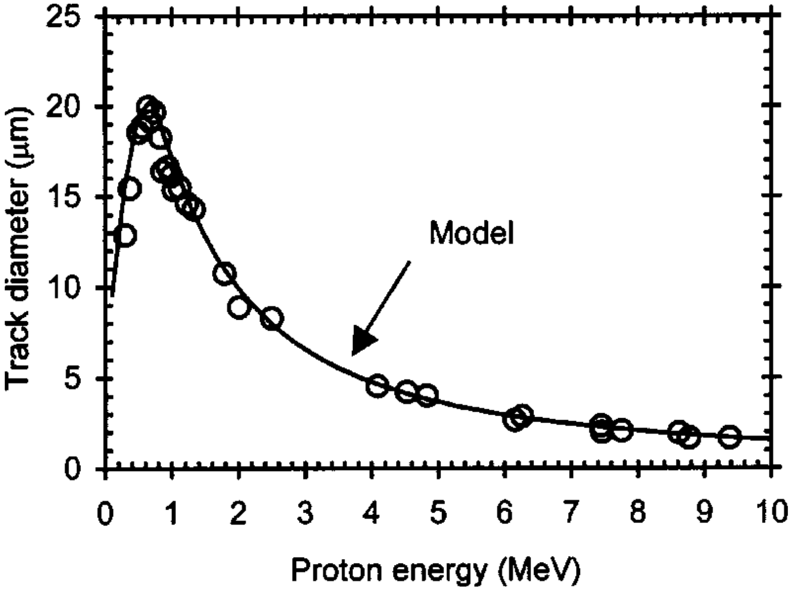

F. H. Seguin *et al.*, Rev. Sci. Instrum. **74**, 975 (2003)

Time dependent magnetic field can be measured using B-dot probe

$$\vec{B} = \vec{B}(t) \qquad \nabla \times \vec{E} = -\frac{\partial \vec{B}}{\partial t}$$

$$\int d\vec{A}\, \nabla \times \vec{E} = \oint \vec{E}\, d\vec{l} = V = -\int d\vec{A}\, \frac{\partial \vec{B}}{\partial t}$$

$$V \sim -A\frac{\partial B}{\partial t} \qquad B = -\int \frac{V}{A}\, dt \sim -\frac{1}{A}\int V dt$$

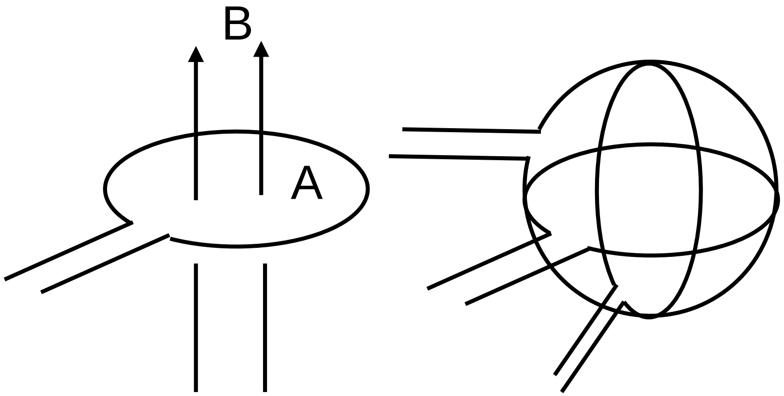

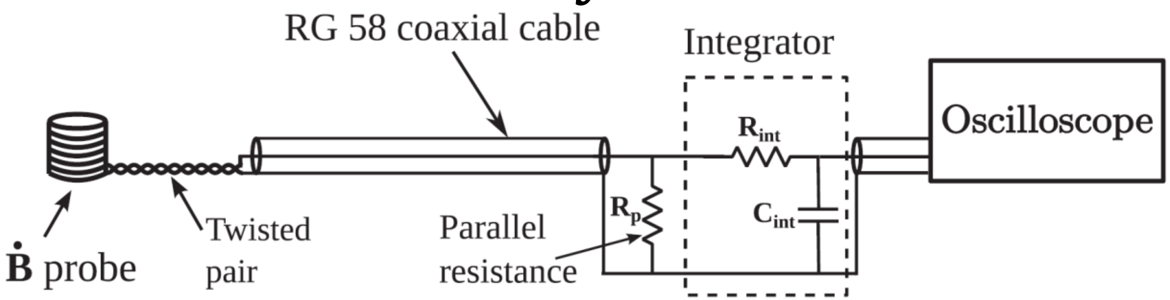

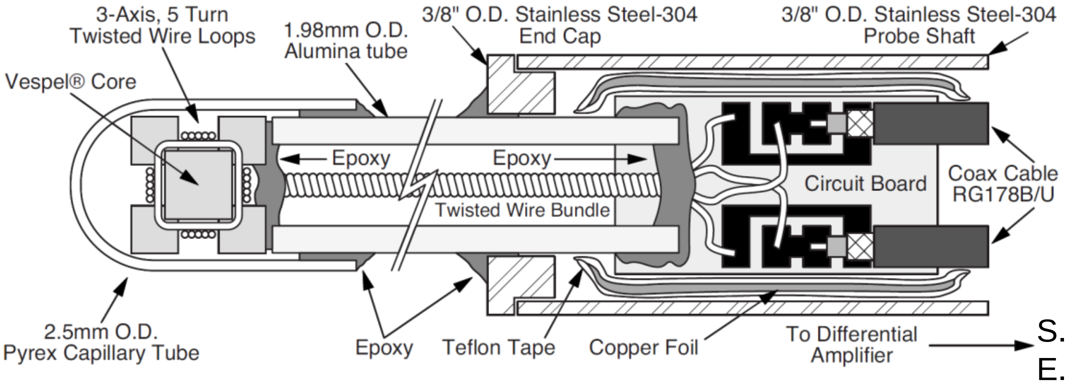

S. Bose *et al.*, Eur. J. Phys. **40**, 015803 (2019)
E. T. Everson *et al.*, Rev. Sci. Instrum. **80**, 113505 (2009)

B-dot probe experiments

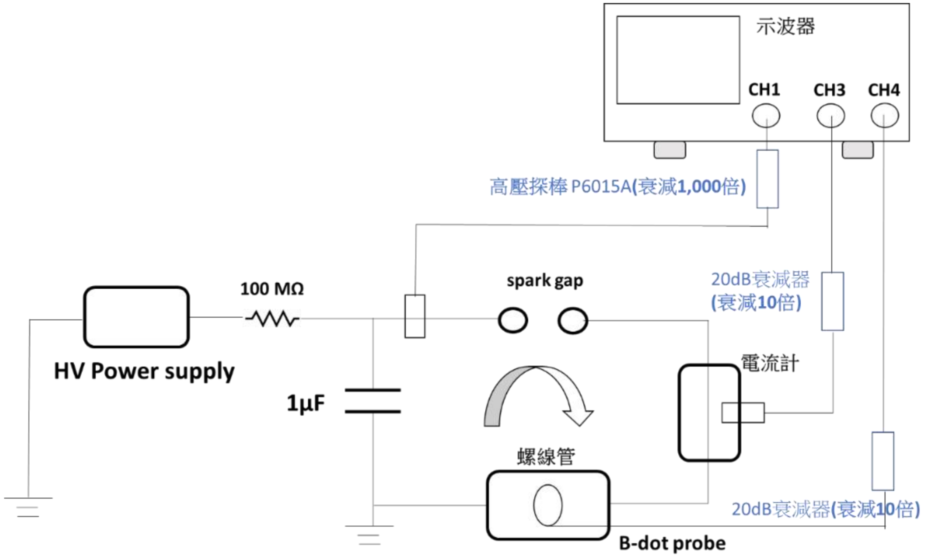

- **Without integrator**

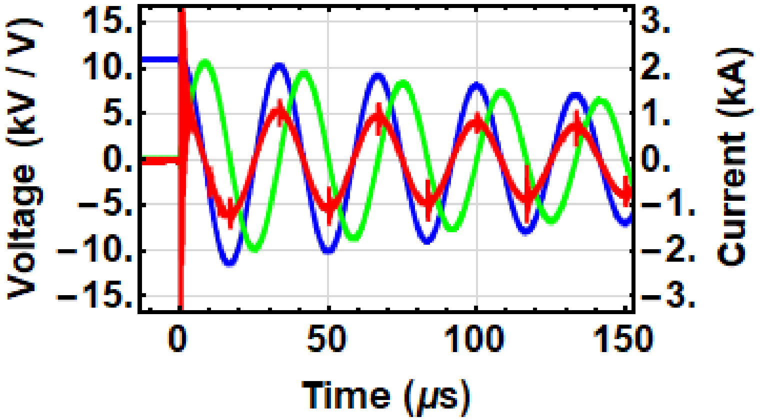

- **With integrator**

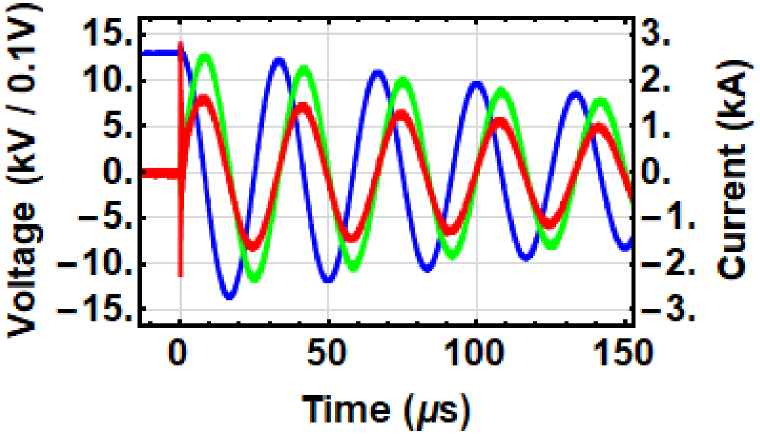

Cheng-Han Du’s experimental report.

A Thomson parabola uses parallel electric and magnetic fields to deflect particles onto parabolic curves that resolve q/m

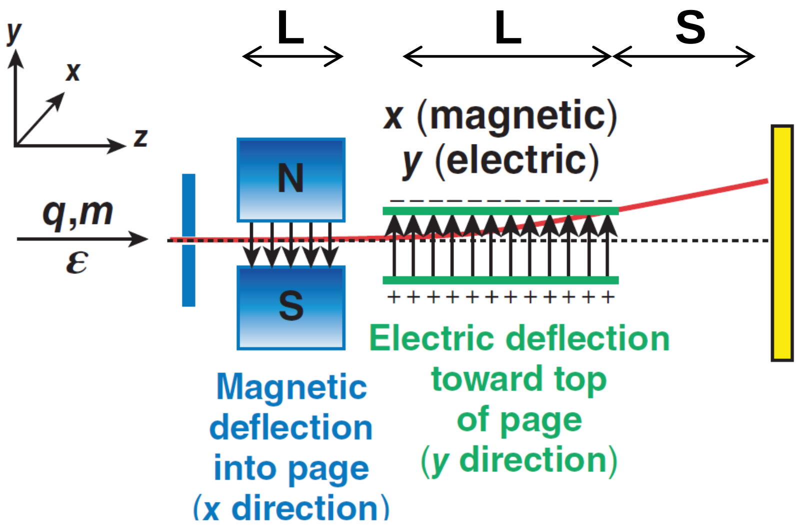

$$F_x = q v_{||} B = m \frac{dv_x}{dt}$$

$$v_x = \frac{q}{m} v_{||} B \Delta t = \frac{q}{m} v_{||} B \frac{L}{v_{||}} = \frac{qBL}{m}$$

$$\tan\theta_x = \frac{v_x}{v_{||}} = \frac{qBL}{m v_{||}} = \frac{qBL}{\sqrt{2m\epsilon}}$$

$$F_y = qE = m \frac{dv_y}{dt}$$

$$v_y = \frac{q}{m} E \Delta t = \frac{q}{m} E \frac{L}{v_{||}} = \frac{qEL}{m v_{||}}$$

- Deflection caused by magnetic field ~*q*/*p*
- Deflection caused by electric field ~*q*/*KE*
- Ion traces form parabolic curves on detector plane

$$y = \frac{m}{q} \frac{E}{B^2 SL} x^2$$

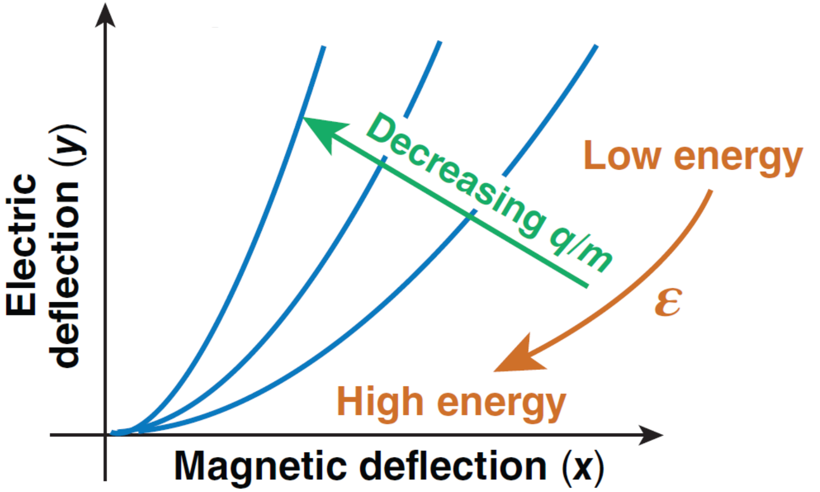

$$\tan\theta_y = \frac{v_y}{v_{||}} = \frac{qEL}{m v_{||}^2} = \frac{qEL}{2\epsilon}$$

E16717b

A faraday cup measures the flux of charge particles

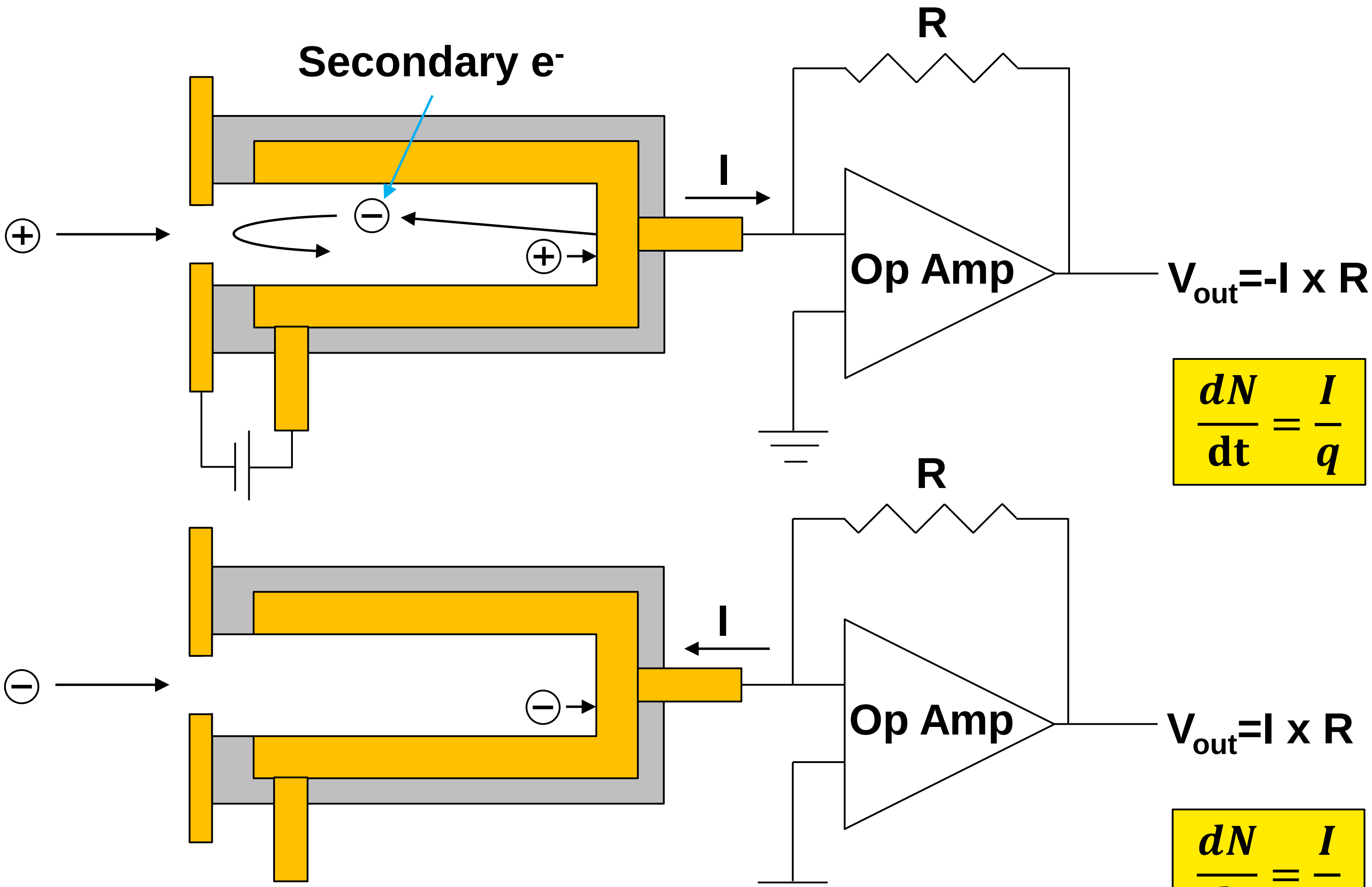

$$\frac{dN}{dt} = \frac{I}{q}$$

$$\frac{dN}{dt} = \frac{I}{q}$$

Retarding potential analyzer measures the energy / velocity distribution function

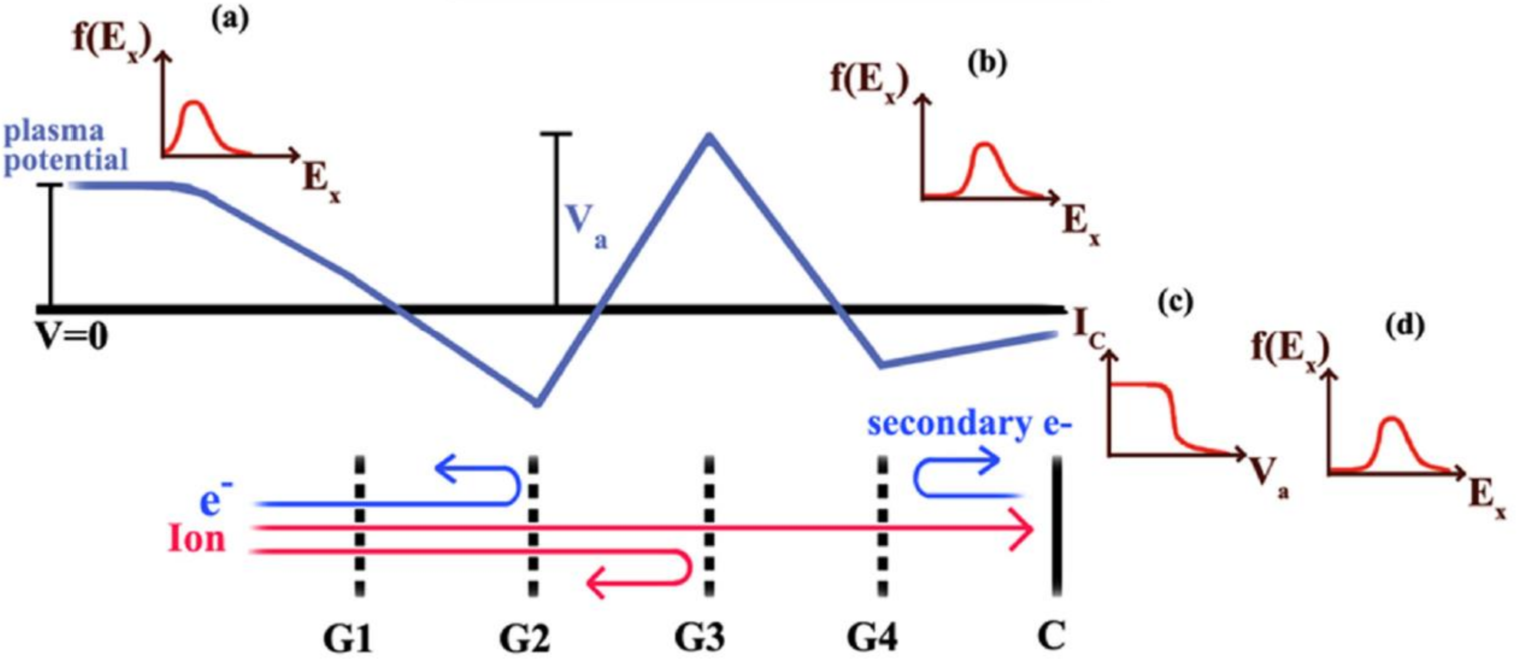

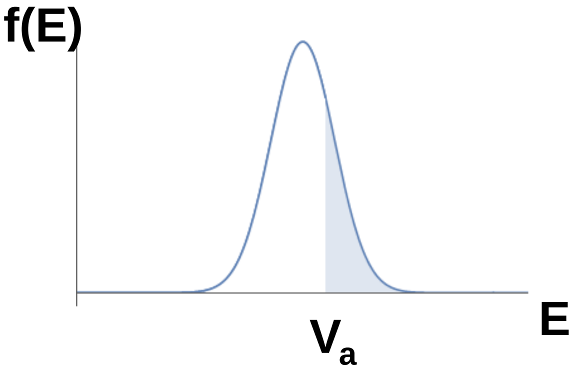

H.-K. Fang, 2015 NCKU Ph. D. Thesis, Ion measurements of ionosphere plasma in space plasma operation chamber

The photon energy spectrum provides valuable information

- Plasma conditions can be determined from the photon spectrum
  - visible light: absorption and laser-plasma interactions
  - x rays: electron temperature, density, plasma flow, material mixing
- There are three basic tools for determining the spectrum detected
  - filtering
  - grating spectrometer
  - Bragg spectrometer

Spectrum can be obtained using grating

- Grating is used to disperse the light

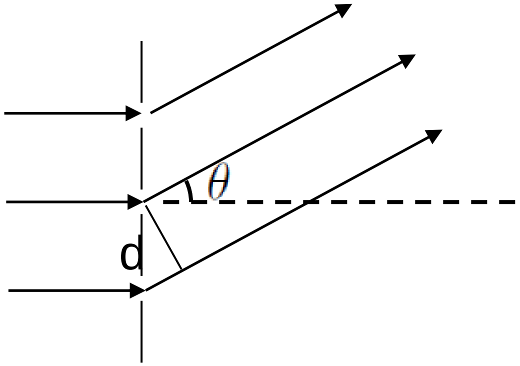

$$d \sin \theta = m\lambda$$

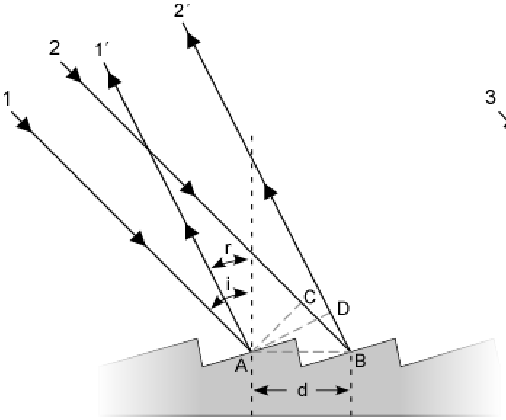

nλ = d(sin(i) + sin (r))

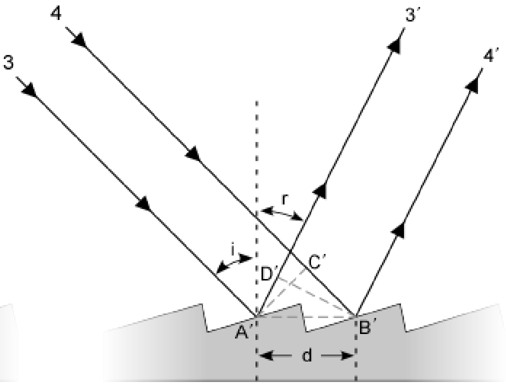

nλ = d(sin(i) - sin (r))

- Bragg condition in the crystal is used for X-ray.

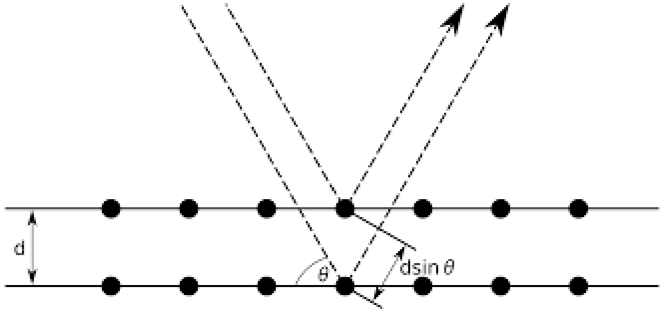

$$2d \sin \theta = m\lambda$$

Temperature and density can be obtained from the emission

Line emission

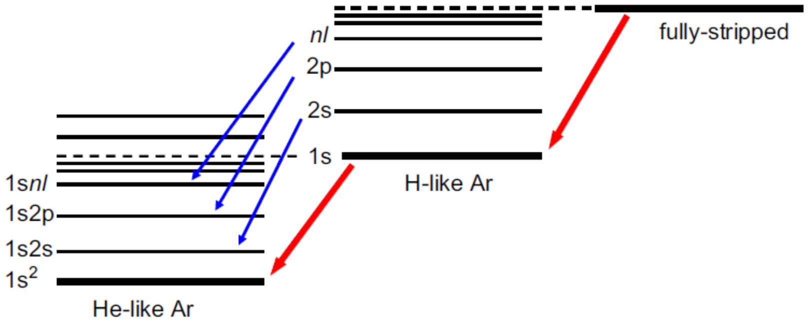

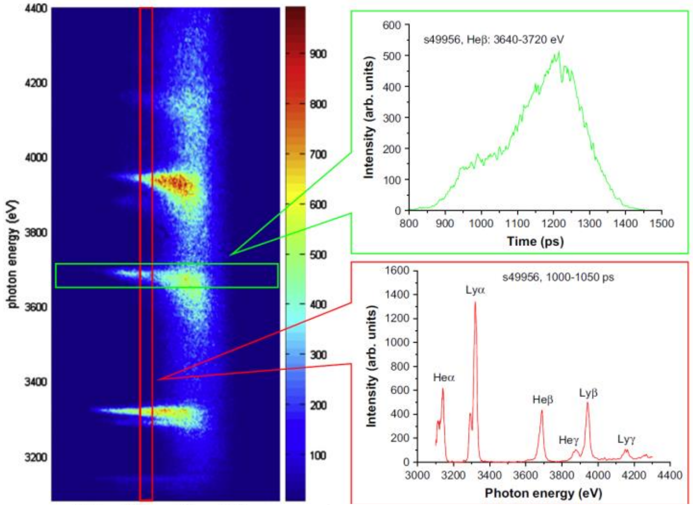

Bremsstrahlung emission

$$\eta_\nu = \frac{16\pi}{3\sqrt{6\pi}}\frac{e^6}{m_\mathrm{e}^2 c^3}\frac{Z_\mathrm{i}^2 n_\mathrm{e}}{\sqrt{k_\mathrm{B} T_\mathrm{e}/m_\mathrm{e} A m_\mathrm{p}}}\exp\left(-\frac{h\nu}{k_\mathrm{B} T_\mathrm{e}}\right)$$

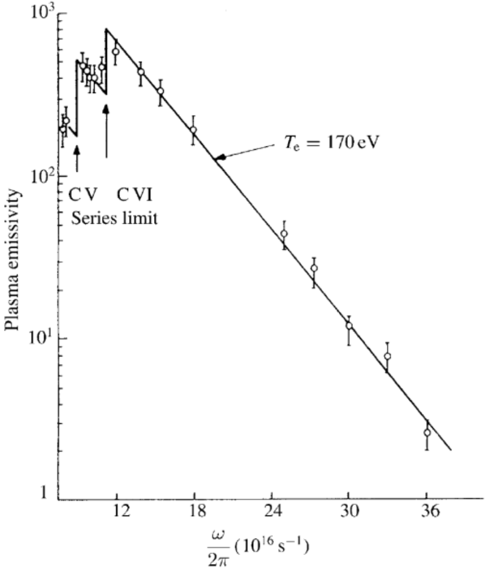

R. Florido *et al.*, High Energy Dens. Phys. **6**, 70 (2010)

Information of x-ray transmission or reflectivity over a surface can be obtained from the Center for X-Ray Optics

- **http://henke.lbl.gov/optical_constants/**

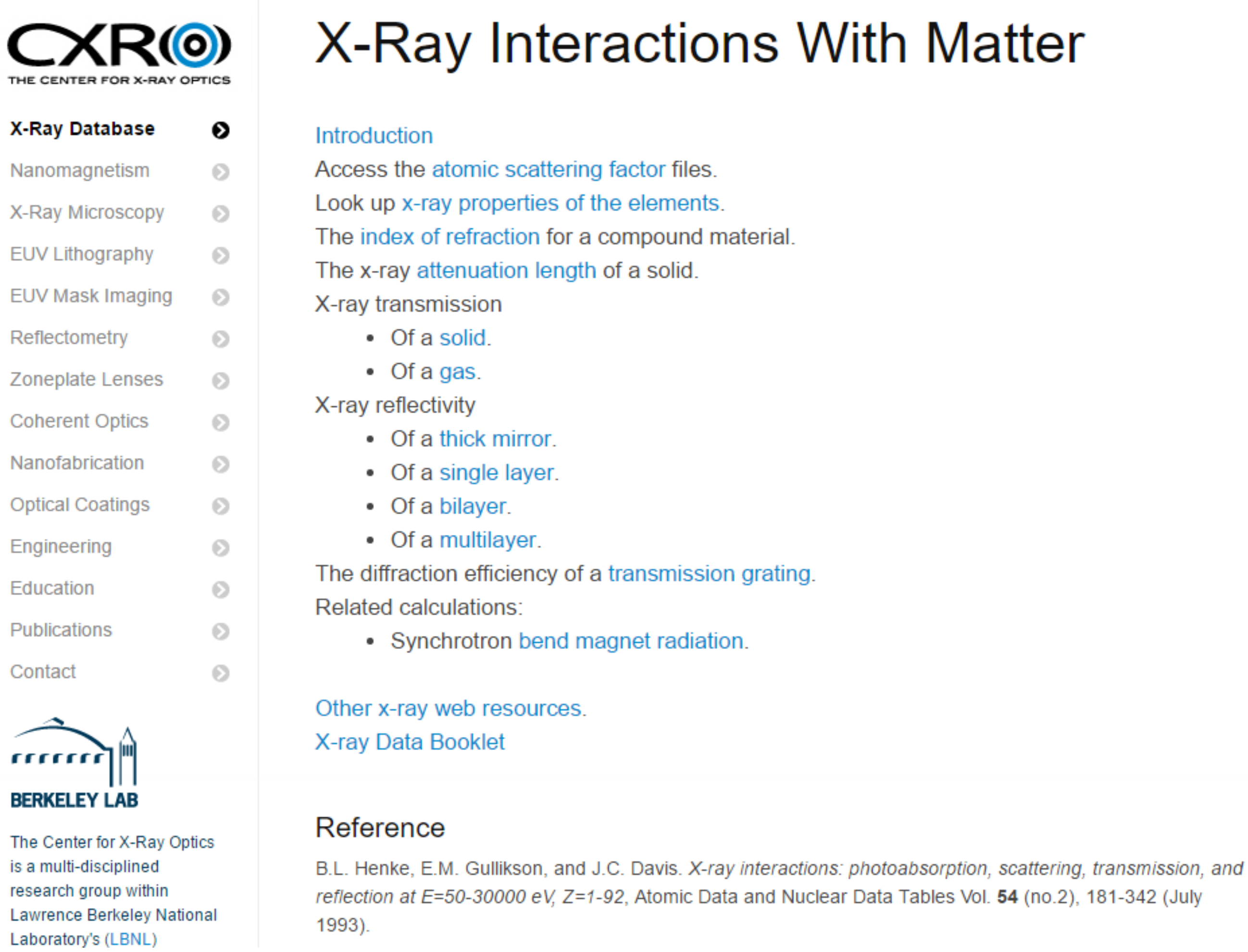

The Center for X-Ray Optics is a multi-disciplined research group within Lawrence Berkeley National Laboratory's (LBNL)

X-Ray Interactions With Matter

Introduction
Access the atomic scattering factor files.
Look up x-ray properties of the elements.
The index of refraction for a compound material.
The x-ray attenuation length of a solid.
X-ray transmission
  - Of a solid.
  - Of a gas.
X-ray reflectivity
  - Of a thick mirror.
  - Of a single layer.
  - Of a bilayer.
  - Of a multilayer.
The diffraction efficiency of a transmission grating.
Related calculations:
  - Synchrotron bend magnet radiation.

Other x-ray web resources.
X-ray Data Booklet

Reference

B.L. Henke, E.M. Gullikson, and J.C. Davis. *X-ray interactions: photoabsorption, scattering, transmission, and reflection at E=50-30000 eV, Z=1-92*, Atomic Data and Nuclear Data Tables Vol. **54** (no.2), 181-342 (July 1993).

A band pass filter is obtained by combing a filter and a mirror

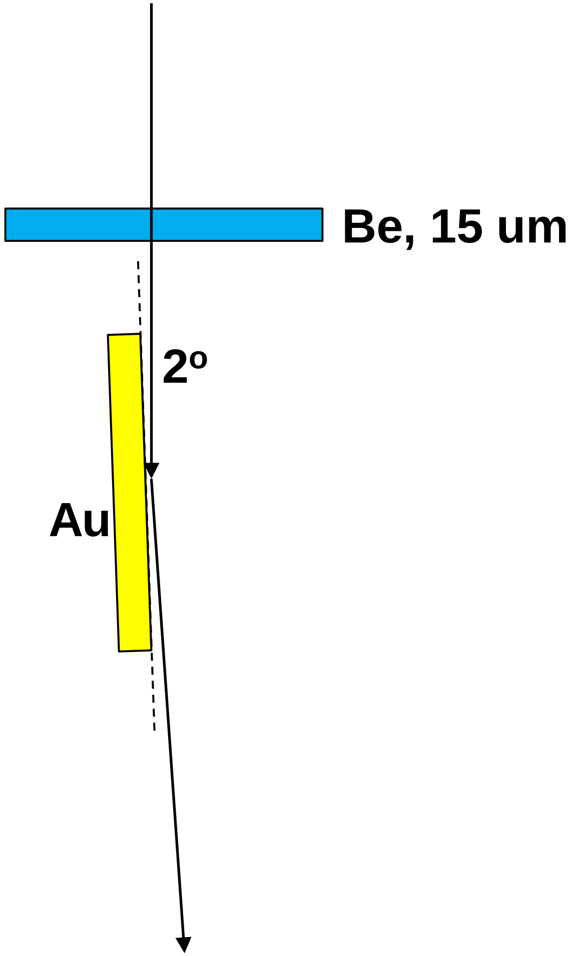

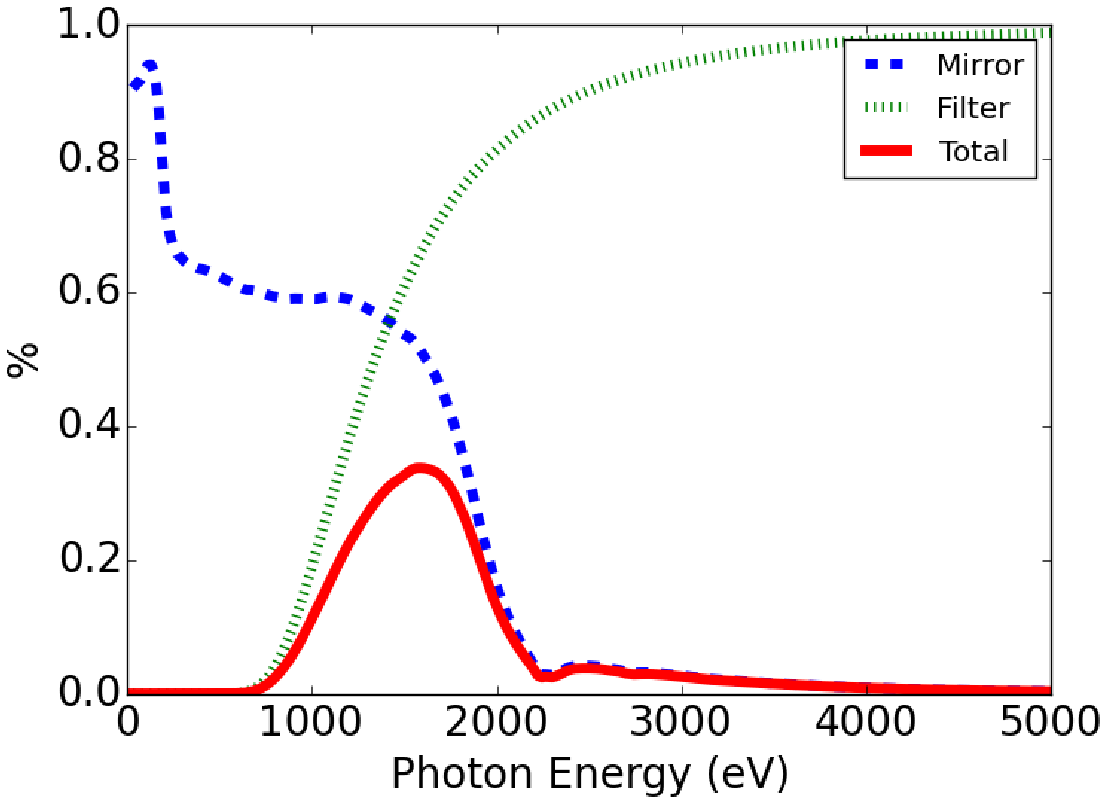

X rays can not be concentrated by lenses

- X-ray refractive indices are less than unity, $n \lesssim 1$
- For those with lower refractive indices, the absorption is also strong
- X-ray mirrors can be made through
  - Bragg reflection
  - External total reflection with a small grazing angle

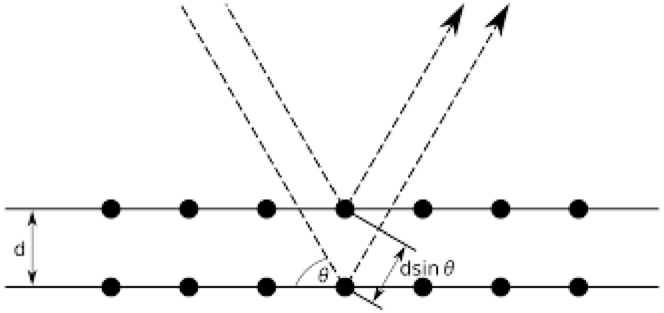

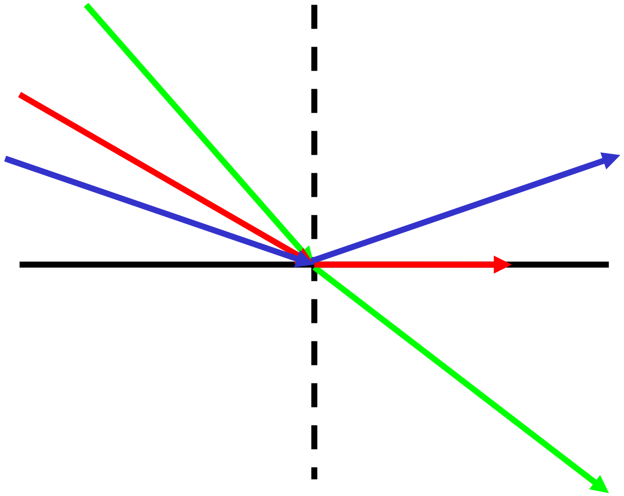

The simplest imaging device is a pinhole camera

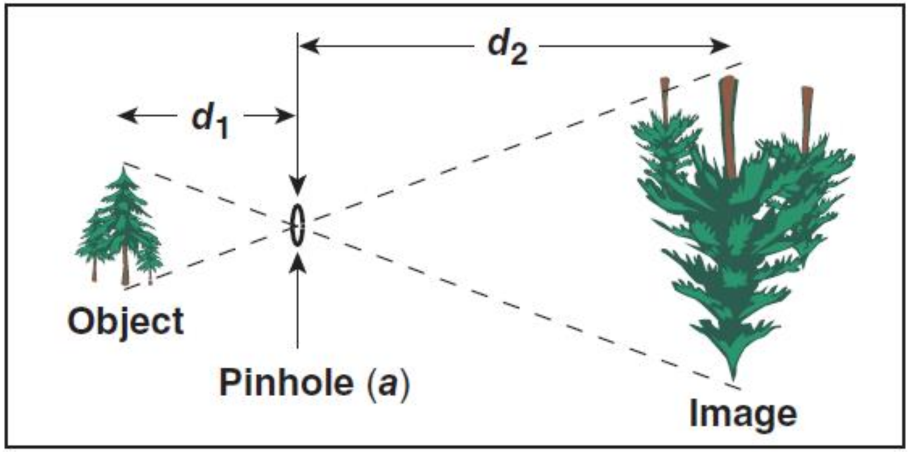

Kodak Brownie camera

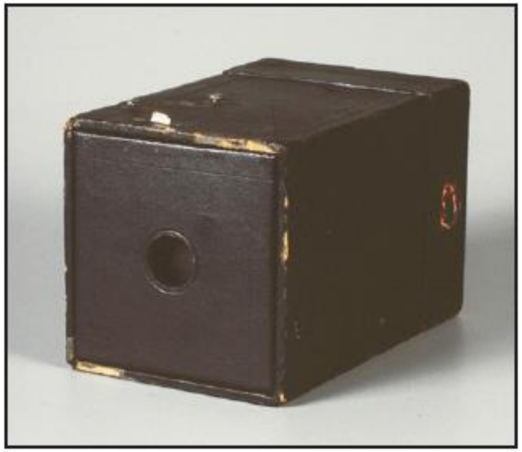

- Magnification = $\dfrac{d_2}{d_1}$
- Infinite depth of field (variable magnification)
- Pinhole diameter determines
  - resolution ~a
  - light collection: $\Delta\Omega = \dfrac{\pi}{4}\,\dfrac{a^2}{d_1^2}$

Imaging optics (e.g., lenses) can be used for higher resolutions with larger solid angles.

E13982a

http://hedpschool.lle.rochester.edu/1000_proc2013.php

2D images can be taken using charge injection device (CID) or charge coupled device (CCD)

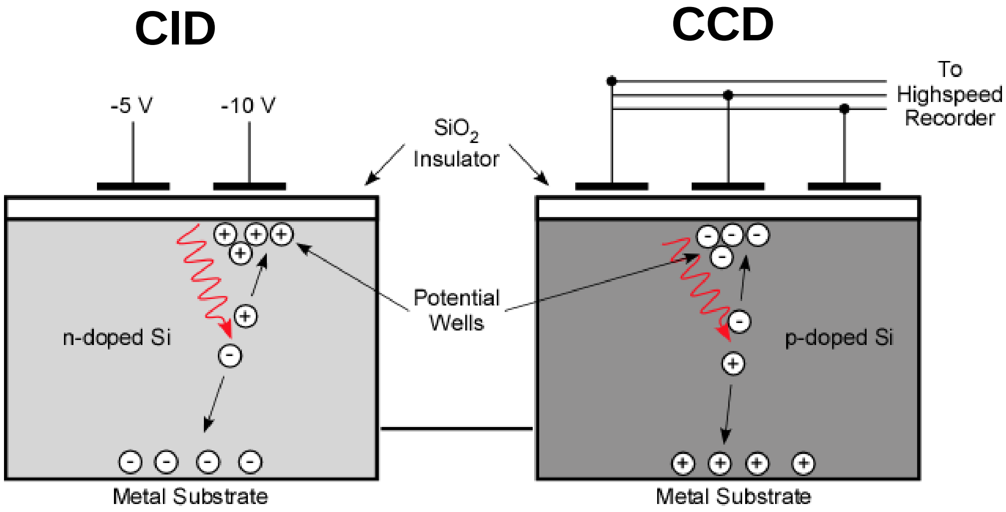

- **Color mask is used for color image**

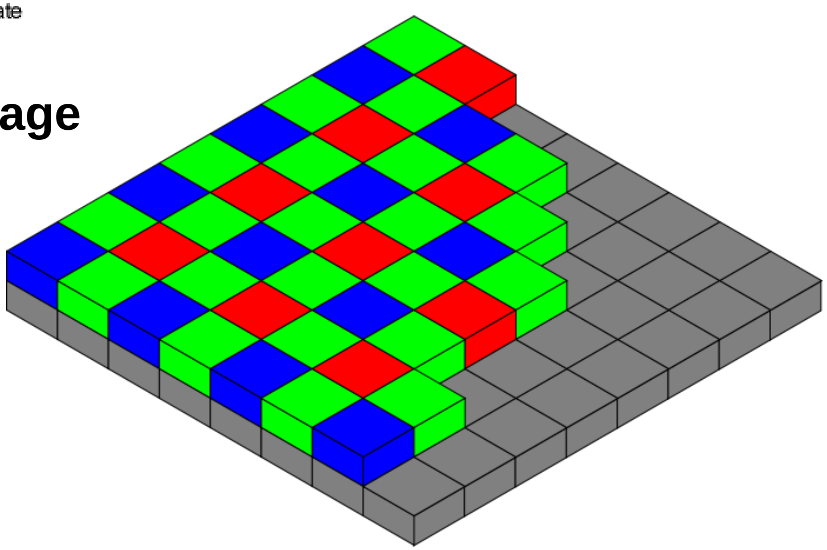

---

http://people.whitman.edu/~dunnivfm/FAASICPMS_Ebook/CH2/2_2_9.html
https://en.wikipedia.org/wiki/Charge-coupled_device

Charges are transferred along the array for readout in CCD

CCD readout:

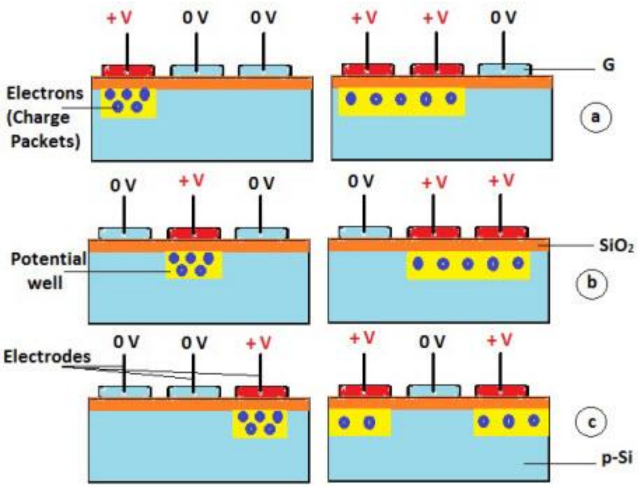

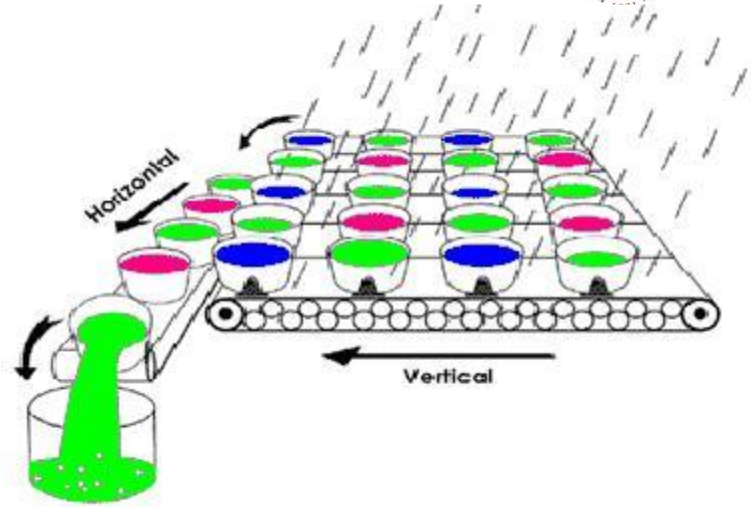

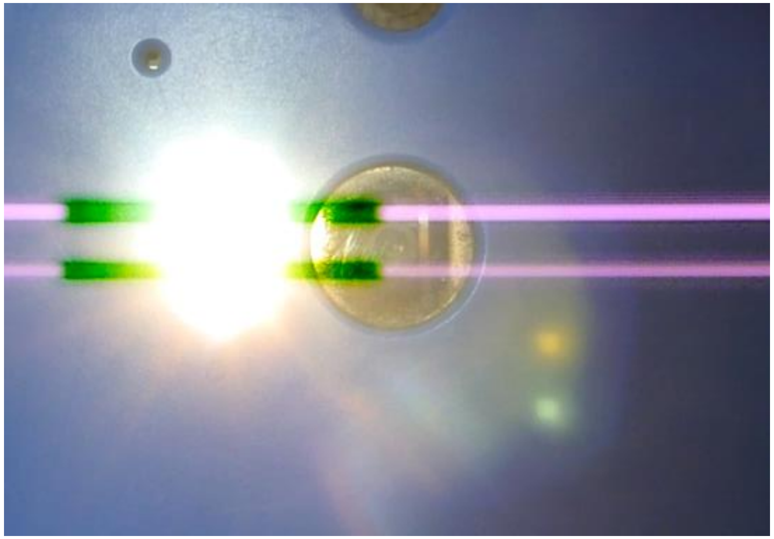

https://www.elprocus.com/know-about-the-working-principle-of-charge-coupled-device/
http://www.siliconimaging.com/ARTICLES/CMOS%20PRIMER.htm

Signal is readout individually in CMOS sensor

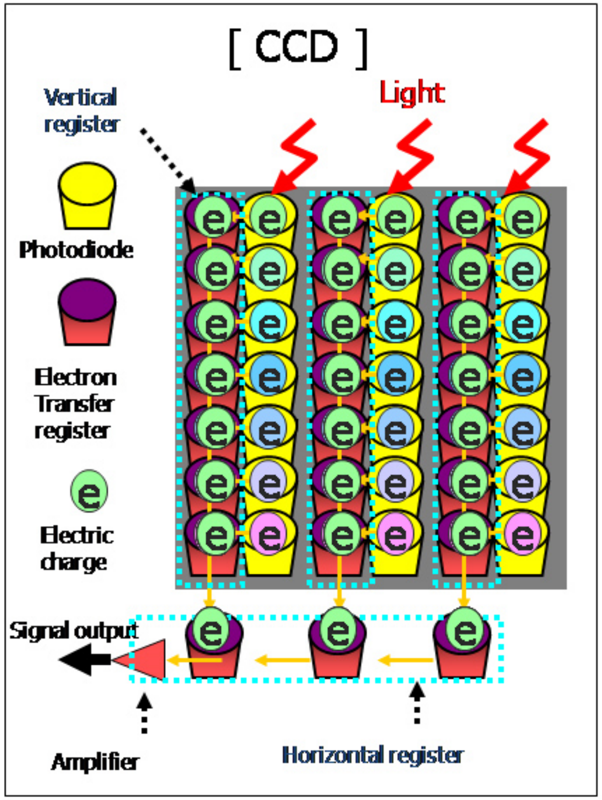

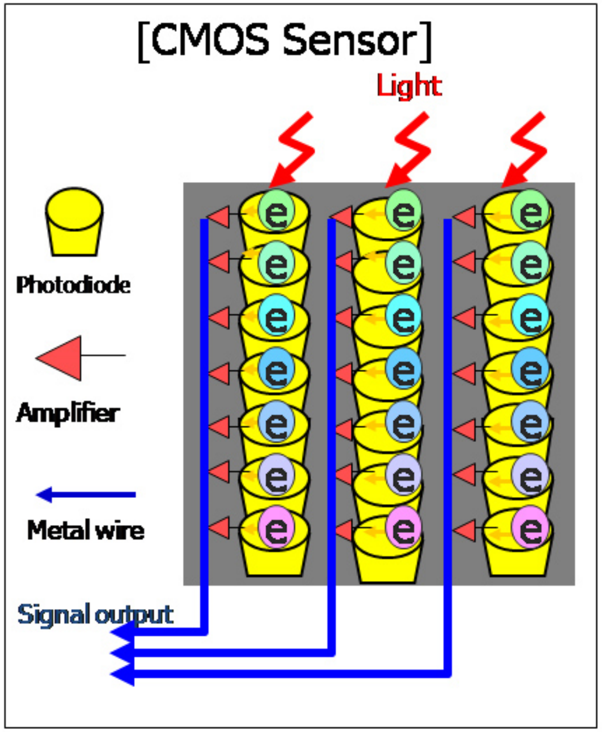

http://www.digitalbolex.com/global-shutter/

Electronic detectors provide rapid readout

- Electronic detectors are typically semiconductors or ionization-based stacks (e.g., photomultipliers)

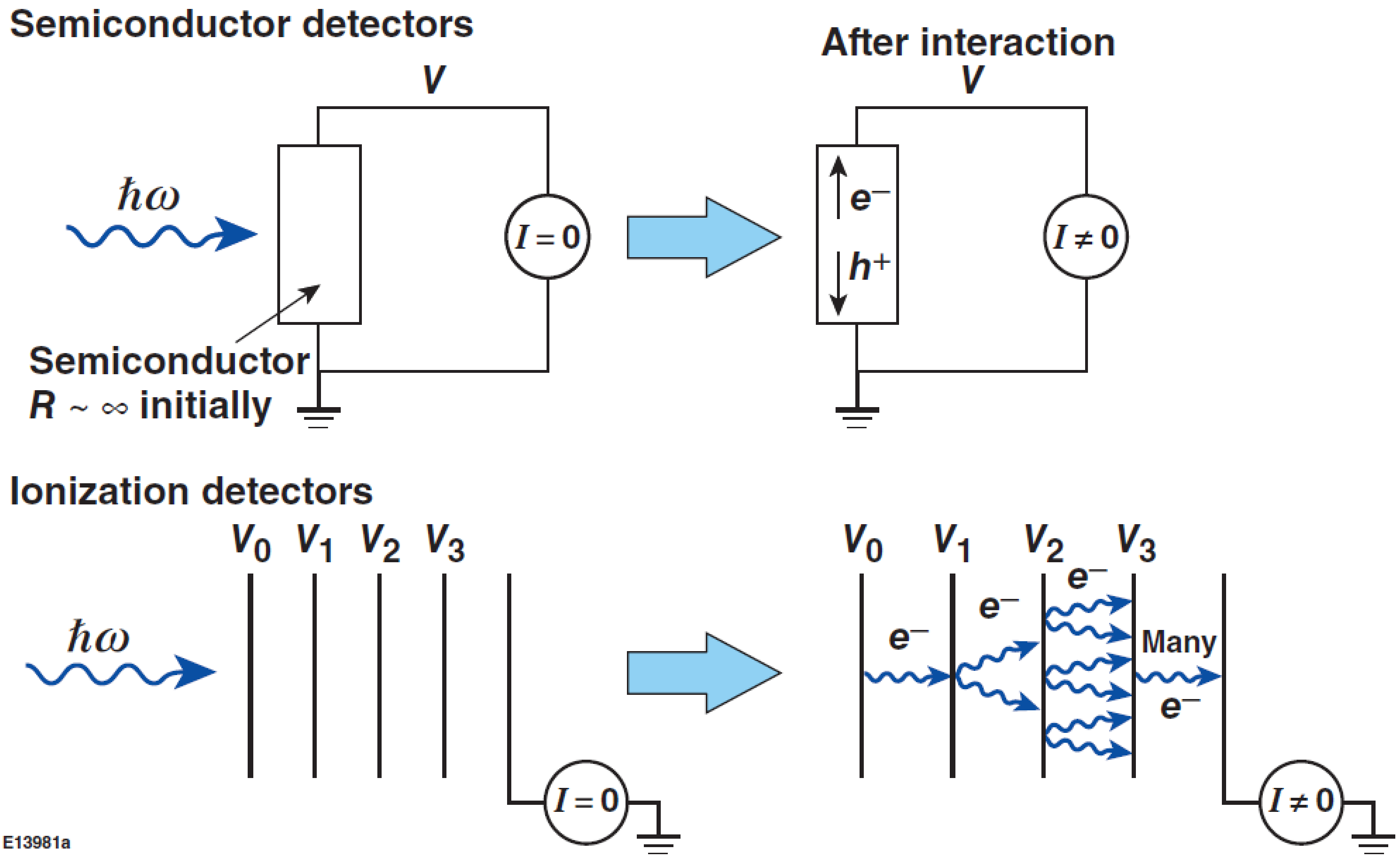

http://hedpschool.lle.rochester.edu/1000_proc2013.php

The number of electrons can be increased through photomultipliers or microchannel plate (MCP)

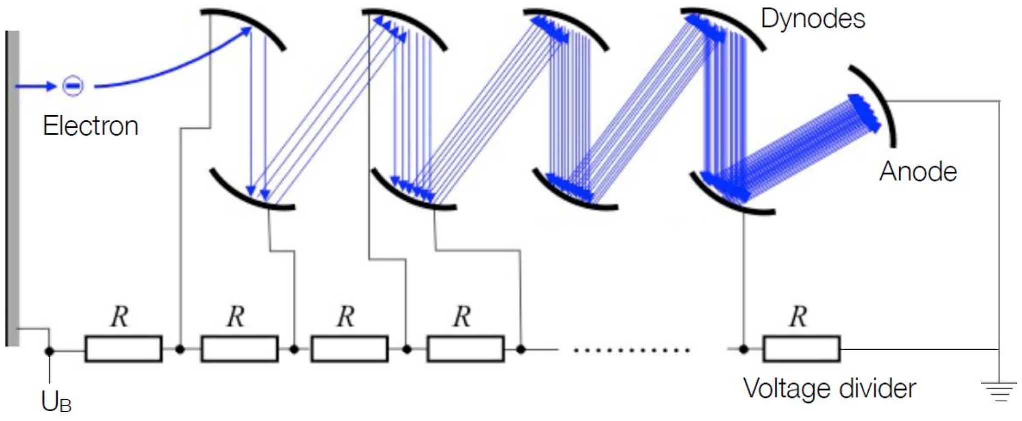

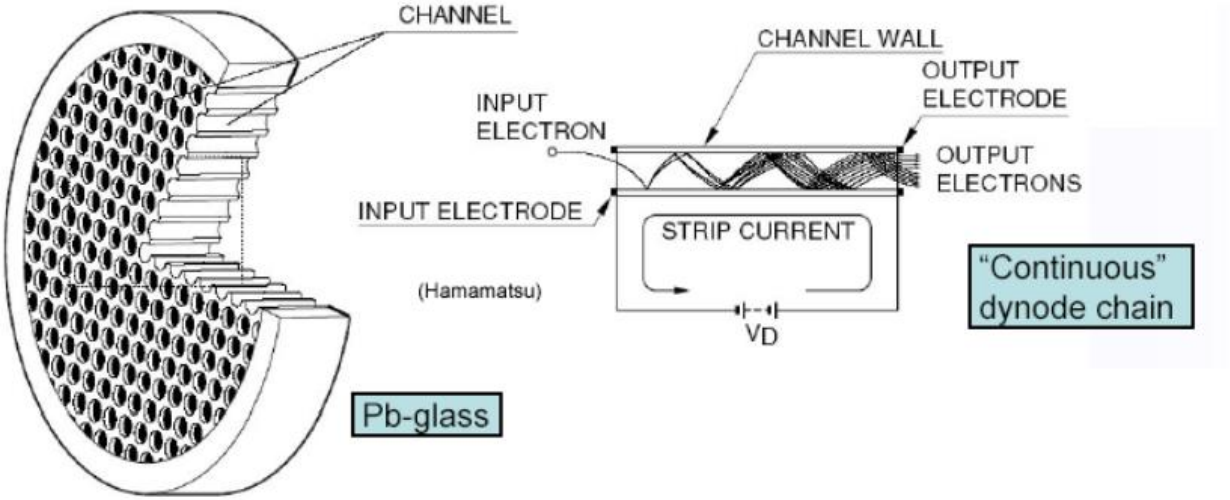

http://www.kip.uni-heidelberg.de/~coulon/Lectures/DetectorsSoSe10/

X-rays are imaged using photocathode, MCP, phosphor, and CCD

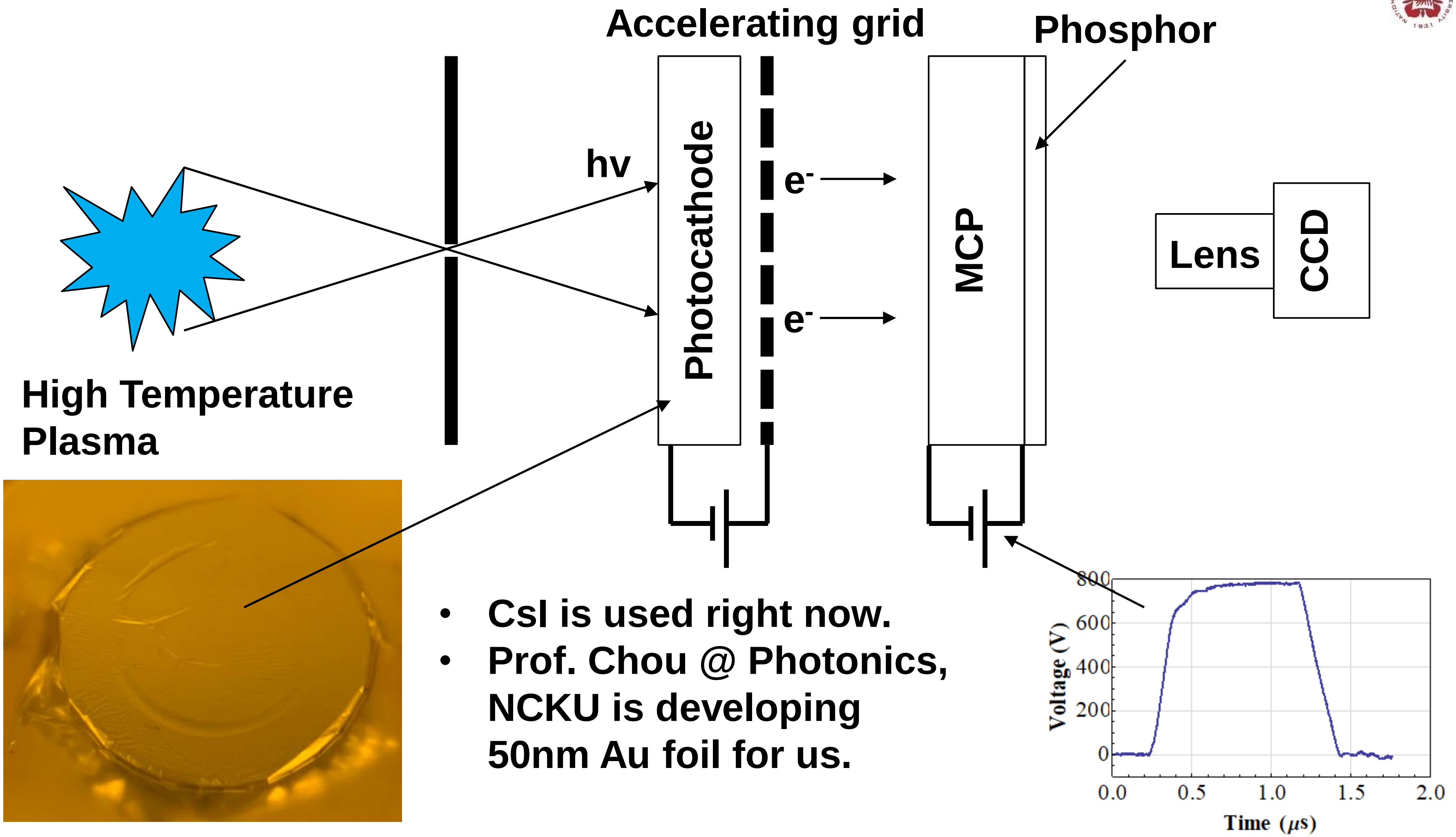

- CsI is used right now.
- Prof. Chou @ Photonics, NCKU is developing 50nm Au foil for us.

- **Images can be gated using fast high voltage pulses.**

A negative high-voltage pulse is used in our x-ray pinhole camera

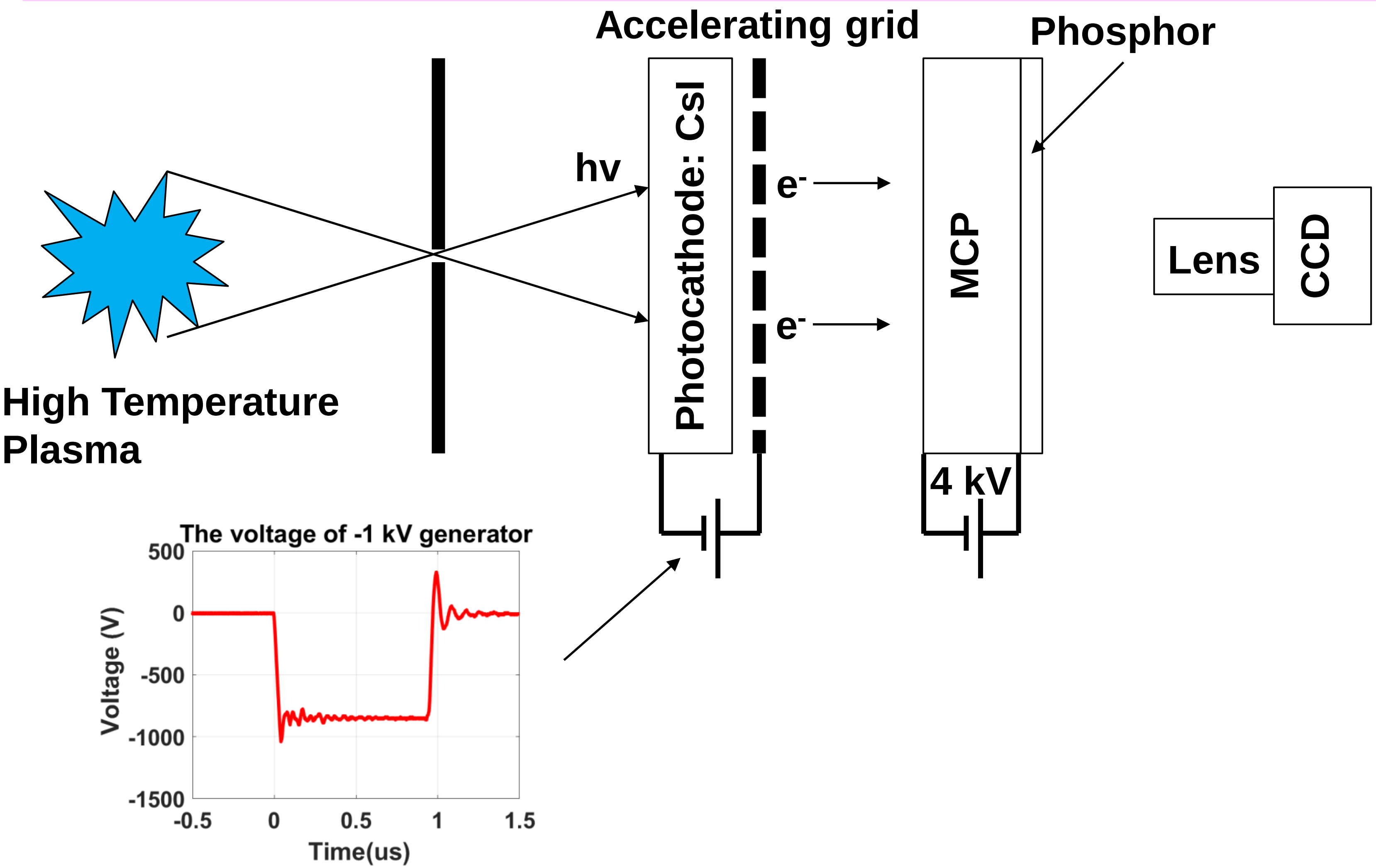

Accelerating grid

Phosphor

hv

Photocathode: CsI

e⁻

e⁻

MCP

Lens

CCD

4 kV

High Temperature Plasma

The voltage of -1 kV generator

- **The x-ray camera with a shutter opening time of ≤ 10 ns will be built.**

Response of components of ICCDs

■Spectral Response Characteristics

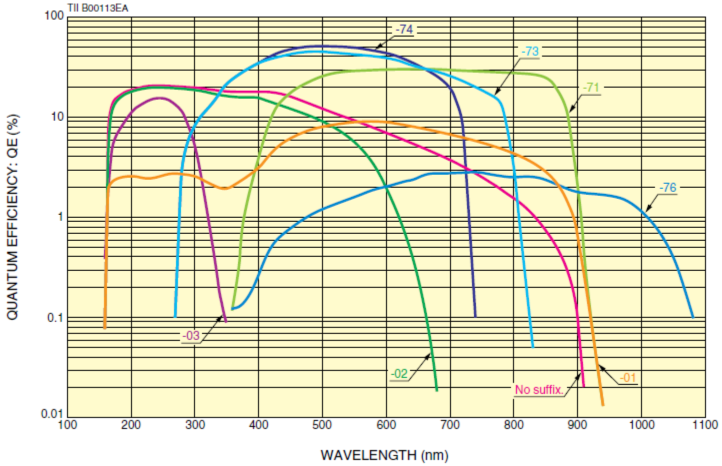

Suffix	Photo Cathode	Input Window
-71	GaAs	Borosilicate Glass
-73	Extended Red GaAsP	Borosilicate Glass
-74	GaAsP	Borosilicate Glass
-76	InGaAs	Borosilicate Glass
Non	Multialkali	Synthetic Silica
-01	Extended Red Multialkali	Synthetic Silica
-02	Bialkali	Synthetic Silica
-03	Cs-Te	Synthetic Silica

The sensitivity at short wavelengths charges with typical transmittance of window materials. Please refer to figure 4 (P6).

NOTE: For Gen II, gate operation types may have slightly lower sensitivity in the ultraviolet region.

An FOP is made up of a bundle of 50 million optical fibers.

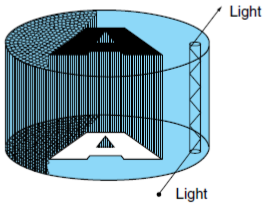

Each individual optical fiber transmits light and this light can be received as an image.

INPUT WINDOWS

Figure 4: Typical Transmittance of Window Materials

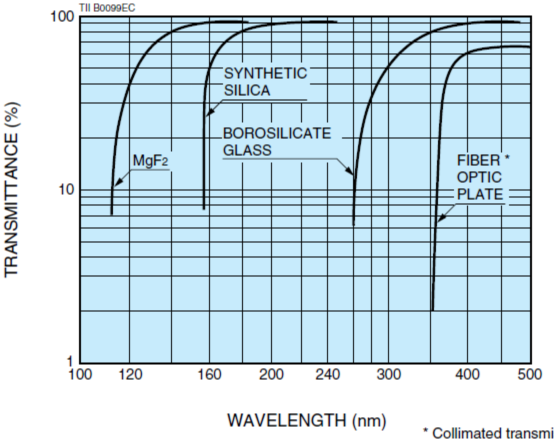

* Collimated transmission

Figure 5: Typical Phosphor Spectral Emission Characteristics

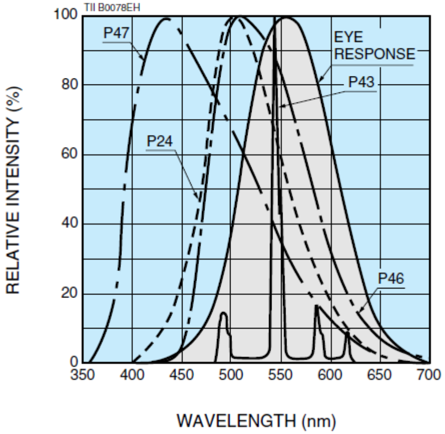

Figure 6: Typical Decay Characteristics

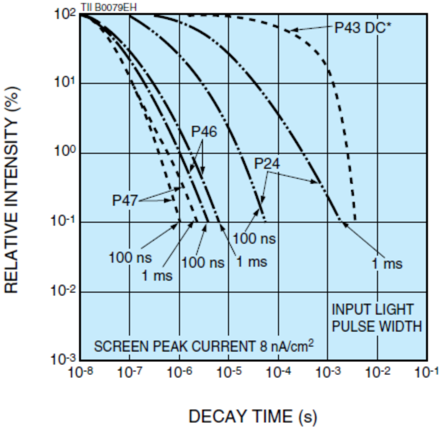

* Decay time obtained following to the continuous input light removal.

Hamamatsu Images Intensifiers brochure

A pinhole camera was designed and was built

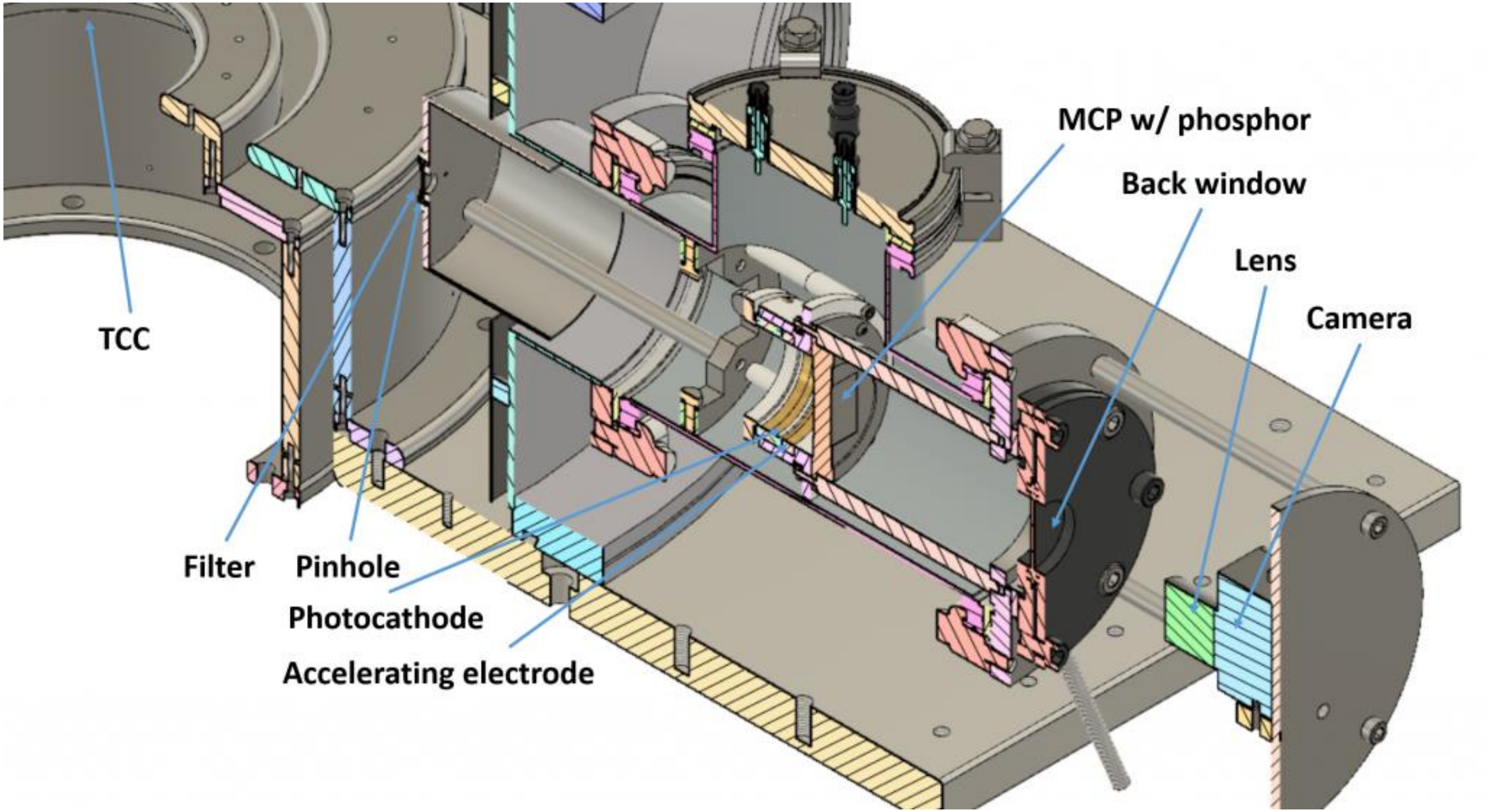

We demonstrated using x-ray pinhole camera to capture the radiation from an imploded x pinch

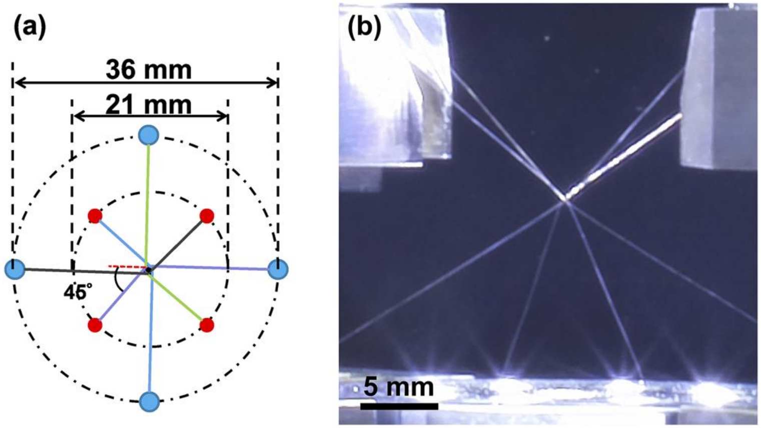

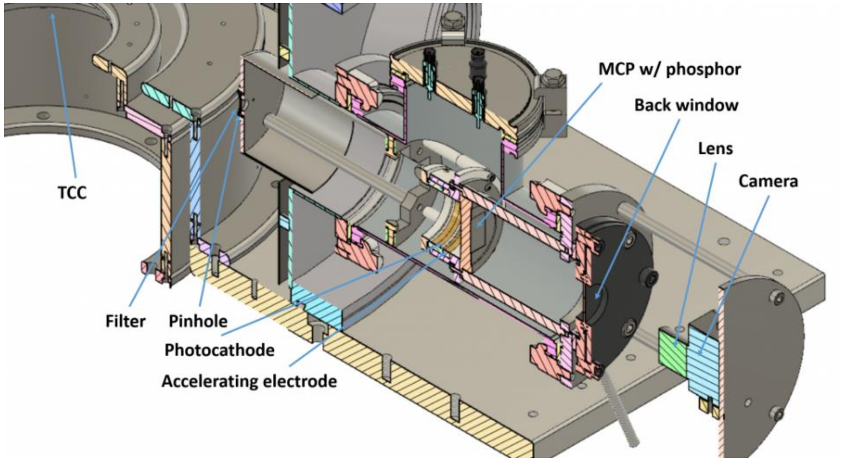

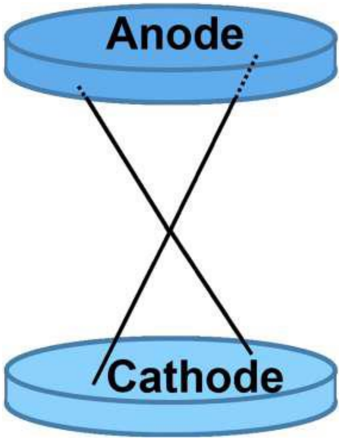

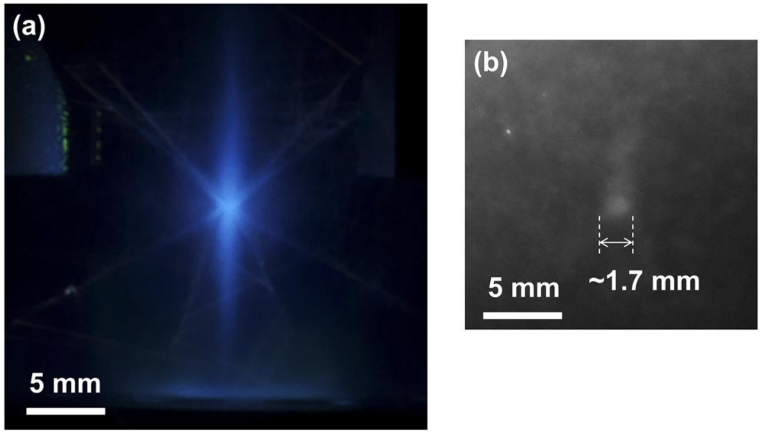

P.-Y. Chang *et al.*, Rev. Sci. Instrum **93**, 043505 (2022)

Electronic detectors provide rapid readout

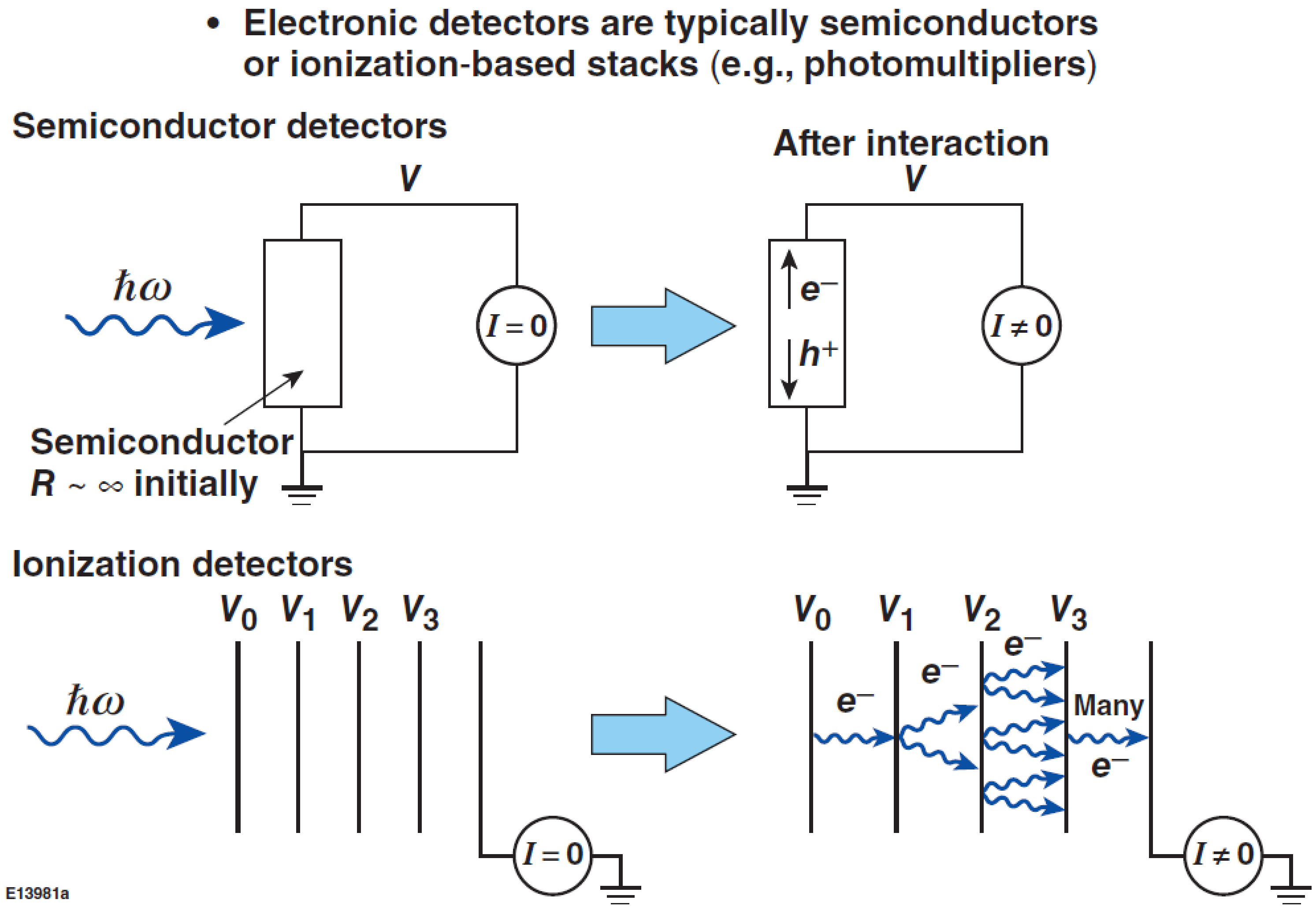
- Electronic detectors are typically semiconductors or ionization-based stacks (e.g., photomultipliers)

http://hedpschool.lle.rochester.edu/1000_proc2013.php

A framing camera provides a series of time-gated 2-D images, similar to a movie camera

- The building block of a framing camera is a gated microchannel-plate (MCP) detector
- An MCP is a plate covered with small holes, each acts as a photomultiplier

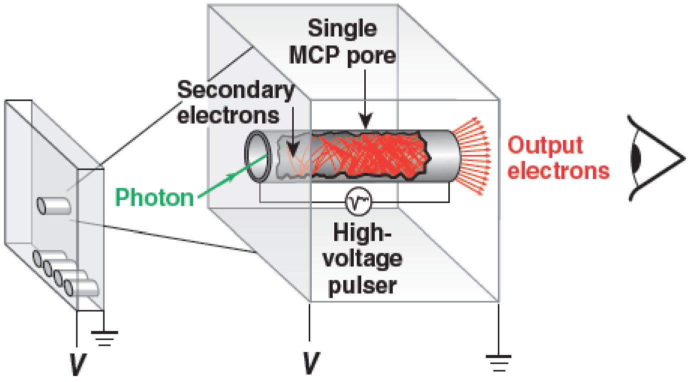

Multiple electrons are produced each time an electron or photon hits the wall

- A voltage pulse is sent down the plate, gating the detector

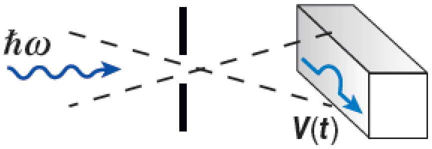

The detector is only on when the voltage pulse is present

E13986b

http://hedpschool.lle.rochester.edu/1000_proc2013.php

A framing camera detector consists of a microchannel plate (MCP) in front of a phosphor screen

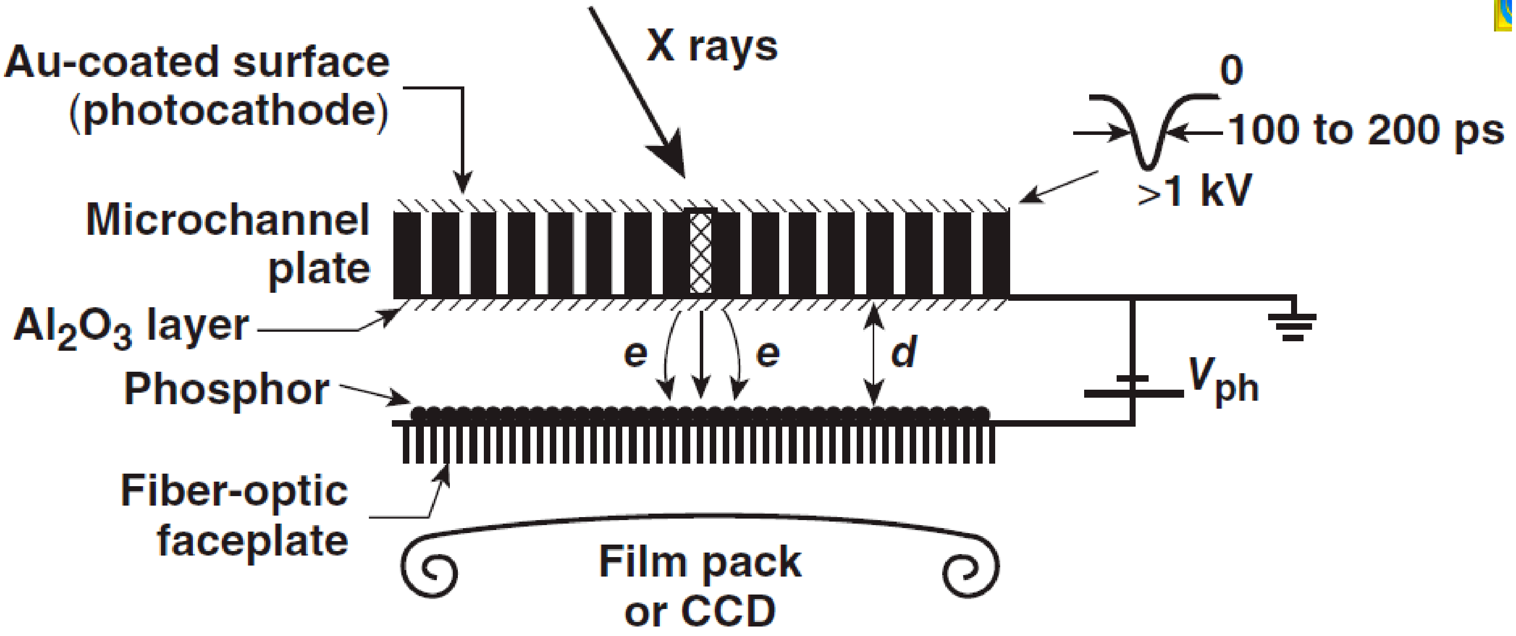

- Electrons are multiplied through MCP by voltage V_c
- Images are recorded on film behind phosphor
- Insulating Al_2O_3 layer allows for V_{ph} to be increased, thereby improving the spatial resolution of phosphor

E7795b

http://hedpschool.lle.rochester.edu/1000_proc2013.php

Framing camera

Two-dimensional time-resolved images are recorded using x-ray framing cameras

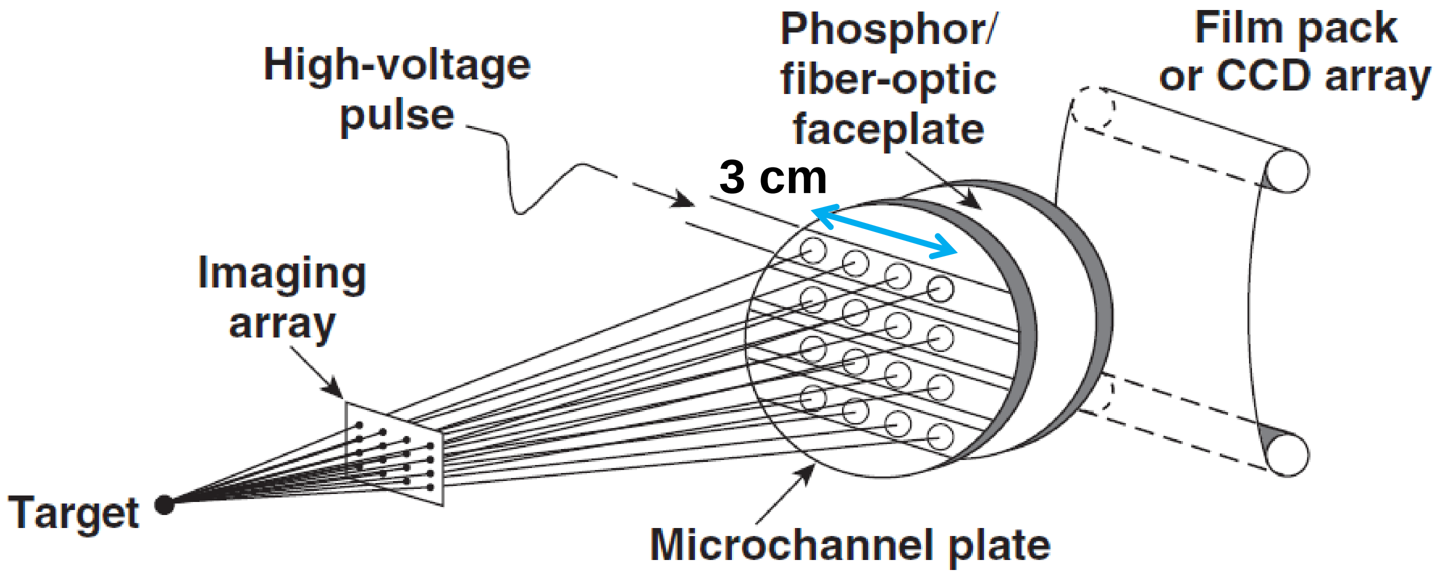

- Temporal resolution = 35 to 40 ps
- Imaging array: Pinholes: 10- to 12-μm resolution, 1 to 4 keV
- Space-resolved x-ray spectra can be obtained by using Bragg crystals and imaging slits

E7105b

Ex:

$$\Delta t = \frac{3\ \mathrm{cm}/3}{3 \times 10^{10}\ \mathrm{cm/s}} = 33\ \mathrm{ps}$$

http://hedpschool.lle.rochester.edu/1000_proc2013.php

X-ray framing cameras for recording two-dimensional time-resolved images will be built by the end of 2021

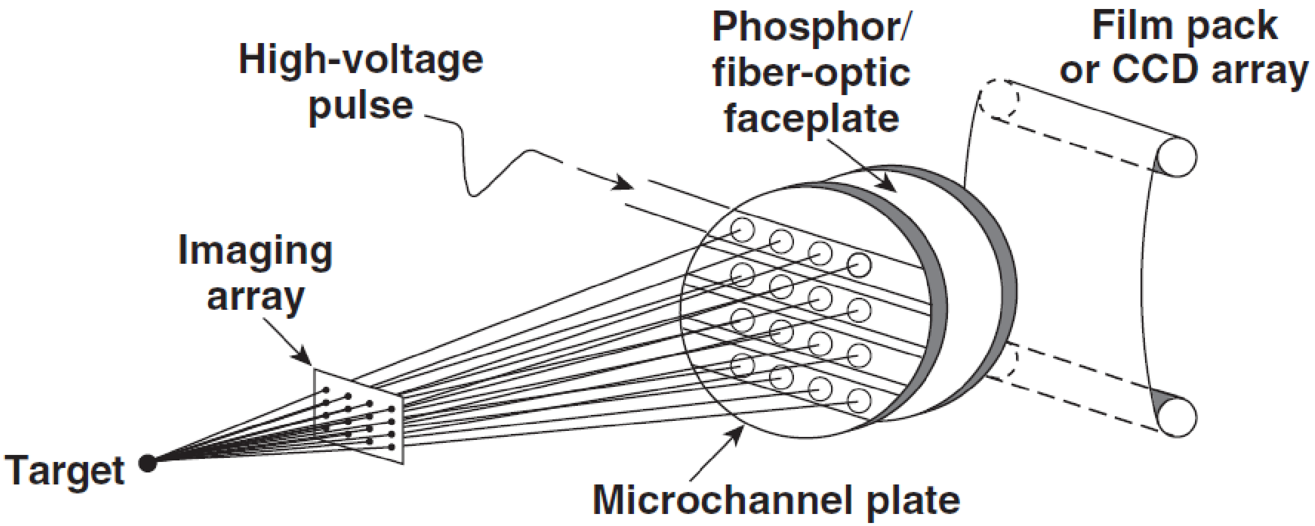

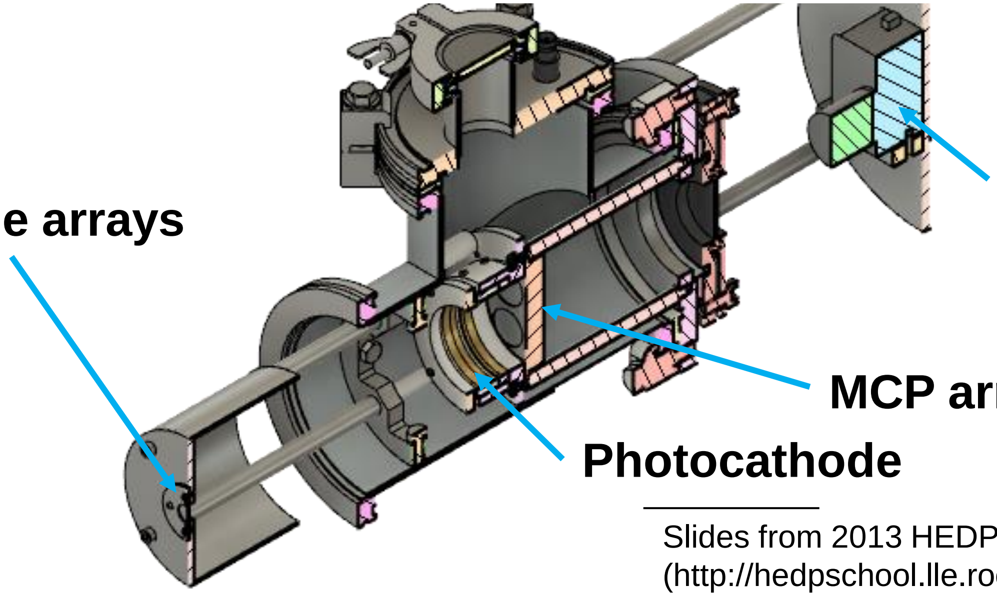

Pinhole arrays

CCD

MCP arrays

Photocathode

Slides from 2013 HEDP Summer School
(http://hedpschool.lle.rochester.edu/1000_proc2013.php)

Each pinhole camera will be triggered separately

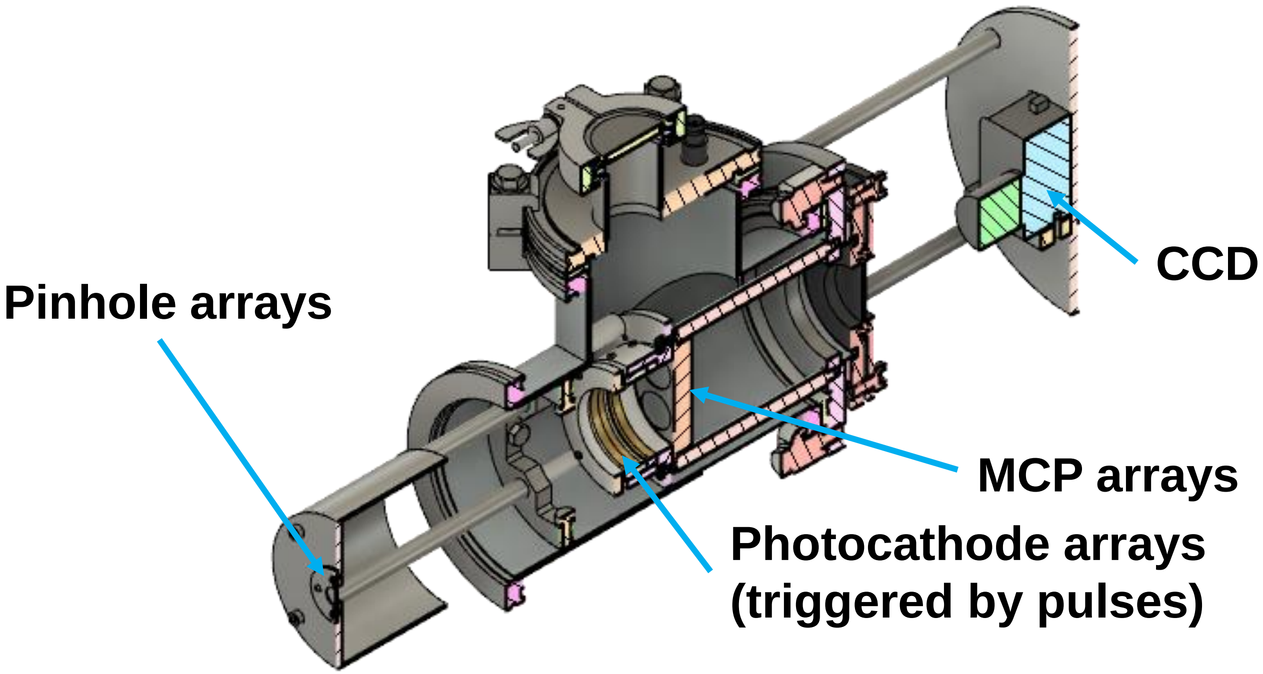

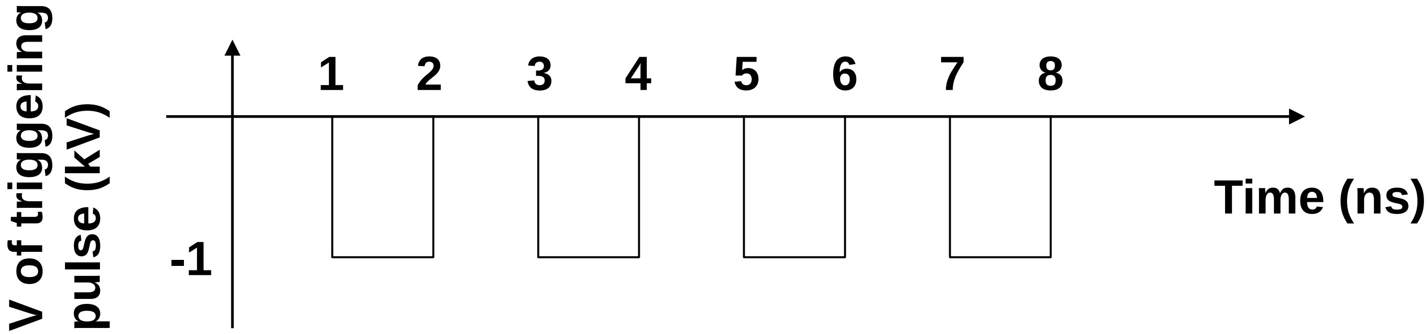

A streak camera provides temporal resolution of 1-D data

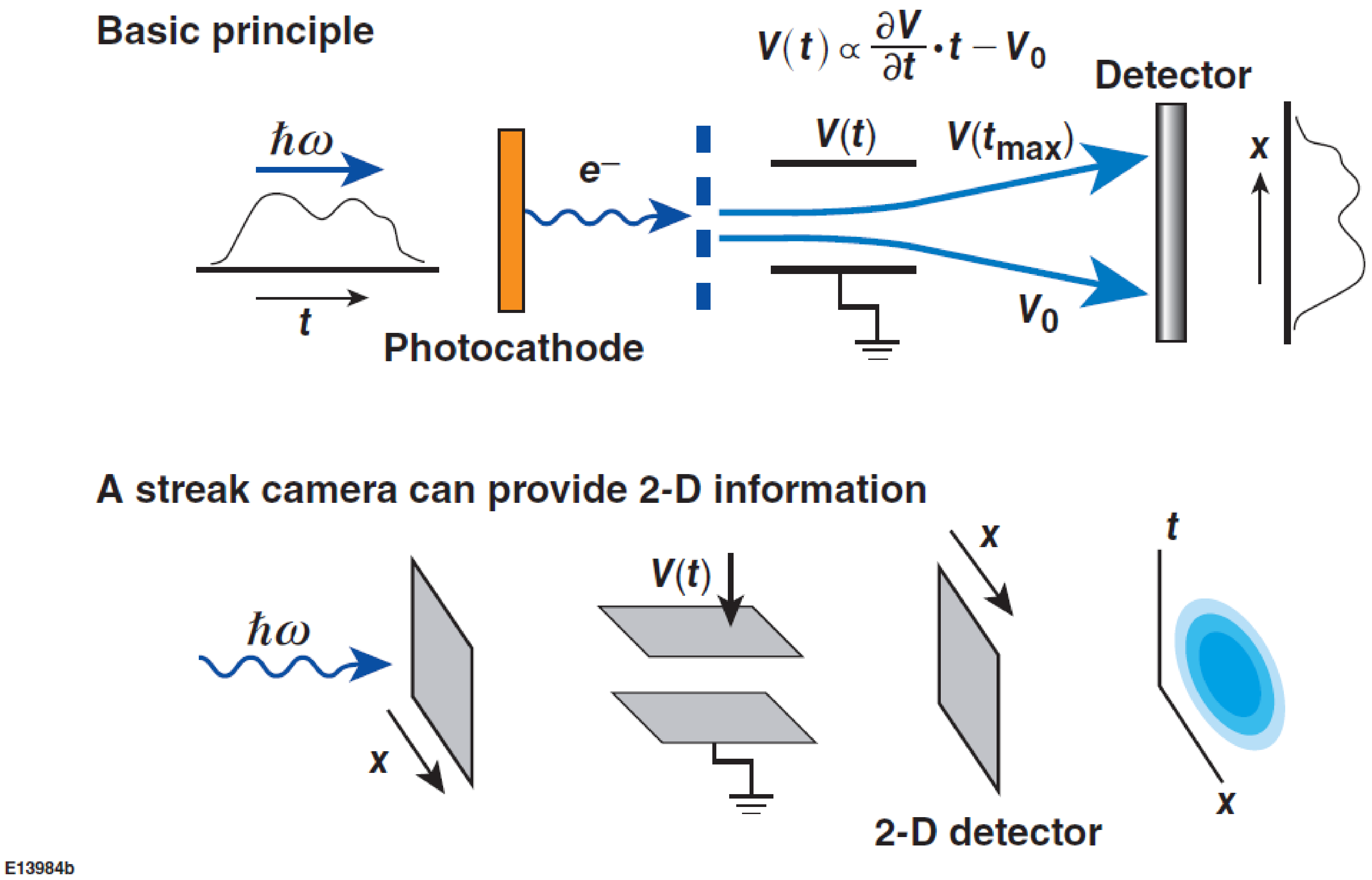

http://hedpschool.lle.rochester.edu/1000_proc2013.php

A slit is to prevent spatial information at different times interfering with each other

Imaging system
- Visible light: regular lens
- X rays: pinhole

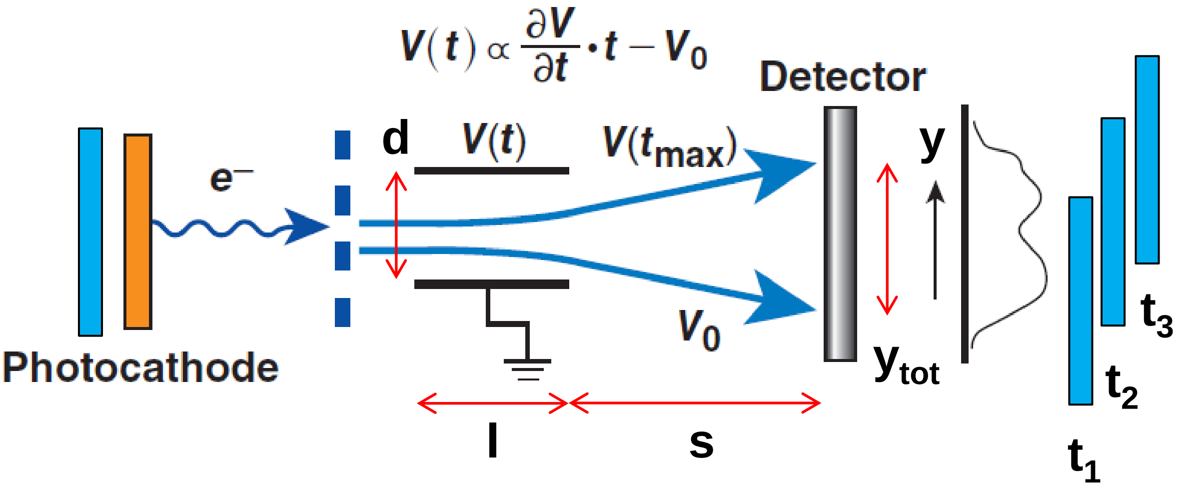

Imaging system
- Visible light: regular lens
- X rays: pinhole

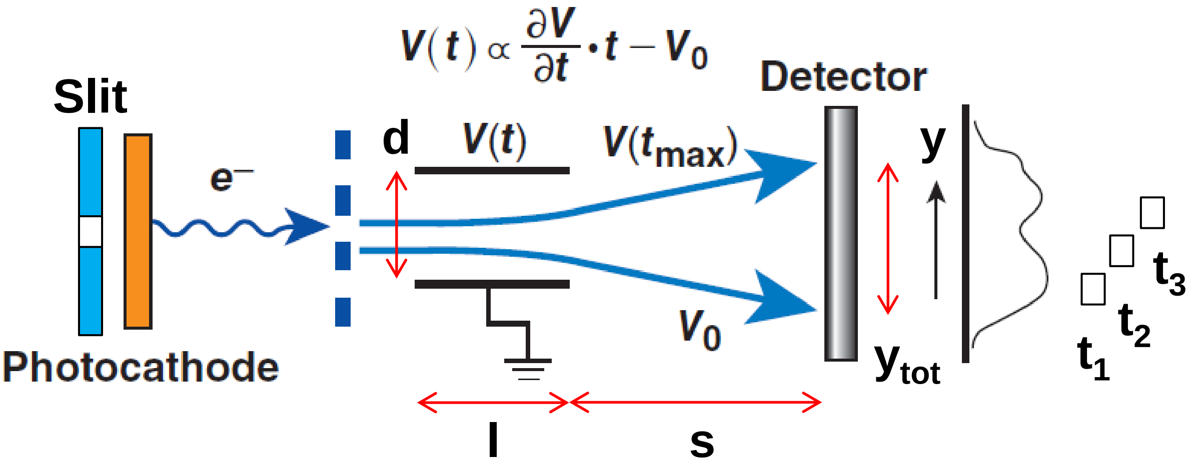

A temporal resolution higher than 15 ps is expected

Imaging system
- Visible light: regular lens
- X rays: pinhole

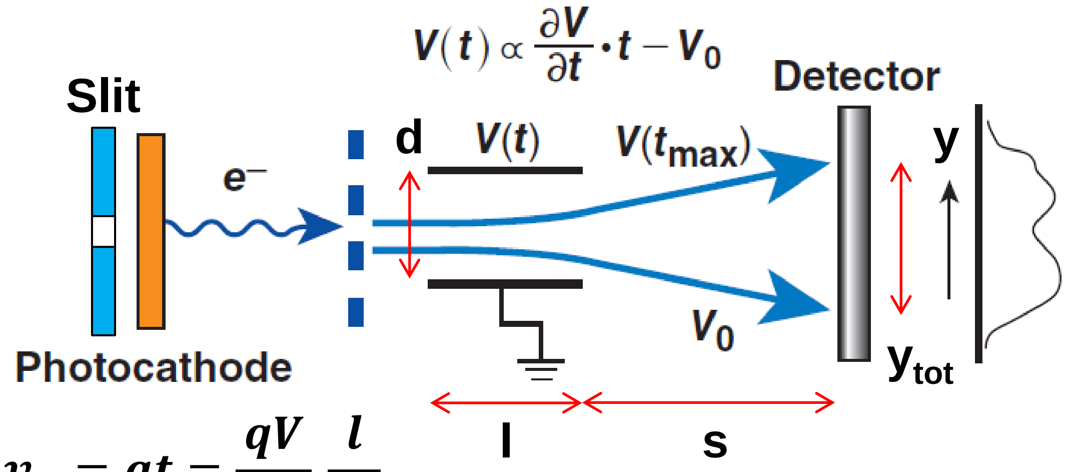

$$a = \frac{F}{m} = \frac{qE}{m} = \frac{qV}{md} \qquad v_\perp = at = \frac{qV}{md}\frac{l}{v_{||}}$$

$$y = s\,\mathrm{Tan}\theta = s\frac{V_\perp}{V_{||}} = \frac{1}{2E_k}\frac{l}{d}sqV = \frac{1}{2E_k}\frac{l}{d}sq(V_0 + V't)$$

- Let d=10 mm, l=20 mm, s=50 mm, E_k=1 keV, V=-200 ~ 200 V

$$V' \equiv \frac{V_{tot}}{t_{tot}} = 0.06\,\mathrm{kV/ns} \qquad y_{tot} = 15\mathrm{mm} \qquad y_{tot} = 15\mathrm{mm}$$

- Temporal resolution:

$$\delta t = \delta y\frac{2E_k d}{lsqV'} = 15\ \mathrm{ps}\quad \mathrm{for}\quad \delta y = 45\mu\mathrm{m}$$

- δt will be adjusted by changing E_k.

A streak camera with temporal resolution of 15 ps has been developed

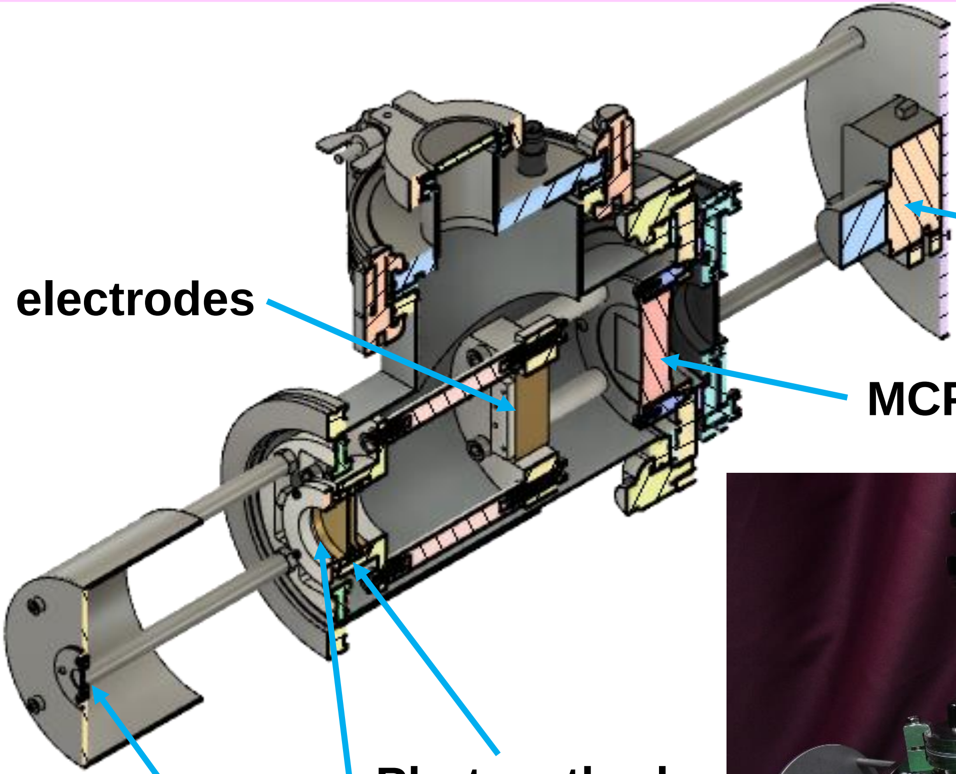

CCD

Sweeping electrodes

MCP

Photocathode

Slit

Pinhole

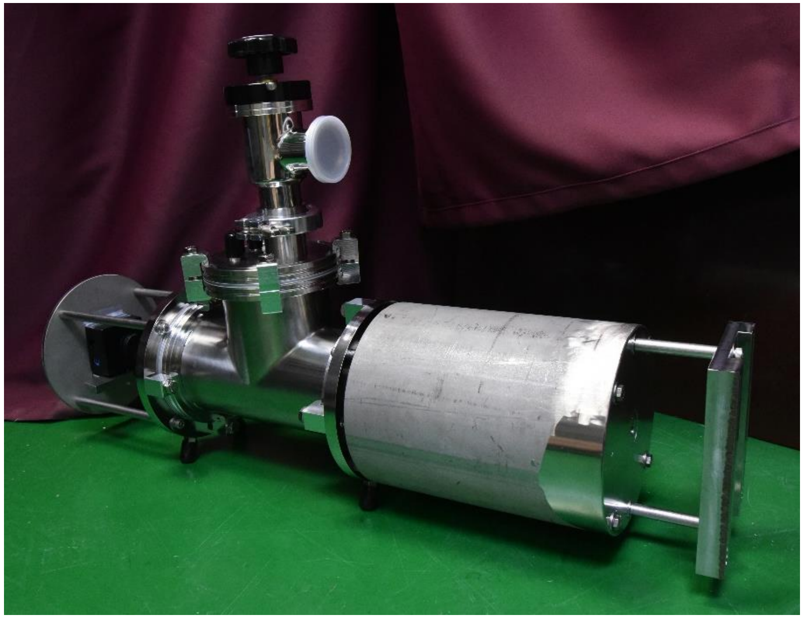

Shell trajectories can be measured using framing camera or streak camera

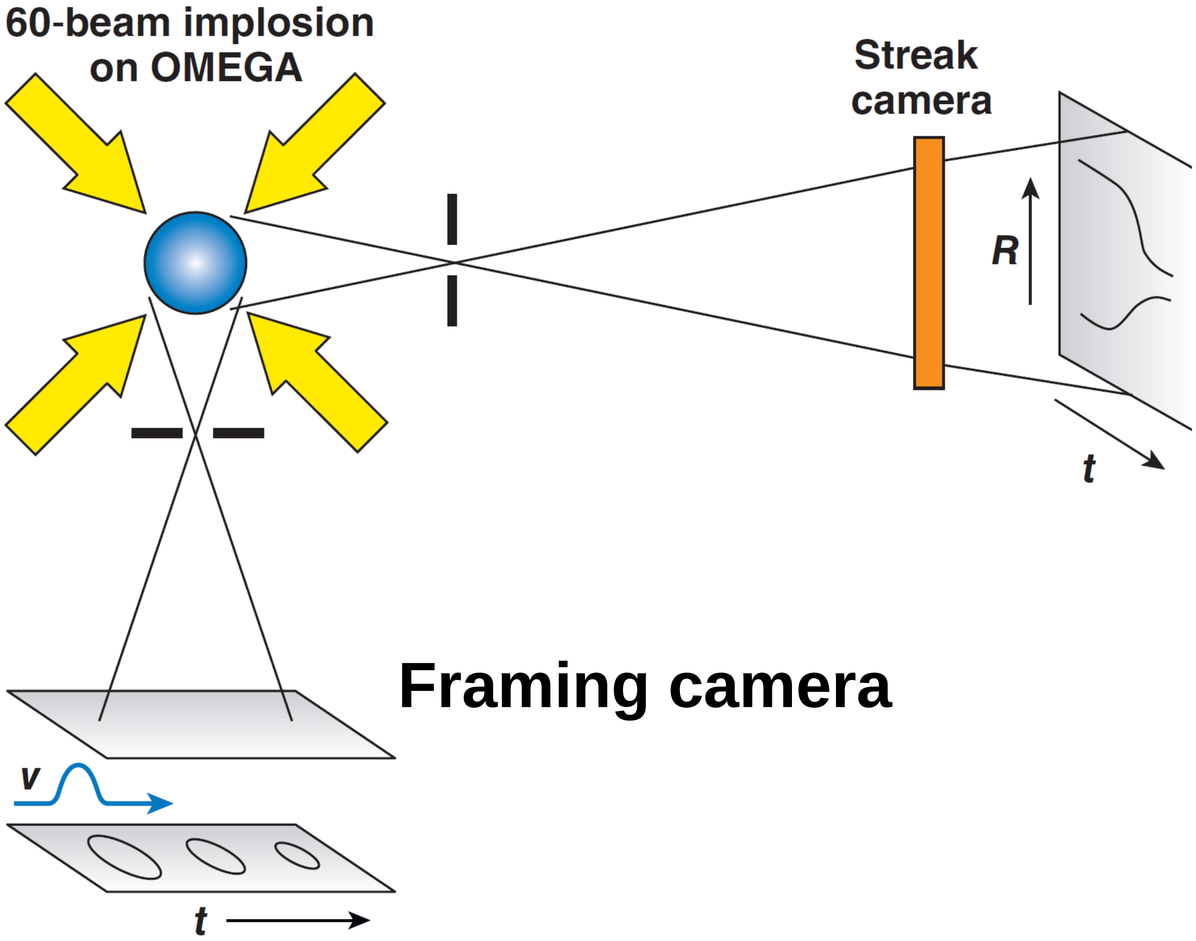

Framing camera

Comparison of images from framing camera versus streak camera

Framing-camera image
6× magnification

Shot 13377

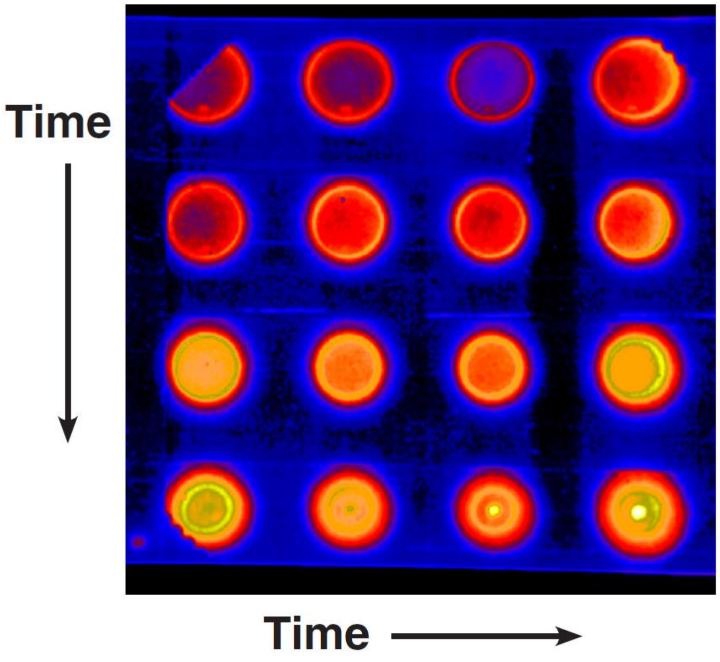

Streak-camera image

Shot 13377

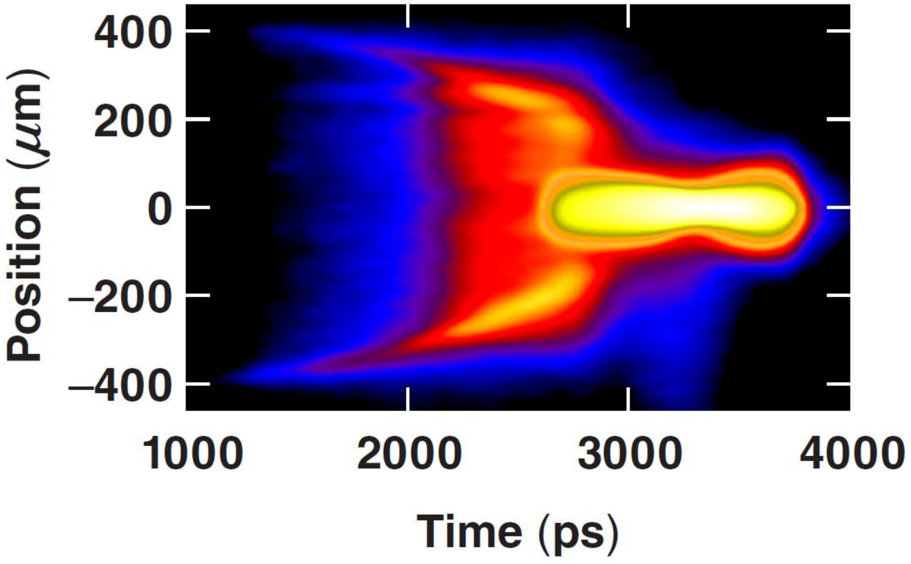

The optical density can be measured using the absorption of a backlighter

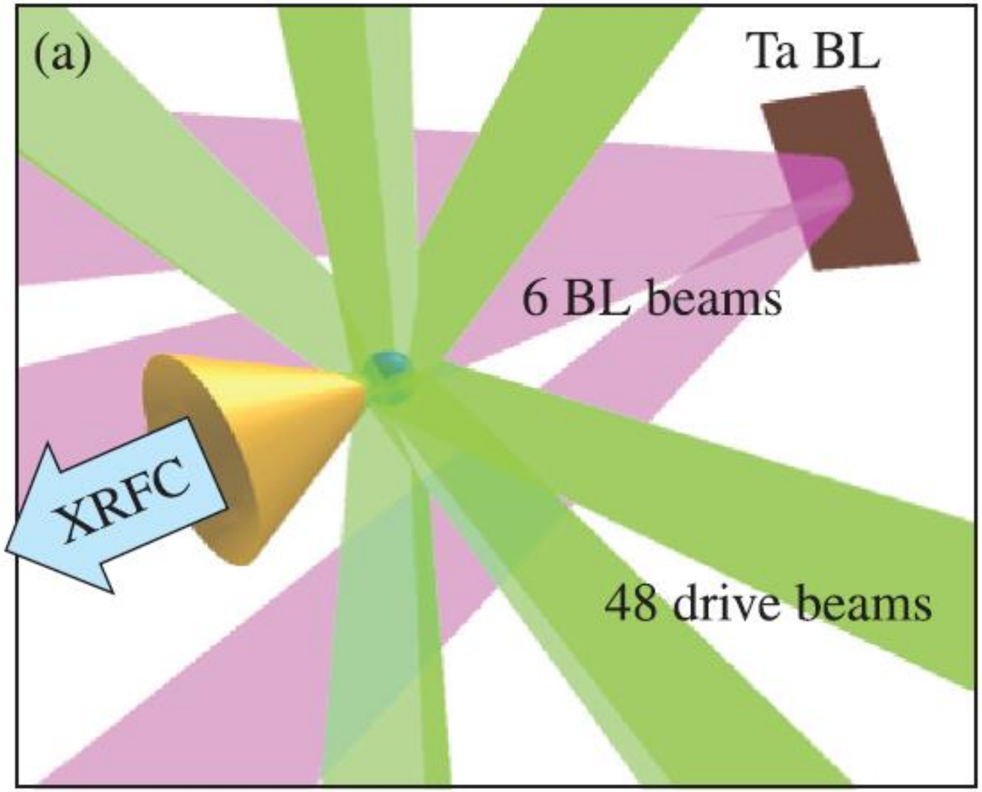

$$I = \int I(\varepsilon)\exp(-\mu(\varepsilon)\rho\delta)d\varepsilon$$

$$I = I_{\mathrm{BL}}\exp(-\bar{\mu}\rho\delta)$$

$$\ln I = \ln I_{BL} - \mu\rho r$$

G. Fiksel *et al.*, Phys. Plasmas **19**, 062704 (2012)

X-ray radiography of an X-pinch by using another X-pinch or two X-pinches as point sources of probing radiation

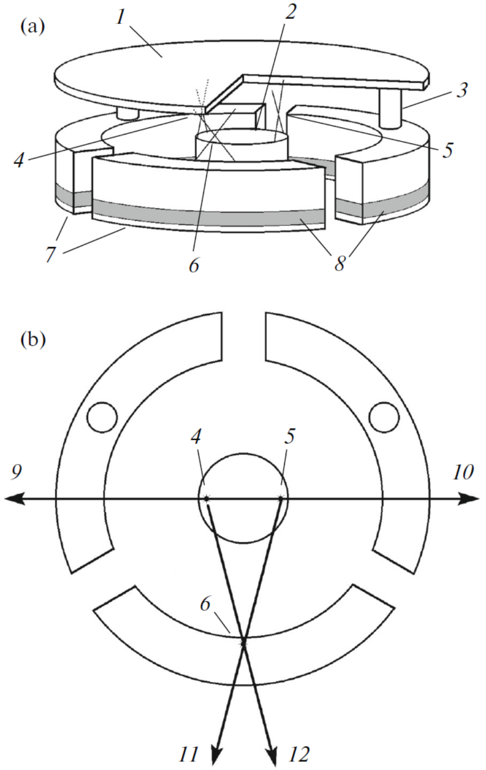

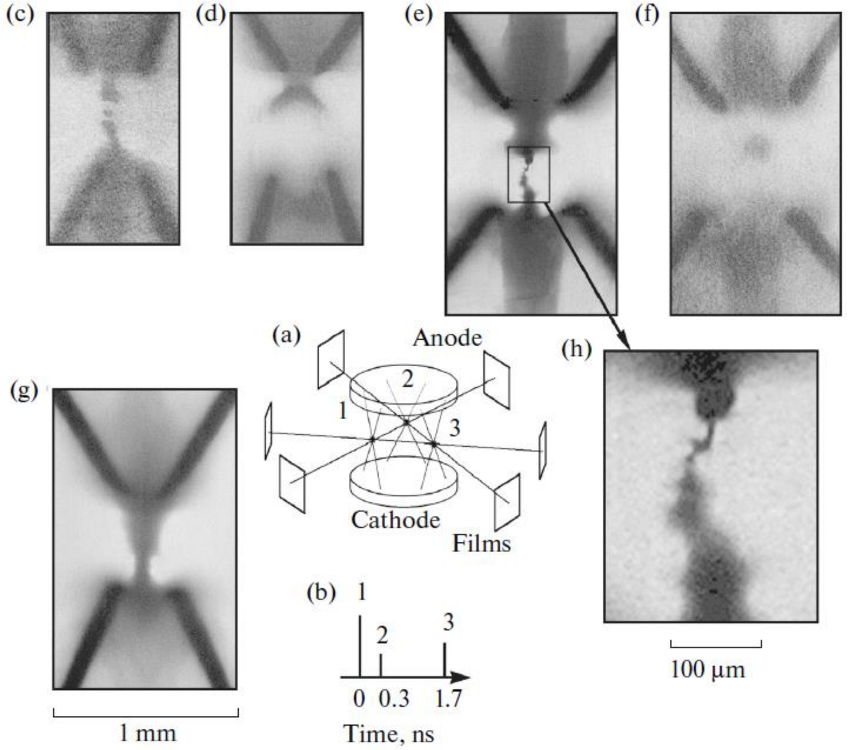

Fig. 44. X-ray radiographs obtained in the system of three parallel 2 × 12.5-μm Mo X-pinches: (a) arrangement of the pinches and films, (b) temporal positions and relative intensities of probing X-ray pulses, (c) image of X-pinch 1 in the radiation of X-pinch 2, (d) image of X-pinch 1 in the radiation of X-pinch 3, (e) image of X-pinch 2 in the radiation of X-pinch 1, (f) image of X-pinch 2 in the radiation of X-pinch 3, (g) image of X-pinch 3 in the radiation of X-pinch 1 emission, and (h) enlarged fragment of the image.

S. A. Pikuz *et al.*, Plasma Phys. Rep. **41**, 291 (2015)

We demonstrated using x-ray pinhole camera to capture the radiation from an imploded x pinch

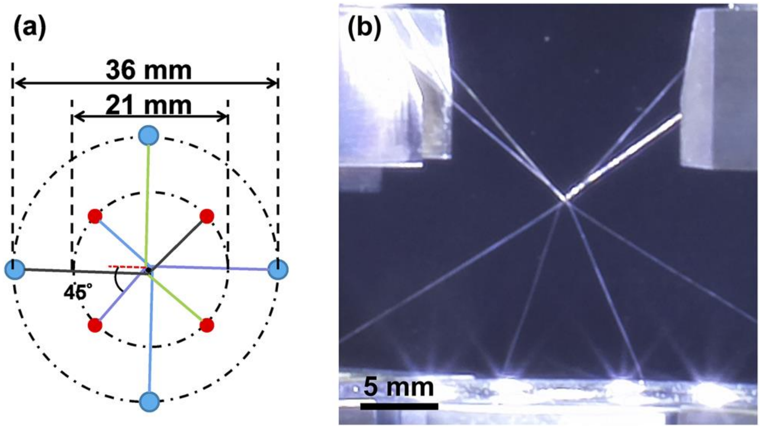

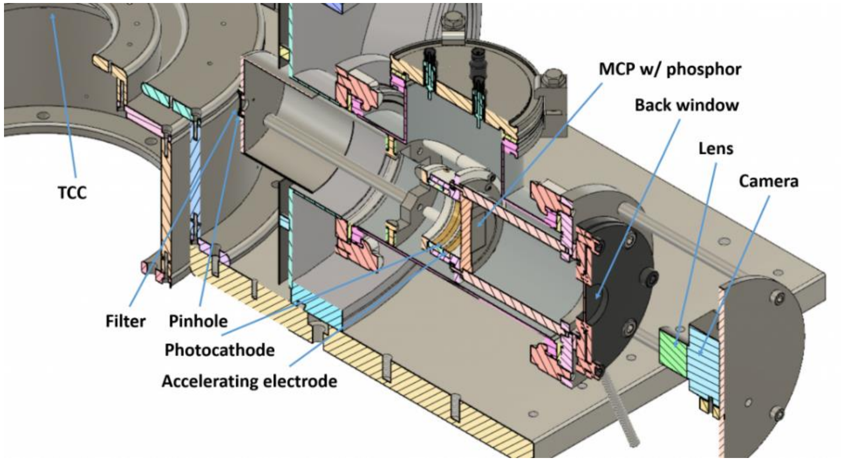

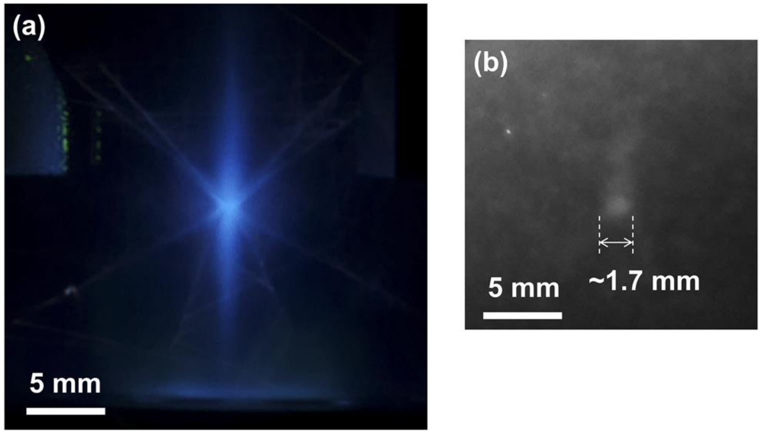

P.-Y. Chang *et al.*, Rev. Sci. Instrum **93**, 043505 (2022)

Shock velocities are measured using time-resolved Velocity Interferometer System for Any Reflector (VISAR)

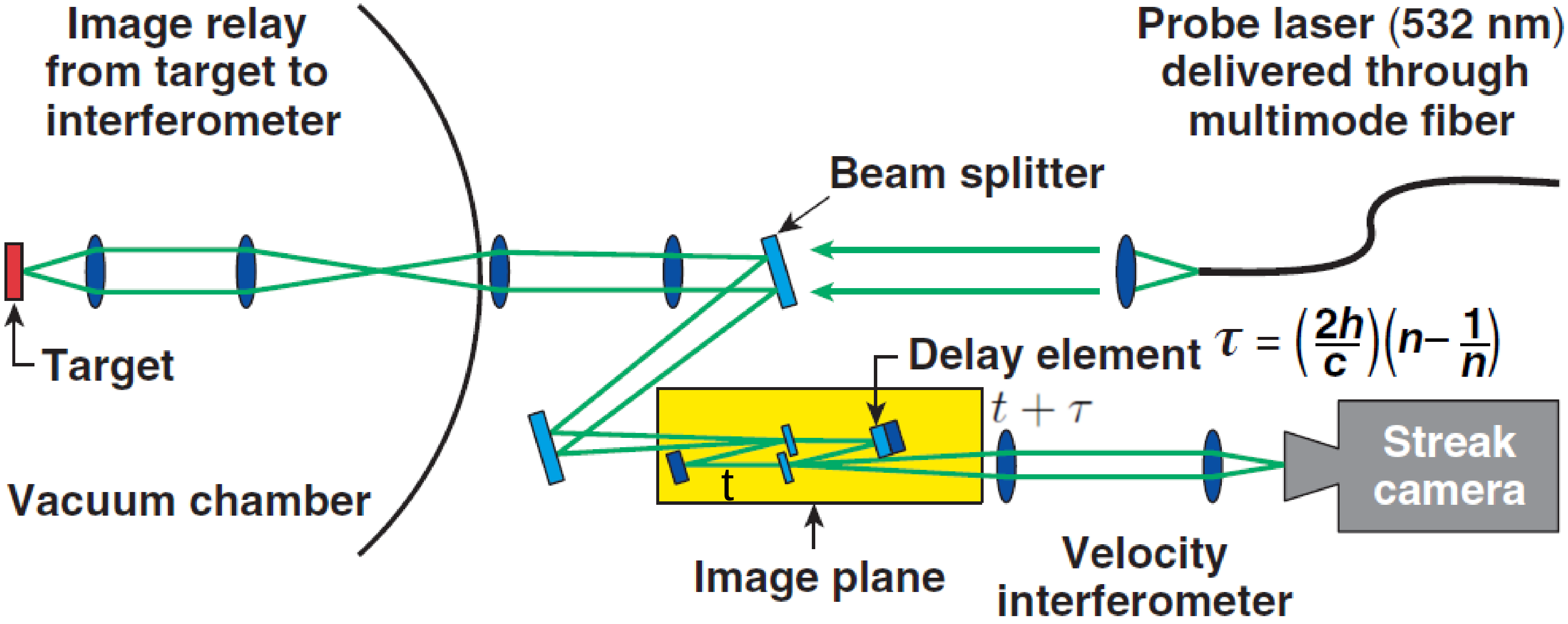

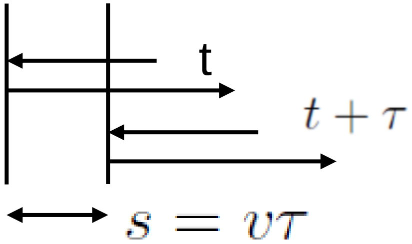

$$\Delta\phi = \frac{v\tau}{\lambda} \propto v$$

---

http://hedpschool.lle.rochester.edu/1000_proc2013.php

Shock velocities are measured using time-resolved Velocity Interferometer System for Any Reflector (VISAR)

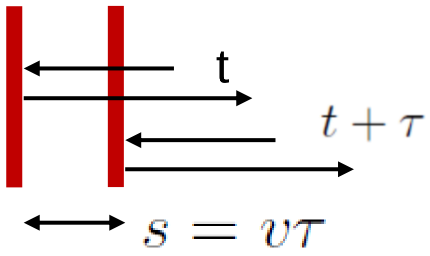

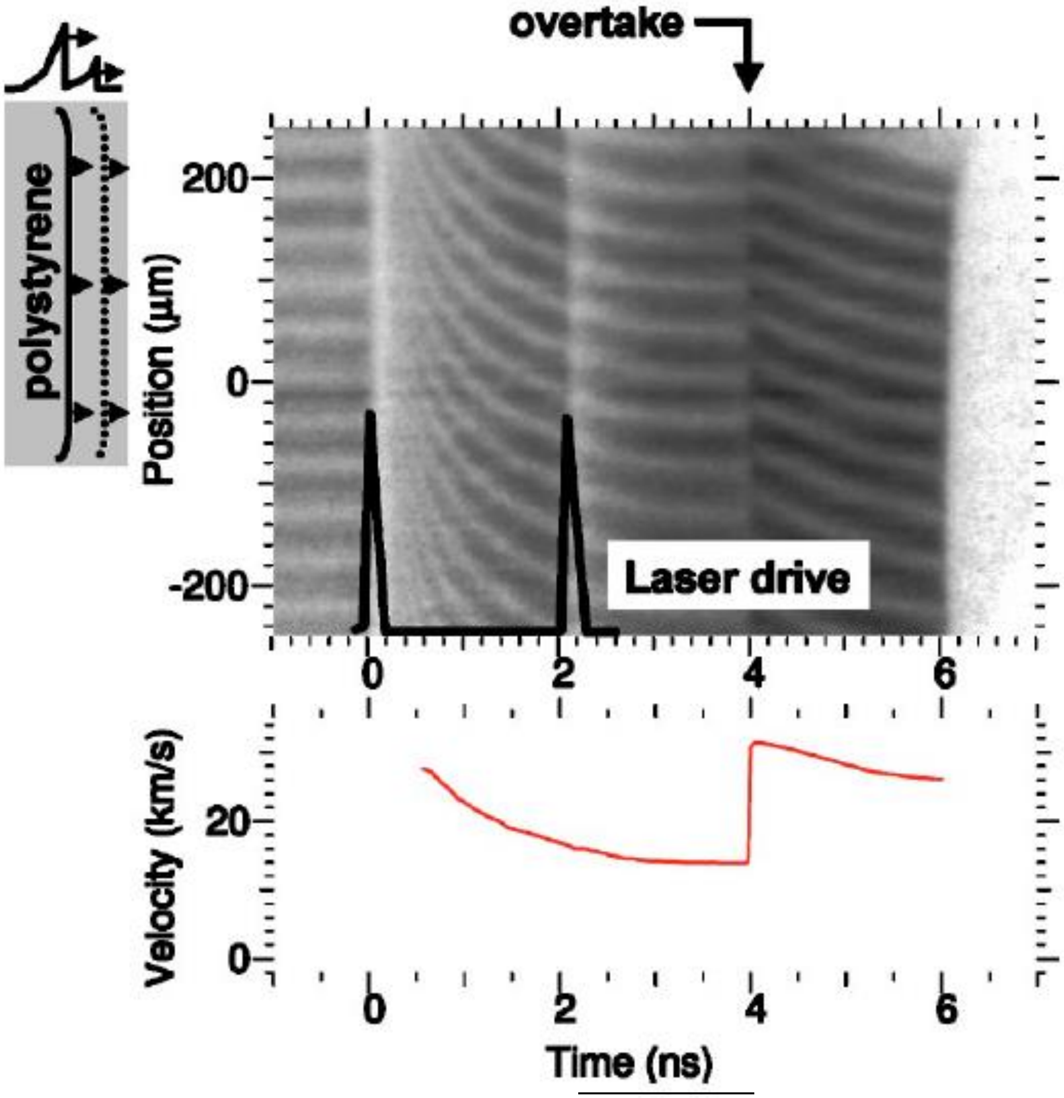

P. M. Celliers *et al.*, Rev. Sci. Insytum. **75**, 4916 (2004)

Neutron average temperature is obtained using Neutron Time of Flight (NToF)

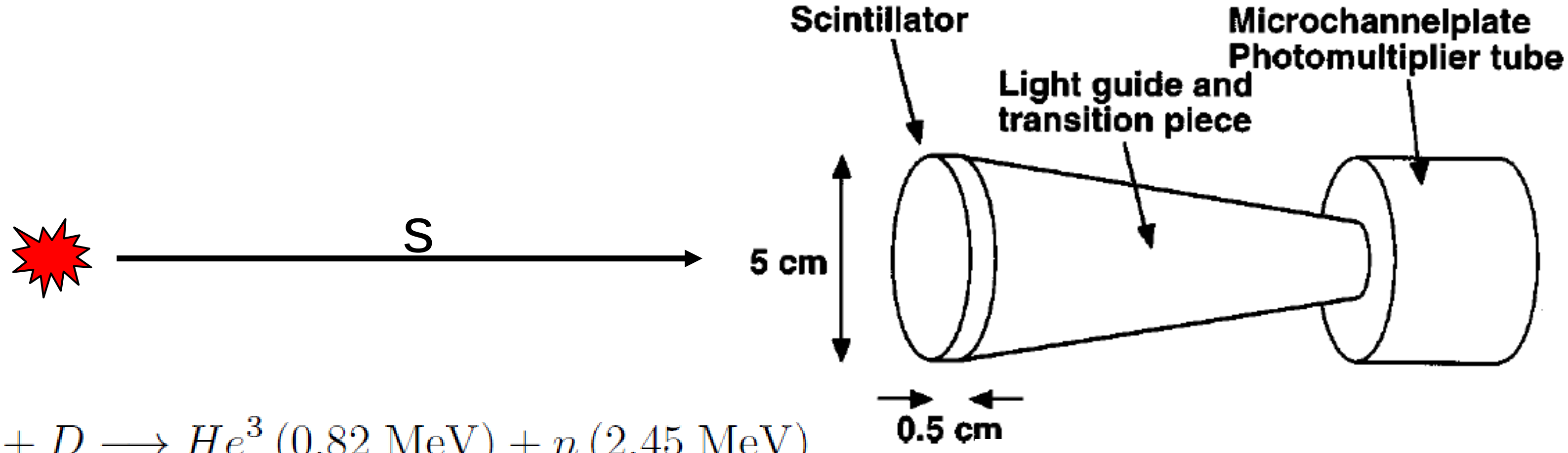

$$D + D \longrightarrow He^3\,(0.82\ \mathrm{MeV}) + n\,(2.45\ \mathrm{MeV})$$

$$D + T \longrightarrow He^4\,(3.5\ \mathrm{MeV}) + n\,(14.1\ \mathrm{MeV})$$

$$s = vt \qquad v = \frac{s}{t}$$

$$f(v) = \sqrt{\left(\frac{m}{2\pi kT}\right)} \exp\left(-\frac{mv^2}{2kT}\right)$$

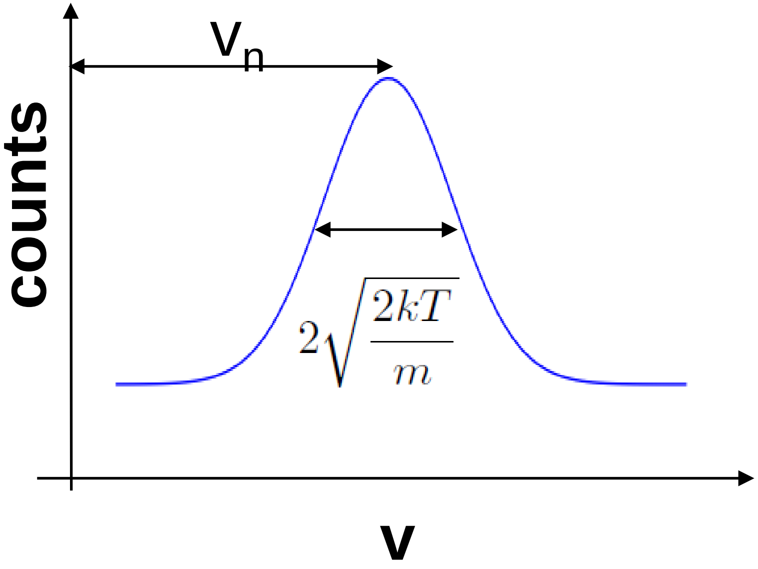

T. J. Murphy *et al.*, Rev. Sci. Instrum. **72**, 773 (2001)

The OMEGA Facility is carrying out ICF experiments using a full suite of target diagnostics

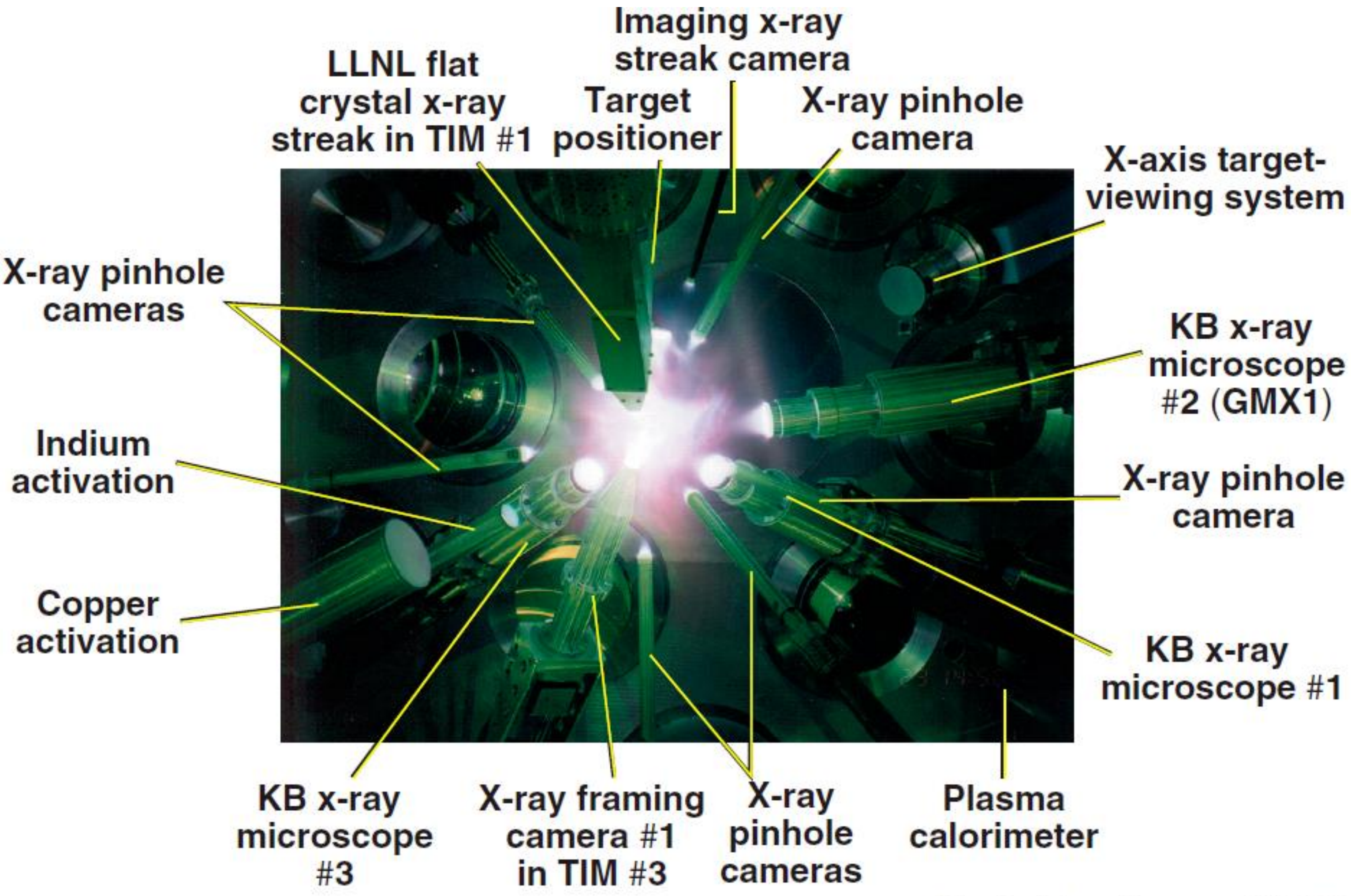

E8012b

Photo taken from port H11B

A peak current of ~135 kA with a rise time of ~1.6 us is provided by the pulsed-power system

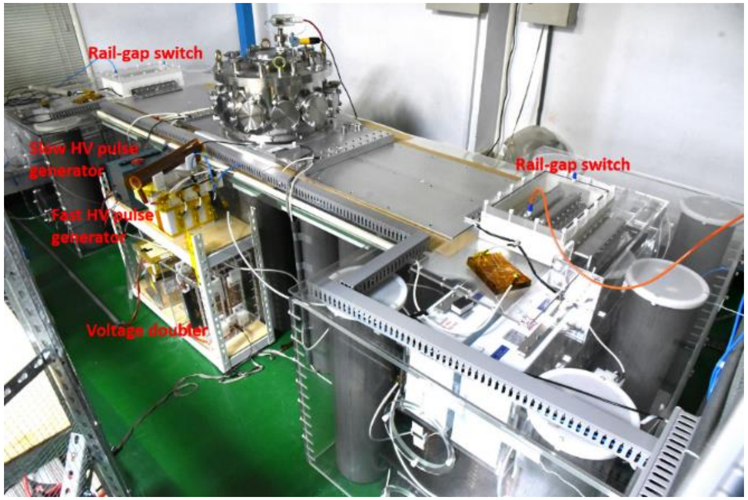

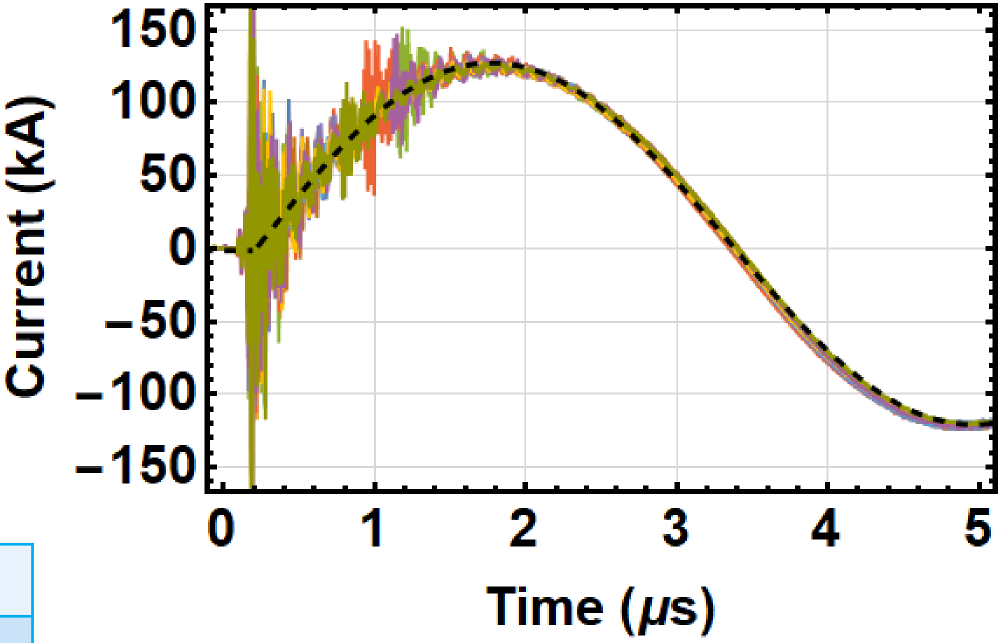

Capacitance (μF)	**5**
V_{charge} (kV)	**20**
Energy (kJ)	**1**
Inductance (nH)	**204 ± 4**
Rise time (quarter period, ns)	**1592 ± 3**
I_{peak} (kA)	**135 ± 1**

A suit of diagnostics in the range of (soft) x-ray are being built

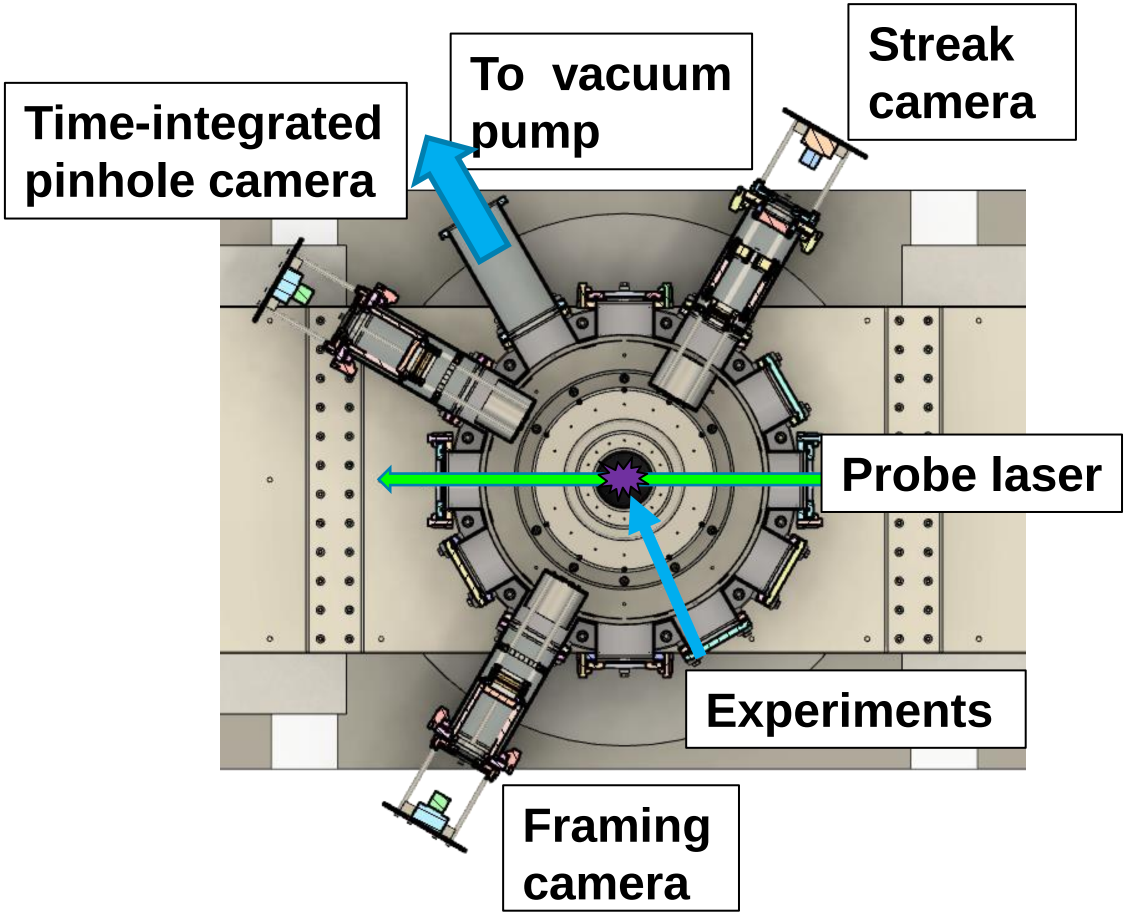

Time-integrated pinhole camera

To vacuum pump

Streak camera

Probe laser

Experiments

Framing camera

- CsI are used as the photocathode for all x-ray imaging system.
- Au photocathode may be used in the future.

- **Pinhole camera:**
  - Magnification: 1x
  - Exposure time: 1 us
- **Streak camera:**
  - Magnification: 1x
  - Temporal resolution: 15 ps
- **Framing camera:**
  - Magnification: 0.3x
  - Temporal resolution: ~ns using 4 individual MCPs
- **Laser probing:**
  - For interferometer, schlieren, shadowgraphy, Thomson scattering.
  - Temporal resolution: ~300 ps using stimulated brillouin scattering (SBS) pulse compression in water

Time-resolved imaging system with temporal resolution in the order of nanoseconds was implemented

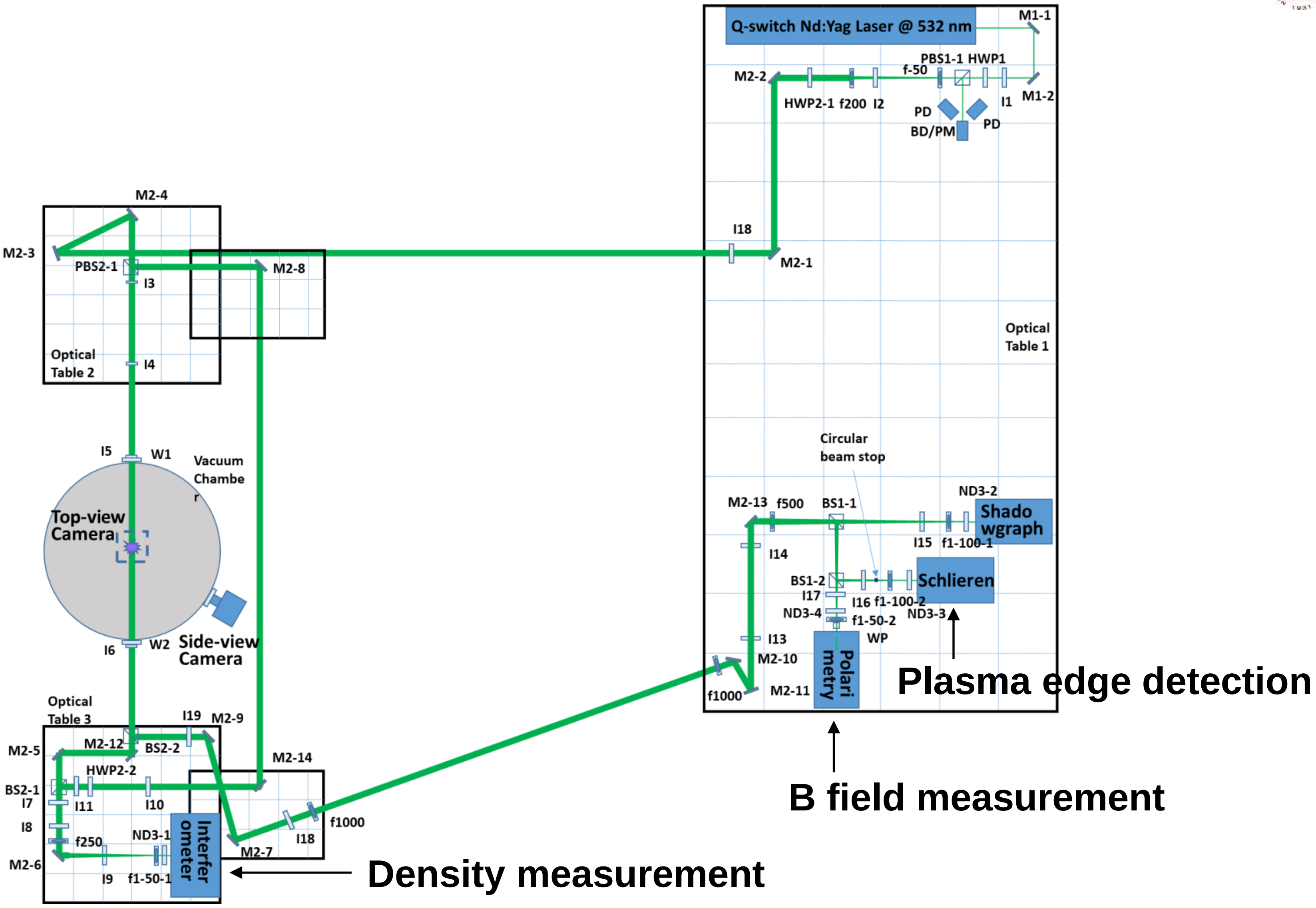

Plasma edge detection

B field measurement

Density measurement

Varies diagnostics were integrated to the system

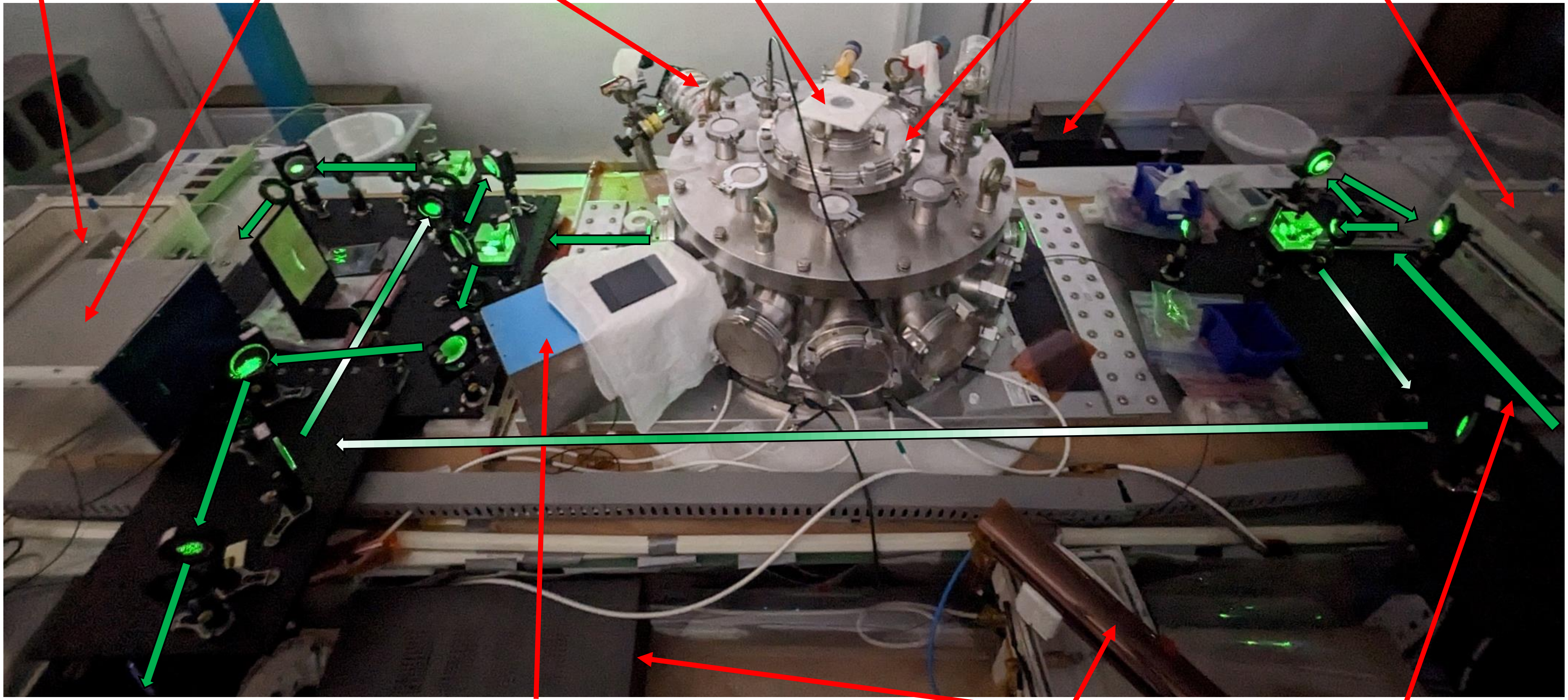

Rail-gap switch

Interferometer

Turbo Pump

Visible-light camera system (Top view)

Vacuum chamber

UPS

Rail-gap switch

To Schlieren /Shadowgraph/ Polarimetry

Visible-light camera system (Side view)

Trigger-Pulse System

532 nm Q-switch Laser In

A plasma jet can be generated by a conical-wire array due to the nonuniform z-pinch effect

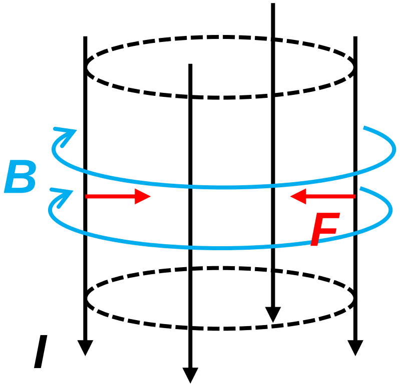

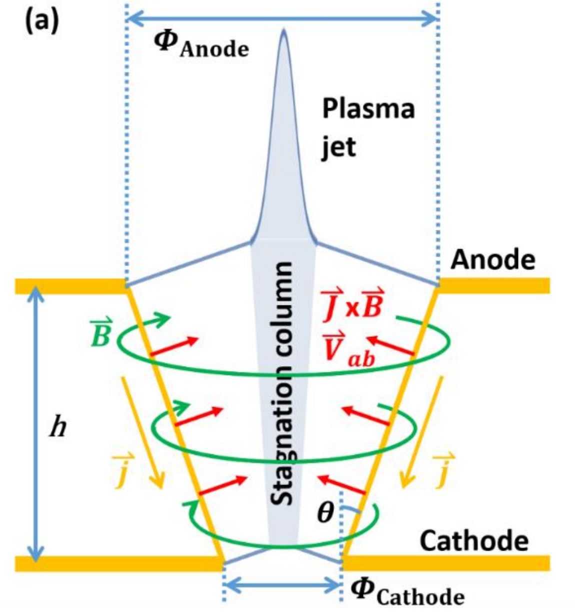

$$V_{\mathrm{j}} = V_{\mathrm{ab}} \frac{1+\cos\theta}{\sin\theta}$$

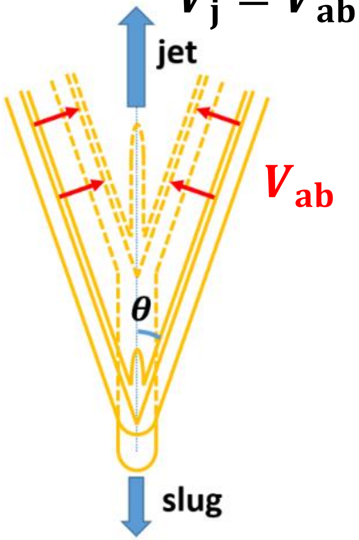

1. Wire ablation : corona plasma is generated by wire ablations.
2. Precursor : corona plasma is pushed by the $\vec{J} \times \vec{B}$ force and accumulated on the axis forming a precursor.
3. Plasma jet is formed by the nonuniform z-pinch effect due to the radius difference between the top and the bottom of the array.

D. J. Ampleforda, et al., Phys. Plasmas 14, 102704 (2007)
G. Birkhoff, et al., J. Applied Physics 19, 563 (1948)

Our conical-wire array consists of 4 tungsten wires with an inclination angle of 30° with respect to the axis

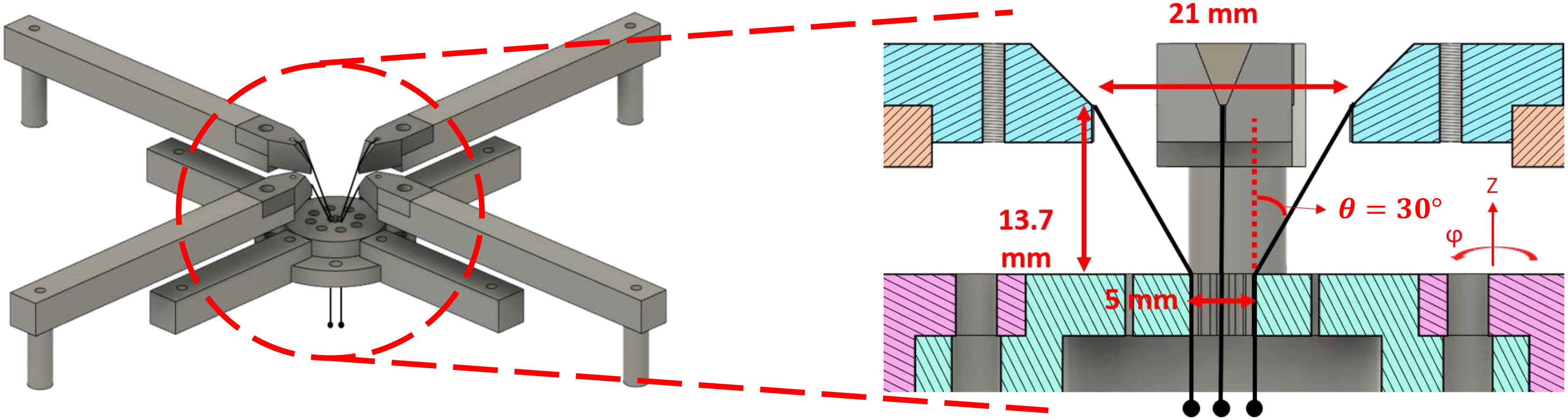

- **Conical-wire array**

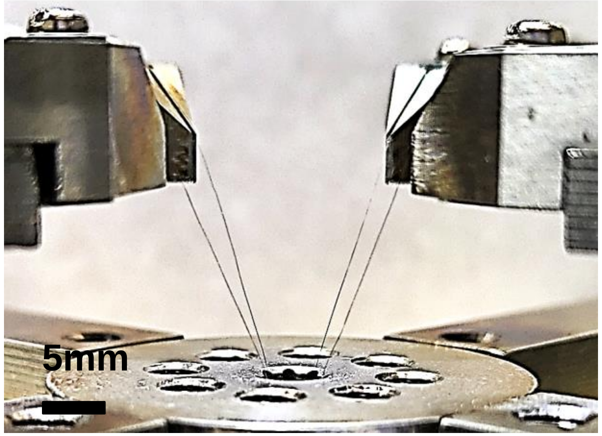

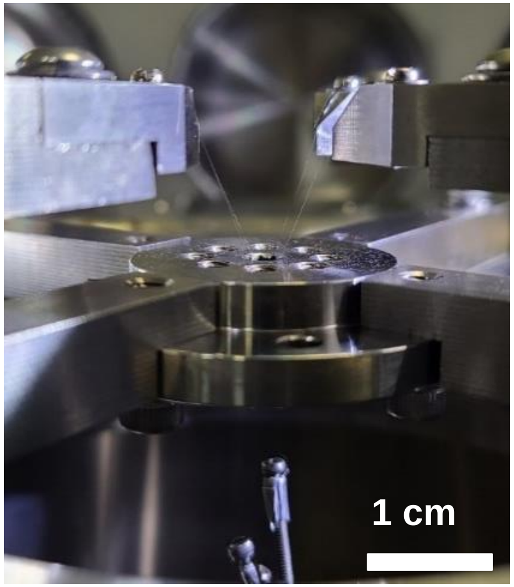

- **Material : Tungsten.**
- **Number of wires : 4.**
- **Diameter : 20 μm.**

Y.-C. Lin, NCKU Master Thesis 2021

Self-emission of the plasma jet in the UV to soft x-ray regions was captured by the pinhole camera

- Image in UV/soft x ray

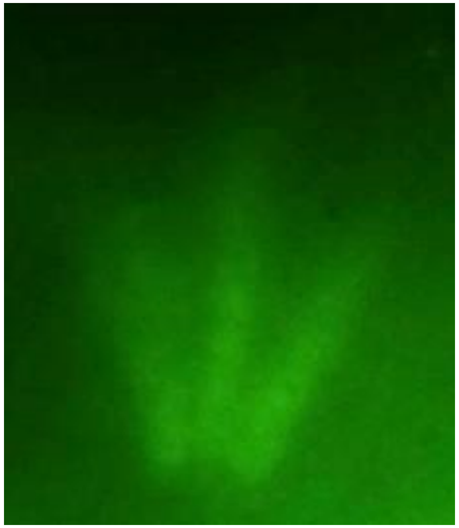

(Brightness is increased by 40 %.)

- Pinhole diameter: 0.5 mm, i.e., spatial resolution: 1 mm.

- Image in visible light

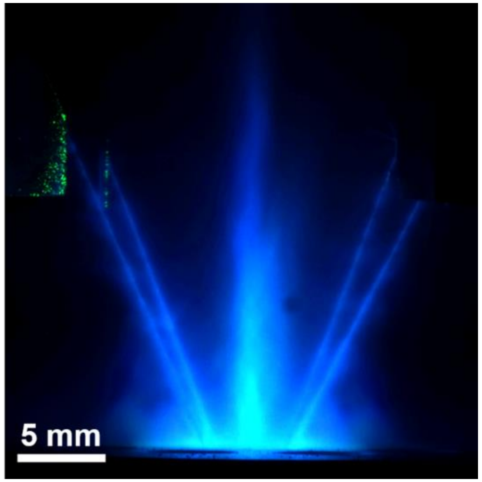

(Enhanced by scaling the intensity range linearly from 0 − 64 to 0 − 255.)

Y.-C. Lin, NCKU Master Thesis 2021

Plasma jet propagation was observed using laser diagnostics

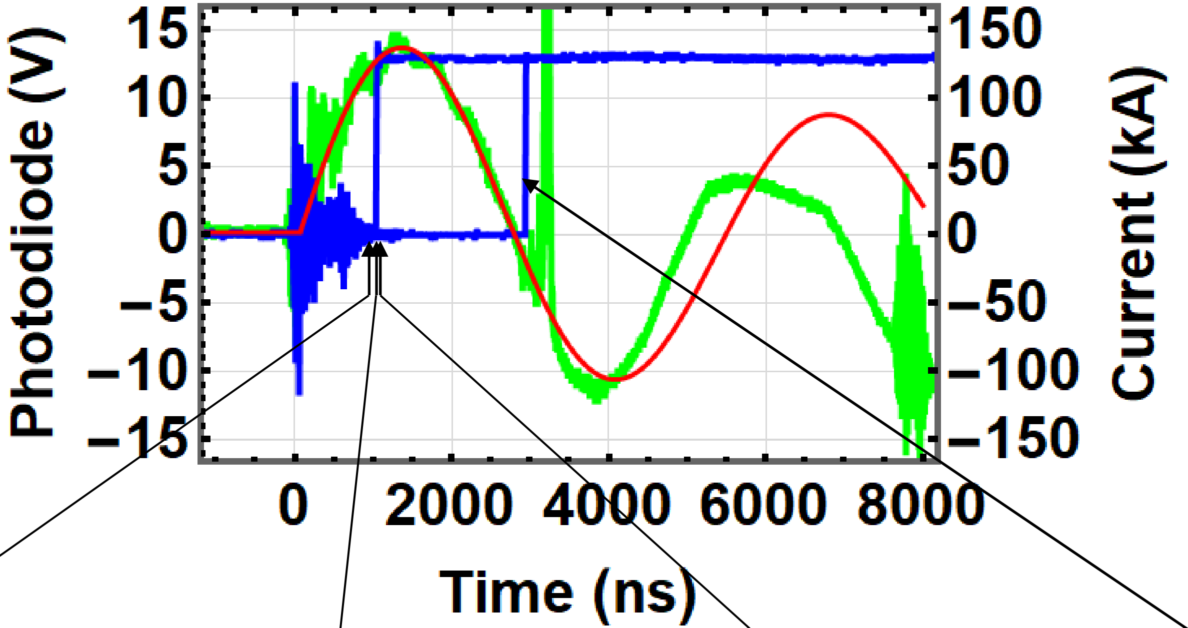

- **Shadowgraph images:**

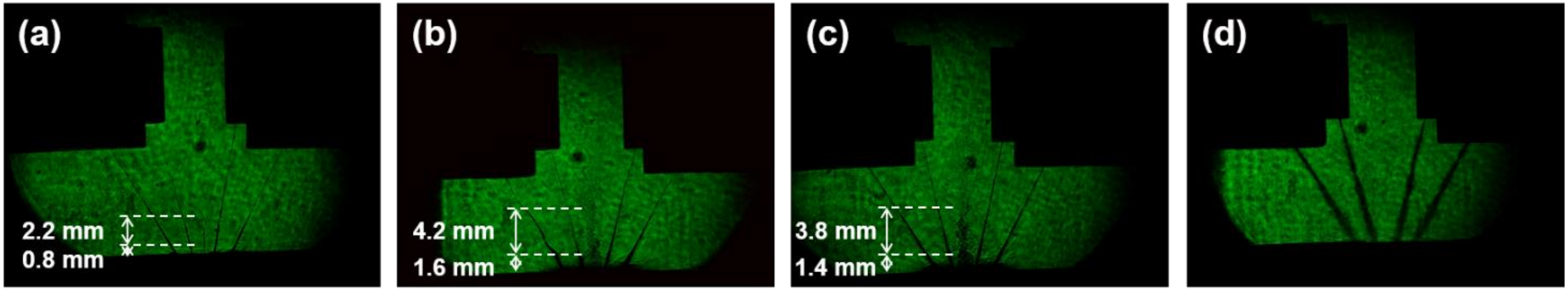

930 ± 20 ns | 975 ± 2 ns | 985 ± 3 ns | 2945 ± 2 ns

Length of the plasma jet at different time was obtained by the Schlieren images at different times

- **Shadowgraph images:**

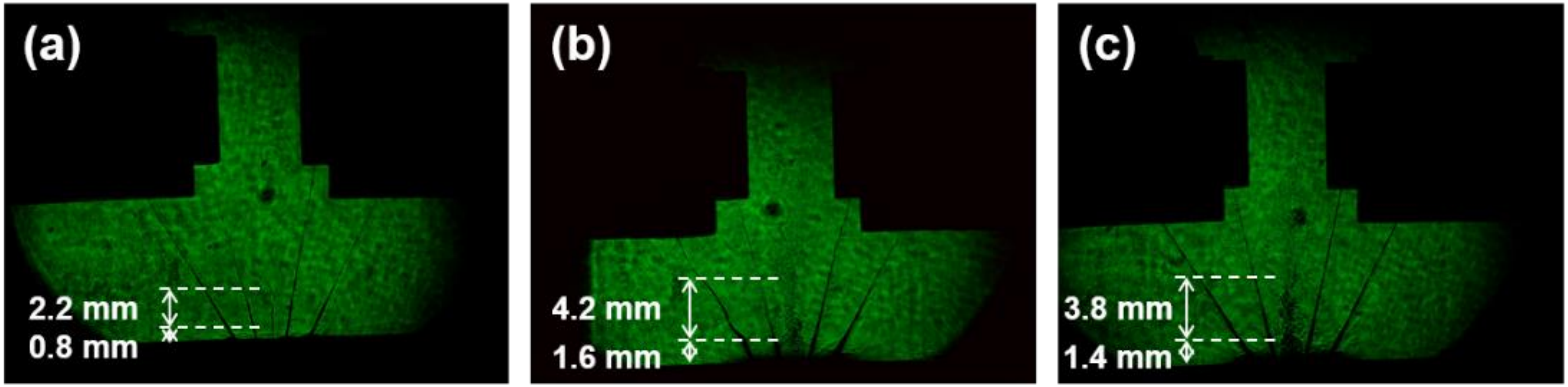

- **Schlieren images:**

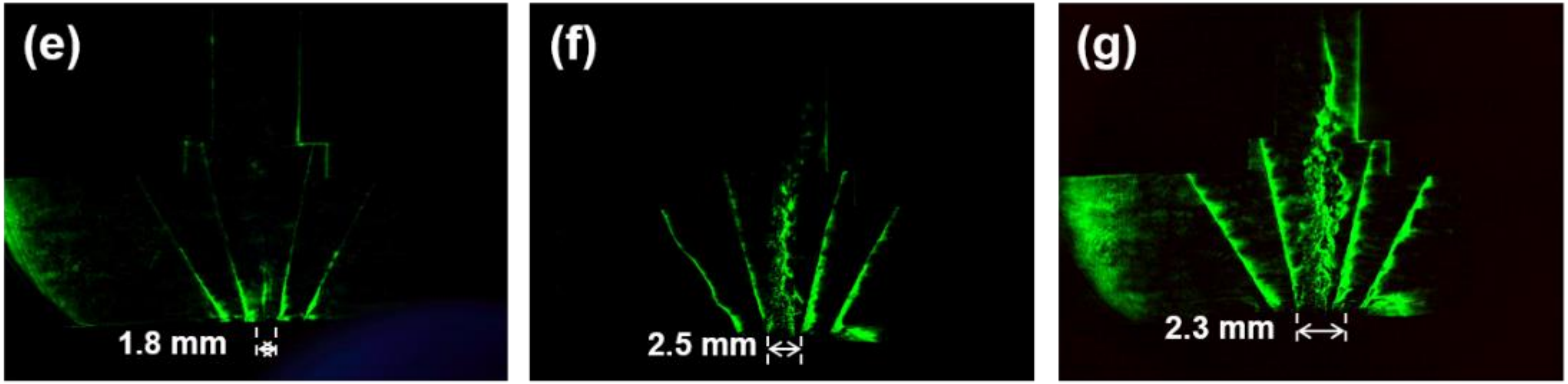

930 ± 20 ns **975 ± 2 ns** **985 ± 3 ns**

The measured plasma jet speed is 170 ± 70 km/s with the corresponding Mach number greater than 5

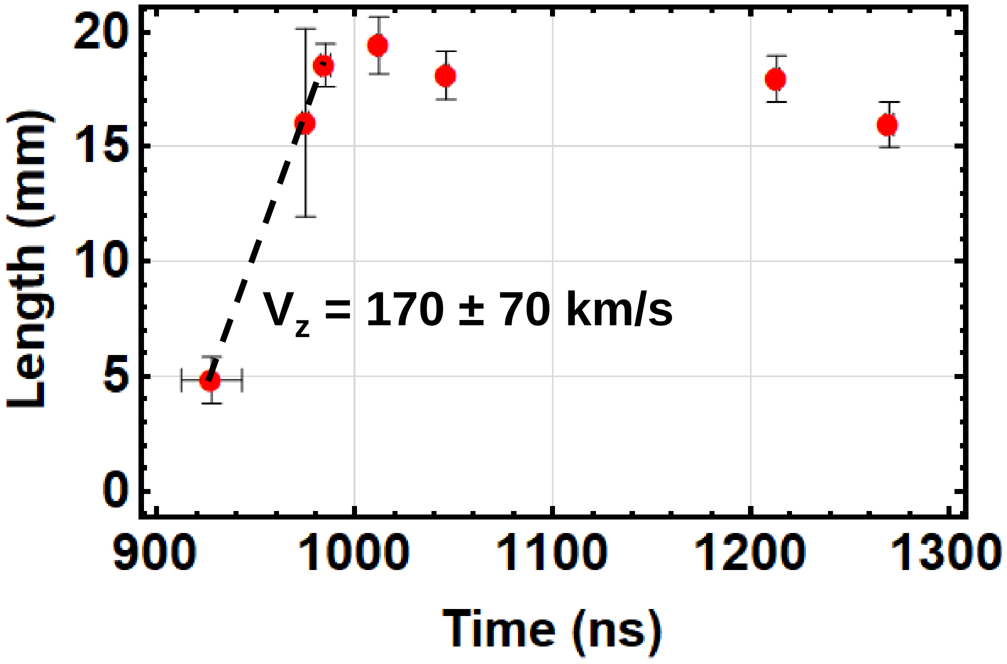

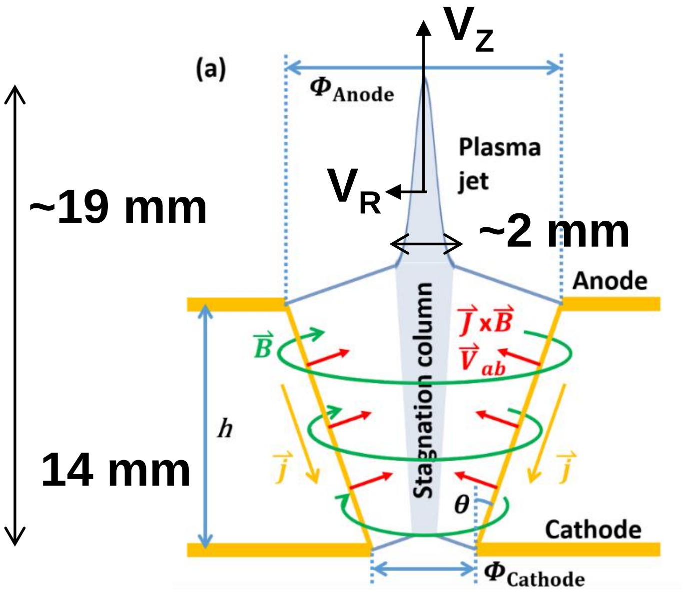

$$M = \frac{V_Z}{V_R} \geq \frac{Z}{r} \approx \frac{(19-14)\ \text{mm}}{\frac{2\ \text{mm}}{2}} = 5$$

$$V_{\text{ab}} = V_{\text{j}} \frac{\sin\theta}{1+\cos\theta} = 50\ \pm 20\ \text{km/s}$$

Plasma disk can be formed when two head-on plasma jets collide with each other

- **Astronomers Find a ‘Break’ in One of the Milky Way’s Spiral Arms.**

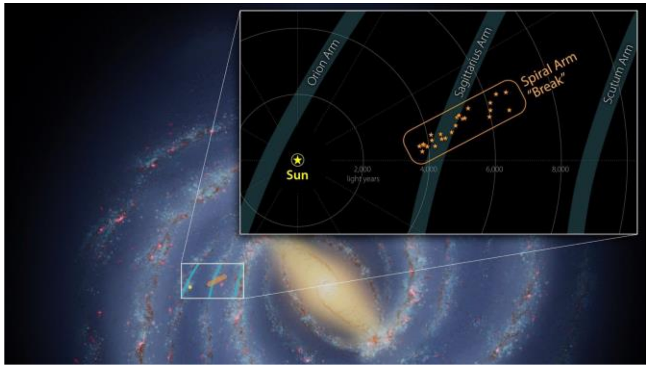

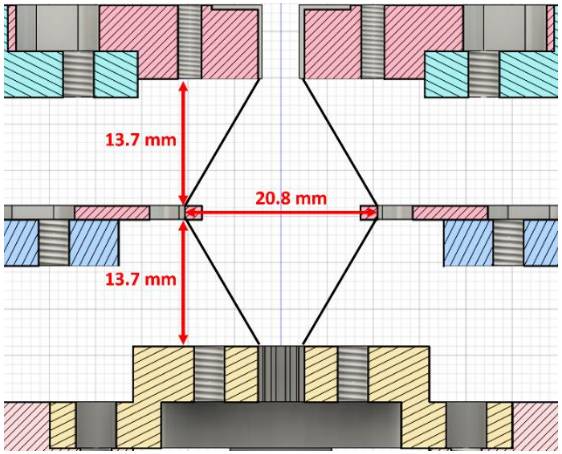

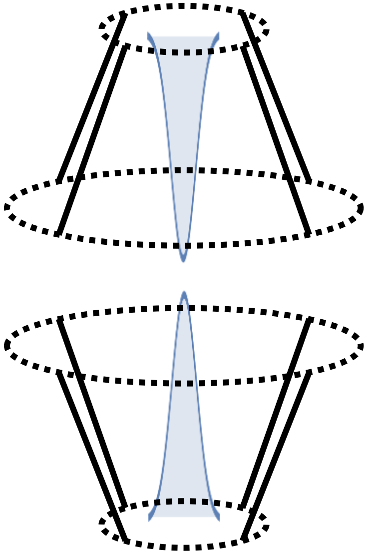

Jet Propulsion Laboratory [NASA/JPL] Astronomers Find a ‘Break’ in One of the Milky Way’s Spiral Arms (Aug 17, 2021)

Plasma disk can be formed when two head-on plasma jets collide with each other

Schlieren

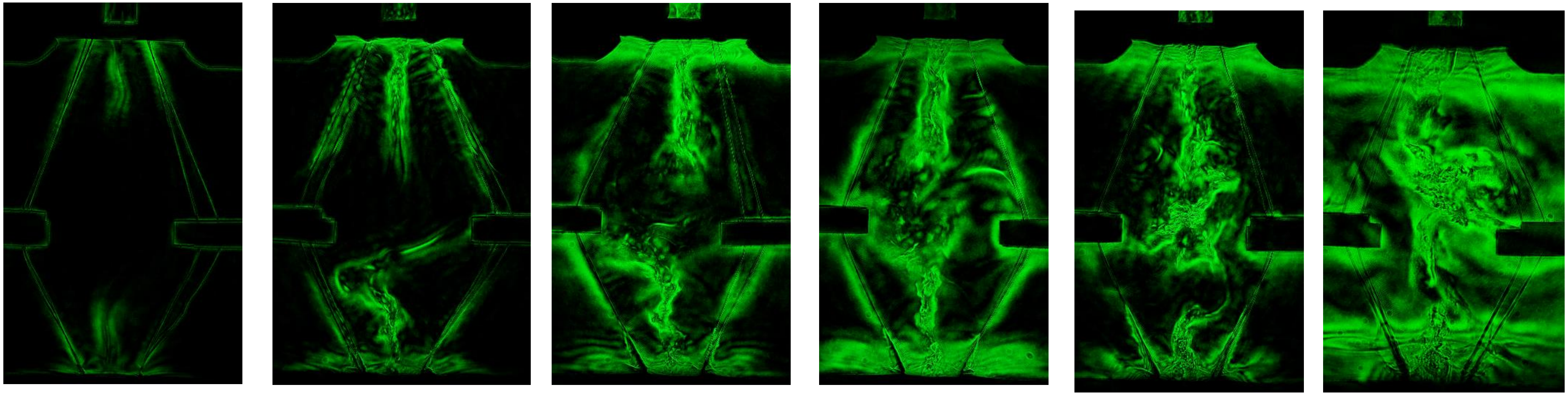

Interferometer

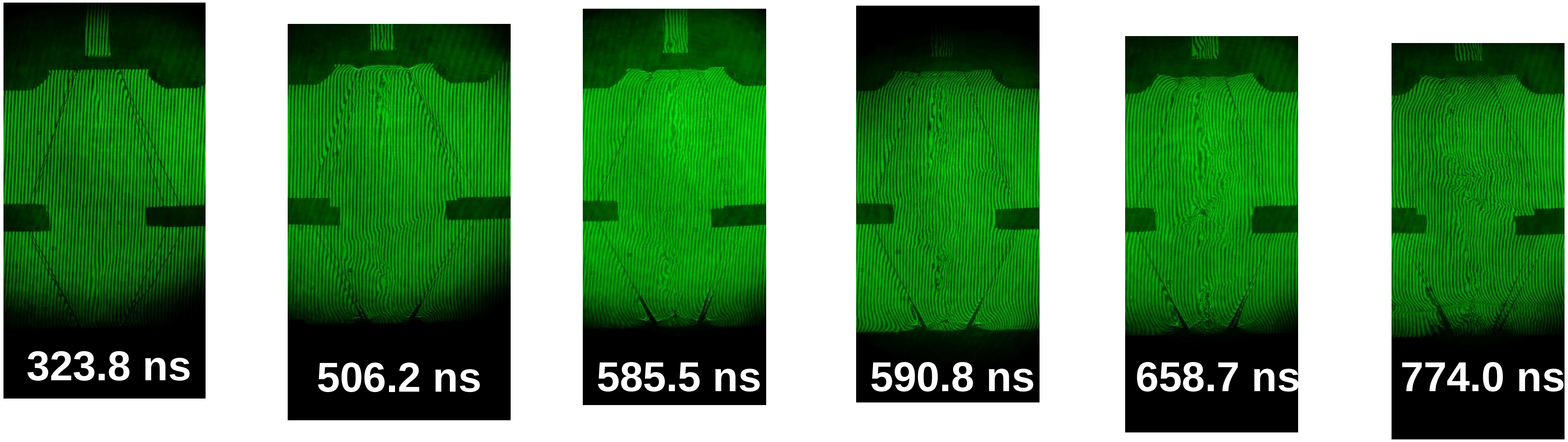

Plasma disk can be formed when two head-on plasma jets collide with each other

Schlieren

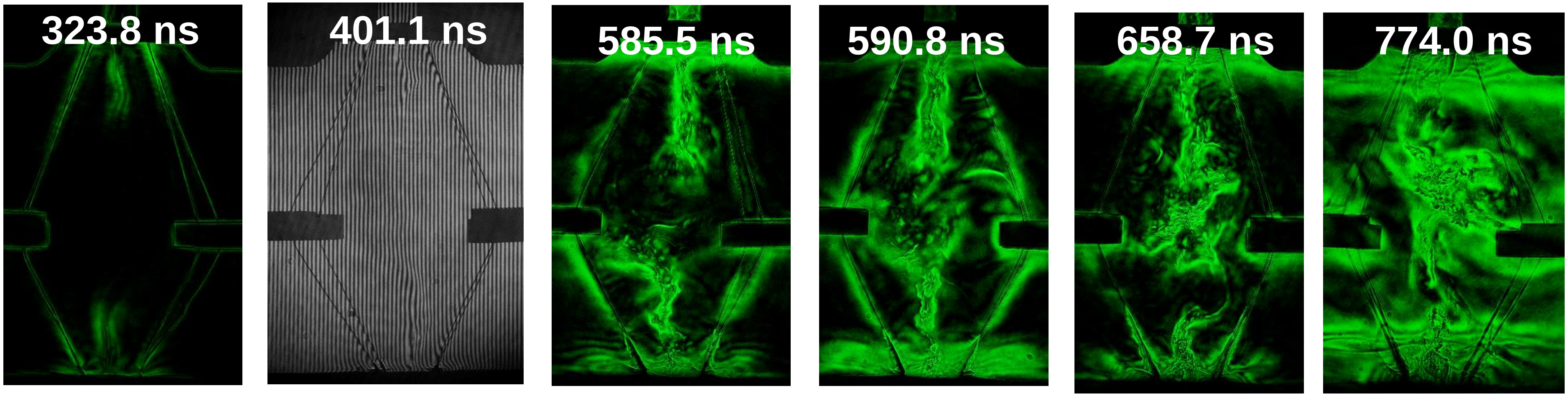

Interferometer

$-2\pi \sim 2\pi \Rightarrow 0 \sim 4.2 \times 10^{17}\ \mathrm{cm}^{-2} \Rightarrow 8.4 \times 10^{17}\ \mathrm{cm}^{-3}$ for l= 5mm

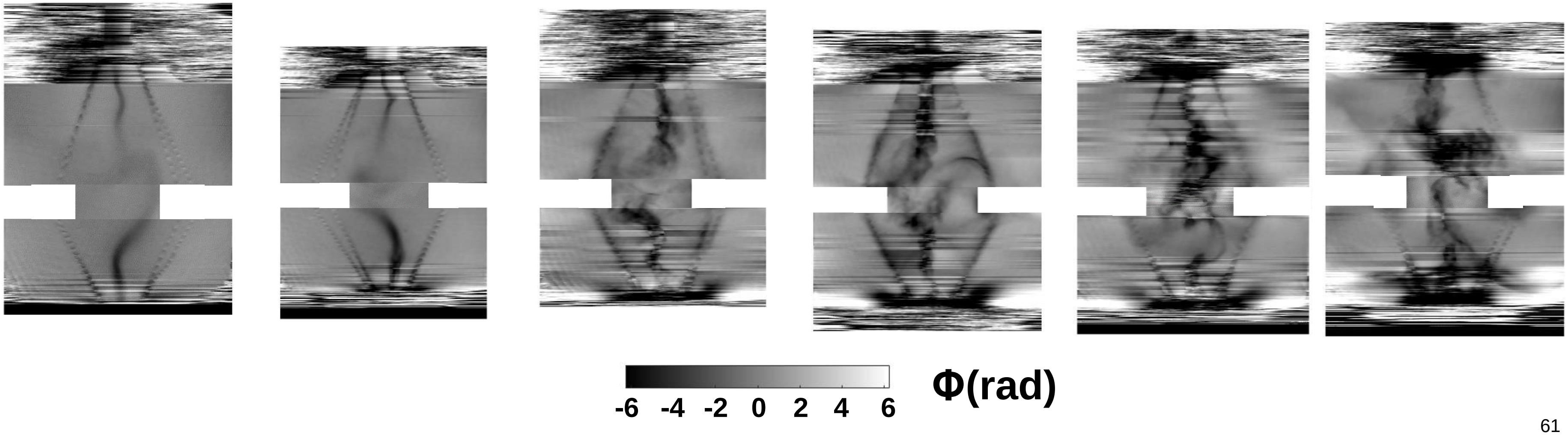

Energetic charged particles losses most of its energy right before it stops

Momentum transfer:

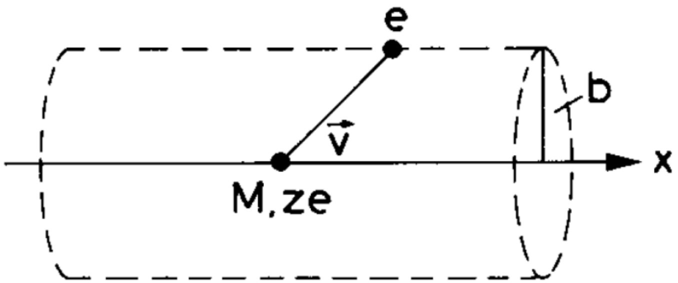

$$\Delta p_\perp = \int F_\perp dt = \int F_\perp \frac{dt}{dx} dx = \int F_\perp \frac{dx}{v}$$

$$= \int_{-\infty}^{\infty} \frac{ze^2}{(x^2+b^2)} \cdot \frac{b}{\sqrt{x^2+b^2}} \cdot \frac{1}{v}\, dx = \frac{ze^2 b}{v} \left[\frac{x}{b^2\sqrt{x^2+b^2}} \right]_{-\infty}^{\infty} = \frac{2ze^2}{bv}$$

$\Delta p_{||}$: averages to zero

$$\Delta E(b) = \frac{\Delta p^2}{2m_e} \qquad N_e = n \cdot (2\pi b) \cdot db\, dx$$

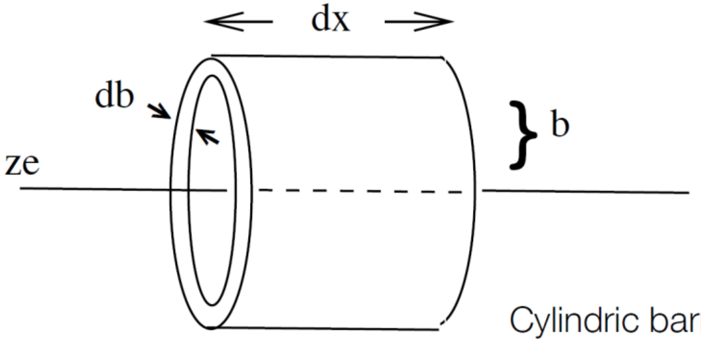

Cylindric barrel
with N_e electrons

$$-dE(b) = \frac{\Delta p^2}{2m_e} \cdot 2\pi n b\, db\, dx$$

$$-\frac{dE}{dx} = \frac{4\pi\, n\, z^2 e^4}{m_e v^2} \cdot \int_{b_{\min}}^{b_{\max}} \frac{db}{b} = \frac{4\pi\, n\, z^2 e^4}{m_e v^2} \ln \frac{b_{\max}}{b_{\min}}$$

http://www.kip.uni-heidelberg.de/~coulon/Lectures/DetectorsSoSe10/

Proton therapy takes the advantage of using Bragg peak

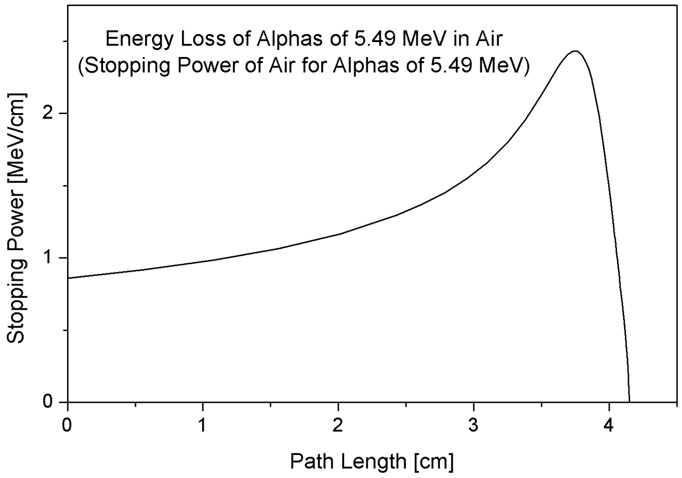

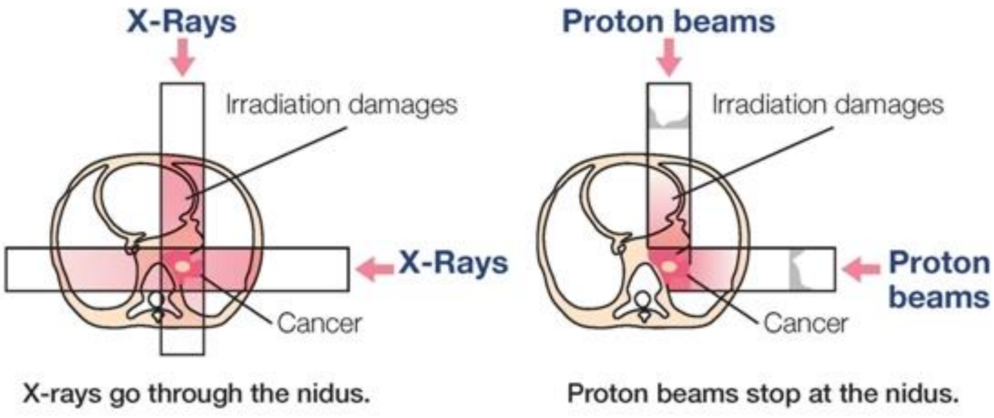

---

http://www.shi.co.jp/quantum/eng/product/proton/proton.html

There are two suggested website for getting the information of proton stopping power in different materials

http://www.nist.gov/pml/data/star/

http://www.srim.org/

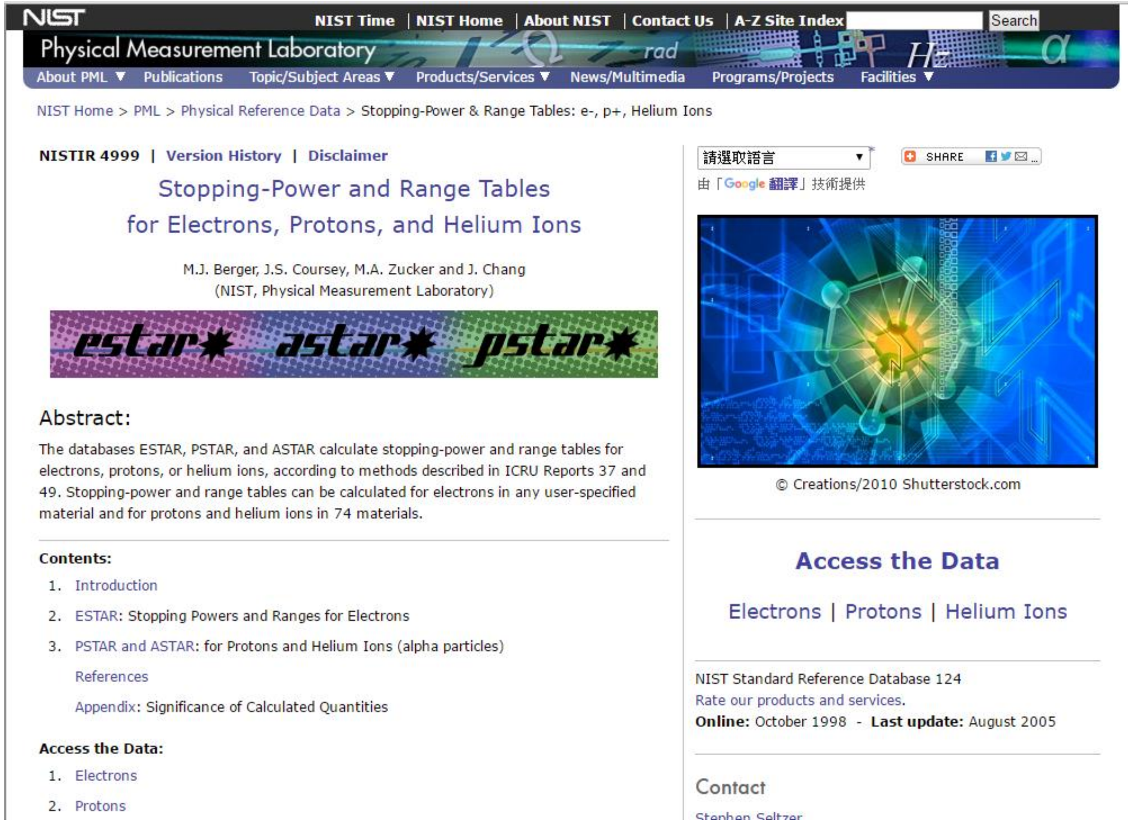

NIST Home > PML > Physical Reference Data > Stopping-Power & Range Tables: e-, p+, Helium Ions

NISTIR 4999 | Version History | Disclaimer

Stopping-Power and Range Tables
for Electrons, Protons, and Helium Ions

M.J. Berger, J.S. Coursey, M.A. Zucker and J. Chang
(NIST, Physical Measurement Laboratory)

Abstract:

The databases ESTAR, PSTAR, and ASTAR calculate stopping-power and range tables for electrons, protons, or helium ions, according to methods described in ICRU Reports 37 and 49. Stopping-power and range tables can be calculated for electrons in any user-specified material and for protons and helium ions in 74 materials.

Contents:

1. Introduction
2. ESTAR: Stopping Powers and Ranges for Electrons
3. PSTAR and ASTAR: for Protons and Helium Ions (alpha particles)

   References

   Appendix: Significance of Calculated Quantities

Access the Data:

1. Electrons
2. Protons

© Creations/2010 Shutterstock.com

Access the Data

Electrons | Protons | Helium Ions

NIST Standard Reference Database 124
Rate our products and services.
Online: October 1998 - **Last update:** August 2005

Contact

Stephen Seltzer

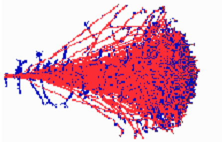

SRIM Textbook

Software	Science
SRIM / TRIM Introduction	Historical Review
Download SRIM-2013	Details of SRIM-2013
SRIM Install Problems	Experimental Data Plots Stopping of Ions in Matter
SRIM Tutorials	Stopping in Compounds
Download TRIM Manual Part-1, Part-2	Scientific Citations of Experimental Data
Stopping, Range and Damage	High Energy Stopping

The thickness of a filter can be decided from the range data from NIST website

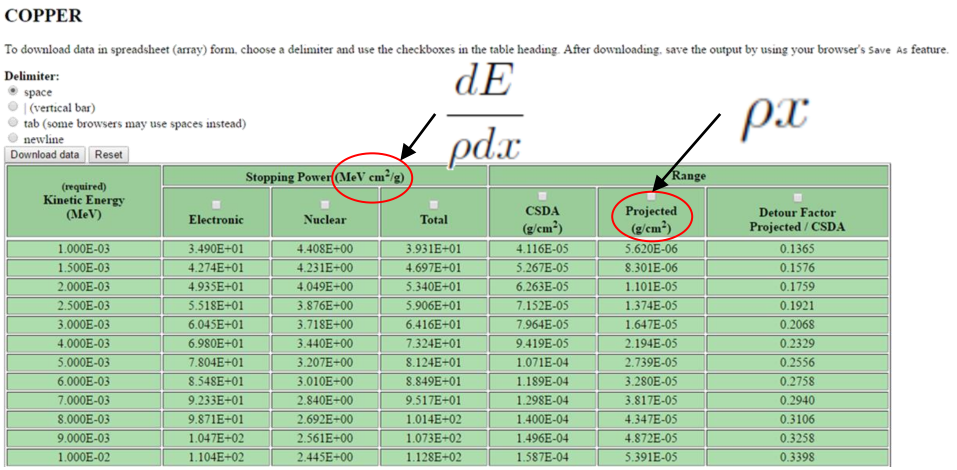

COPPER

To download data in spreadsheet (array) form, choose a delimiter and use the checkboxes in the table heading. After downloading, save the output by using your browser's `Save As` feature.

Delimiter:

● space

○ | (vertical bar)

○ tab (some browsers may use spaces instead)

○ newline

$$\frac{dE}{\rho dx}$$

$$\rho x$$

(required) Kinetic Energy (MeV)	Stopping Power (MeV cm^2/g)			Range		
	☐ Electronic	☐ Nuclear	☐ Total	☐ CSDA (g/cm^2)	☐ Projected (g/cm^2)	☐ Detour Factor Projected / CSDA
1.000E-03	3.490E+01	4.408E+00	3.931E+01	4.116E-05	5.620E-06	0.1365
1.500E-03	4.274E+01	4.231E+00	4.697E+01	5.267E-05	8.301E-06	0.1576
2.000E-03	4.935E+01	4.049E+00	5.340E+01	6.263E-05	1.101E-05	0.1759
2.500E-03	5.518E+01	3.876E+00	5.906E+01	7.152E-05	1.374E-05	0.1921
3.000E-03	6.045E+01	3.718E+00	6.416E+01	7.964E-05	1.647E-05	0.2068
4.000E-03	6.980E+01	3.440E+00	7.324E+01	9.419E-05	2.194E-05	0.2329
5.000E-03	7.804E+01	3.207E+00	8.124E+01	1.071E-04	2.739E-05	0.2556
6.000E-03	8.548E+01	3.010E+00	8.849E+01	1.189E-04	3.280E-05	0.2758
7.000E-03	9.233E+01	2.840E+00	9.517E+01	1.298E-04	3.817E-05	0.2940
8.000E-03	9.871E+01	2.692E+00	1.014E+02	1.400E-04	4.347E-05	0.3106
9.000E-03	1.047E+02	2.561E+00	1.073E+02	1.496E-04	4.872E-05	0.3258
1.000E-02	1.104E+02	2.445E+00	1.128E+02	1.587E-04	5.391E-05	0.3398

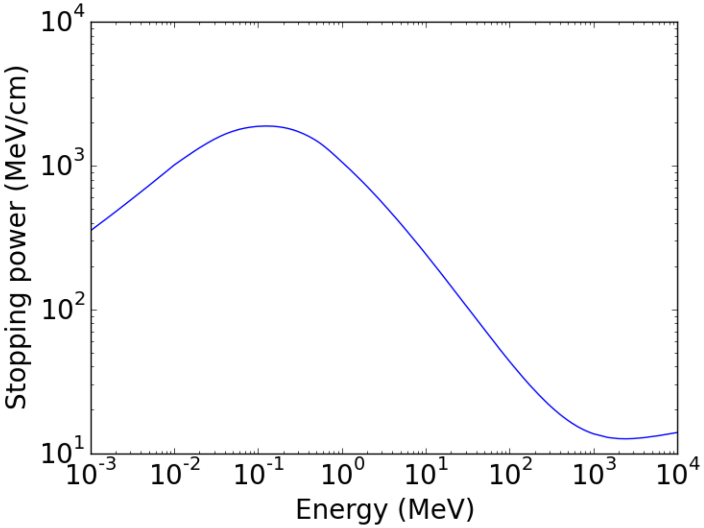

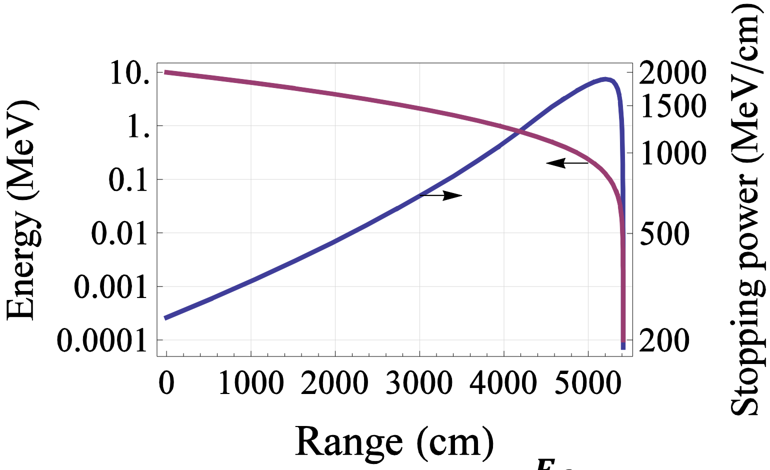

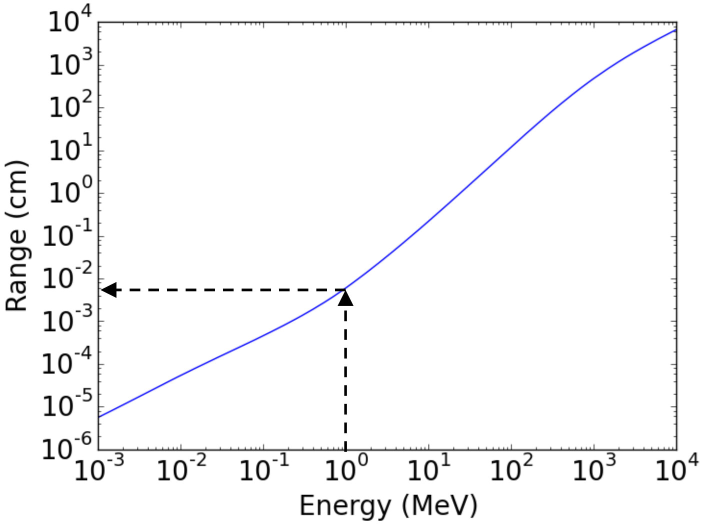

$$\frac{dE}{dx} = f(E) \Rightarrow x = \int_{E_i}^{E_f} \frac{dE}{f(E)}$$

Proton therapy takes the advantage of using Bragg peak

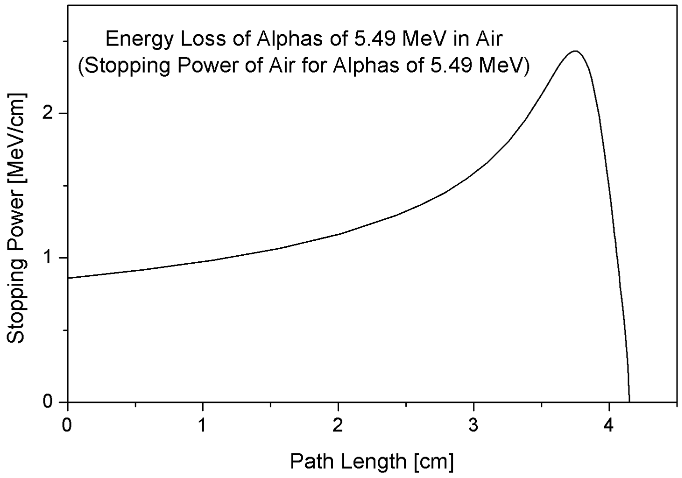

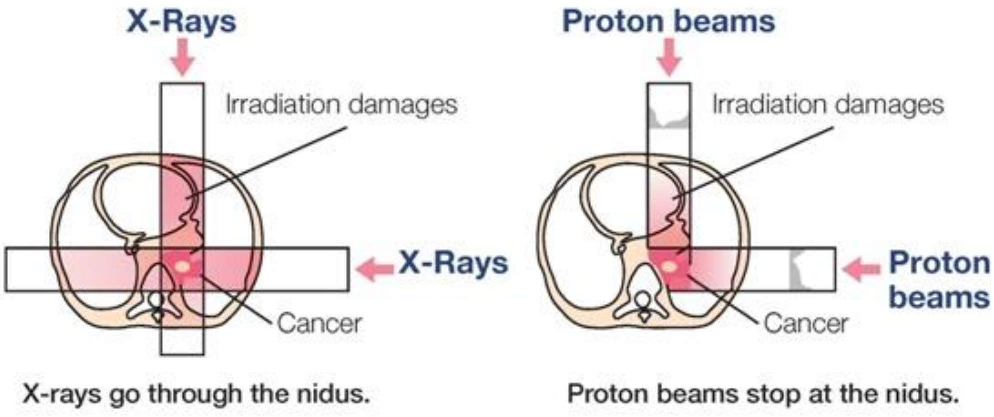

http://www.shi.co.jp/quantum/eng/product/proton/proton.html

Saha equation gives the relative proportions of atoms of a certain species that are in two different states of ionization in thermal equilibrium

$$\frac{n_{r+1}n_e}{n_r} = \frac{G_{r+1}g_e}{G_r}\frac{(2\pi m_e KT)^{3/2}}{h^3}\exp\left(-\frac{\chi_r}{KT}\right)$$

- n_{r+1}, n_r: Density of atoms in ionization state r+1, r (m^{-3})
- n_e: Density of electrons (m^{-3})
- G_{r+1}, G_r: Partition function of ionization state r+1, r
- $g_e=2$: Statistical weight of the electron
- m_e: Mass of the electron
- χ_r: Ionization potential of ground level of state r to reach to the ground level of state r+1
- T: Temperature
- h: Planck's constant
- K: Boltzmann constant

Supplement to Ch. 6 of Astrophysics Processes by Hale Bradt
(http://homepages.spa.umn.edu/~kd/Ast4001-2015/NOTES/n052-saha-bradt.pdf)

Some backgrounds of quantum mechanics

- **Planck blackbody function:**

$$u(\nu, T) = \frac{8\pi h\nu^3}{c^3} \frac{1}{e^{\mathrm{h\nu/KT}} - 1} \left(W/m^3\,\mathrm{Hz}\right)$$

- **Boltzmann formula:**
  - **g_i, g_j: statistical weight**

$$\frac{n_i}{n_j} = \frac{g_i e^{-\epsilon_i/\mathrm{KT}}}{g_j e^{-\epsilon_j/\mathrm{KT}}} = \frac{g_i}{g_j} e^{-h\nu_{\mathrm{ij}}/\mathrm{KT}} \qquad \frac{g_i}{g_j} = \frac{2J_i + 1}{2J_j + 1}$$

(J: angular momenta quantum number)

  - **Number in the i^{th} state to the total atom:**

$$\frac{n_i}{n} = \frac{n_i}{\Sigma n_j} \equiv \frac{g_i e^{-\epsilon_i/\mathrm{KT}}}{G} \qquad G \equiv \Sigma g_j e^{-\epsilon_j/\mathrm{KT}}$$

G: partition function of statistical weight for the atom, taking into account all its excited states.

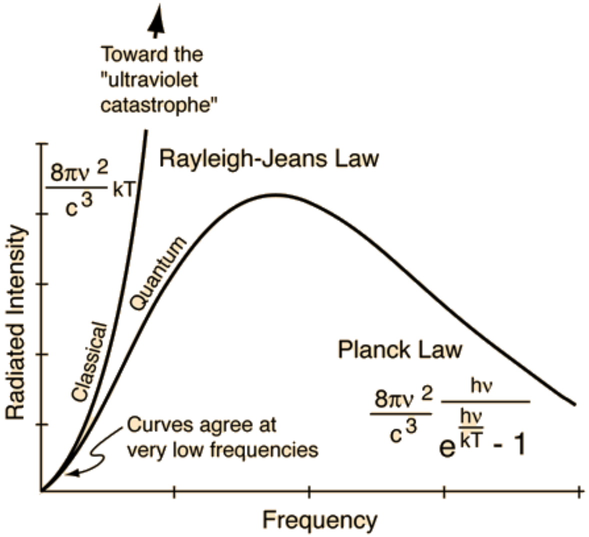

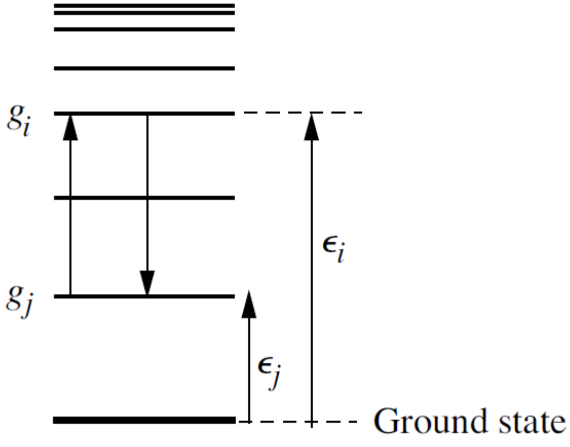

http://hyperphysics.phy-astr.gsu.edu/hbase/mod6.html

Einstein coefficient

- **Probability of electron energy transition:**
  - **Excitation (↑):** $P_{\mathrm{ji}} = B_{\mathrm{ji}} u(\nu, T)$
  - **De-excitation (↓):** $P_{\mathrm{ij}} = A_{\mathrm{ij}} + B_{\mathrm{ij}} u(\nu, T)$
- **In thermal equilibrium:**

$$n_i\left(A_{\mathrm{ij}} + B_{\mathrm{ij}} u\right) = n_j B_{\mathrm{ji}} u$$

$$\frac{g_i}{g_j} e^{-x}\left(A_{\mathrm{ij}} + B_{\mathrm{ij}} u\right) = B_{\mathrm{ji}} u \qquad x \equiv \frac{\mathrm{h}\nu}{\mathrm{KT}}$$

$$u = a\left(e^x - 1\right)^{-1} \qquad a \equiv \frac{8\pi \mathrm{h}\nu^3}{c^3}$$

$$a\left(e^x B_{\mathrm{ji}} - \frac{g_i}{g_j} B_{\mathrm{ij}}\right) = \left(e^x - 1\right)\frac{g_i}{g_j} A_{\mathrm{ij}}$$

- **The Einstein coefficients are independent of T or ν.**

$$x \to 0, e^x \to 1 \qquad x \to \infty, e^x \to \infty$$

$$\frac{B_{\mathrm{ij}}}{B_{\mathrm{ji}}} = \frac{g_j}{g_i} \qquad a B_{\mathrm{ji}} = \frac{g_i}{g_j} A_{\mathrm{ij}} \qquad \frac{A_{\mathrm{ij}}}{B_{\mathrm{ij}}} = \frac{8\pi h \nu^3}{c^3}$$

- **Photoexcitation:**

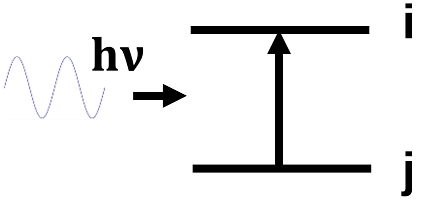

- **Induced radiation:**

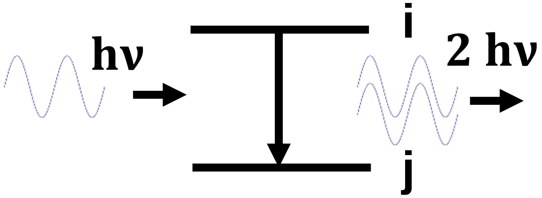

- **Spontaneous radiation:**

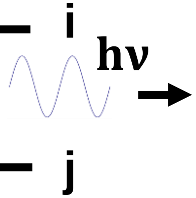

Saha equation is derived using the transition between different ionization states

- **Required photon energy for transition 1 from the ground state of r ionization state to the ground state of r+1 ionization state:**

$$\mathbf{h\nu} = \chi_r + \frac{p^2}{2m}$$

Energy of the free electron

- **Required photon energy for transition 2 from the energy level k of r ionization state to the energy level j of r+1 ionization state:**

$$\mathbf{h\nu} = \chi_r + \epsilon_{r+1,j} - \epsilon_{r,k} + \frac{p^2}{2m}$$

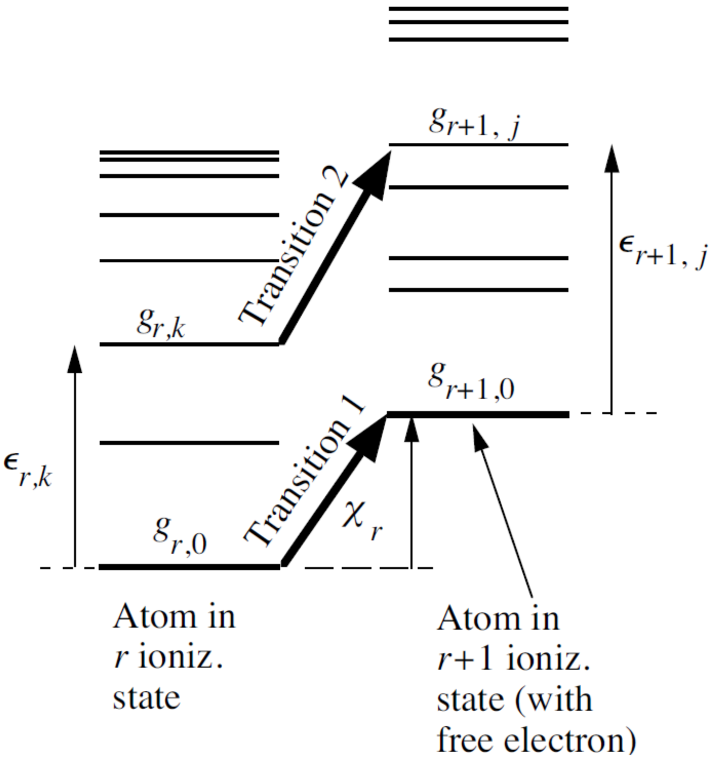

Saha equation is derived using the transition between different ionization states

- **Photoionization:**

$$R_{\mathrm{pi}} = n_{r,k} u(\nu) B_{r,k\rightarrow r+1,j}$$

- **Induced radiation:**

$$R_{\mathrm{ir}} = n_{r+1,j} n_{e,p}(p) u(\nu) B_{r+1,j\rightarrow r,k}$$

- **Spontaneous emission:**

$$R_{\mathrm{sr}} = n_{r+1,j} n_{e,p}(p) A_{r+1,j\rightarrow r,k}$$

- **In thermal equilibrium:**

$$n_{r+1,j} n_{e,p} A_{r+1,j\rightarrow r,k} + n_{r+1,j} n_{e,p} u B_{r+1,j\rightarrow r,k} = n_{r,k} u B_{r,k\rightarrow r+1,j}$$

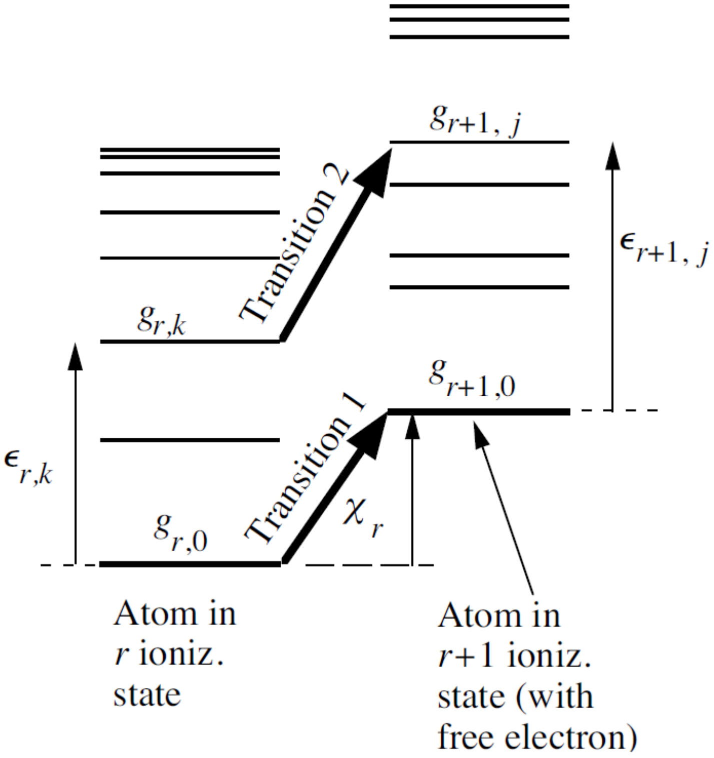

- **Einstein coefficients:**

$$\frac{B_{r,k\rightarrow r+1,j}}{B_{r+1,j\rightarrow r,k}} = \frac{g_{r+1,j}}{g_{r,k}} \frac{g_e 4\pi p^2}{h^3} \qquad \frac{A_{r+1,j\rightarrow r,k}}{B_{r+1,j\rightarrow r,k}} = \frac{8\pi h\nu^3}{c^3}$$

Saha equation - continued

$$n_{r+1,j}n_{e,p}A_{r+1,j\to r,k}+n_{r+1,j}n_{e,p}uB_{r+1,j\to r,k}=n_{r,k}uB_{r,k\to r+1,j}$$

$$n_{r+1,j}n_{e,p}\frac{A_{r+1,j\to r,k}}{B_{r+1,j\to r,k}}+n_{r+1,j}n_{e,p}u=n_{r,k}u\frac{B_{r,k\to r+1,j}}{B_{r+1,j\to r,k}}$$

$$\frac{n_{r+1,j}n_{e,p}}{n_{r,k}}=\left(\frac{A_{r+1,j\to r,k}}{uB_{r+1,j\to r,k}}+1\right)^{-1}\frac{B_{r,k\to r+1,j}}{B_{r+1,j\to r,k}}$$

$$\frac{B_{r,k\to r+1,j}}{B_{r+1,j\to r,k}}=\frac{g_{r+1,j}}{g_{r,k}}\frac{g_e4\pi p^2}{h^3}$$

$$n_{e,p}(p)=\frac{n_e4\pi p^2}{(2\pi\mathrm{mKT})^{3/2}}\exp\left(-\frac{p^2}{2\mathrm{mKT}}\right)$$

$$\frac{A_{r+1,j\to r,k}}{B_{r+1,j\to r,k}}=\frac{8\pi h\nu^3}{c^3}$$

$$\frac{n_{r+1,j}n_e}{n_{r,k}}=\frac{(2\pi\mathrm{mKT})^{3/2}}{4\pi p^2}\exp\left(\frac{p^2}{2\mathrm{mKT}}\right)\left[\frac{c^3}{8\pi h\nu^3}\left(e^{\mathrm{h\nu/KT}}-1\right)\frac{8\pi h\nu^3}{c^3}+1\right]^{-1}\frac{g_{r+1,j}}{g_{r,k}}\frac{g_e4\pi p^2}{h^3}$$

$$\frac{n_{r+1,j}n_e}{n_{r,k}}=\frac{(2\pi\mathrm{mKT})^{3/2}}{h^3}\frac{g_{r+1,j}g_e}{g_{r,k}}\exp\left[\frac{1}{\mathrm{KT}}\left(\frac{p^2}{2m}-\mathrm{h\nu}\right)\right]$$

Saha equation - continued

$$\frac{n_{r+1,j}n_e}{n_{r,k}} = \frac{(2\pi \mathrm{mKT})^{3/2}}{h^3}\frac{g_{r+1,j}g_e}{g_{r,k}}\exp\left[\frac{1}{\mathrm{KT}}\left(\frac{p^2}{2m} - \mathrm{h\nu}\right)\right]$$

$$\frac{n_{r+1,j}n_e}{n_{r,k}} = \frac{(2\pi \mathrm{mKT})^{3/2}}{h^3}\frac{g_{r+1,j}g_e}{g_{r,k}}\exp\left[\frac{1}{\mathrm{KT}}\left(\frac{p^2}{2m} - \chi_r - \epsilon_{r+1,j} + \epsilon_{r,k} - \frac{p^2}{2m}\right)\right]$$

$$\frac{n_{r+1,j}n_e}{n_{r,k}} = \frac{(2\pi \mathrm{mKT})^{3/2}}{h^3}\frac{g_{r+1,j}\exp\left(\frac{\epsilon_{r+1,j}}{\mathrm{KT}}\right)g_e}{g_{r,k}\exp\left(\frac{\epsilon_{r,k}}{\mathrm{KT}}\right)}\exp\left(-\frac{\chi_r}{\mathrm{KT}}\right)$$

$$\frac{n_{r,k}}{n_r} = \frac{g_{r,k}e^{-\epsilon_{r,k}/\mathrm{KT}}}{G_r} \qquad G_r = \Sigma g_{r,k}e^{-\epsilon_{r,k}/\mathrm{KT}}$$

$$\frac{n_{r+1,j}}{n_{r+1}} = \frac{g_{r+1,j}e^{-\epsilon_{r+1,j}/\mathrm{KT}}}{G_{r+1}} \qquad G_{r+1} = \Sigma g_{r+1,j}e^{-\epsilon_{r+1,j}/\mathrm{KT}}$$

$$\boxed{\frac{n_{r+1}n_e}{n_r} = \frac{G_{r+1}g_e}{G_r}\frac{(2\pi m_e KT)^{3/2}}{h^3}\exp\left(-\frac{\chi_r}{KT}\right)}$$

Saha equation – example: hydrogen plasma of the sun

- Photosphere of the sun – hydrogen atoms in an optically thick gas in thermal equilibrium at temperature T=6400 K.
  - Neutral hydrogen (r state / ground state)

$$G_r = \Sigma \mathrm{g}_{r,k} = g_{r,0} + g_{r,1}\exp\left(-\frac{\epsilon_{r,1}}{\mathrm{KT}}\right) + \cdots = 2 + 8\exp\left(-\frac{10.2\mathrm{eV}}{0.56\mathrm{eV}}\right) + \cdots$$

$$= 2 + 9.8 \times 10^{-8} + \cdots \approx 2$$

  - Ionized state (r+1 state)

$$G_{r+1} = \Sigma \mathrm{g}_{r+1,j} = g_{r+1,0} + g_{r+1,1}\exp\left(-\frac{\epsilon_{r+1,1}}{\mathrm{KT}}\right) + \cdots \approx 1$$

  - Other information: $g_e = 2$ $\chi_r = 13.6\mathrm{eV};$ $\mathrm{kT} = 0.56\mathrm{eV}$ $n_{r+1} = n_e$

$$\frac{{n_{r+1}}^2}{n_r} = 2.41 \times 10^{21}\,\frac{1 \times 2}{2}\,(6400)^{3/2}\exp\left(-\frac{13.6}{0.56}\right) = 3.5 \times 10^{16} m^{-3}$$

It is mostly neutral in the photosphere of the sun

- **Assuming 50 % ionization:**

$$n_{r+1} = n_r = 3.5 \times 10^{16} m^{-3} \qquad n = n_{r+1} + n_r = 7 \times 10^{16} m^{-3}$$

- **In the photosphere of the sun:**

$$\rho \sim 3 \times 10^{-4}\, \mathrm{kg}/m^3 \rightarrow n = 2 \times 10^{23} m^{-3} \gg 7 \times 10^{16} m^{-3}$$

- **At higher densities n at the same temperature, there should be more collisions leading to higher recombination rate and thus the plasma is less than 50 % ionization.**

$\Rightarrow$ **Less than 50 % ionization**

- **Use the total number density to estimate the ionization percentage:**

$$n_{r+1} + n_r = 2 \times 10^{23}$$

$$\frac{n_{r+1}}{n_r} = 4 \times 10^{-4} @ 6400K$$

A semiconductor device is fabricated by many repetitive production process

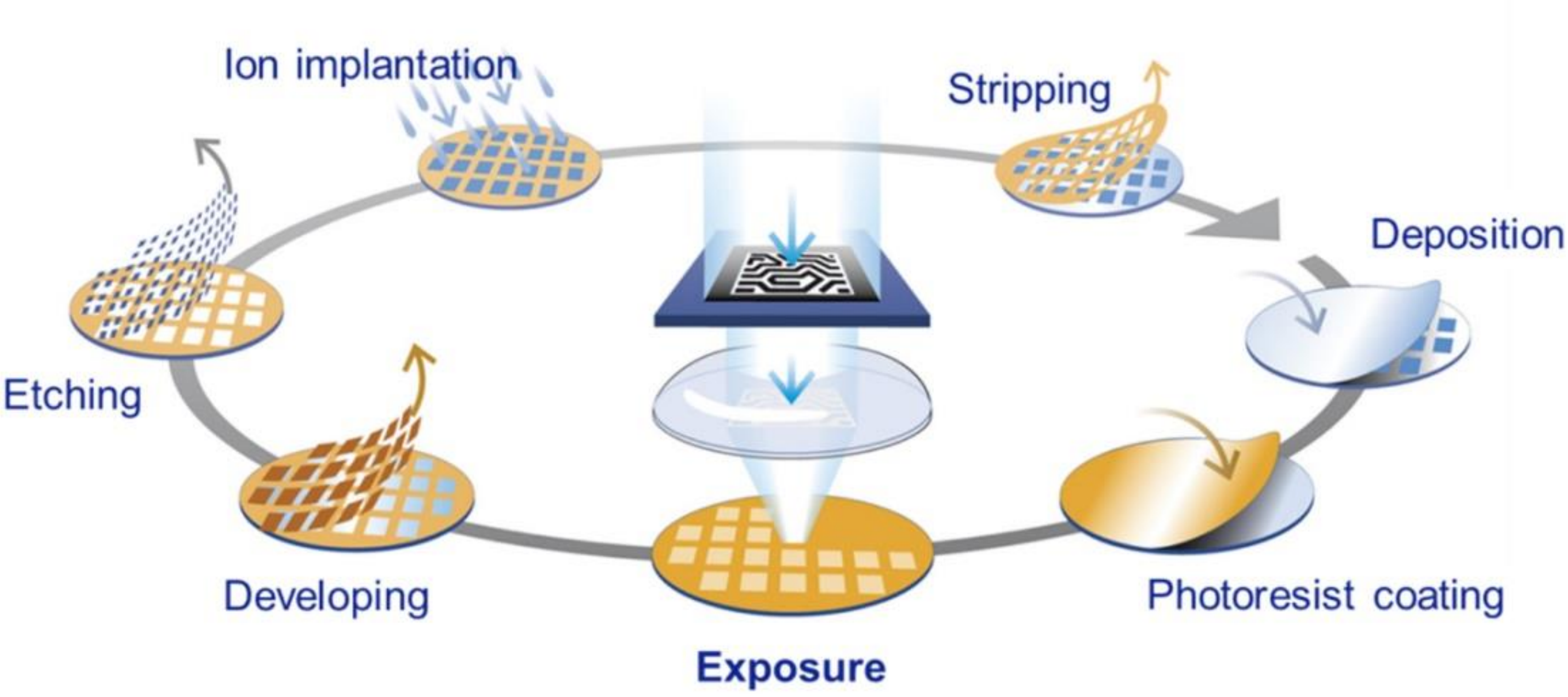

Surf. Topogr.: Metrol. Prop. **4** (2016) 023001

Reference for material processing

- **Principles of plasma discharges and materials processing, 2nd edition, by Michael A. Lieberman and Allan J. Lichtenberg**
- **http://www.eecs.berkeley.edu/~lieber/**
- **Materials science of thin films, 2nd edition, by Milton Ohring**
- **Plasma etching, by Dennis M. Manos and Daniel L. Flamm**
- **Industrial plasma engineering, volume 1, by J. Reece Roth**

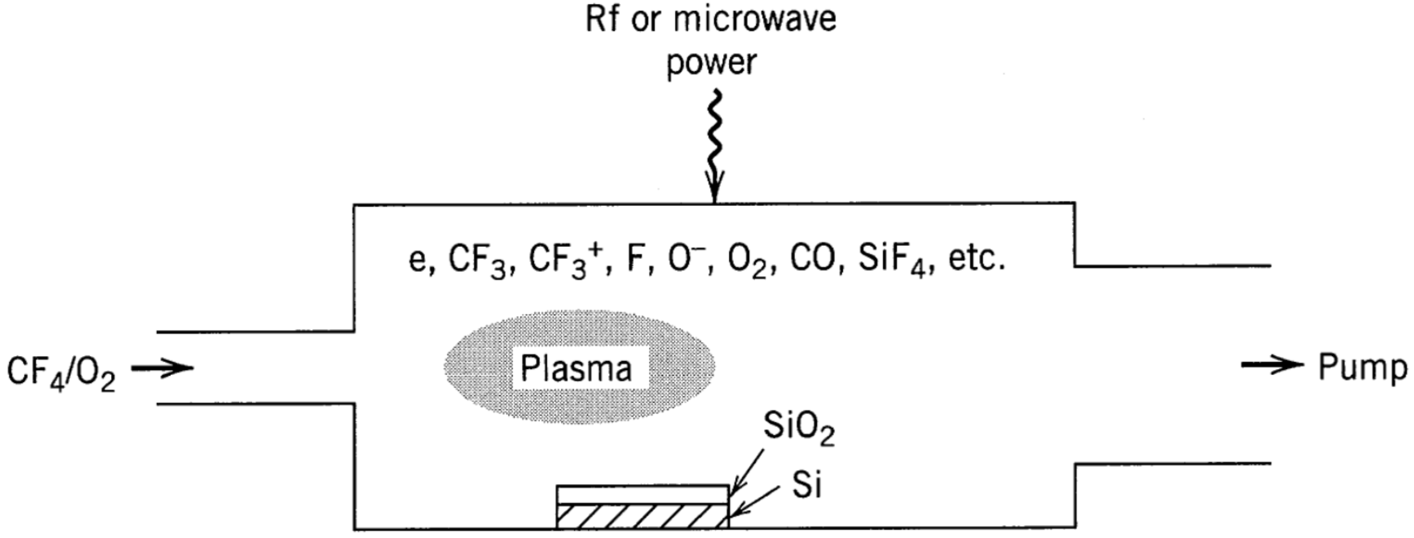

Evolution of etching discharges

1st generation
(1 source, multi-wafer,
low density)

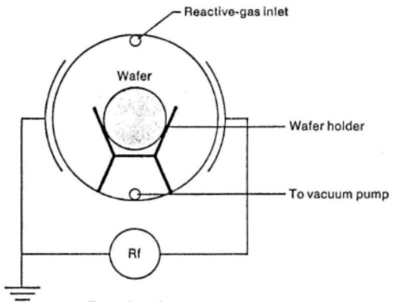

Barrel etcher
(Isotropic etch)

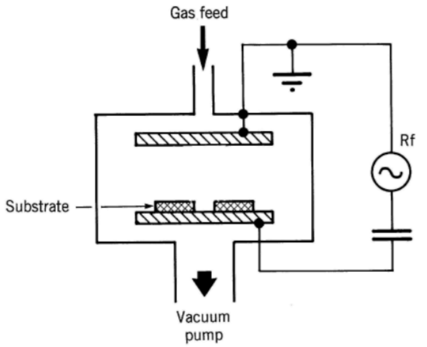

Capacitive
(Anisotropic etch)

2nd generation
(2 sources, single-wafer,
high density)

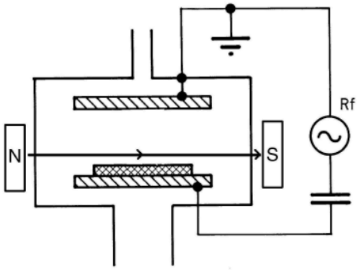

Magnetically enhanced
capacitive discharge

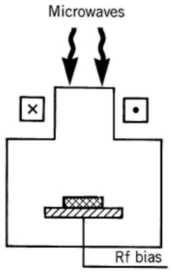

ECR

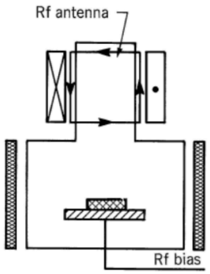

Helicon

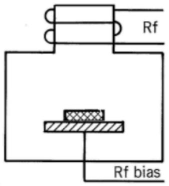

Inductive

3rd generation
(multi-sources, single-
wafer, moderate density)

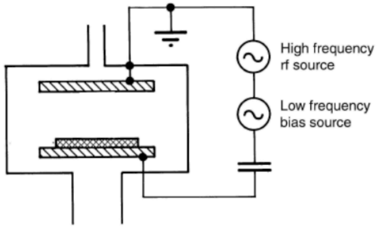

Dual frequency
capacitive discharge

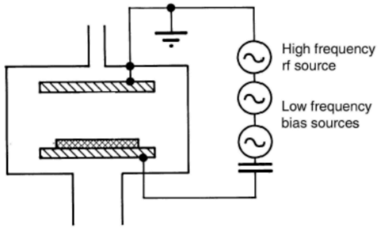

Triple frequency
capacitive discharge

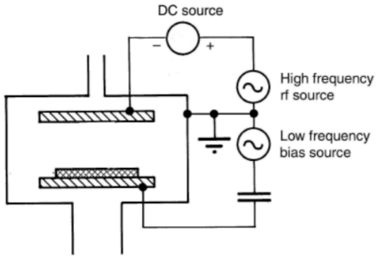

DC/dual frequency
capacitive discharge

There are two types of etching: isotropic vs anistropic

- Isotropic etching

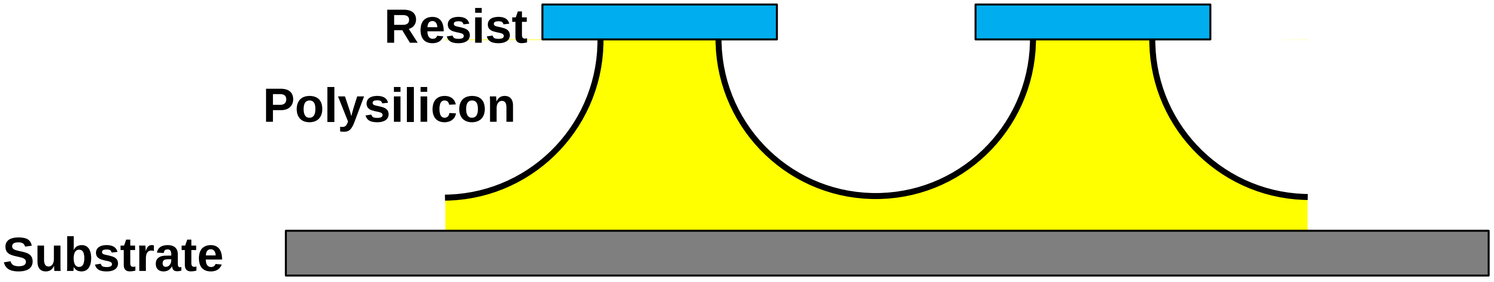

- Anisotropic etching

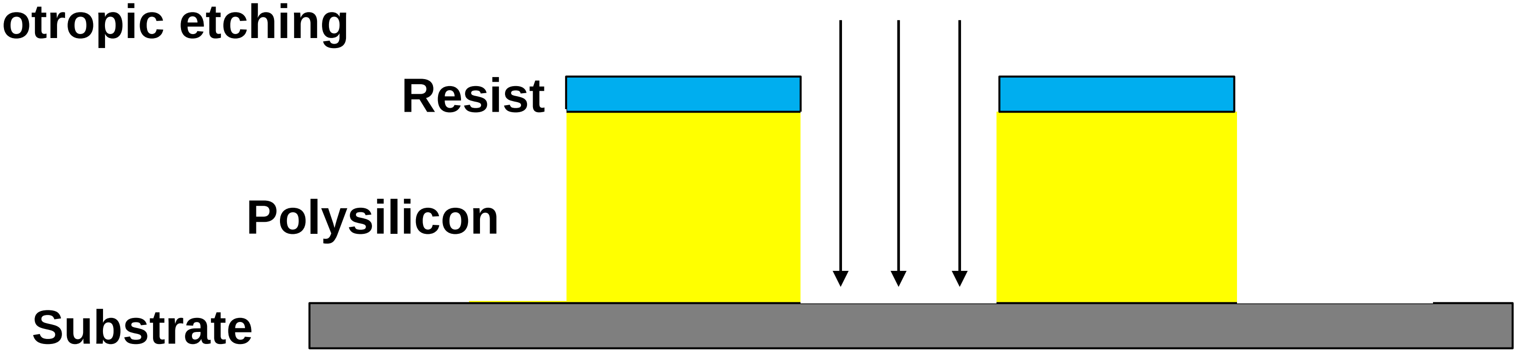

Plasma etch requirements – etch rate

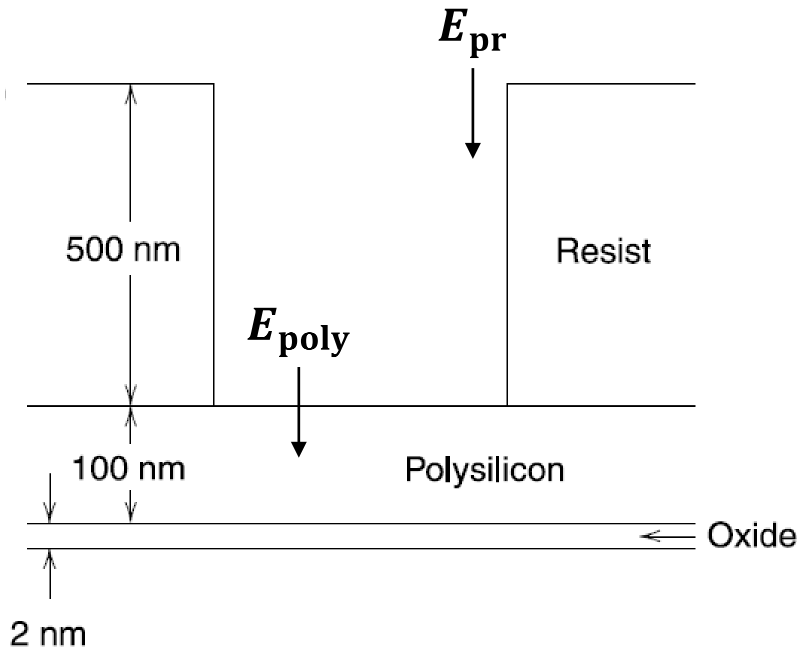

- **Etch time needs to be within a few minutes:**

$$E_{\mathrm{pr}} \geq 250\,\mathrm{nm/min}$$

$$E_{\mathrm{poly}} \geq 50\,\mathrm{nm/min}$$

Principles of plasma discharges and materials processing, 2nd edition, by Michael A. Lieberman and Allan J. Lichtenberg

Plasma etch requirements - selectivity

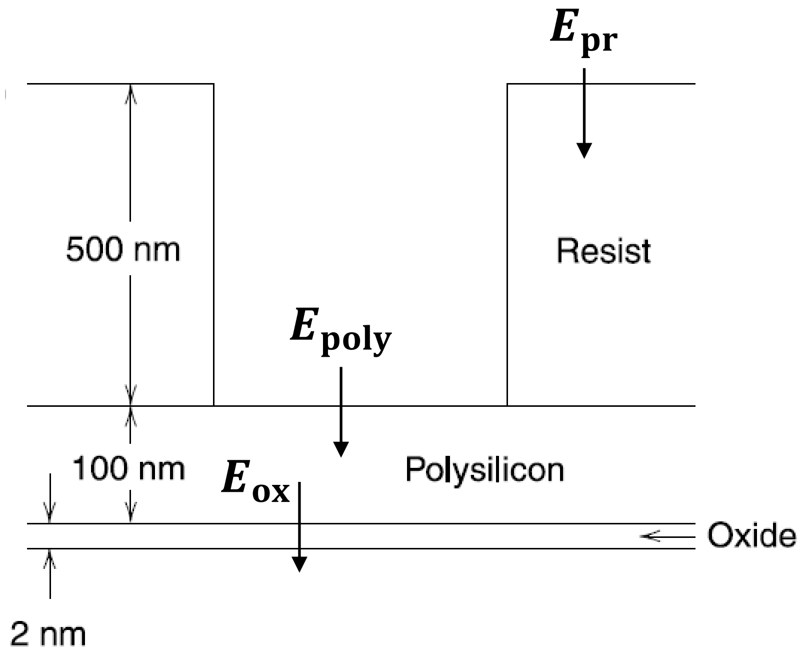

- **Selectivity between polysilicon and resist:**

$$s = \frac{E_{\mathrm{poly}} \triangle t}{E_{\mathrm{pr}} \triangle t} >> \frac{100\mathrm{nm}}{500\mathrm{nm}} = 0.2$$

- **Assuming 20% non-uniformity on the wafer:**

$$s = \frac{E_{\mathrm{poly}} \triangle t}{E_{\mathrm{ox}} \triangle t} >> \frac{20\% \times 100\mathrm{nm}}{2\mathrm{nm}} = 10$$

Principles of plasma discharges and materials processing, 2nd edition, by Michael A. Lieberman and Allan J. Lichtenberg

Plasma etch requirements – Anisotropy

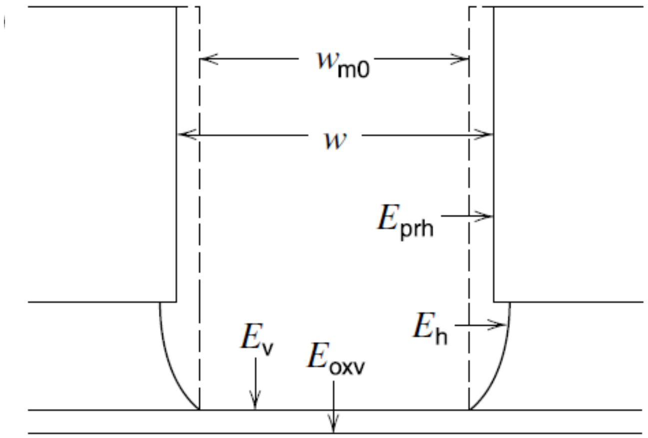

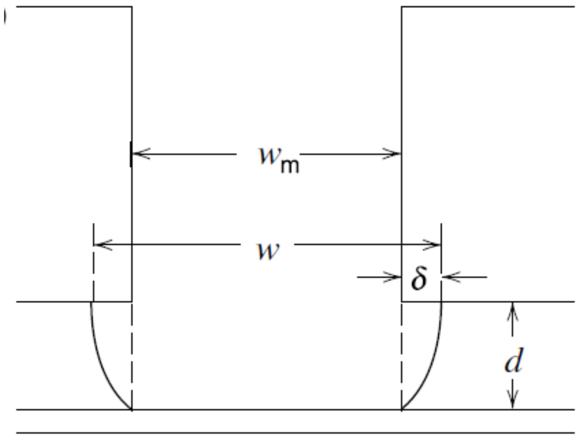

- **Anisotropy**

$$a_h = \frac{E_v}{E_h} = \frac{d}{\delta}$$

$$w = w_m + 2\delta$$

$$a_h \geq \frac{2d}{w - w_m}$$

- **The smallest feature size where w_m=0:**

$$w \approx \frac{2d}{a_h}$$

Principles of plasma discharges and materials processing, 2nd edition, by Michael A. Lieberman and Allan J. Lichtenberg

Plasma etch requirements – Anisotropy including etching on photoresist

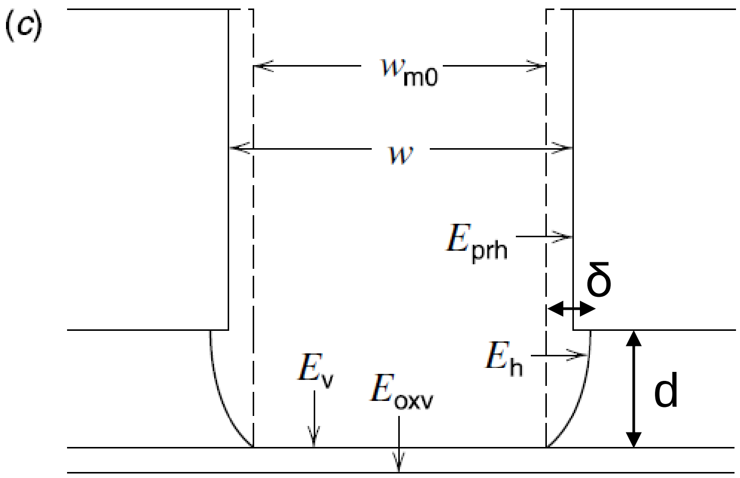

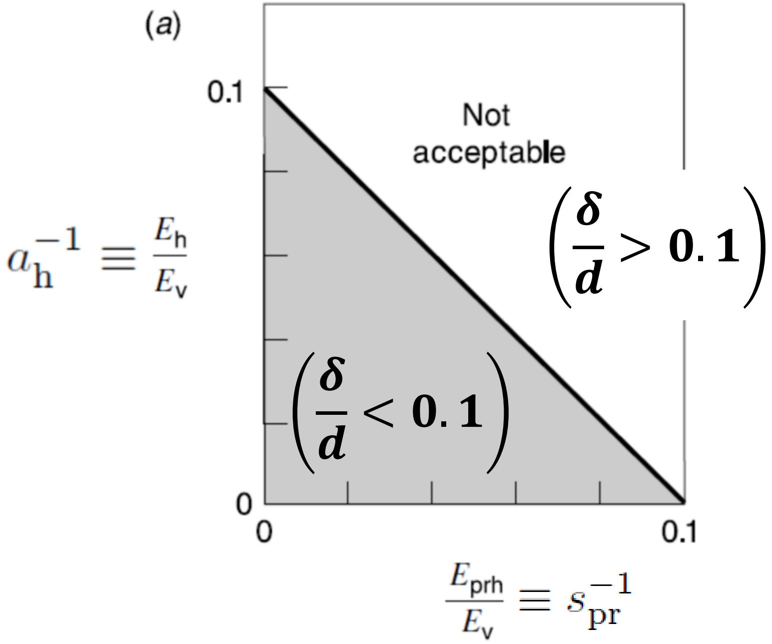

$$\delta \approx (E_h + E_{prh})\, t$$

$$t = \frac{d}{E_v}$$

$$\delta \approx d \frac{E_h + E_{prh}}{E_v}$$

$$\frac{E_h + E_{prh}}{E_v} \approx \frac{\delta}{d}$$

$$\frac{E_h}{E_V} + \frac{E_{prh}}{E_V} = a_h{}^{-1} + s_{pr}{}^{-1} \approx \frac{\delta}{d} \equiv 0.1$$

- The contribution of the horizontal etching is from both E_h and E_{prh}.

Principles of plasma discharges and materials processing, 2nd edition, by Michael A. Lieberman and Allan J. Lichtenberg

Plasma etch requirements – Uniformity on selectivity and anisotropy

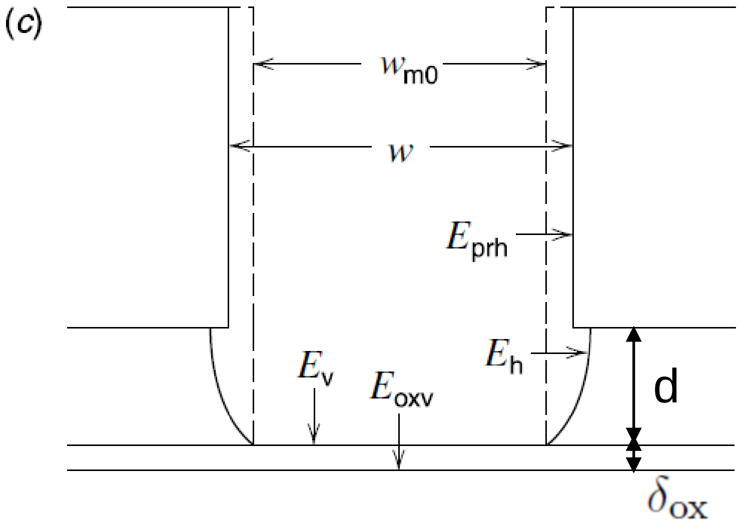

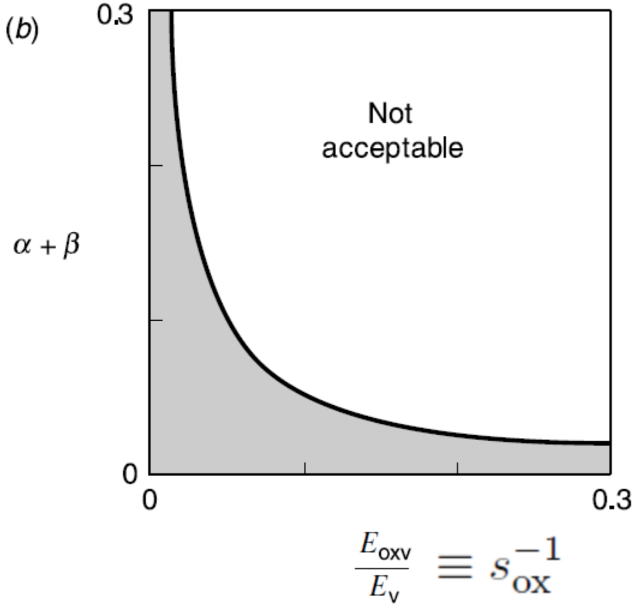

$$d \rightarrow d(1 \pm \alpha) \qquad E_v \rightarrow E_v(1 \pm \beta)$$

where α, β are variations.

$$t_{max} = \frac{d(1+\alpha)}{E_v(1-\beta)} \approx \frac{d}{E_v}(1+\alpha+\beta)$$

$$t_{min} = \frac{d(1-\alpha)}{E_v(1+\beta)} \approx \frac{d}{E_v}(1-\alpha-\beta)$$

$$\begin{aligned}\delta_{ox} &= (t_{max} - t_{min})E_{oxv} \\ &= \frac{d}{E_v} 2(\alpha+\beta) E_{oxv}\end{aligned}$$

$$2(\alpha+\beta)\frac{E_{oxv}}{E_v} = \frac{\delta_{ox}}{d}$$

Principles of plasma discharges and materials processing, 2nd edition, by Michael A. Lieberman and Allan J. Lichtenberg

There are four major plasma etching mechanisms

- **Sputtering**
- **Pure chemical etching**

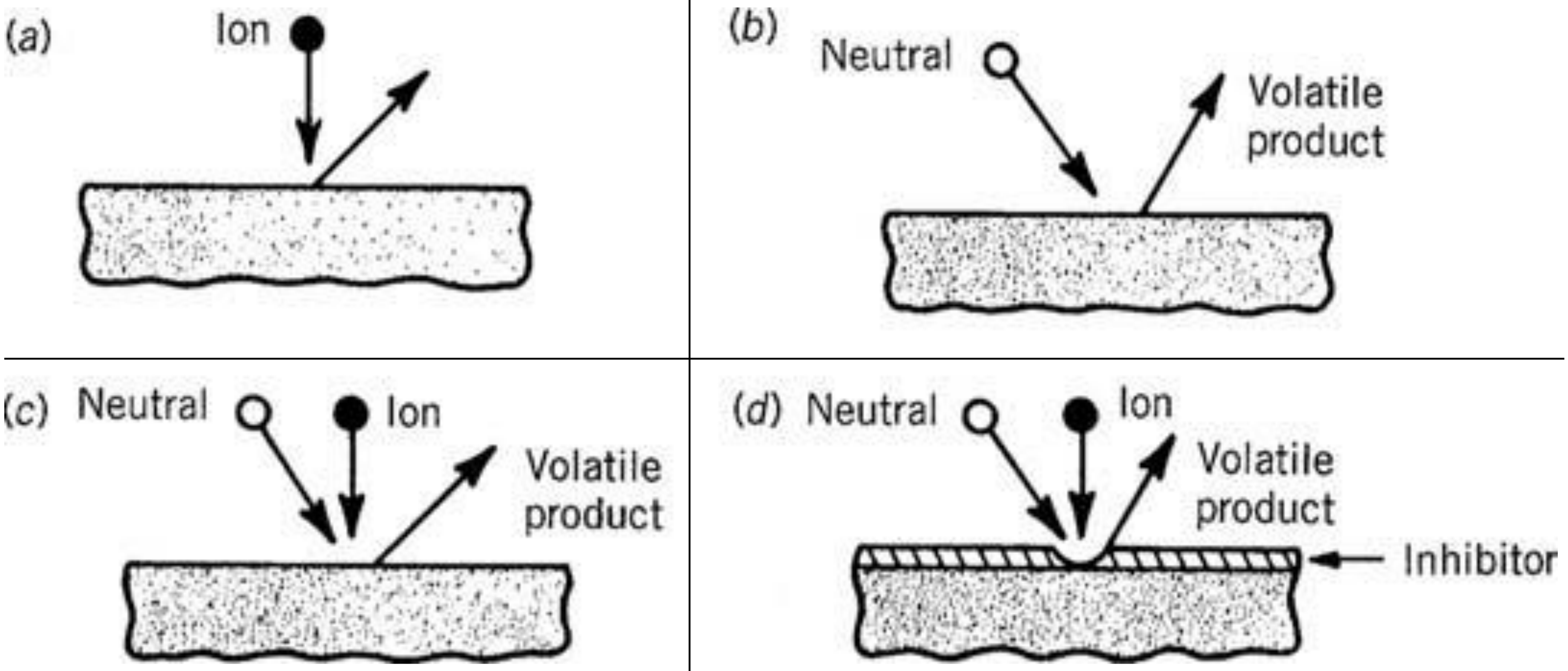

- **Ion energy-driven etching**
- **Ion-enhanced inhibitor etching**

Principles of plasma discharges and materials processing, 2nd edition, by Michael A. Lieberman and Allan J. Lichtenberg

Sputtering is an unselective but anisotropic process

- **Unselective process.**
- **Anisotropic process, strongly sensitive to the angle of incidence of the ion.**
- **Sputtering rates of different materials are roughly the same.**
- **Sputtering rates are generally low because the yield is typically of order one atom per incident ion.**
- **Sputtering is the only one of the four etch processes that can remove nonvolatile products from a surface.**
- **The process is generally under low pressure since the mean free path of the sputtered atoms must be large enough to prevent redeposition on the substrate or target.**

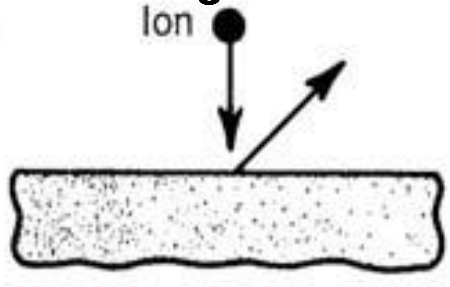

Principles of plasma discharges and materials processing, 2nd edition, by Michael A. Lieberman and Allan J. Lichtenberg

Topographical patterns might not be faithfully transferred during sputter etching

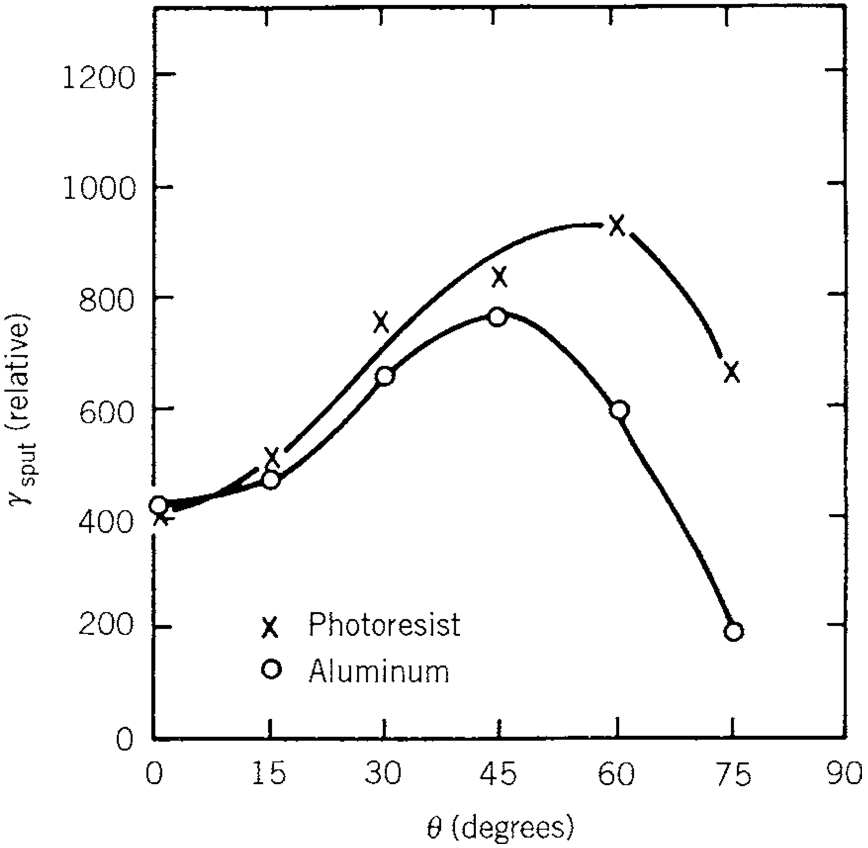

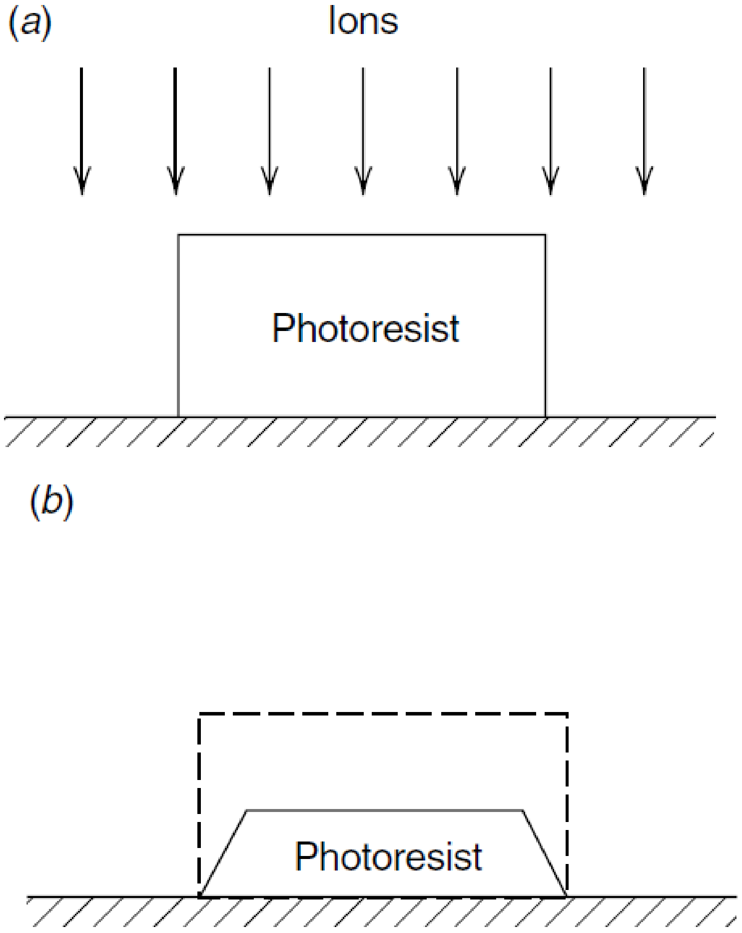

Principles of plasma discharges and materials processing, 2nd edition, by Michael A. Lieberman and Allan J. Lichtenberg

Pure chemical etching

Atoms or molecules chemically react with the surface to form gas-phase products

- **Highly chemically selective, e.g.,**

$$\mathrm{Si(s)} + 4\mathrm{F} \longrightarrow \mathrm{SiF_4(g)}$$

$$\mathrm{photoresist} + \mathrm{O(g)} \longrightarrow \mathrm{CO_2(g)} + \mathrm{H_2O(g)}$$

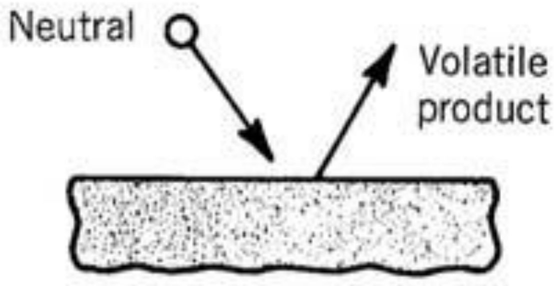

- **Almost invariably isotropic.**
- **Etch products must be volatile.**
- **The etch rate can be quite large.**
- **Etch rate are generally not limited by the rate of arrival of etchant atoms, but by one of a complex set of reactions at the surface leading to formation of etch products.**

Principles of plasma discharges and materials processing, 2nd edition, by Michael A. Lieberman and Allan J. Lichtenberg

Ion-enhanced energy-driven etching

The discharge supplies both etchants and energetic ions to the surface

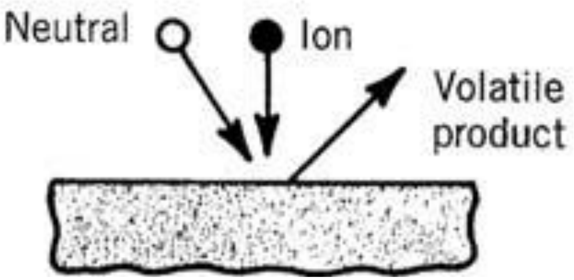

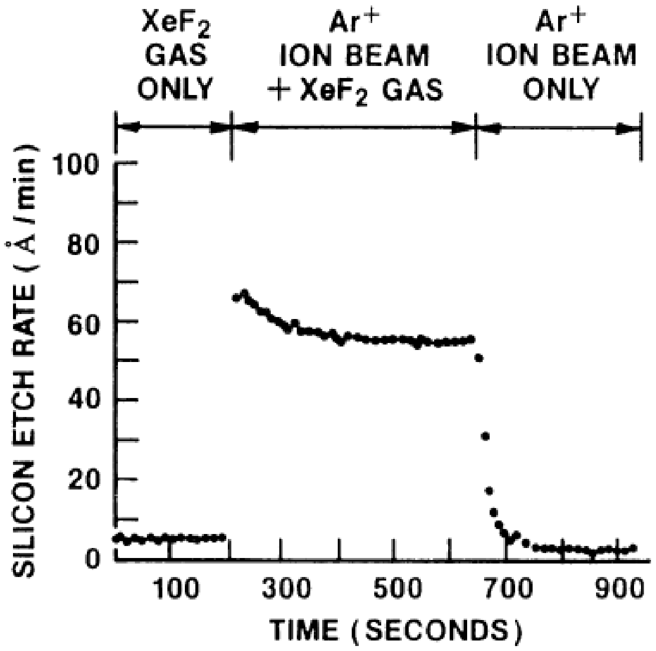

- **Low chemical etch rate of silicon substrate in XeF2 etchant gas.**
- **Tenfold increase in etch rate with XeF_2 + 500 V argon ions, simulating ion-enhanced plasma etching.**
- **Very low “etch rate” due to the physical sputtering of silicon by ion bombardment alone.**

Plasma etching, by Daniel L. Flamm and G. Kenneth Herb

Ion-enhanced energy-driven etching has the characteristic of both sputtering and pure chemical etching

- Chemical in nature but with a reaction rate determined by the energetic ion bombardment.
- Product must be volatile.
- Highly anisotropic.

Ion-enhanced inhibitor etching

An inhibitor species is used

- Inhibitor precursor molecules that absorb or deposit on the substrate form a protective layer or polymer film.
- Etchant is chosen to produce a high chemical etch rate of the substrate in the absence of either ion bombardment or the inhibitor.
- Ion bombardment flux prevents the inhibitor layer from forming or clears it as it forms.
- Where the ion flux does not fall, the inhibitor protects the surface (side wall) from the etchant.
- May not be as selective as pure chemical etching.
- A volatile etch product must be formed.
- Contamination of the substrate and final removal of the protective inhibitor film are other issues.

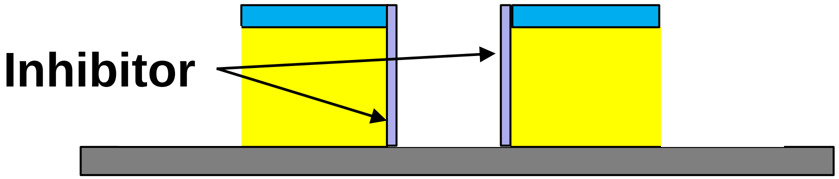

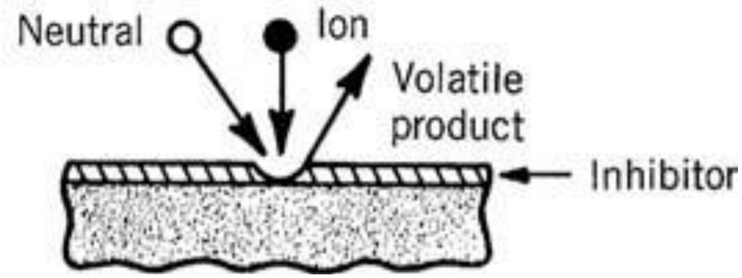

Comparison of different processes

	Sputtering etching	Pure chemical etching	Ion energy-driven etching	Ion-enhanced Inhibitor etching
Selectivity	X	O	O	O
Anisotropic	O	X	O	O
Volatile product	X	O	O	O

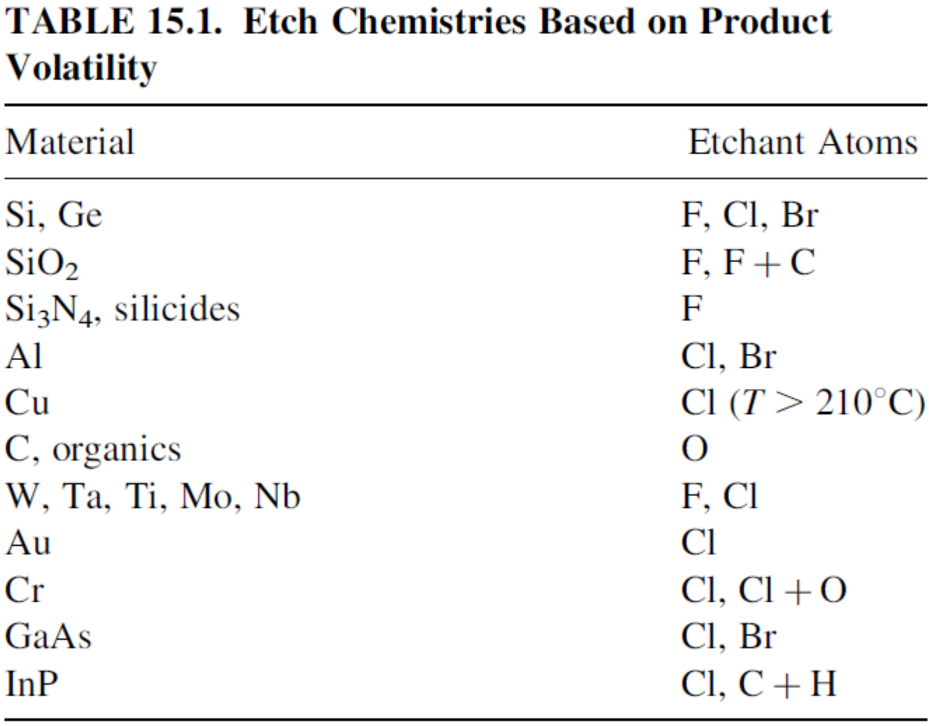

TABLE 15.1. Etch Chemistries Based on Product Volatility

Material	Etchant Atoms
Si, Ge	F, Cl, Br
SiO_2	F, F + C
Si_3N_4, silicides	F
Al	Cl, Br
Cu	Cl ($T > 210°C$)
C, organics	O
W, Ta, Ti, Mo, Nb	F, Cl
Au	Cl
Cr	Cl, Cl + O
GaAs	Cl, Br
InP	Cl, C + H

Deposition and implementation

- **Plasma-assisted deposition, implantation, and surface modification are important material processes for producing films on surfaces and modifying their properties**
- **Example processes:**
  - **Plasma-enhanced chemical vapor deposition (PECVD)**
  - **Sputter deposition / physical vapor deposition (PVD)**
  - **Plasma-immersion ion implantation (PIII)**

Chemical Vapor Deposition (CVD)

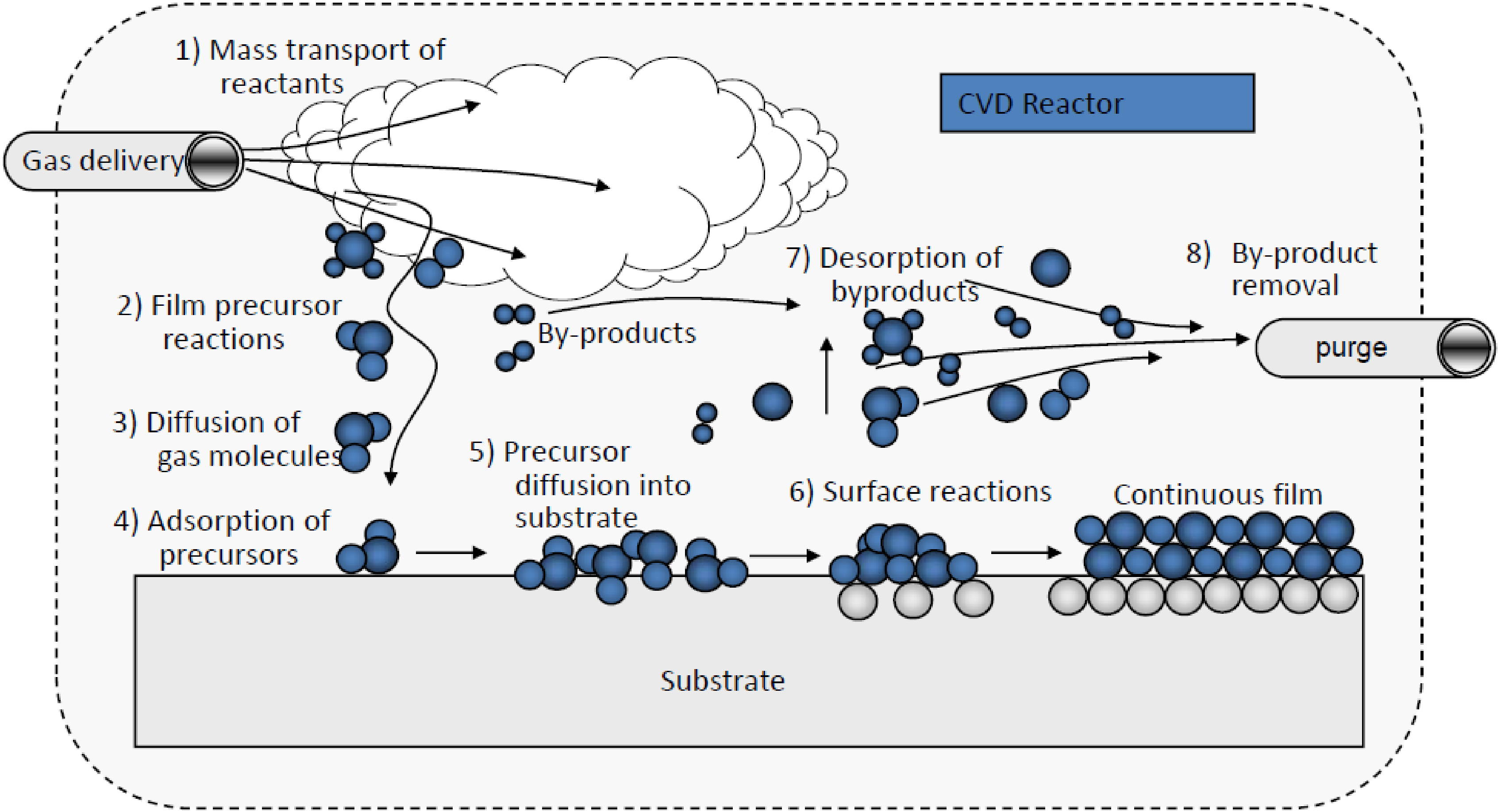

http://www.ece.uah.edu/courses/material/EE410-Wms/

Plasma-enhanced chemical vapor deposition (PECVD)

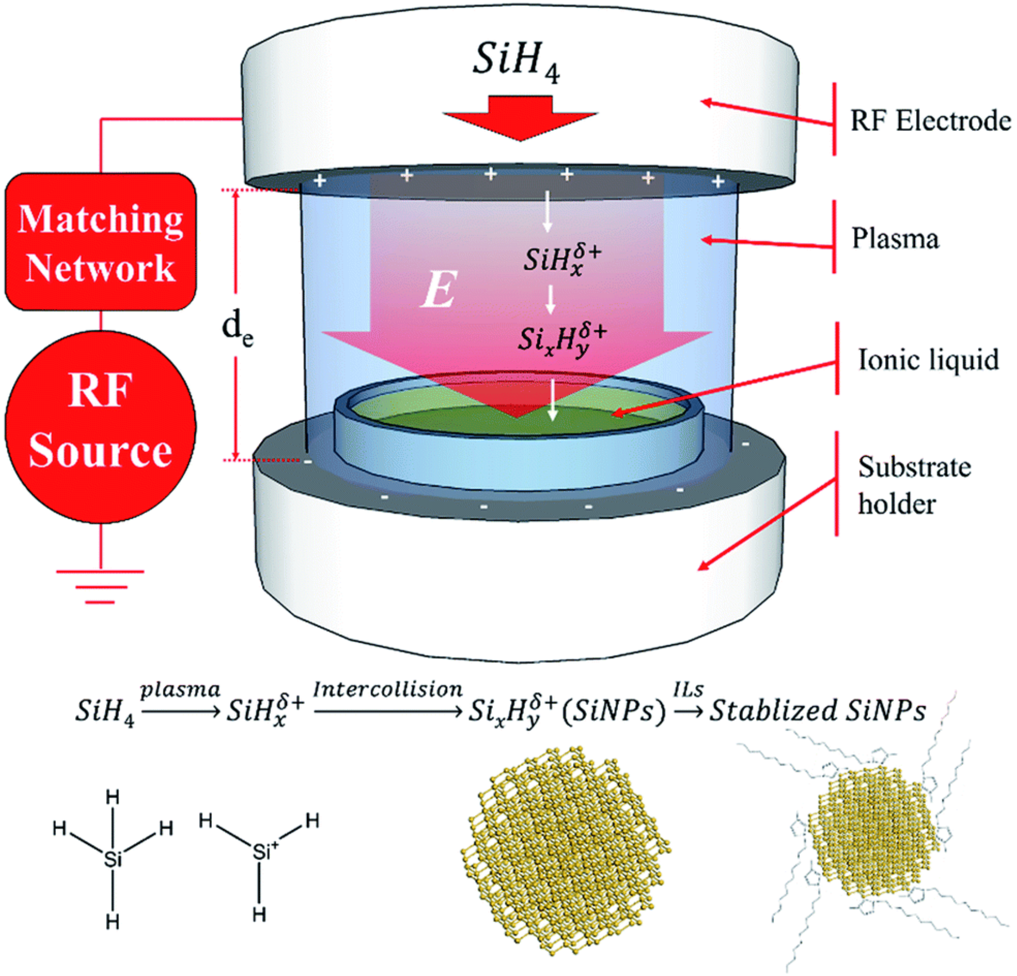

$$SiH_4 \xrightarrow{plasma} SiH_x^{\delta+} \xrightarrow{Intercollision} Si_xH_y^{\delta+}(SiNPs) \xrightarrow{ILs} Stablized\ SiNPs$$

Films can be deposited in low temperatures using plasma deposition

- **Device structures are sensitive to temperature, high-temperature deposition processes cannot be used in many cases.**
- **High-temperature films can be deposited at low temperatures.**
- **Unique films not found in nature can be deposited, e.g., diamond.**

Working temperature is determined by the desired film properties

- CVD – consists of a thermally activated set of gas-phase and surface reactions that produce a solid product at a surface.
- PECVD – gas-phase and the surface reactions are controlled or modified by the plasma properties.
- Te~2-5 eV in PECVD is much greater than the substrate temperature, the temperature in PECVD is much less that CVD.
- Deposition rates are usually not very sensitive to the substrate temperature T.
- Film properties such as composition, stress, and morphology, are functions of T.
- Low-temperature PECVD films are amorphous, not crystalline, which can more easily be achieved with chemical vapor deposition (CVD).

Example of using PECVD – amorphous silicon

- **Amorphous silicon thin films are used in solar cells**

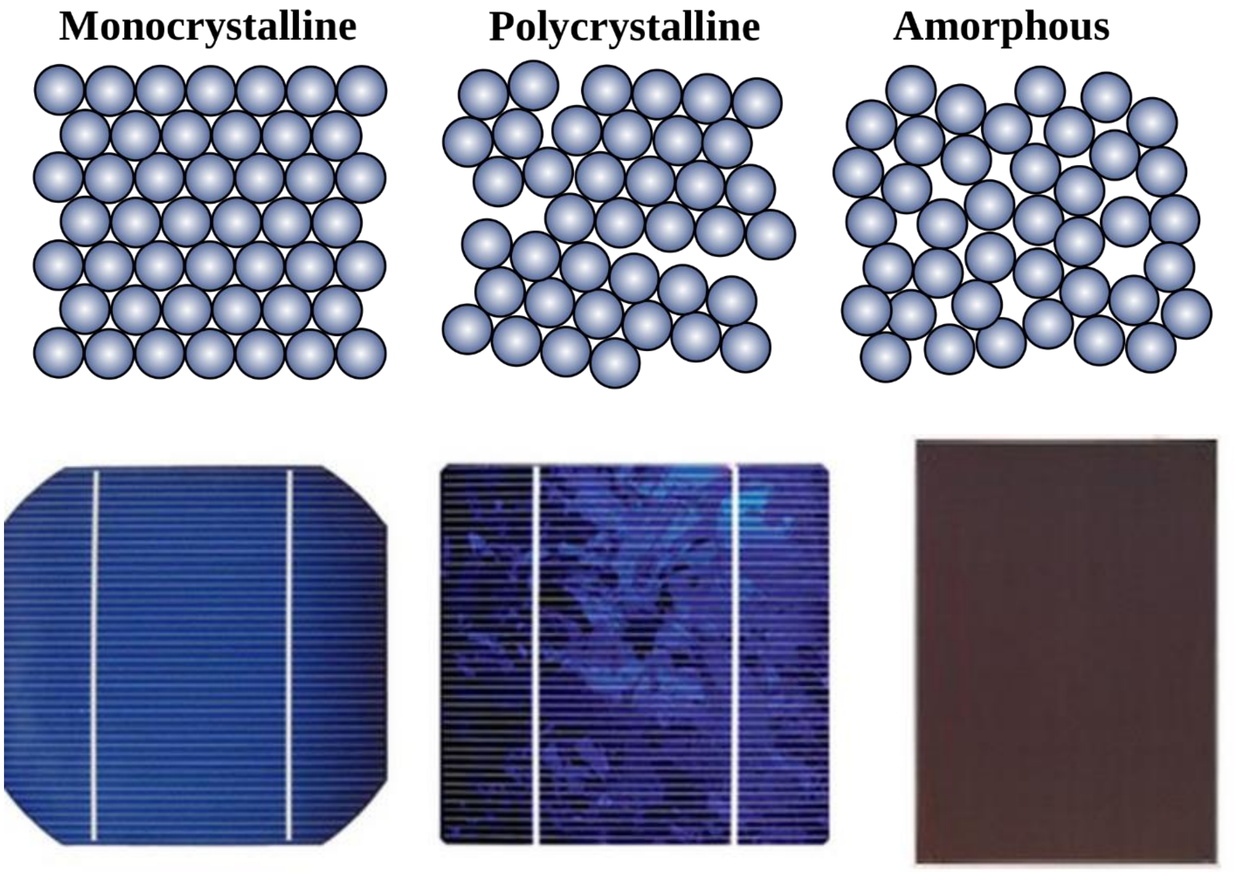

Example of using PECVD – amorphous silicon

- H is required so that SiH_4 is used
  - For the material to be semiconducting.
  - Terminate the dangling bonds.
  - The dangling bonds are created by ion bombardment (SiH_3^+) which also removes hydrogen from the surface.
  - SiH_3 and SiH_2 radicals are important precursors for film growth while SiH_4 also participates in surface reactions.

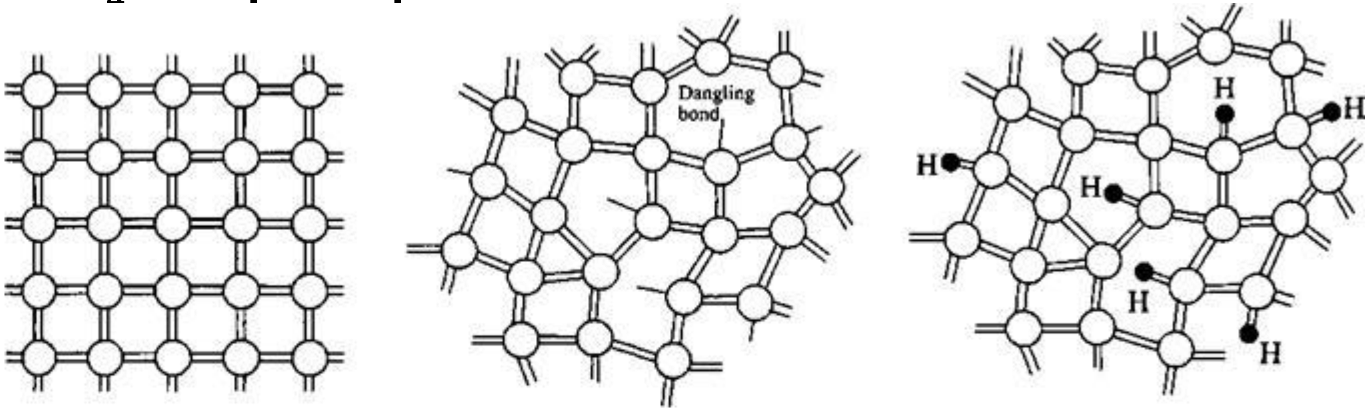

PVD

Physical vapor deposition can be achieved by heating the deposited material

- **Thermal evaporator**

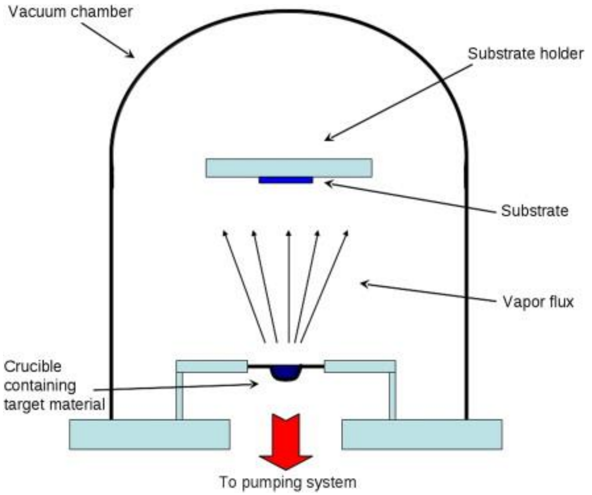

- **Electron-beam evaporator**

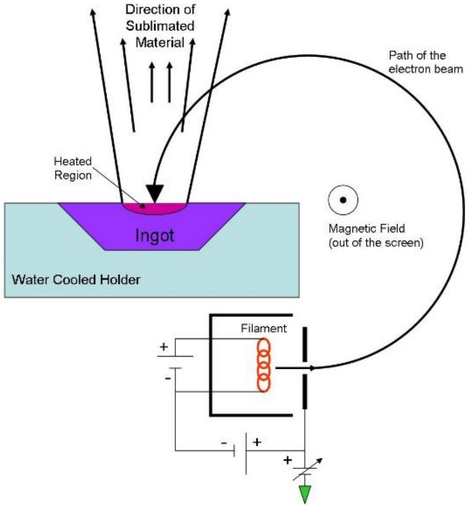

- **Pulsed-laser deposition**

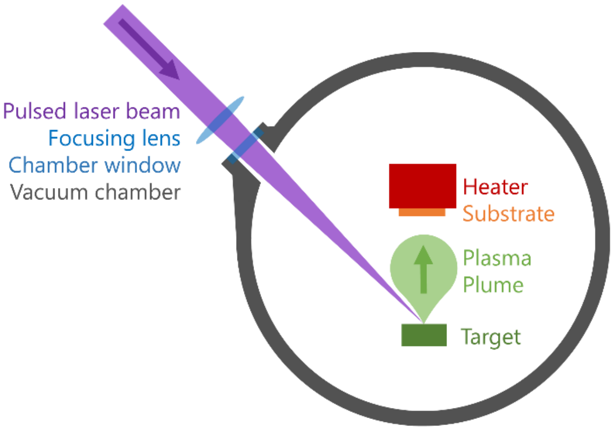

---

https://en.wikipedia.org/wiki/Pulsed_laser_deposition
Engineered biomimicry by A. Lakhtakia and R. J. Martin-Palma
https://en.wikipedia.org/wiki/Electron-beam_physical_vapor_deposition

Sputtering deposition

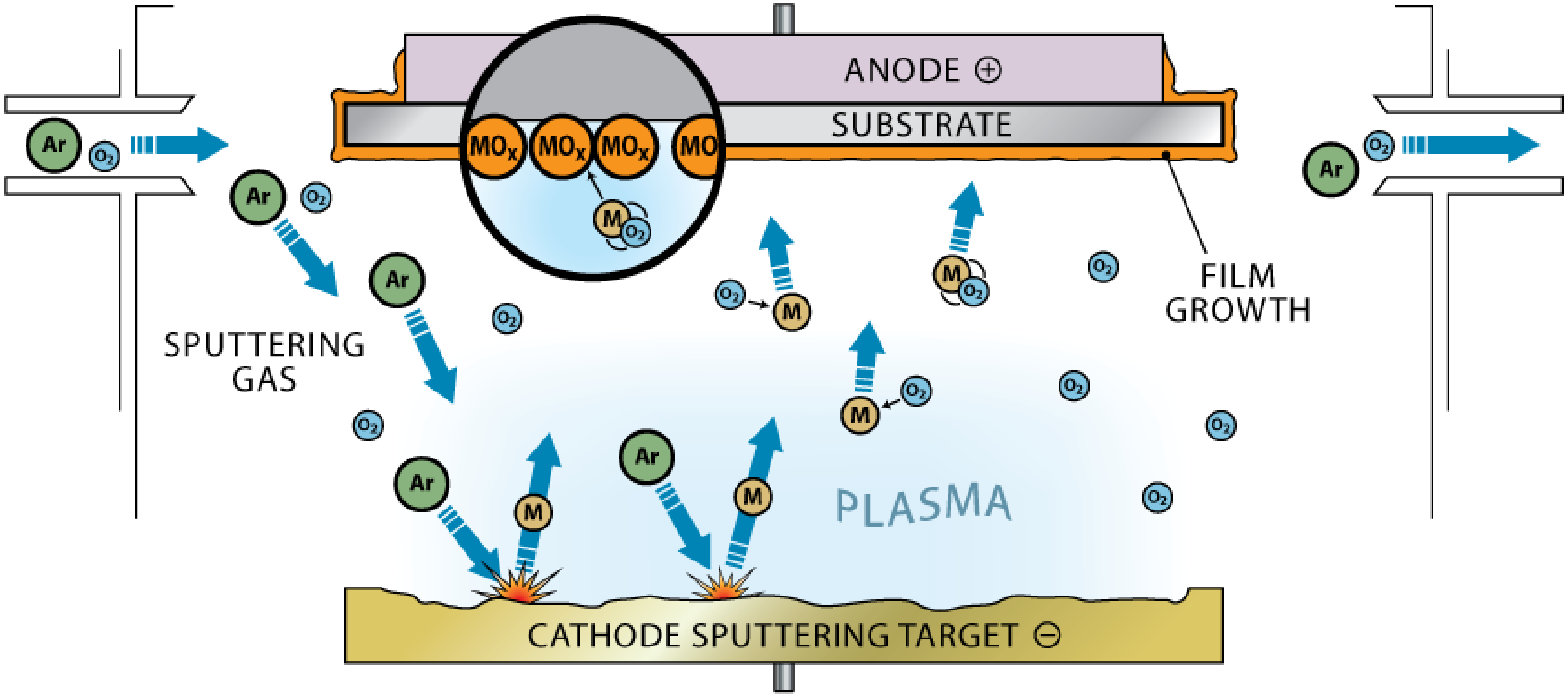

http://lnf-wiki.eecs.umich.edu/wiki/Sputter_deposition

Plasma-immersion ion implantation (PIII)

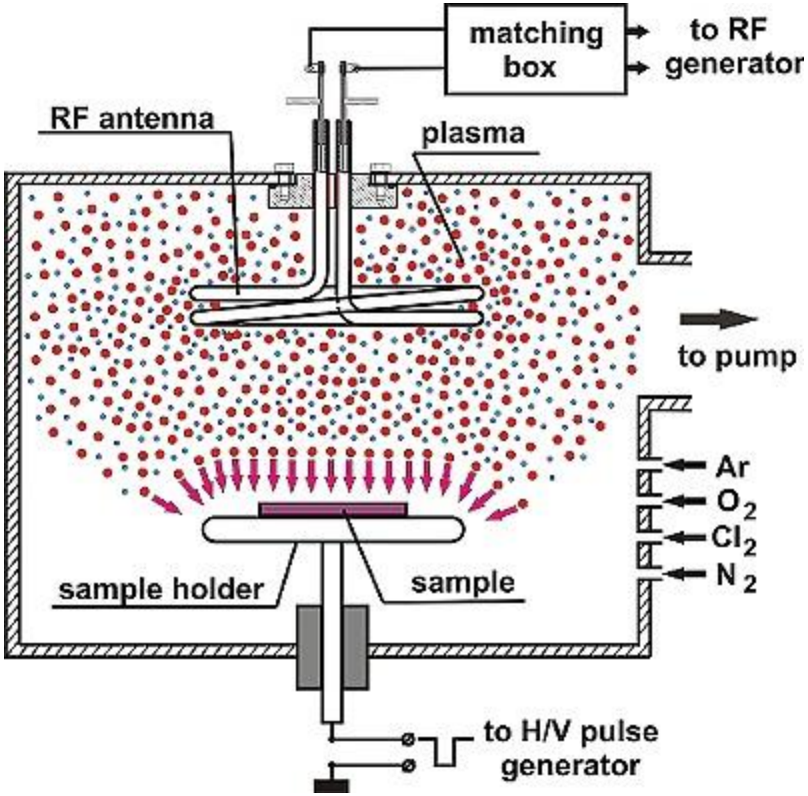

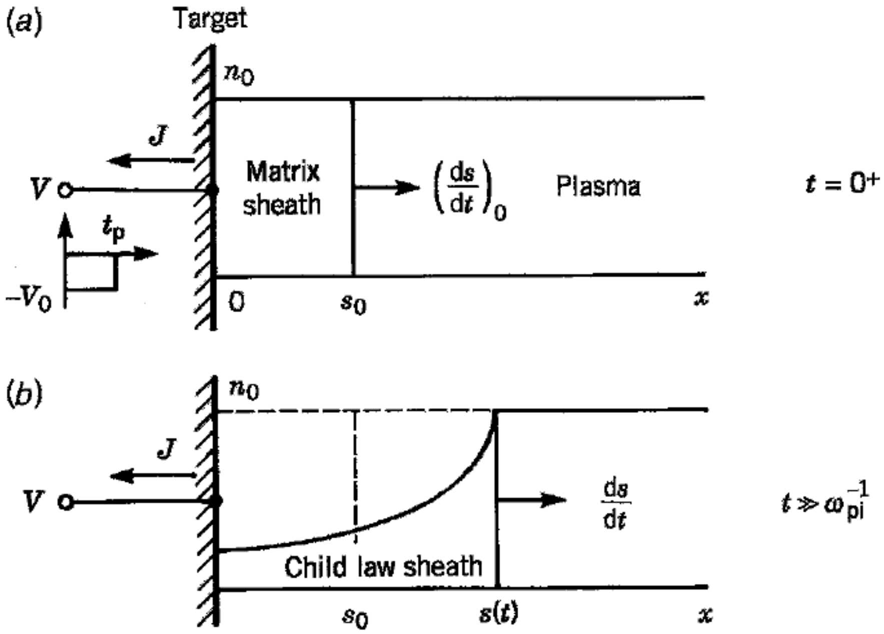

- **Silicon doping – ions such as B, P, As are implanted**
- **Surface hardening of metals – N, C are implanted**

https://www.hzdr.de/db/Cms?pOid=10890&pNid=306

Magnetron sputtering provides higher deposition rates than conventional sputtering

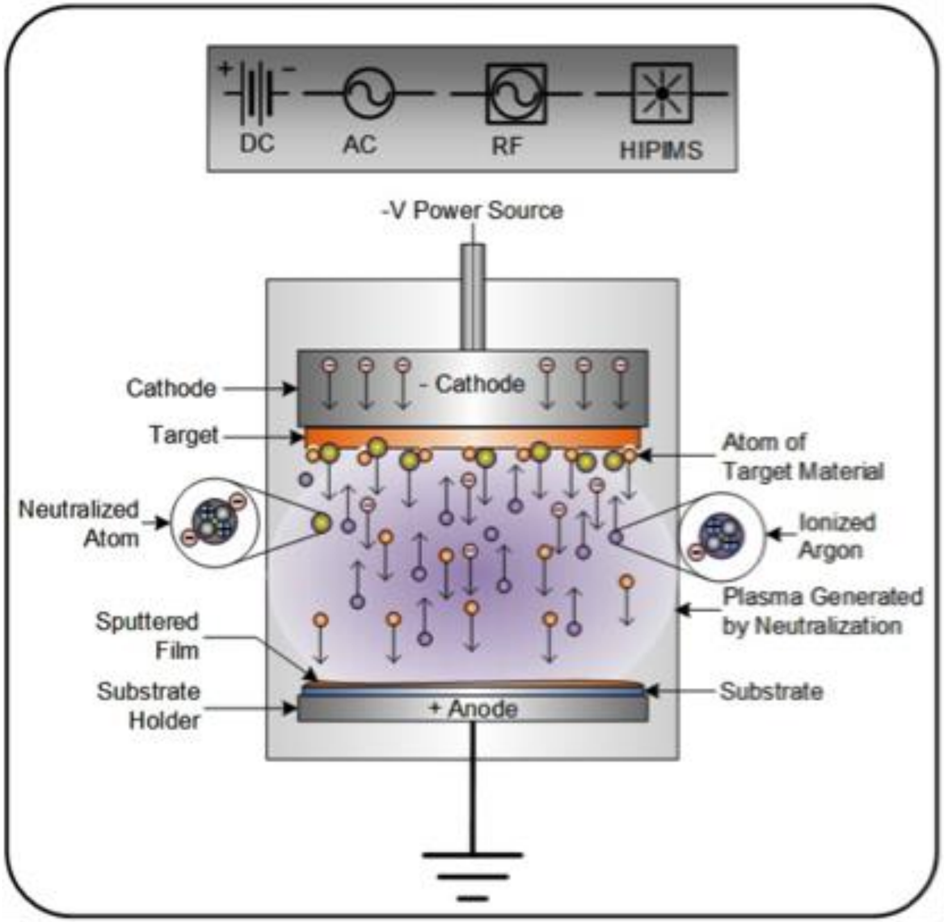

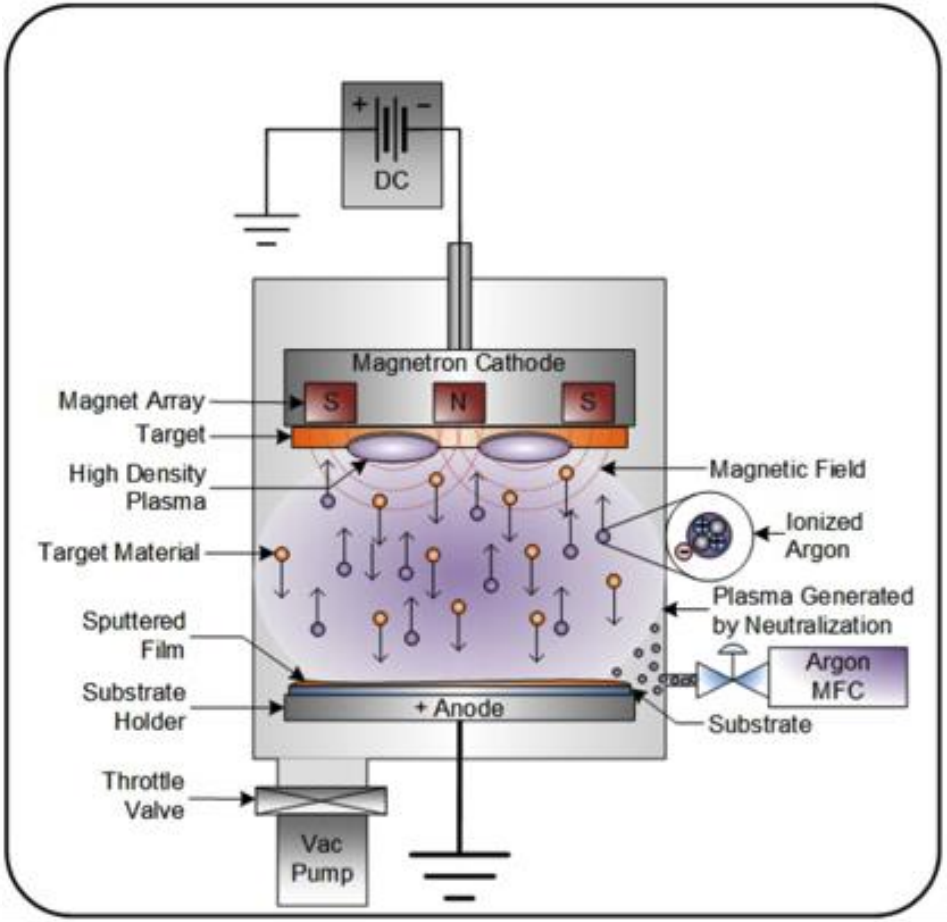

http://www.semicore.com/what-is-sputtering

Demonstration experiments – magnetron sputtering

- System

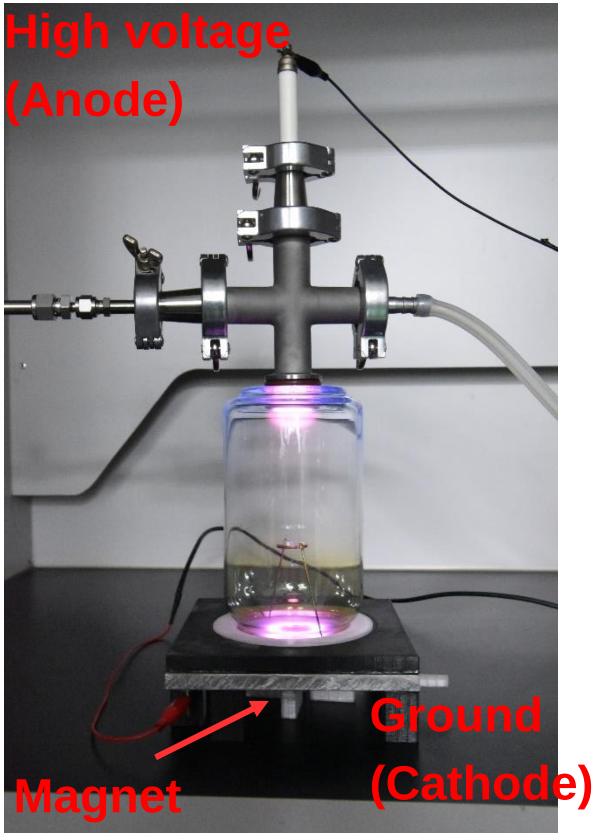

- Without magnet

- With magnet

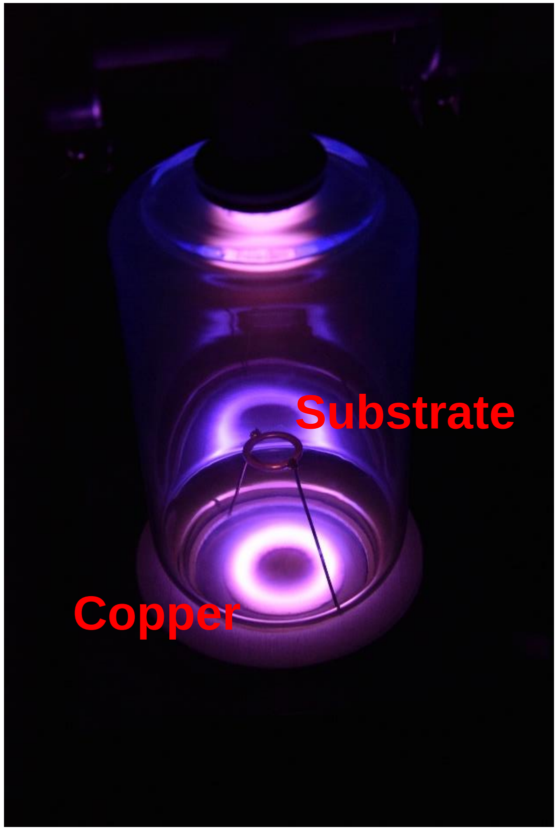

self-aligned quadruple patterning

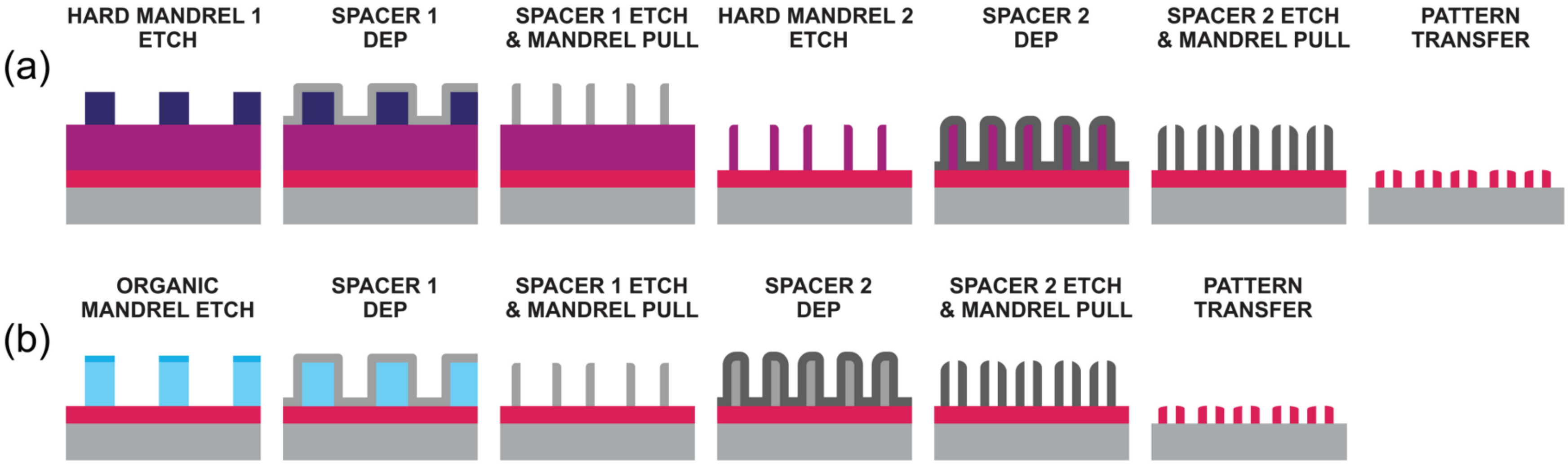

H. C. M. Knoops *et al.*, J. Vac. Sci. Technol. **A 37**, 030902 (2019)

Plasma can be used for cleaning surface

- **Cleaning mechanisms:**
  - **Chemical reactions by free radicals**
  - **Physical sputtering by high energy ions**

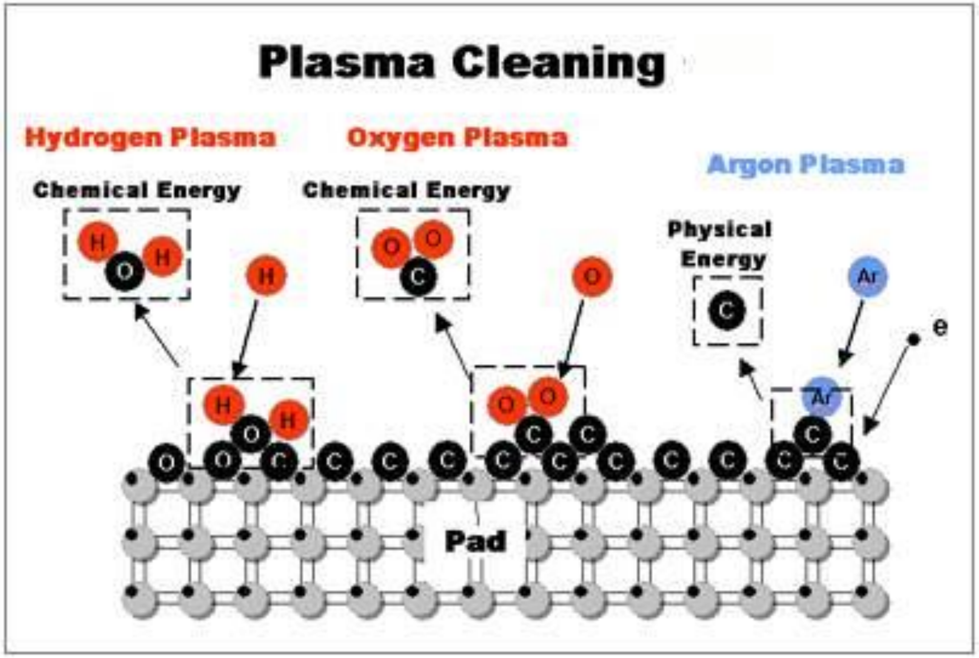

埴鼎奈米科技股份有限公司
https://www.ecplaza.net/products/plasma-cleaning_111807

Free radicals are generated and used in chemical reactions

$$e^- + H_2 \rightarrow 2H\bullet \qquad e^- + O_2 \rightarrow 2O\bullet \qquad \mathrm{O}\bullet + O_2 \rightarrow O_3$$

- **Highly reactive free radicals generated in plasma may react with the hydrocarbon contaminants of surface oxide.**
- **Both H• and O• can react with grease or oil on surface to form volatile hydrocarbons.**

$$\mathrm{H}\bullet_{(g)} + C_n H_{2n+2(s)} \rightarrow \mathrm{CH}_{4(s)}$$

$$\mathrm{O}\bullet_{(g)} + C_n H_{2n+2(s)} \rightarrow \mathrm{CO}_{(s)} + \mathrm{CH}_x O_{y(g)} + H_2 O_{(g)}$$

- **O• is more reactive than H•. But O• may also react with surface metal to form oxide, deteriorating the material properties. Nevertheless, H• can make metal oxide back to metal.**

$$\mathrm{O}\bullet + \mathrm{Me} \rightarrow \mathrm{MeO}$$

$$\mathrm{H}\bullet + \mathrm{MeO} \rightarrow \mathrm{Me} + H_2 O$$

The effect of chemical reactions is increased as the pressure increases

- **Advantages:**
  - **Stable gas products are formed.**
  - **No redeposition problem.**
  - **High etching selectivity.**

- **Disadvantages:**
  - **Higher concentration of H_2 or O_2 is required to ensure an appropriate etching rate.**
  - **H_2 safety or O_2 strong oxidation ability needs to be monitored.**

High energy ions are used in physical sputtering cleaning

- **Ions generated in plasma can be accelerated toward the substrate to physically bombard away the atoms of contaminants.**
- **The physical sputtering rate increases as the following quantities increase:**
  - **Plasma density;**
  - **Accelerating voltage;**
  - **Mass of bombardment atoms.**
- **The physical sputtering is also enhanced by lowering the pressure.**
- **High cathode bias is used.**
- **Ar^+ has strong sputtering effect.**

The physical sputtering rate increases with higher cathode bias and Ar concentration and lower pressure

- **Advantages:**
  - **Highly efficient cleaning effect can be achieved.**
  - **Gas consumption rate can be very low.**

- **Disadvantages:**
  - **Etching problems – non-selective etching by physical sputtering.**
  - **Redeposition problems: the products sputtered out may be highly unstable and tend to deposit again downstream.**

Plasma cleaning examples

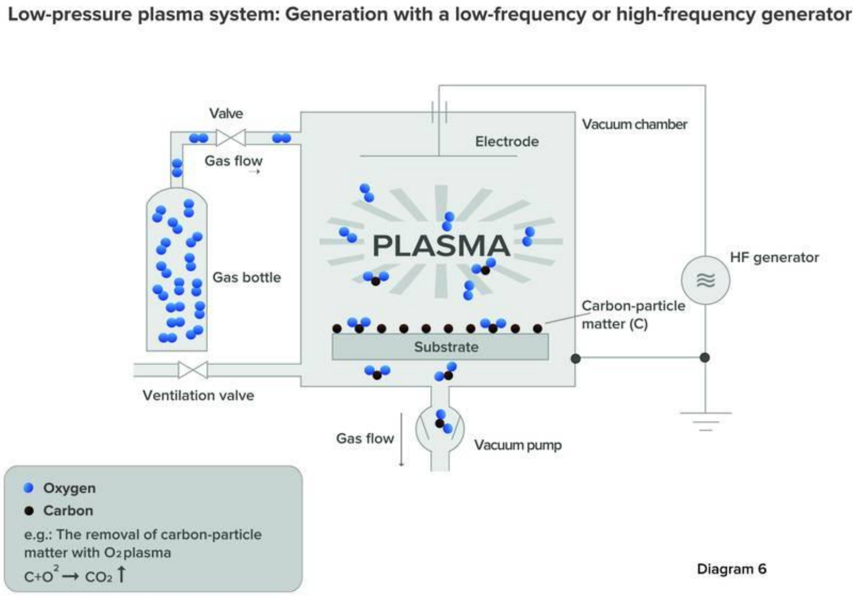

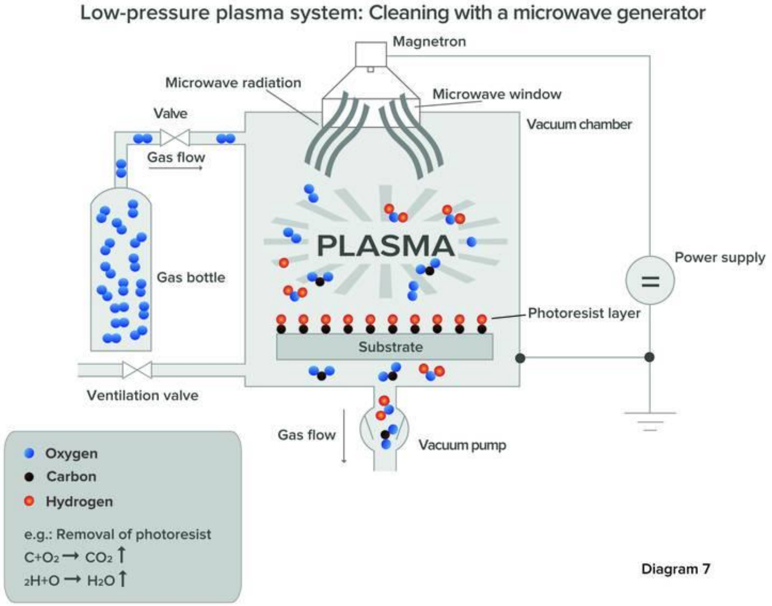

---

https://www.plasma.com/en/plasmatechnik/low-pressure-plasma/cleaning/

Plasma cleaning needs to work in the regime of abnormal glow discharge

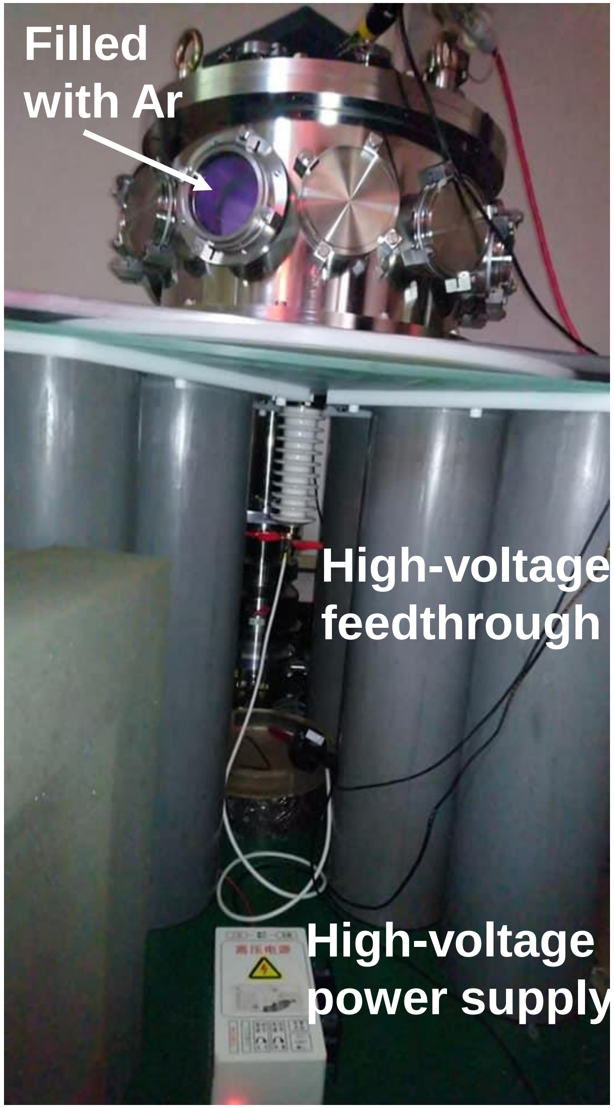

A semiconductor device is fabricated by many repetitive production process

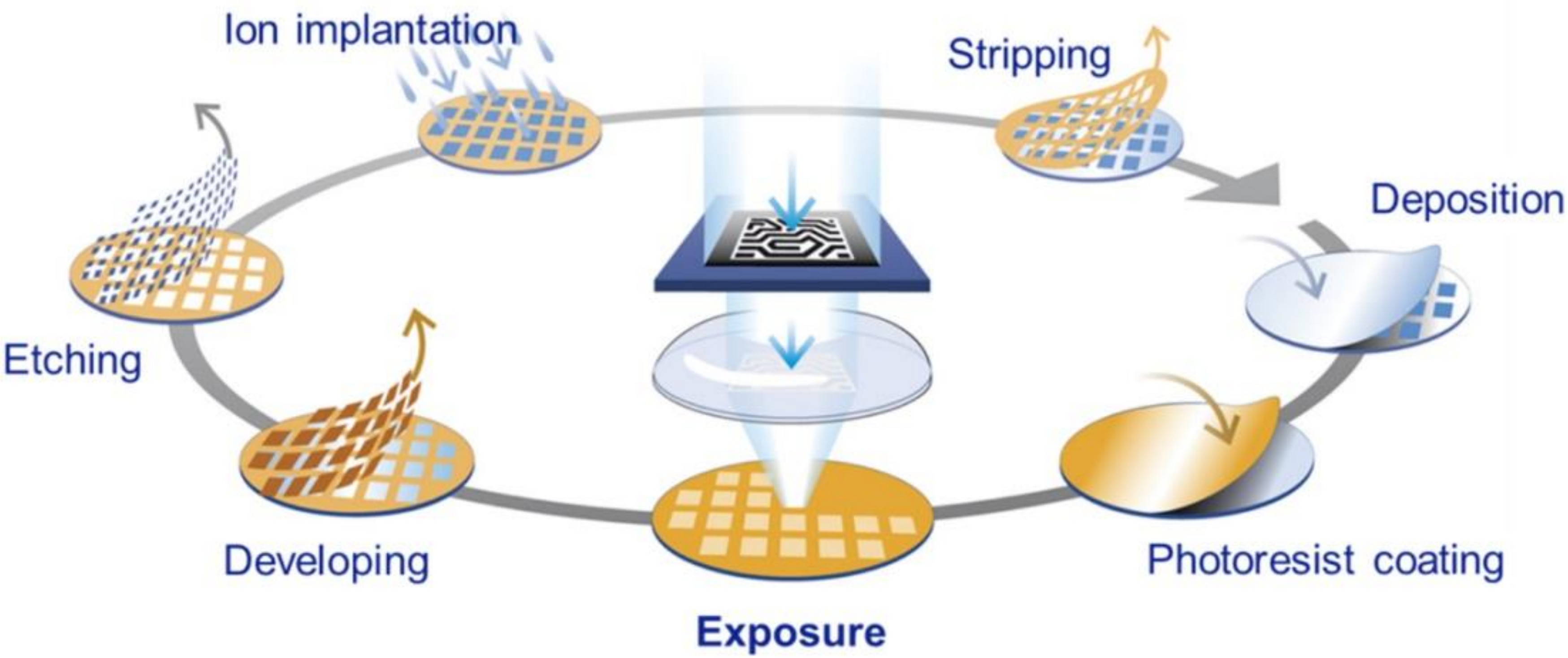

Surf. Topogr.: Metrol. Prop. **4** (2016) 023001

Ultraviolet lithography (EUVL) is one of the key technologies in semiconductor manufacturing nowadays

- The process technology of Taiwan Semiconductor Manufacturing Company Limited (TSMC):

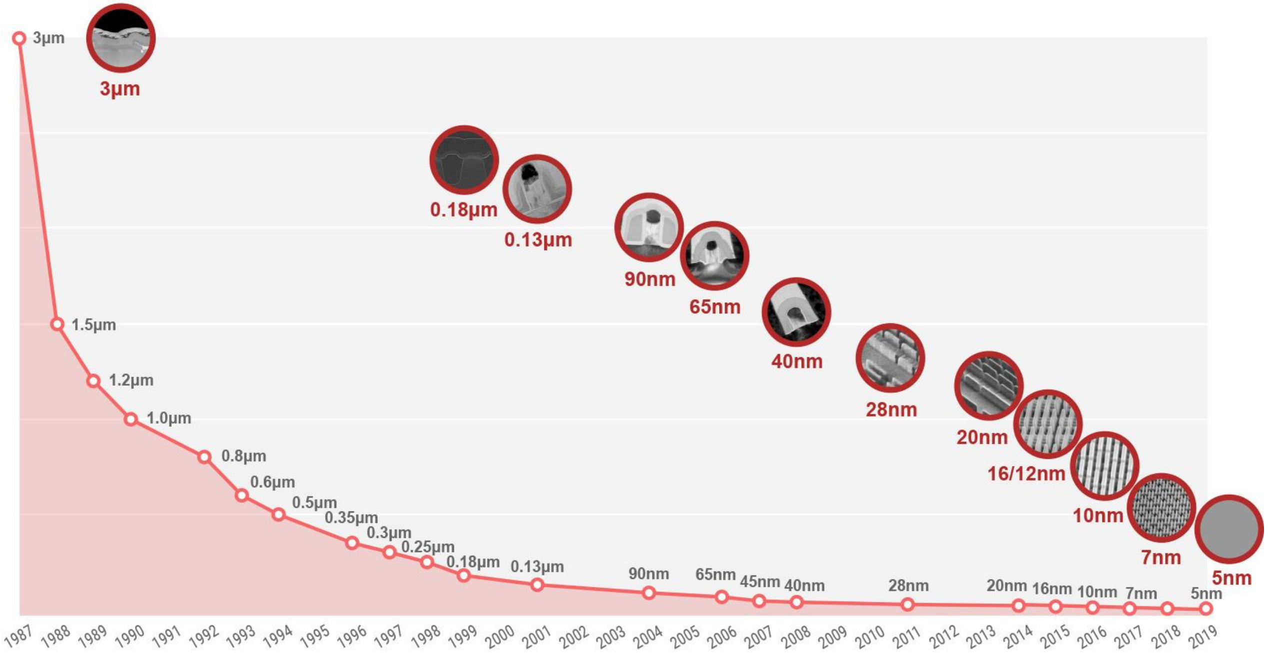

- Optical diffraction needs to be taken into account.
- Shorter wavelength is preferred.

- **Light source with a center wavelength of 13.5 nm is used.**

---

https://www.tsmc.com/chinese/dedicatedFoundry/technology/logic.htm

EUV lithography becomes important for semiconductor industry

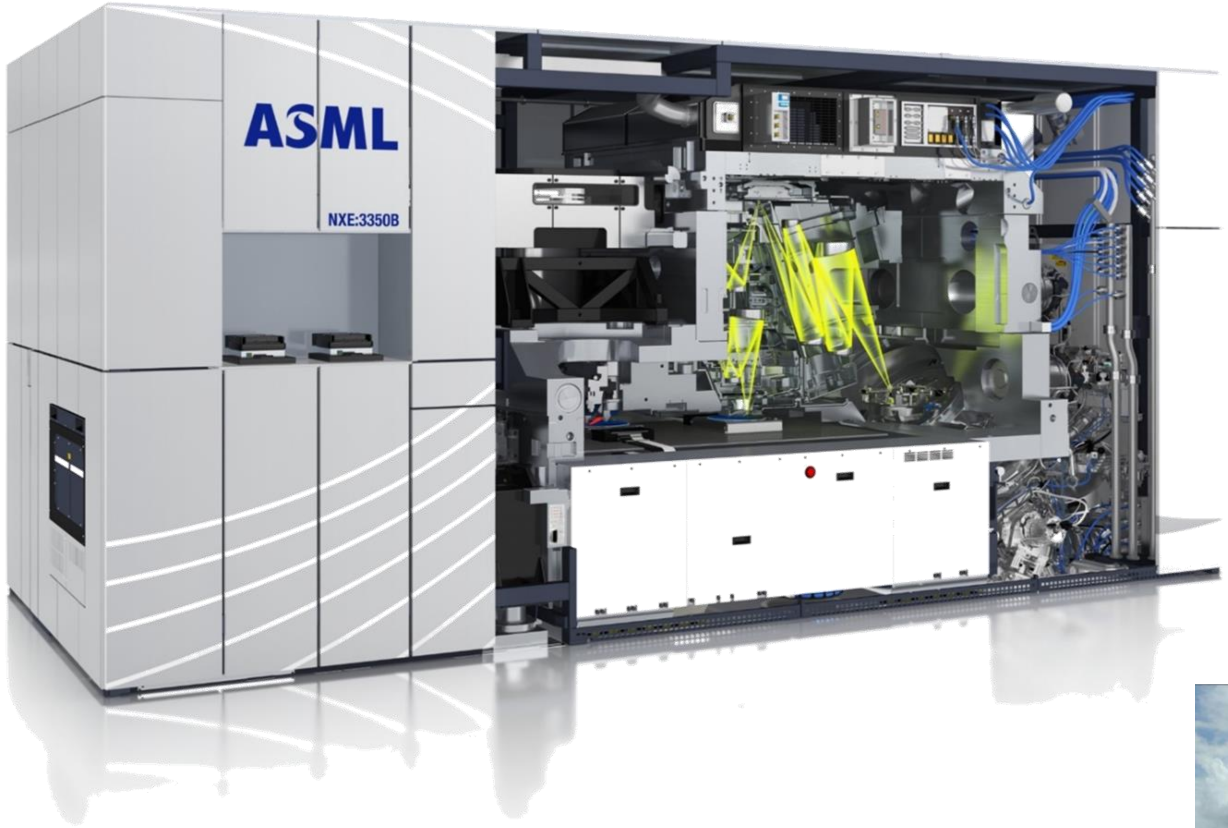

- **0.15 billion USD for each EUV light source.**

https://www.youtube.com/watch?v=NHSR6AHNiDs

---

http://finance.technews.tw/2019/01/25/euv-asml-2018/

EUV light can only be reflected using multilayer mirrors

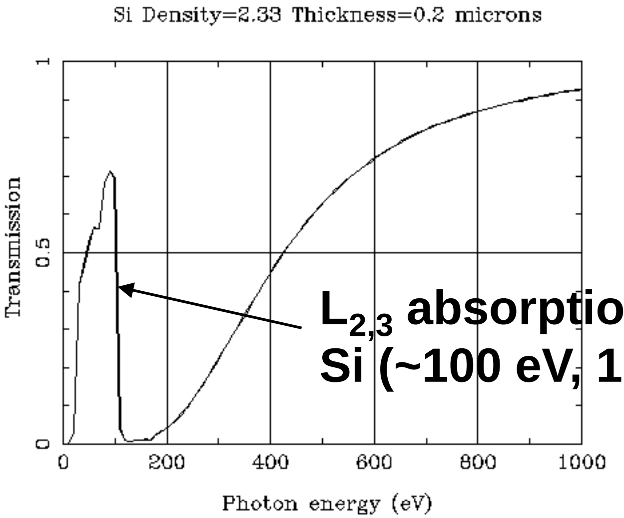

$L_{2,3}$ absorption edge of Si (~100 eV, 12.4 nm)

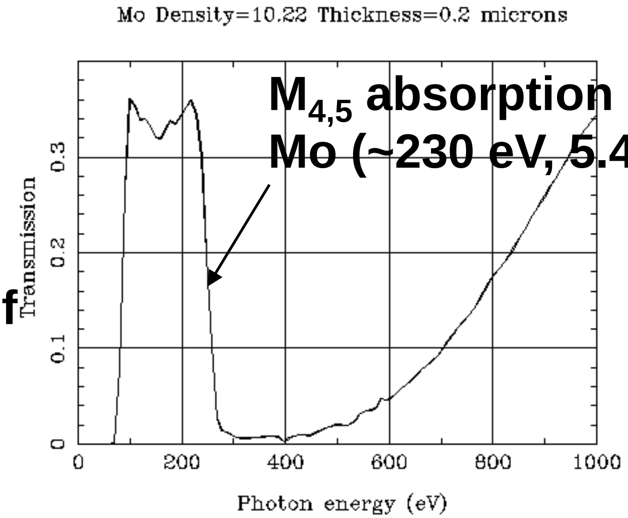

$M_{4,5}$ absorption edge of Mo (~230 eV, 5.4 nm)

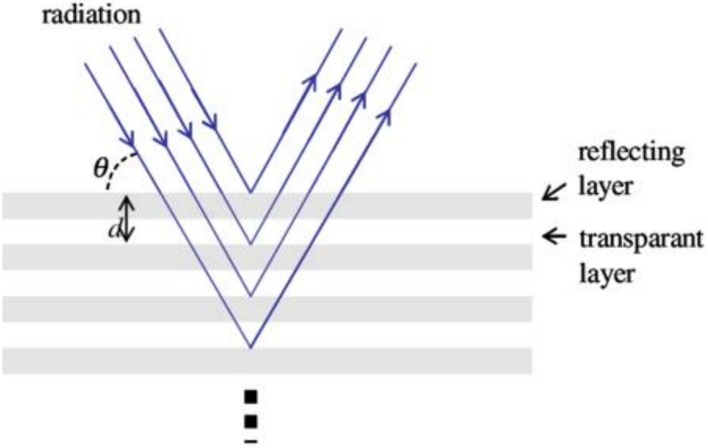

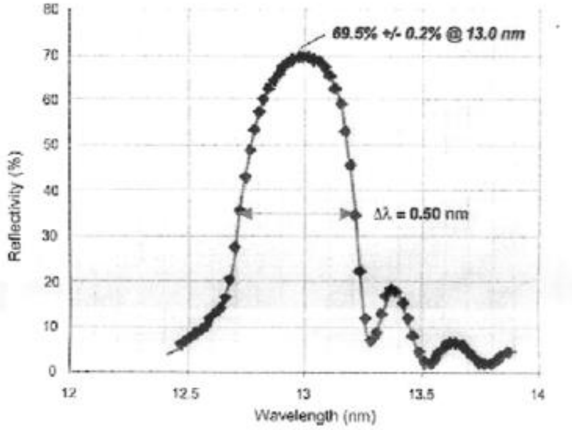

https://henke.lbl.gov/optical_constants/
Mo/Si multilayer coating technology for EUVL, coating uniformity and time stability; E. Louis et al.; SPIE 4146-06, Soft X-ray and EUV Imaging Systems, San Diego, 2000.

13.5-nm EUV light is picked for EUV lithography

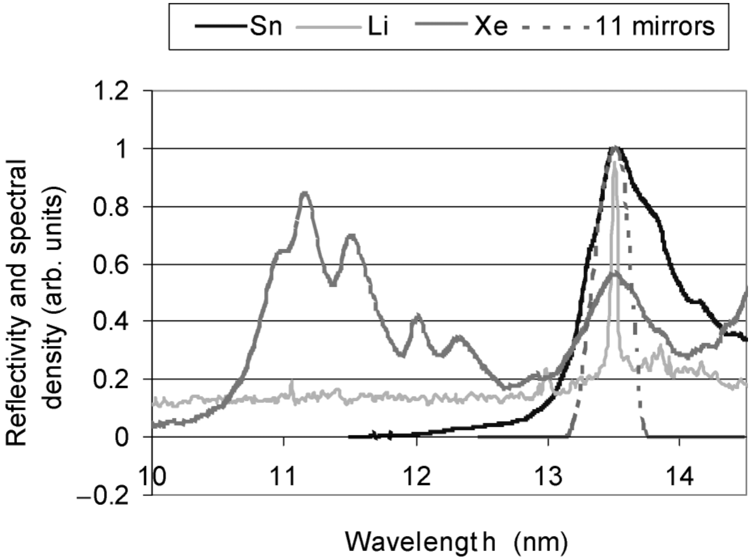

- $\lambda = 13.5\ \mathrm{nm} \pm 1\%$ **is required.**
- **At T=35-40 eV (~450,000 K), in-band emission occurs.**
- **Xenon:**
  - $4p^64d^8 \rightarrow 4p^64d^75p$ **from single ion stage** Xe^{10+}
  - **UTA @ 11 nm**

- **Tin:**
  - $4p^64d^N \rightarrow 4p^54d^{N+1} + 4p^64d^{N-1}4f$ $(1 \leq N \leq 6)$ **in ions ranging from** Sn^{8+} **to** Sn^{12+}
  - **UTA @ 13.5 nm**

- UTA: unresolved transition array

V. Bakshi, EUV sources for lithography

R. S. Abhari, etc., J. Micro/Nanolithography, MEMS, and MOEMS, 11, 021114 (2012)

EUV light is generated from laser-produced plasma (LPP)

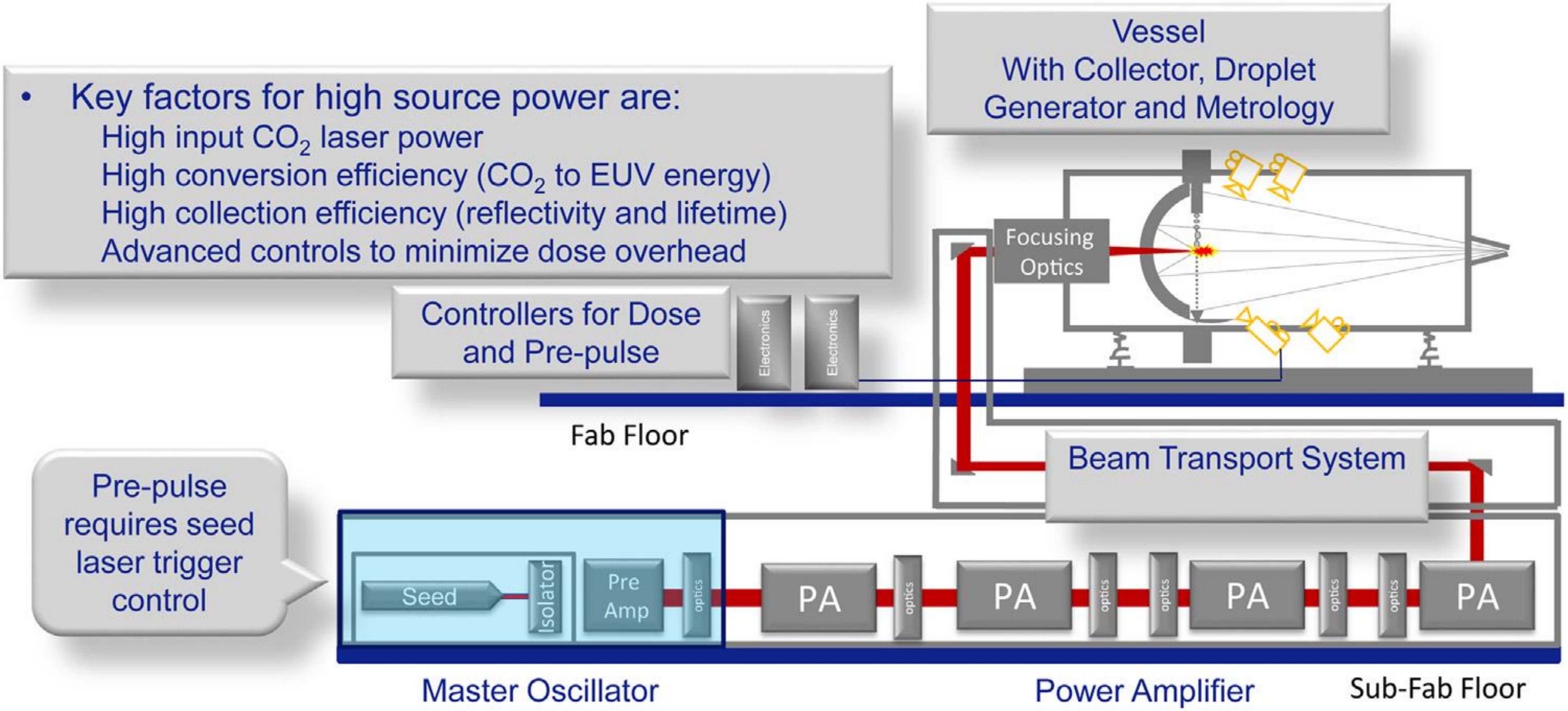

- Key factors for high source power are:
  - High input CO_2 laser power
  - High conversion efficiency (CO_2 to EUV energy)
  - High collection efficiency (reflectivity and lifetime)
  - Advanced controls to minimize dose overhead

D.-K. Yang, etc., *Chip*, **1**, 100019 (2022)

Two laser pulses are used to heat the plasma

Temporal View

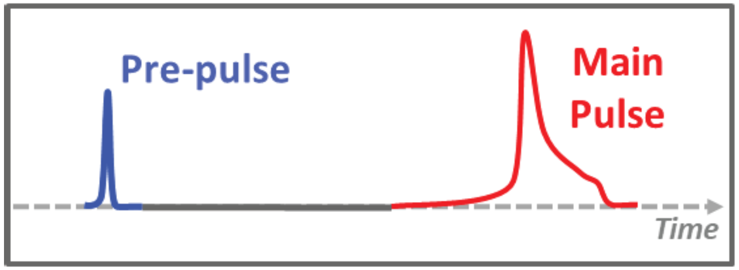

Spatial View

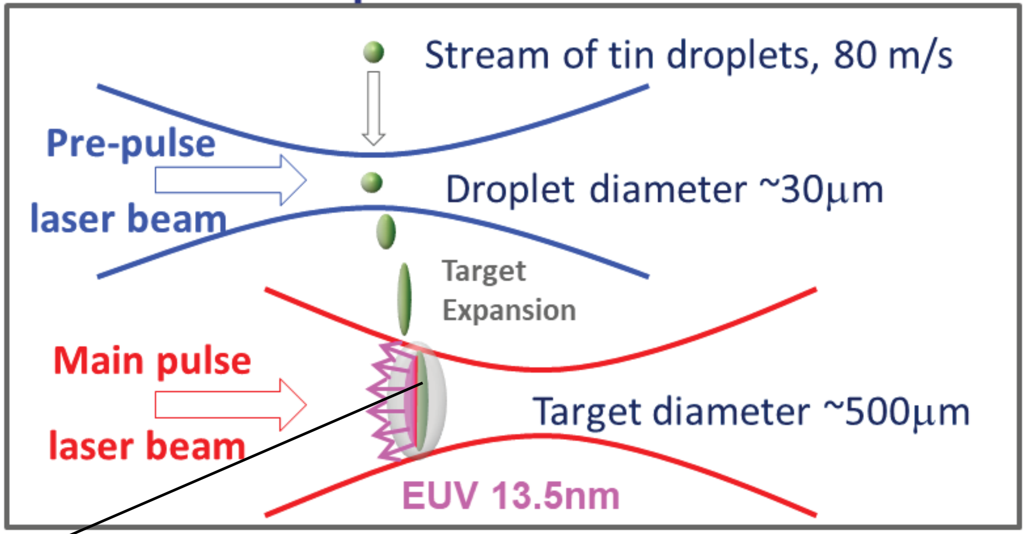

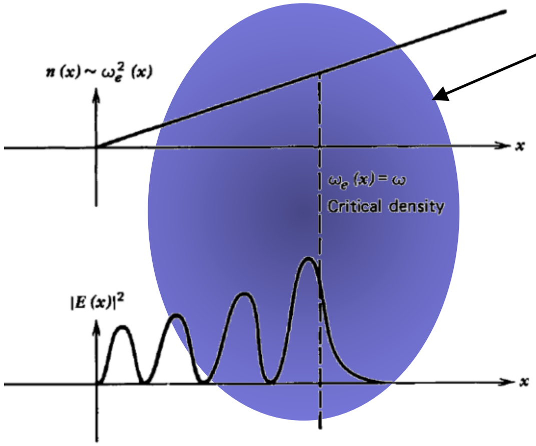

I. Fomenkov, etc., *Synch. Rad. News*, **32**, 3 (2019)

Hydrogen buffer gas with a pressure of ~100 Pa is used to protect the collector mirror

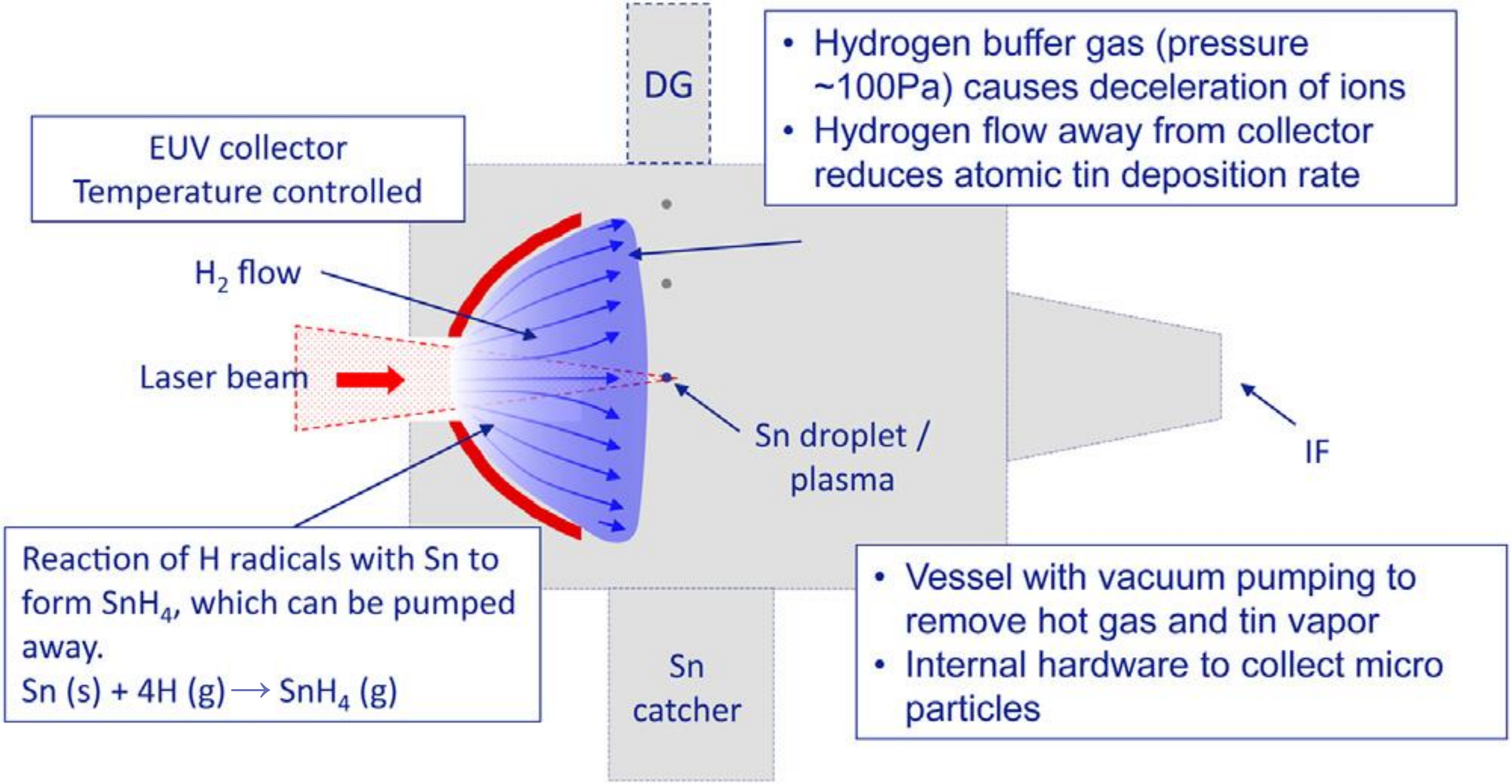

EUV collector
Temperature controlled

- Hydrogen buffer gas (pressure ~100Pa) causes deceleration of ions
- Hydrogen flow away from collector reduces atomic tin deposition rate

Reaction of H radicals with Sn to form SnH_4, which can be pumped away.
$Sn\ (s) + 4H\ (g) \longrightarrow SnH_4\ (g)$

- Vessel with vacuum pumping to remove hot gas and tin vapor
- Internal hardware to collect micro particles

D.-K. Yang, etc., *Chip*, **1**, 100019 (2022)

Laser-produced plasma (LPP) is used in the EUV lithography

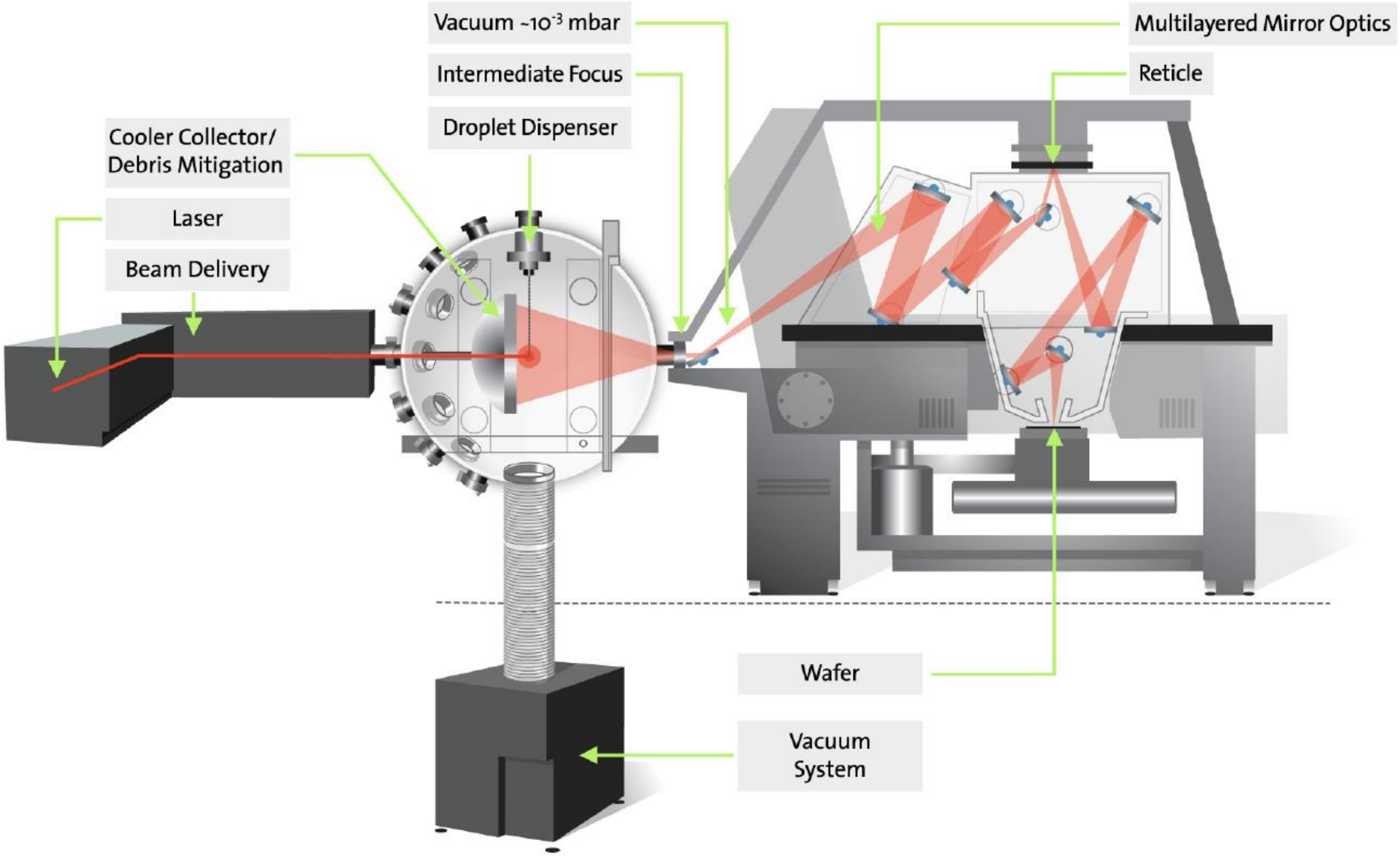

R. S. Abhari, etc., J. Micro/Nanolithography, MEMS, and MOEMS, 11, 021114 (2012)

High harmonic generation from high-power laser

- **For I < 10^{18} w/cm^2**

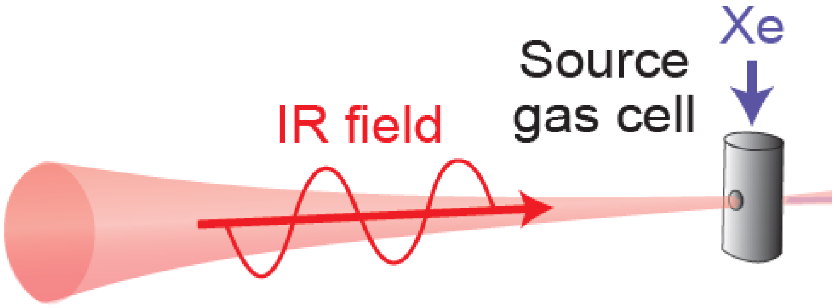

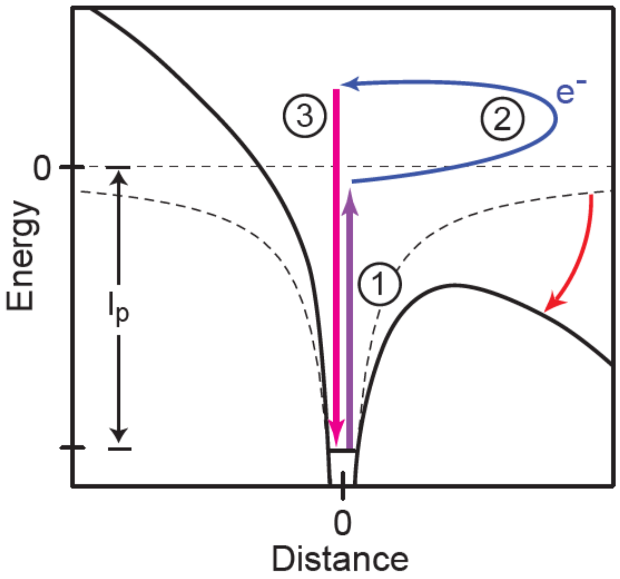

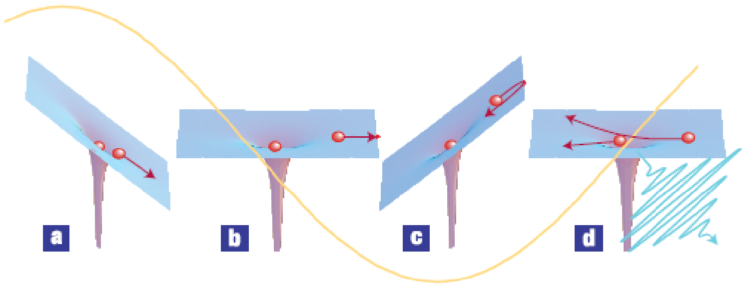

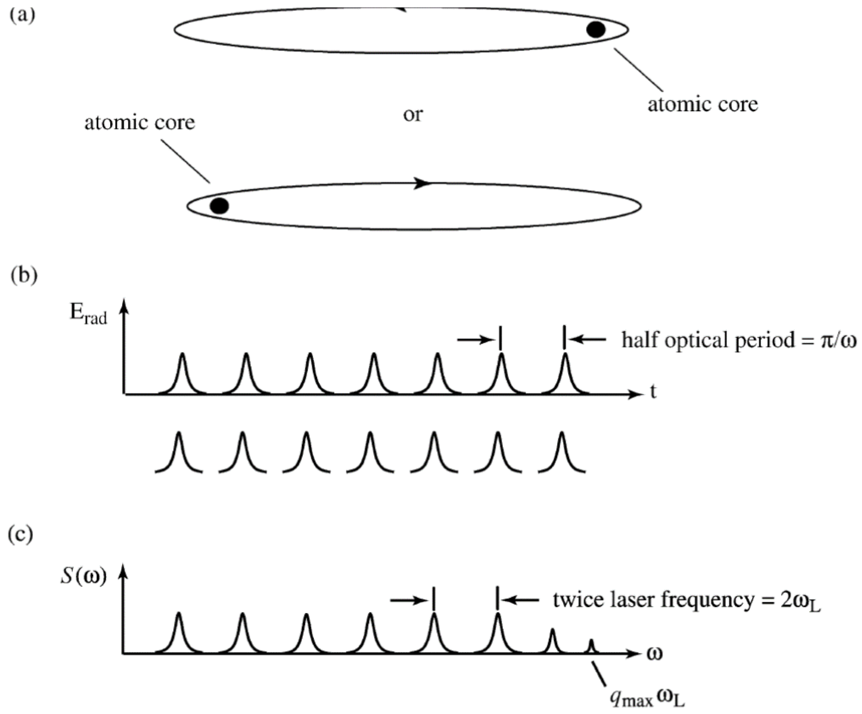

- M. Krüger, etc., Appl. Sci. 9, 378 (2019)
- Nonlinear Optics 3rd edition , by Robert W. Boyd
- P. B. Corkum and F. Krausz, Nature Phys., 3, 381 (2007)

EUV light can be generated using discharged-produced plasma

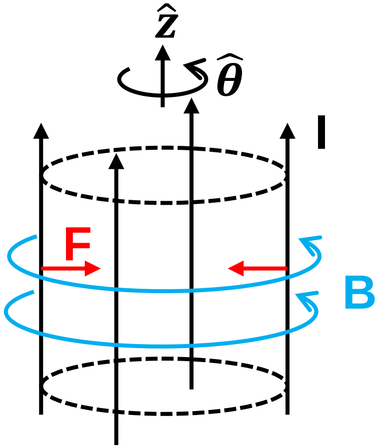

- **Adiabatic compression:**

$$TV^{\gamma-1} = \text{const} \quad T_f = T_o\left(\frac{r_o}{r_f}\right)^{4/3}$$

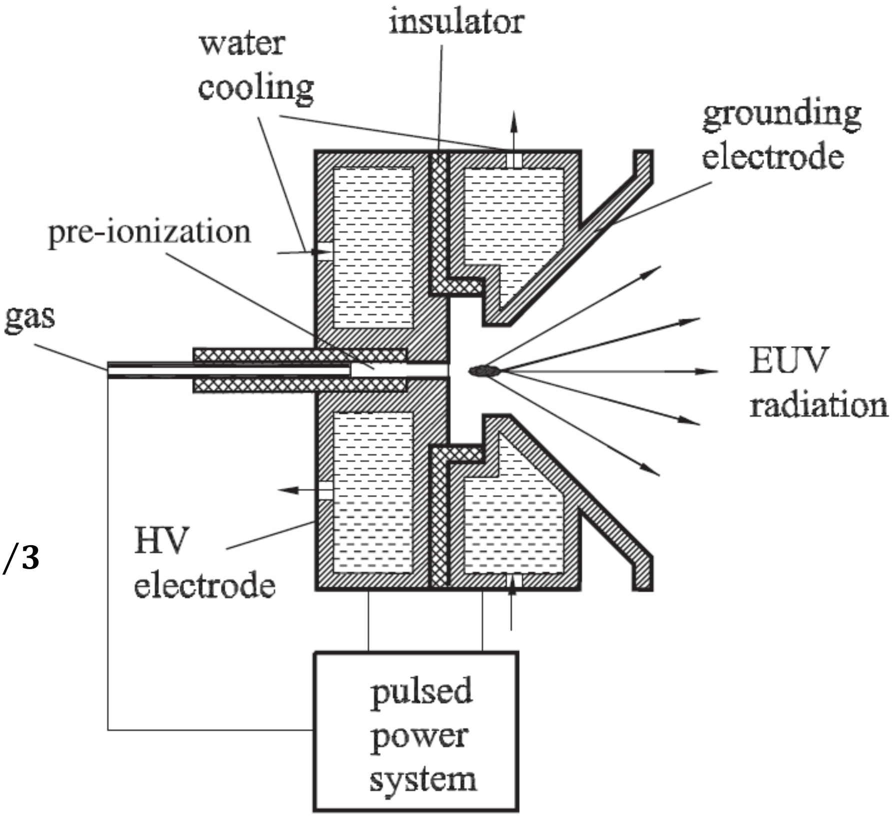

- JPDAP_37_p3254_2004_EUV sources using Xe and Sn discharge plasmas

Light source and display systems

Plasma display panel (PDP)

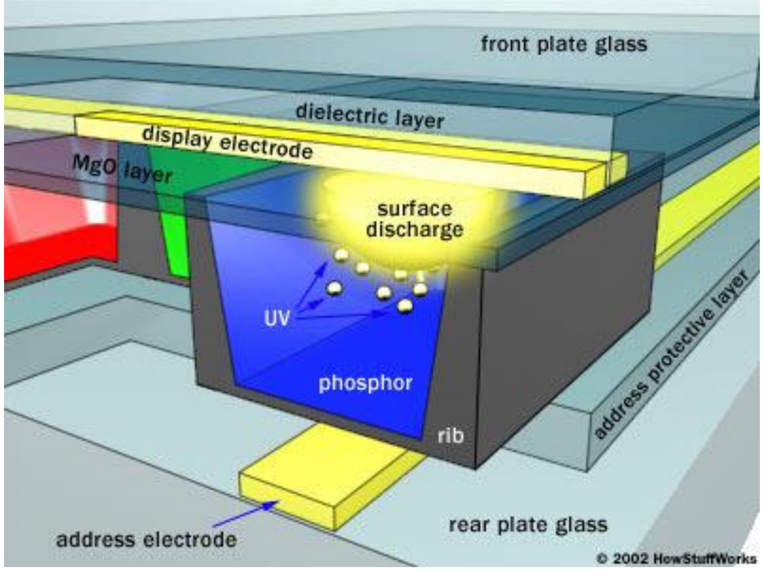

Liquid crystal display (LCD)

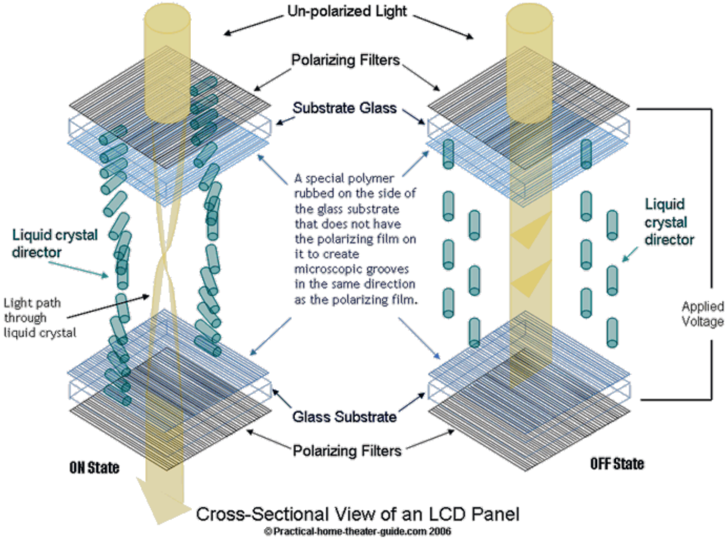

Outlines

- Cathode Ray Tube
- Color space (CIE 1931 color spaces)
- History of plasma display panel (PDP)
- Design of PDP
- Liquid crystal display (LCD)
- LCD vs PDP

CRT

Cathode Ray Tube uses electron beams to light the fluorescent screen

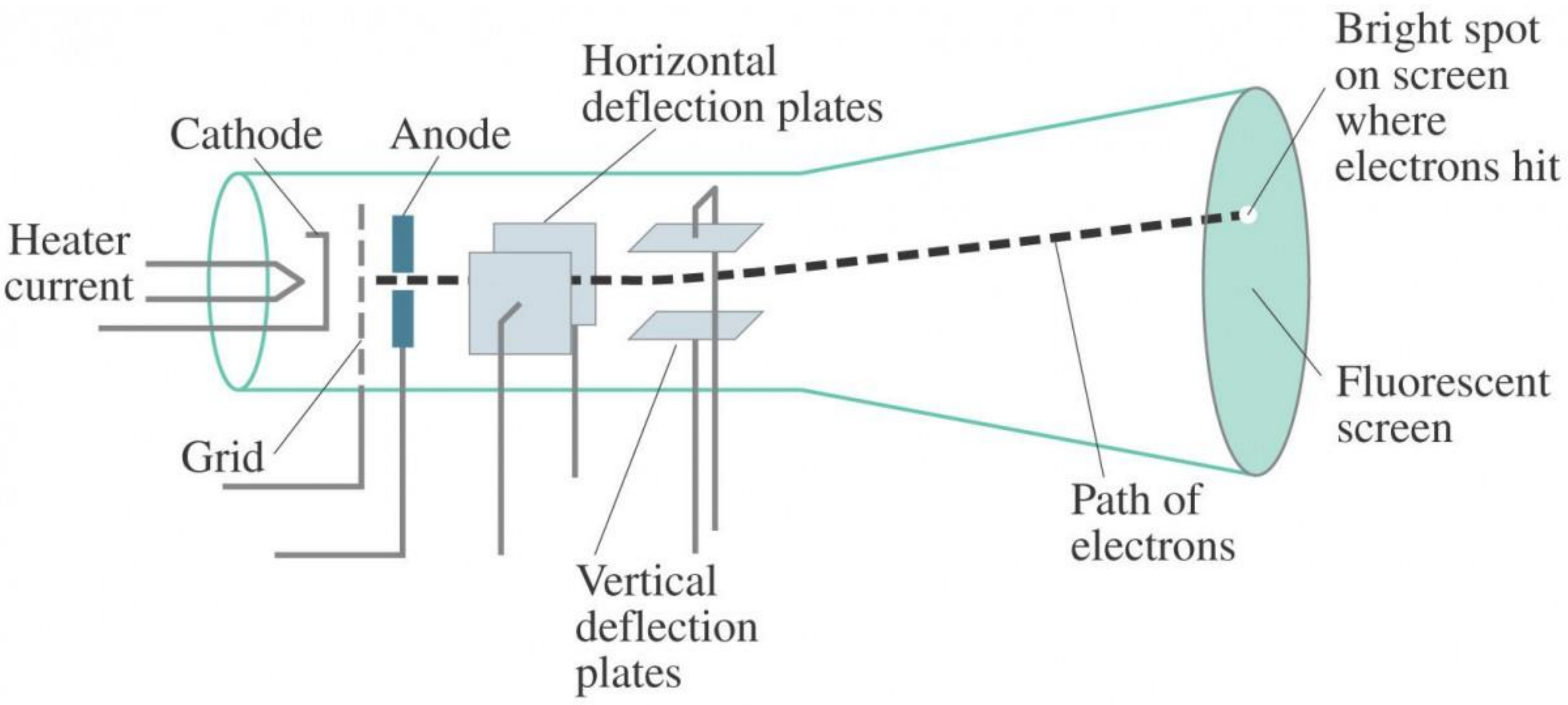

http://www.sciencefacts.net/cathode-ray-tube-crt.html

The image is shown by scanning through the whole screen with the single electron beam

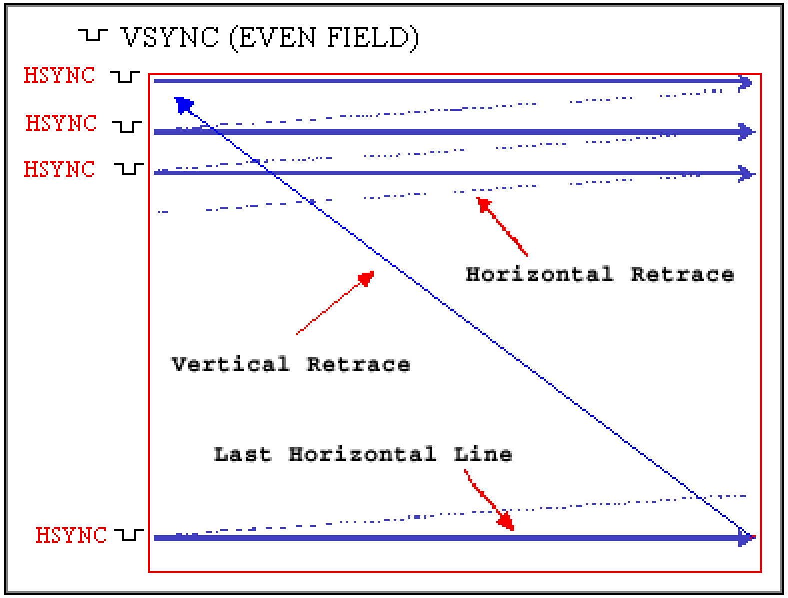

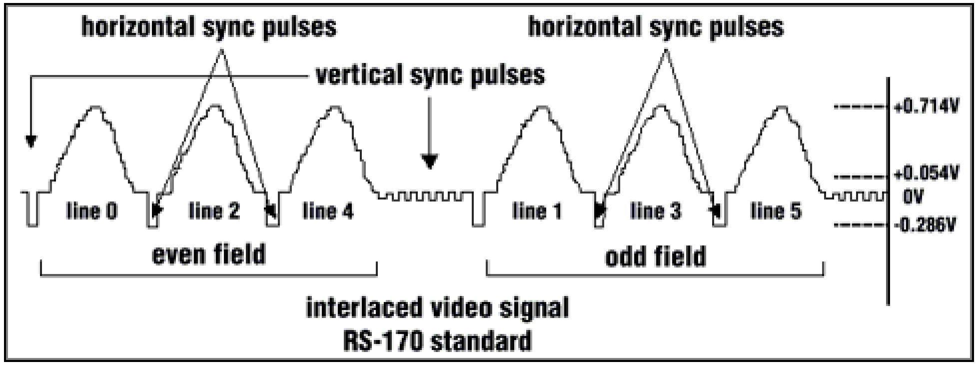

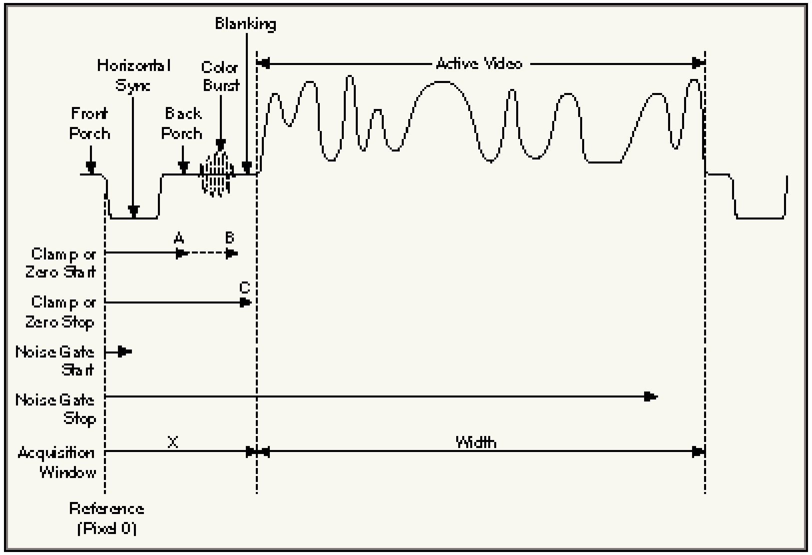

http://www.ni.com/white-paper/3020/en/#toc2

Color image is formed by using three electron beams scanning through three different color channels

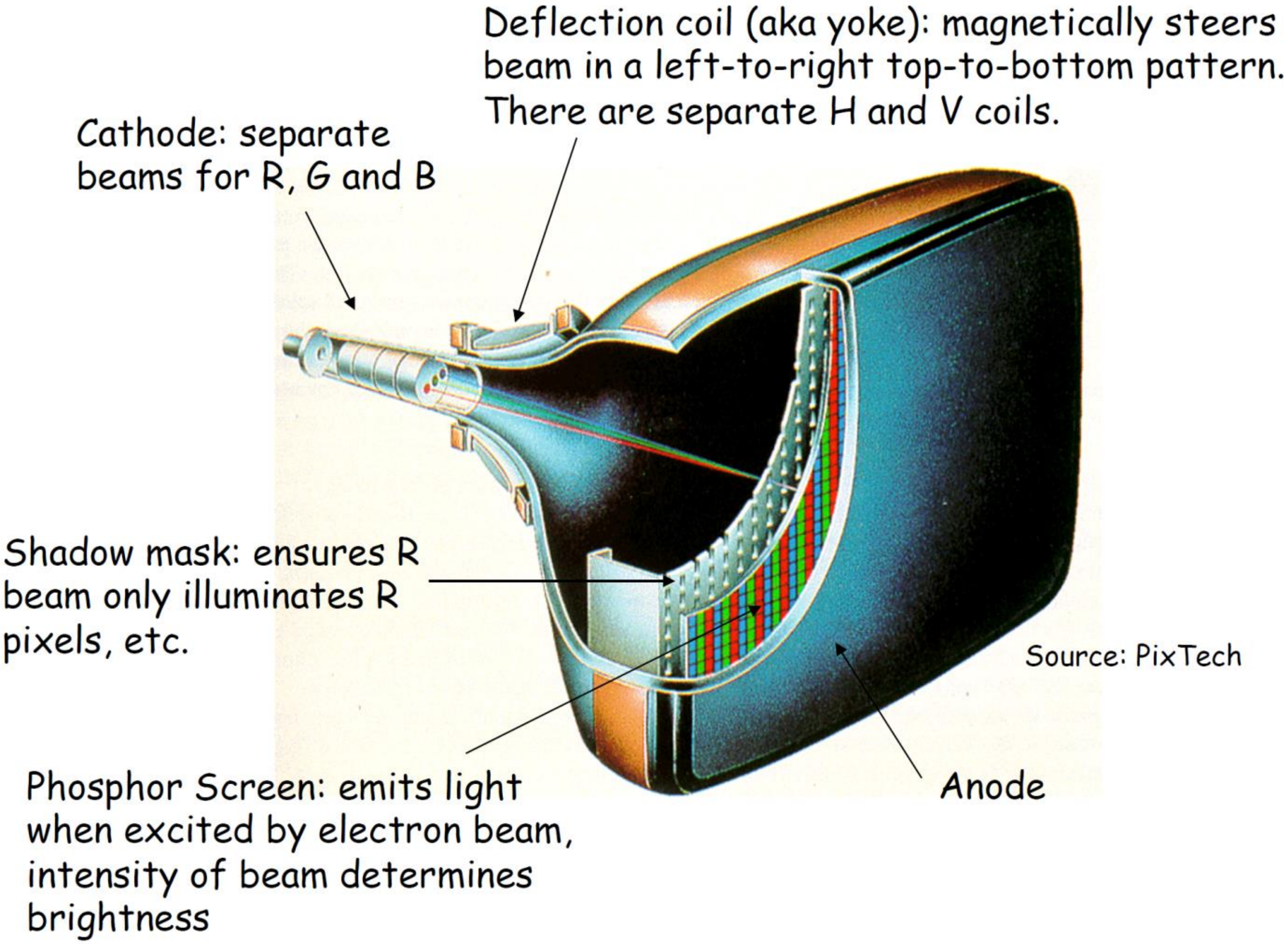

Deflection coil (aka yoke): magnetically steers beam in a left-to-right top-to-bottom pattern. There are separate H and V coils.

Cathode: separate beams for R, G and B

Shadow mask: ensures R beam only illuminates R pixels, etc.

Source: PixTech

Phosphor Screen: emits light when excited by electron beam, intensity of beam determines brightness

Anode

http://web.mit.edu/6.111/www/f2008/handouts/L12.pdf

Color space

Color can be created using three primary colors

Additive primaries

Subtractive primaries

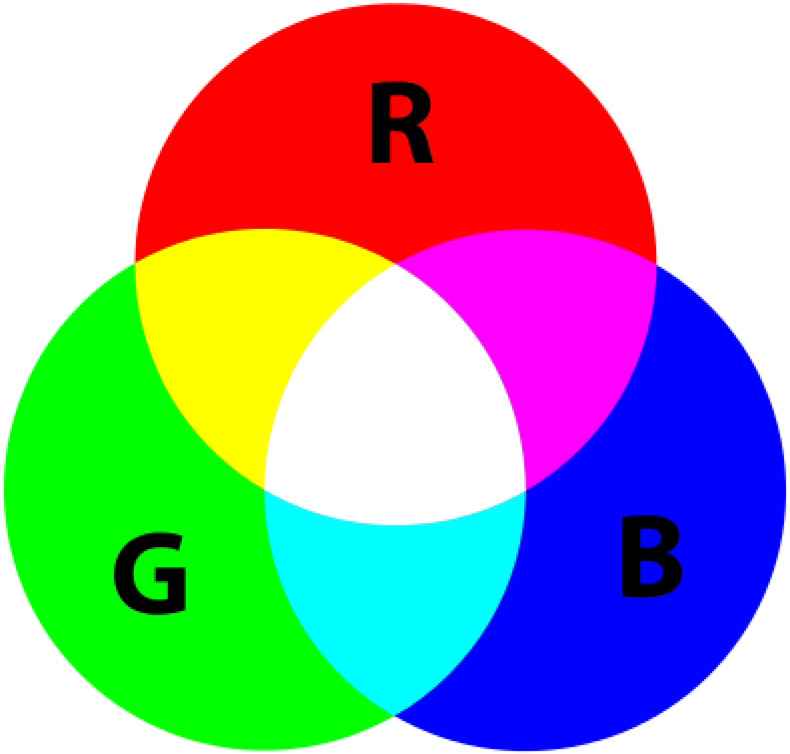

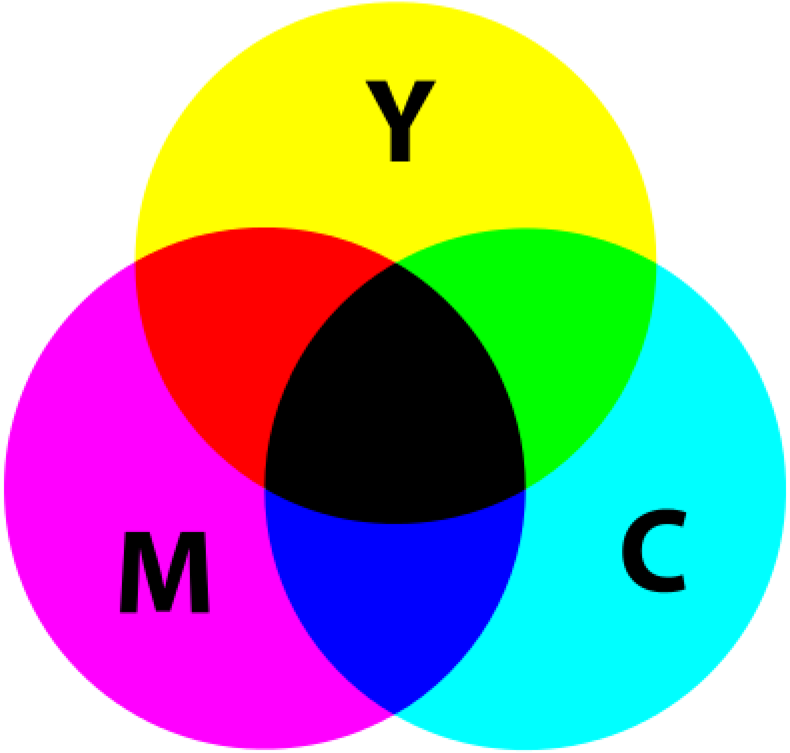

https://en.wikipedia.org/wiki/Primary_color

Human retina has three kinds of “cones” that have different spectral response

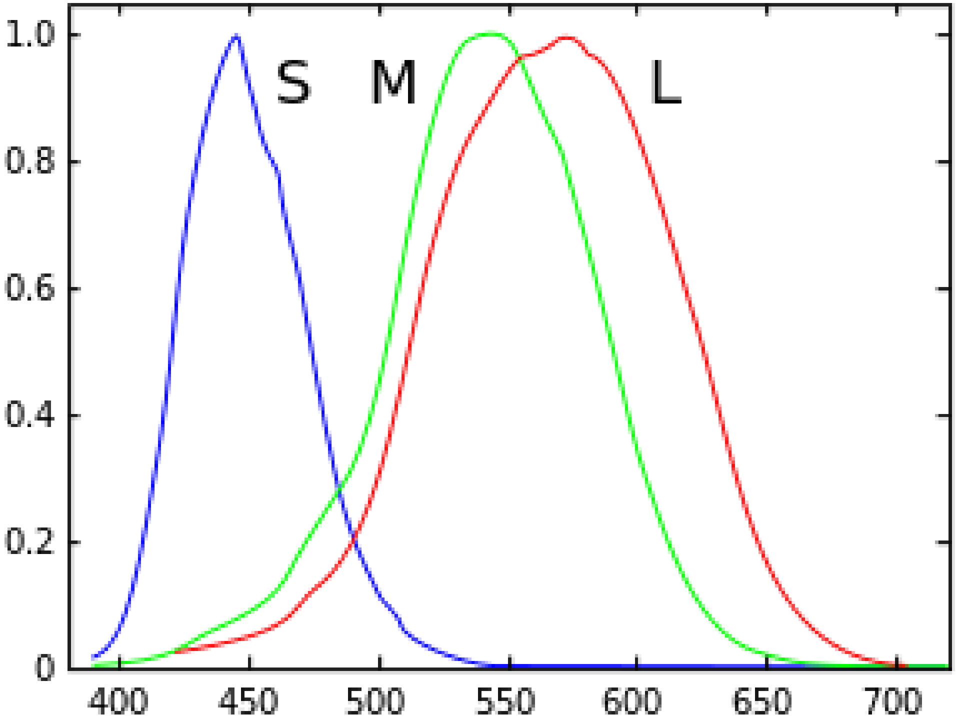

Spectral response of retina “cones” are tested using light sources with single wavelength

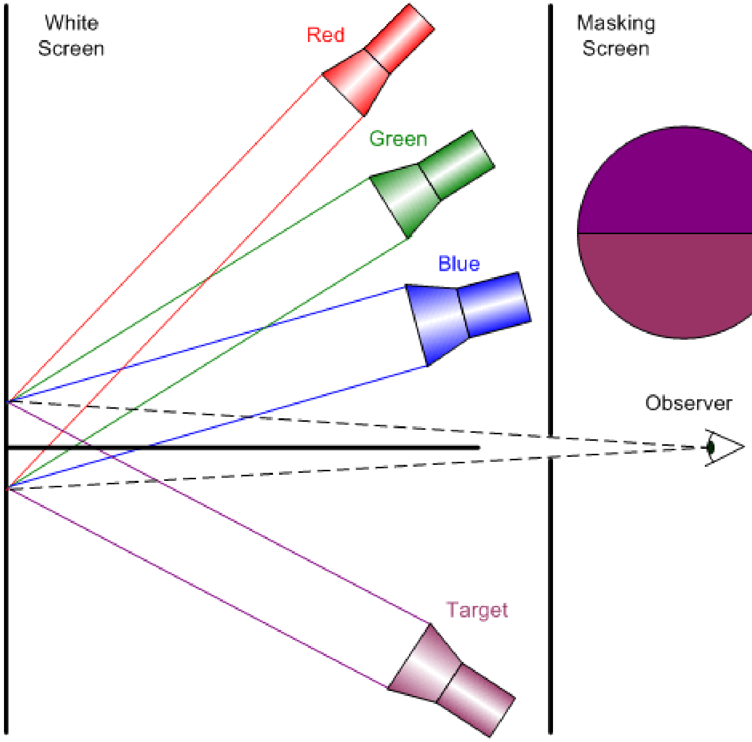

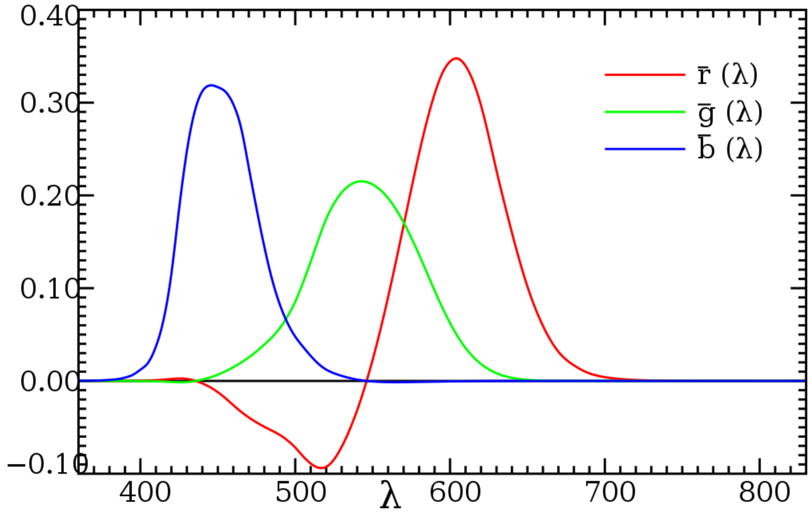

http://betterphotographytutorials.com/2011/08/01/light-and-colors-%E2%80%93-part-3/
https://en.wikipedia.org/wiki/CIE_1931_color_space

The CIE 1931 color space chromaticity diagram is the standard color space

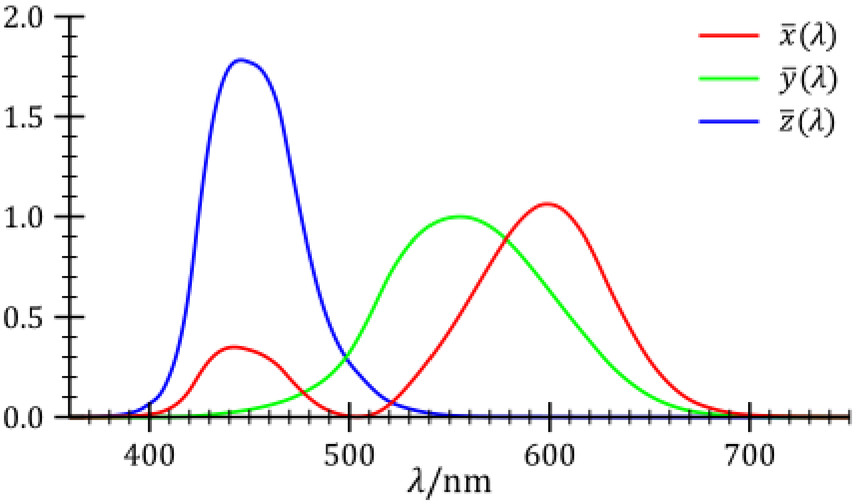

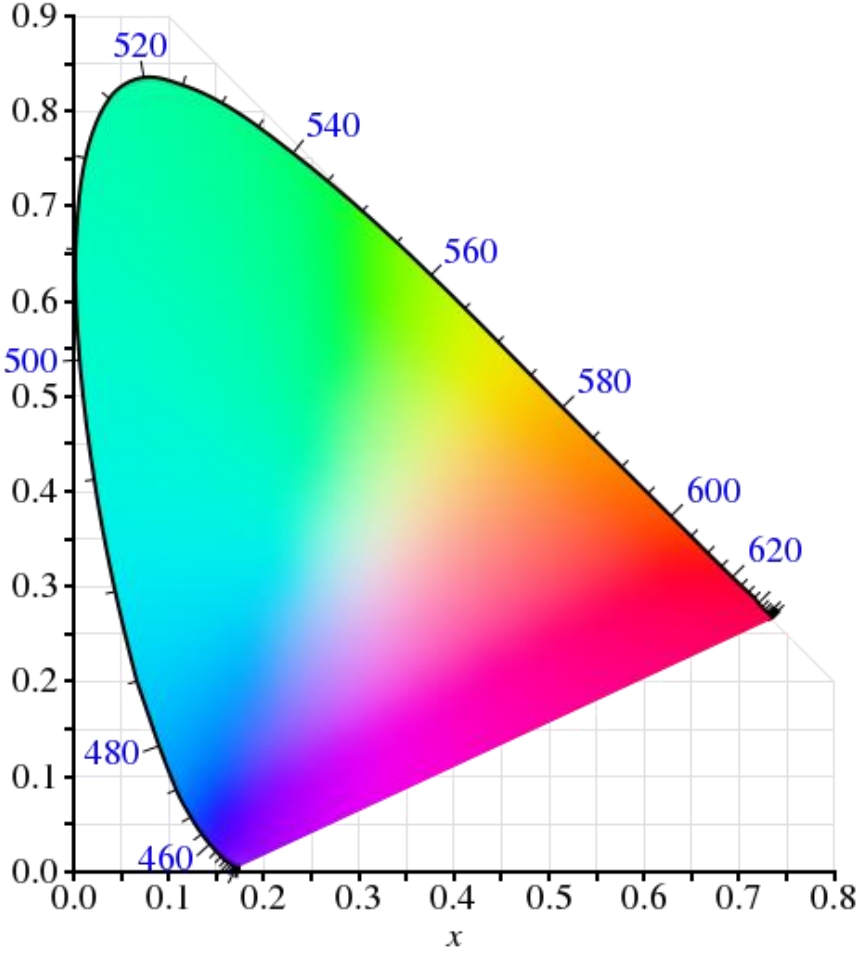

https://en.wikipedia.org/wiki/CIE_1931_color_space

Plasma display panel was invented at the University of Illinois in 1967

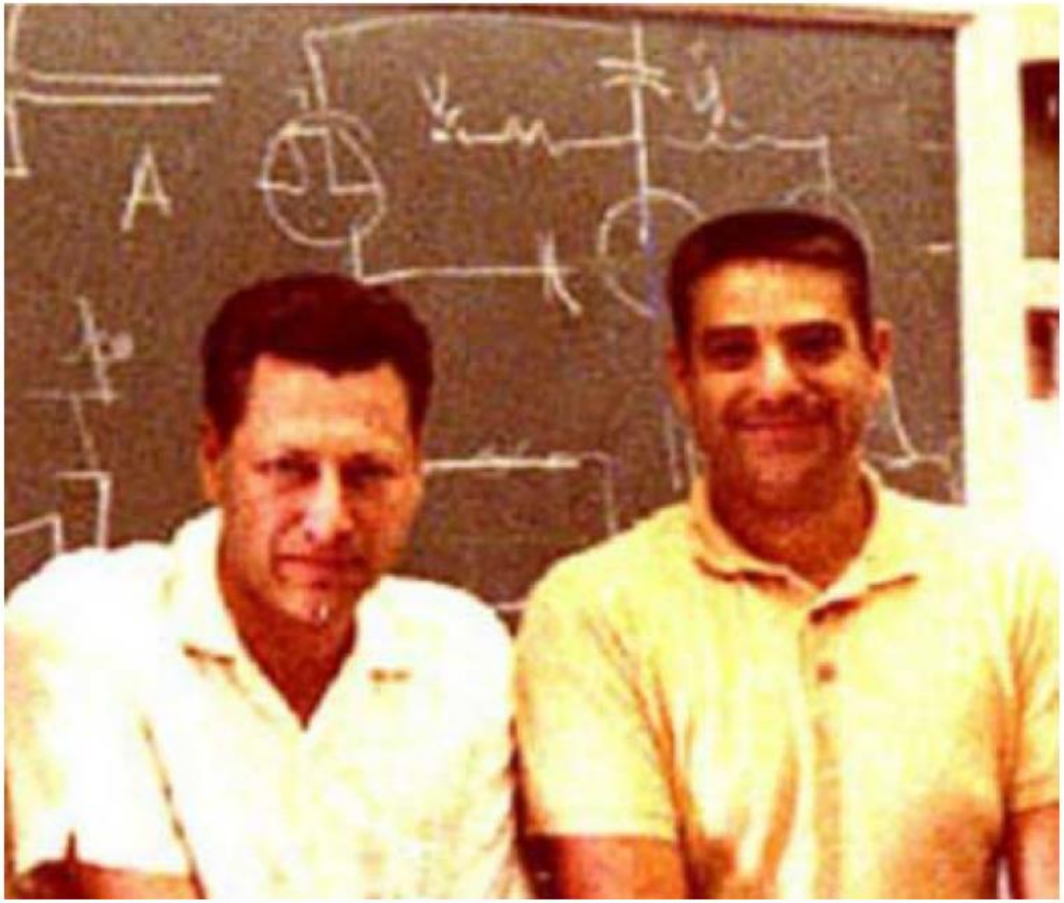

Prof. H. Gene Slottow **Prof. Donald L. Bitzer**

L. F. Weber, IEEE Trans. Plas. Scien., *34*, 268, 2006

PDP was invented due to a need for Programmed Logic for Automatic Teaching Operations (PLATO) in 1960s

1981 Plato V

https://topwallpapers.pw/computer/keyboards-computers-history-teletype-typewriters-desktop-hd-wallpaper-1035981/
https://en.wikipedia.org/wiki/Punched_tape
https://en.wikipedia.org/wiki/PLATO_(computer_system)

The positive column in a glow discharge is used to excite phosphors in color PDP

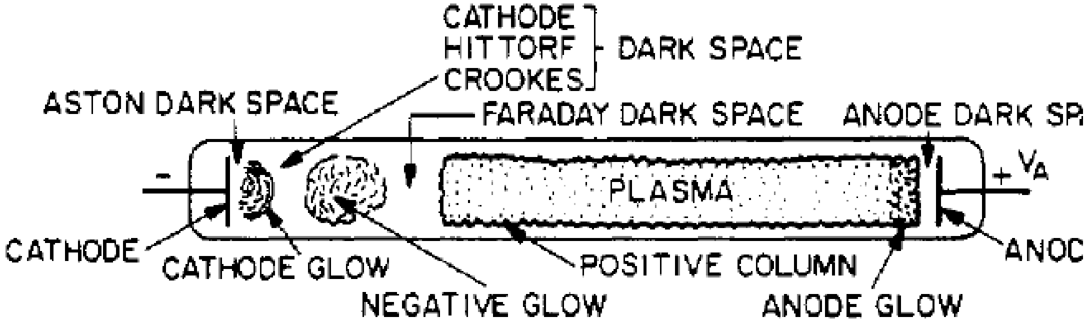

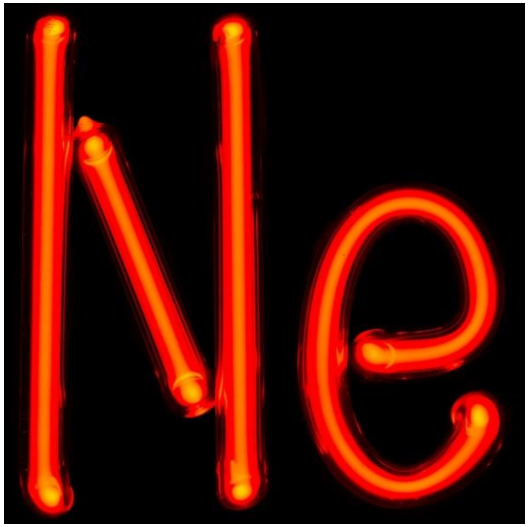

- **Majority of monochrome PDPs use the negative glow as the light source**
- **The positive column is used to excite phosphors in fluorescent lamps and in color PDPs**

Industrial plasma engineering, volume 1, by J. Reece Roth
https://en.wikipedia.org/wiki/Neon_lighting

Early plasma panel (PD) attached to the glass vacuum system used for the first plasma displays at UI

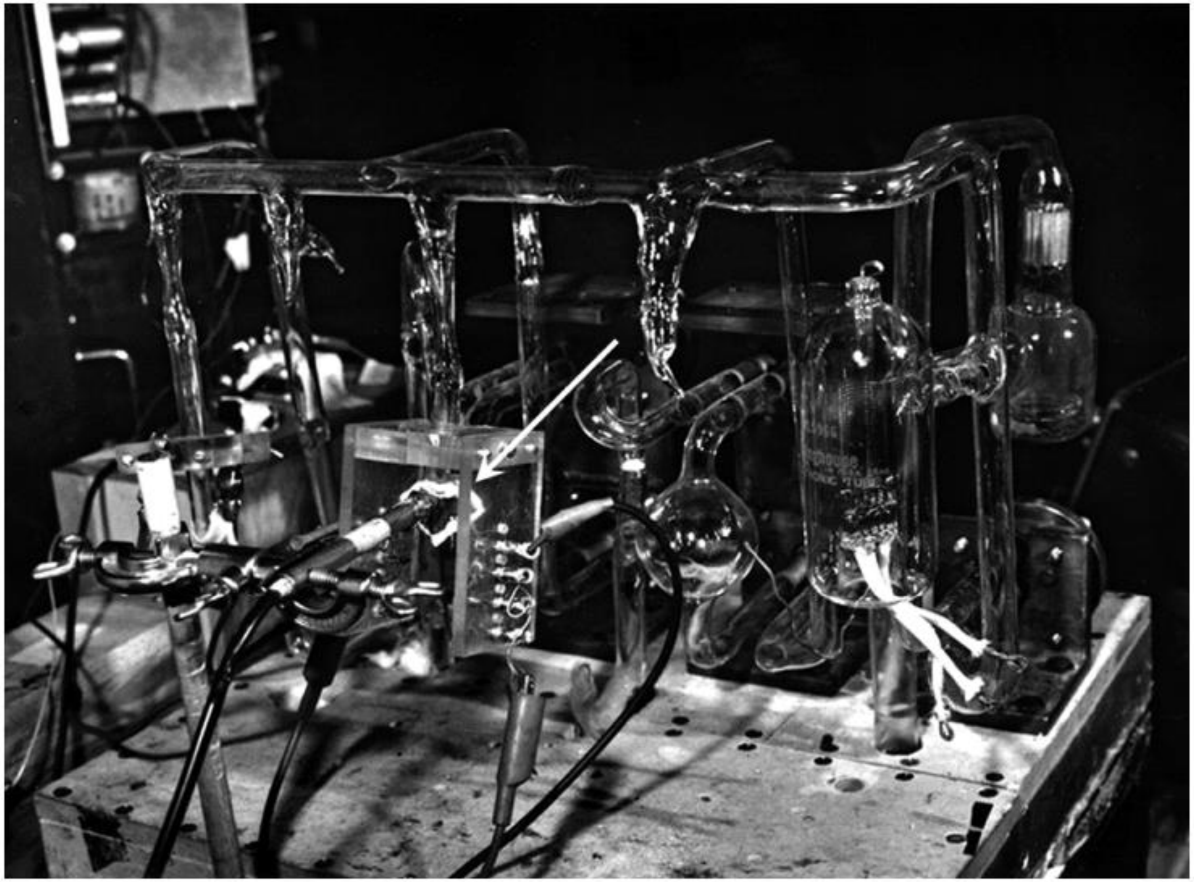

- **It had the same alternating sustain voltage, neon, gas, and dielectric glass insulated electrodes that are used for plasma TVs today.**

L. F. Weber, IEEE Trans. Plas. Scien., *34*, 268, 2006

Early plasma panel (PD) attached to the glass vacuum system used for the first plasma displays at UI

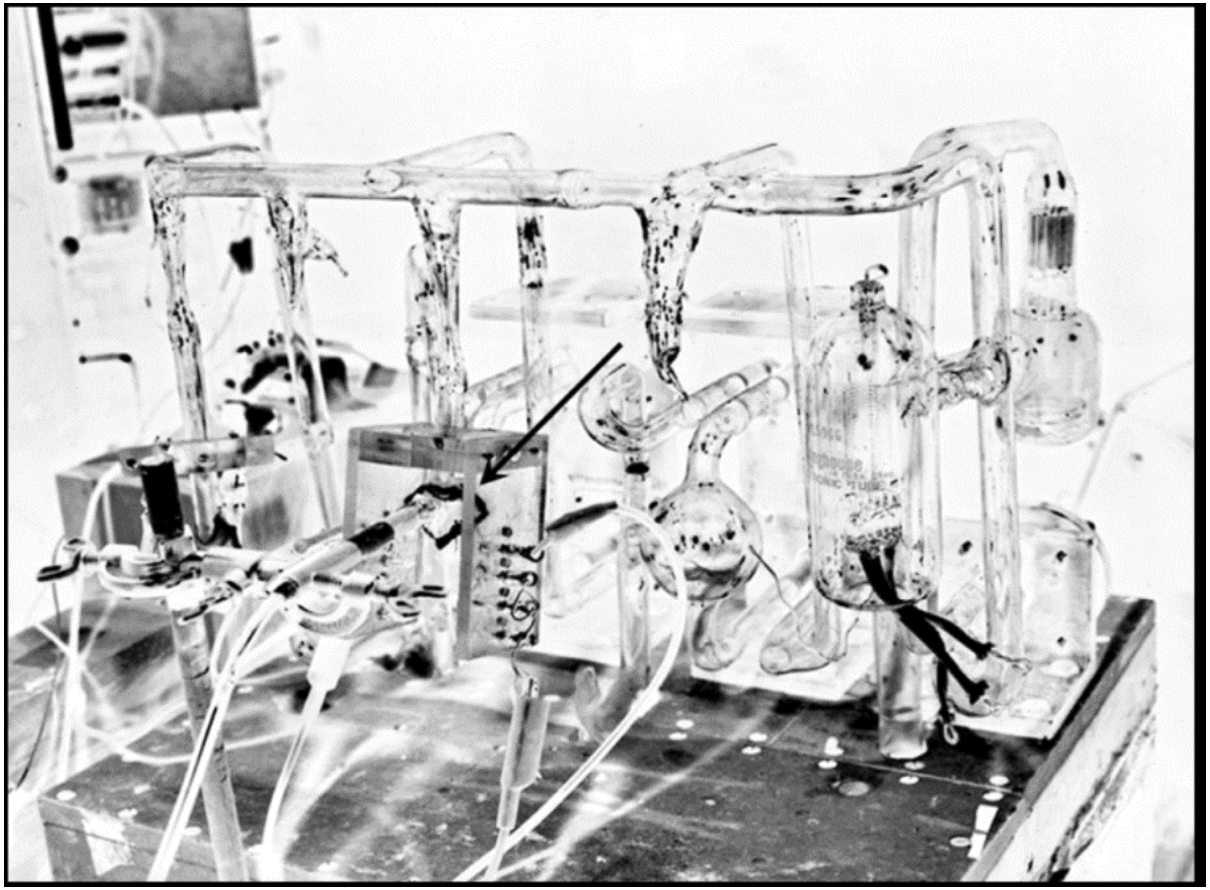

- **It had the same alternating sustain voltage, neon, gas, and dielectric glass insulated electrodes that are used for plasma TVs today.**

L. F. Weber, IEEE Trans. Plas. Scien., *34*, 268, 2006

Early 4x4 pixel panel has achieved matrix addressability for the first time

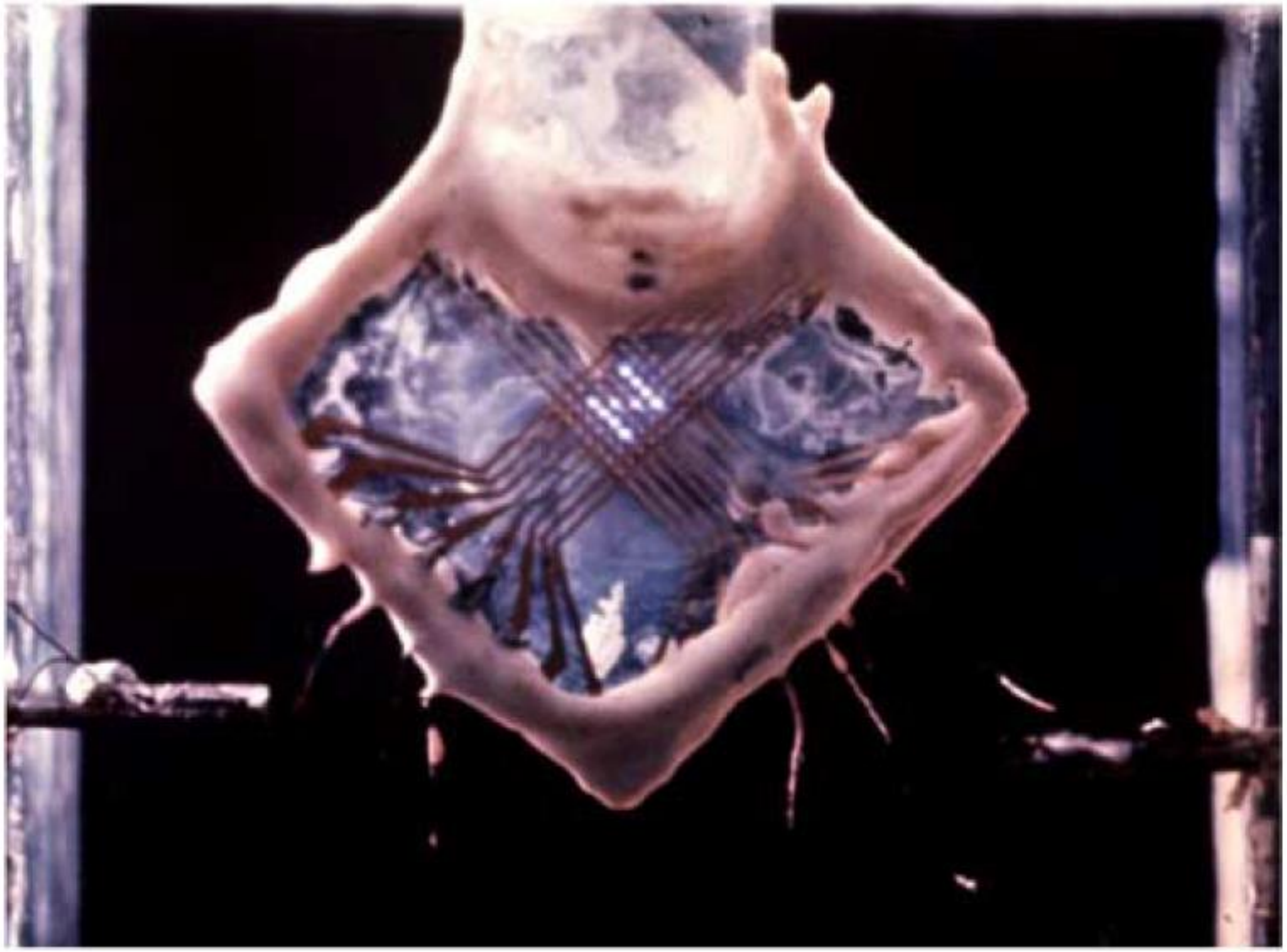

L. F. Weber, IEEE Trans. Plas. Scien., *34*, 268, 2006

Early 4x4 pixel panel has achieved matrix addressability for the first time

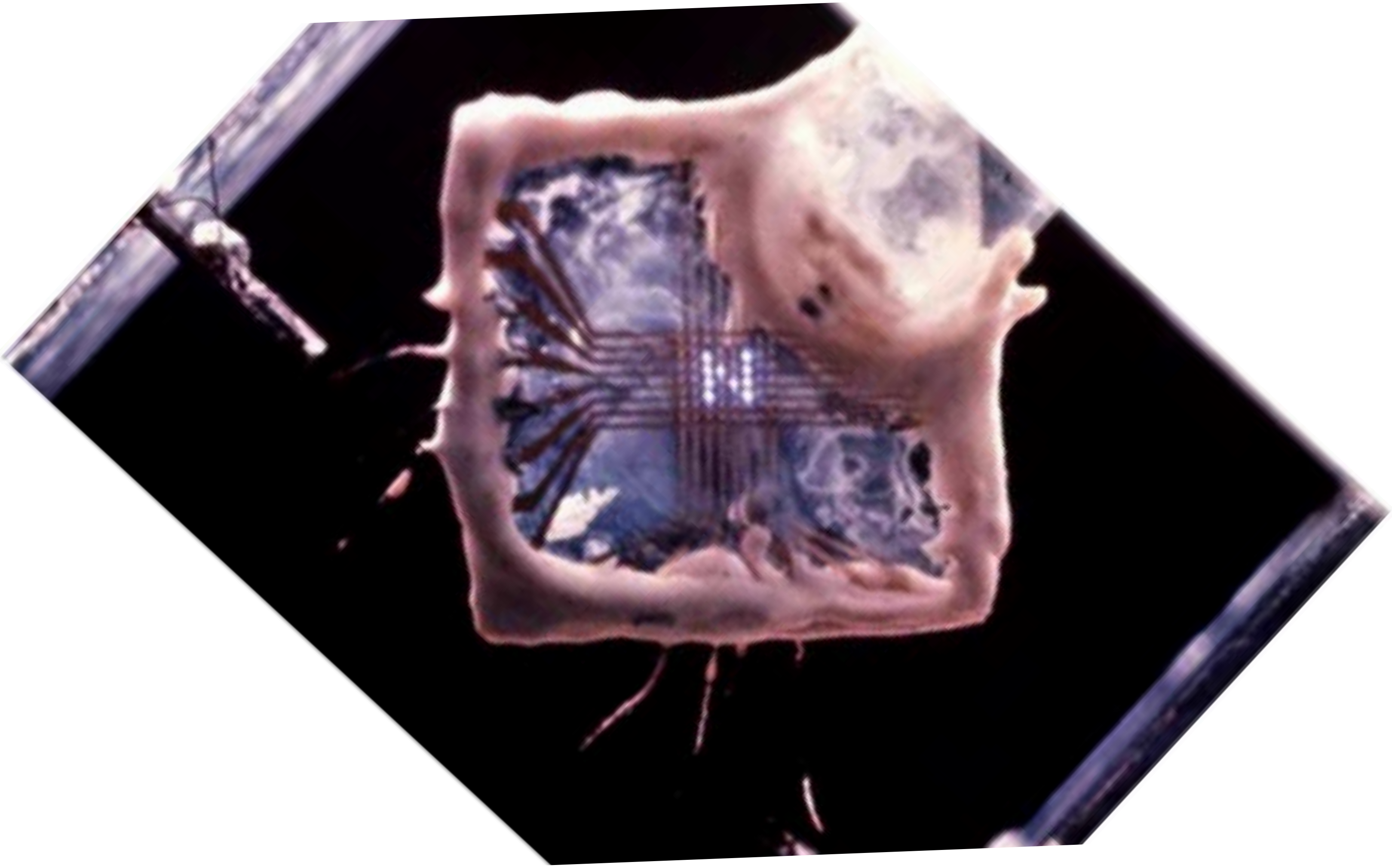

L. F. Weber, IEEE Trans. Plas. Scien., *34*, 268, 2006

A 16x16 pixel PD, developed in 1967, needed to be addressed manually

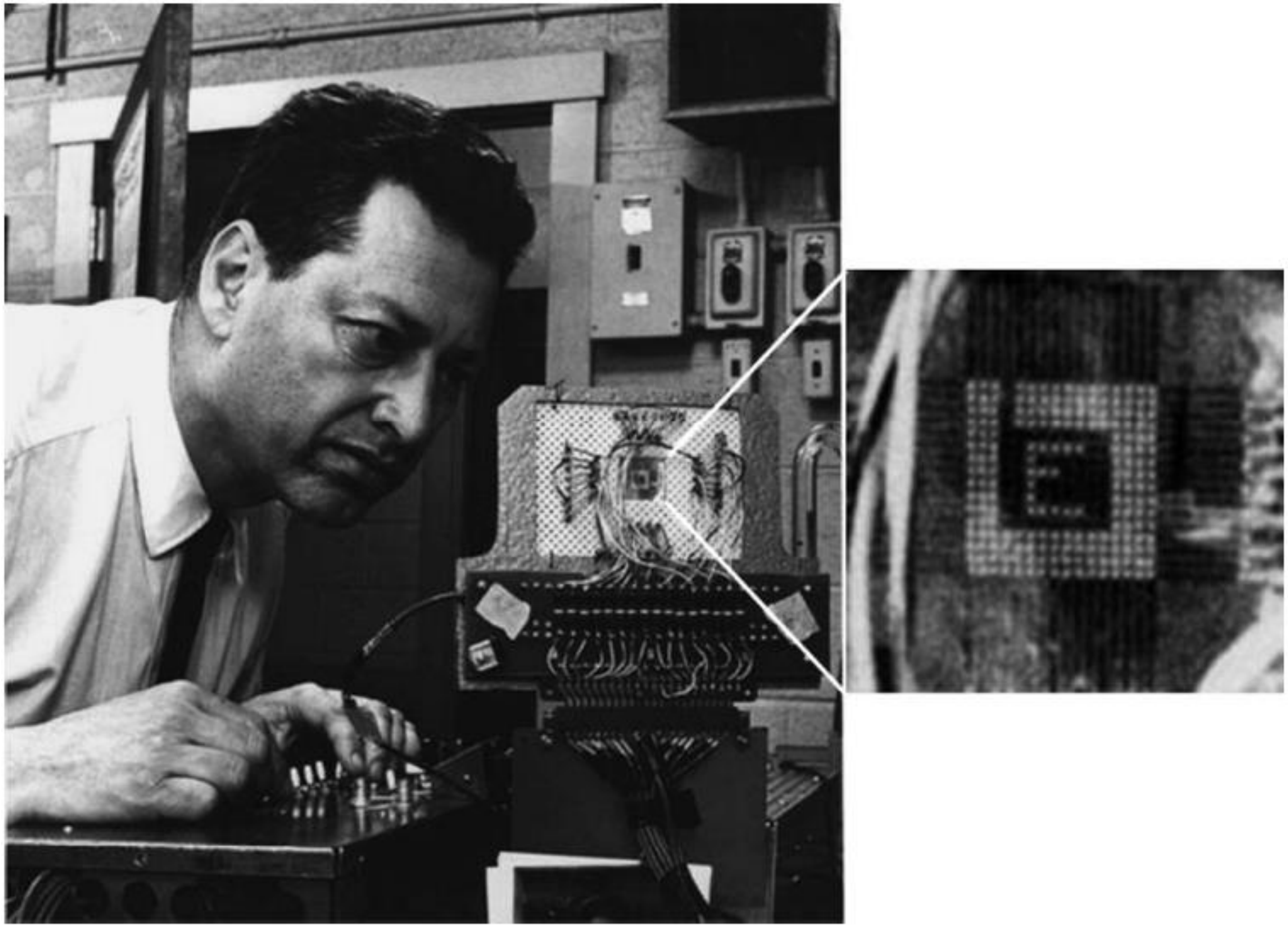

L. F. Weber, IEEE Trans. Plas. Scien., *34*, 268, 2006

First color PD was three cell prototype with red and green color phosphors excited by a xenon gas discharge

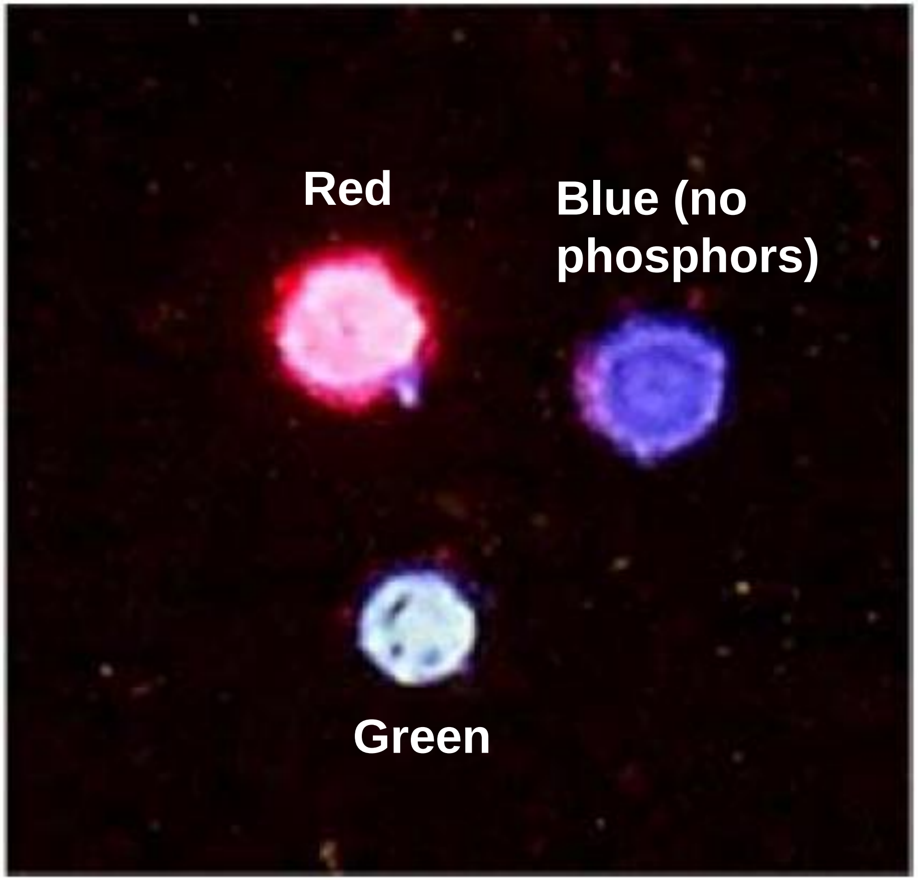

L. F. Weber, IEEE Trans. Plas. Scien., *34*, 268, 2006

Open-cell structure developed in 1968

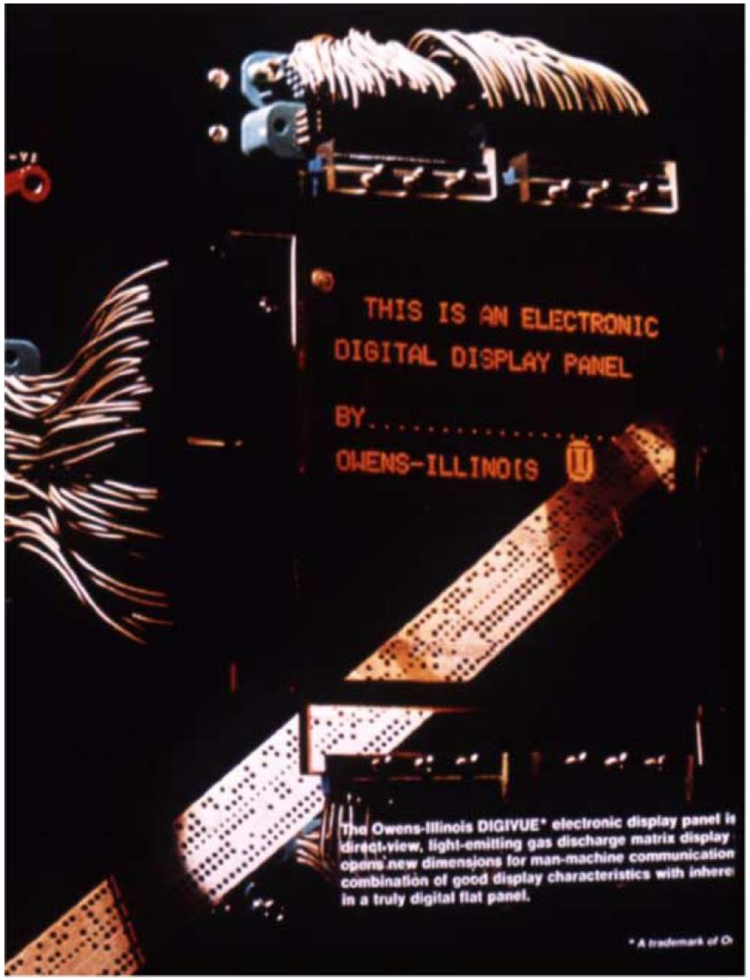

The Owens-Illinois DIGIVUE* electronic display panel is
direct-view, light-emitting gas discharge matrix display
opens new dimensions for man-machine communication
combination of good display characteristics with inhere
in a truly digital flat panel.

* A trademark of O

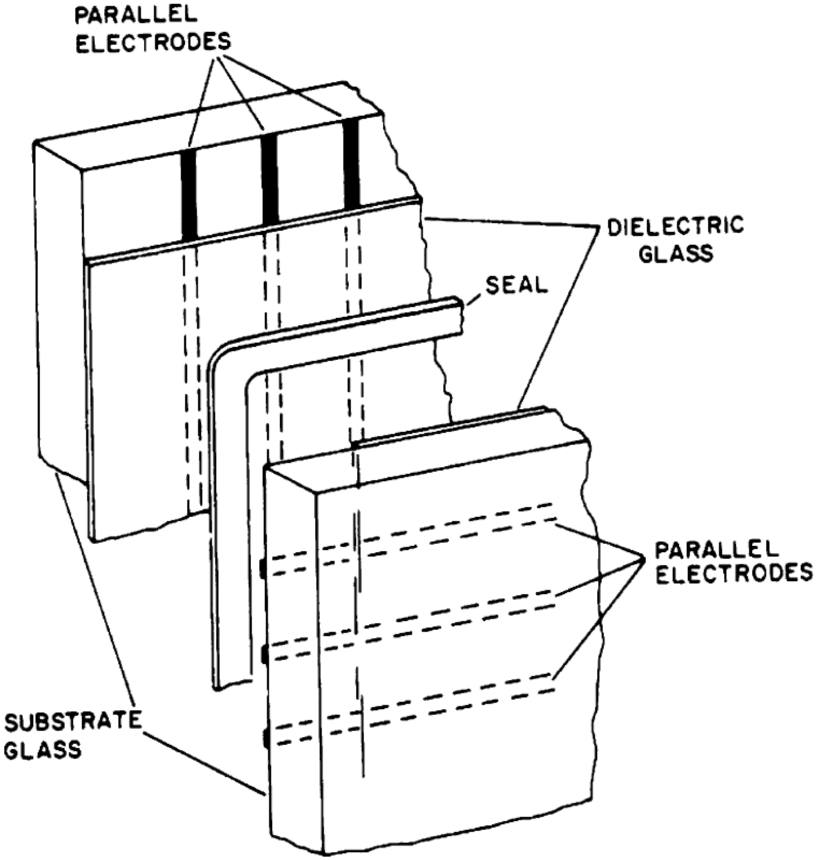

- **It could be baked under vacuum at 350 ^{o}C to drive out contaminants.**

L. F. Weber, IEEE Trans. Plas. Scien., *34*, 268, 2006

More progress

1968, University of Illinois
16x16 pixels

1971, Owens-Illinois
512x512 pixels

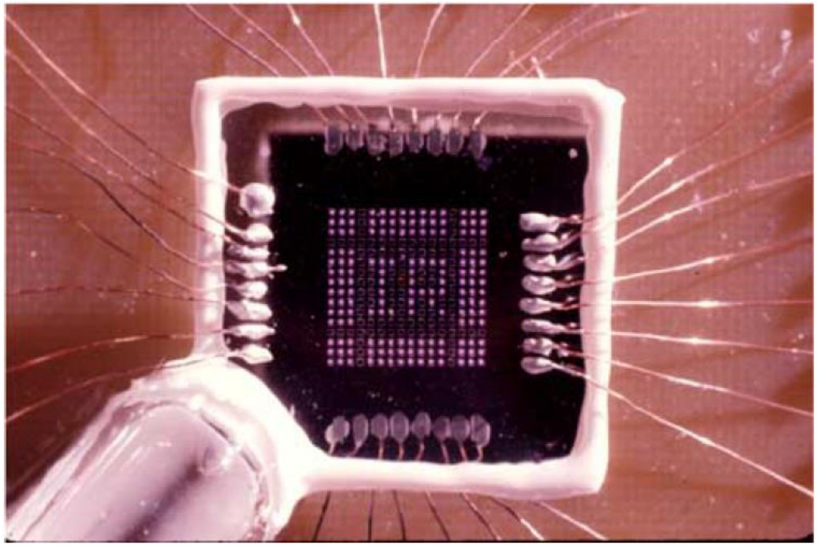

L. F. Weber, IEEE Trans. Plas. Scien., *34*, 268, 2006

Color PDPs had short display lifetime due to the degradation of color phosphors caused by ion sputtering

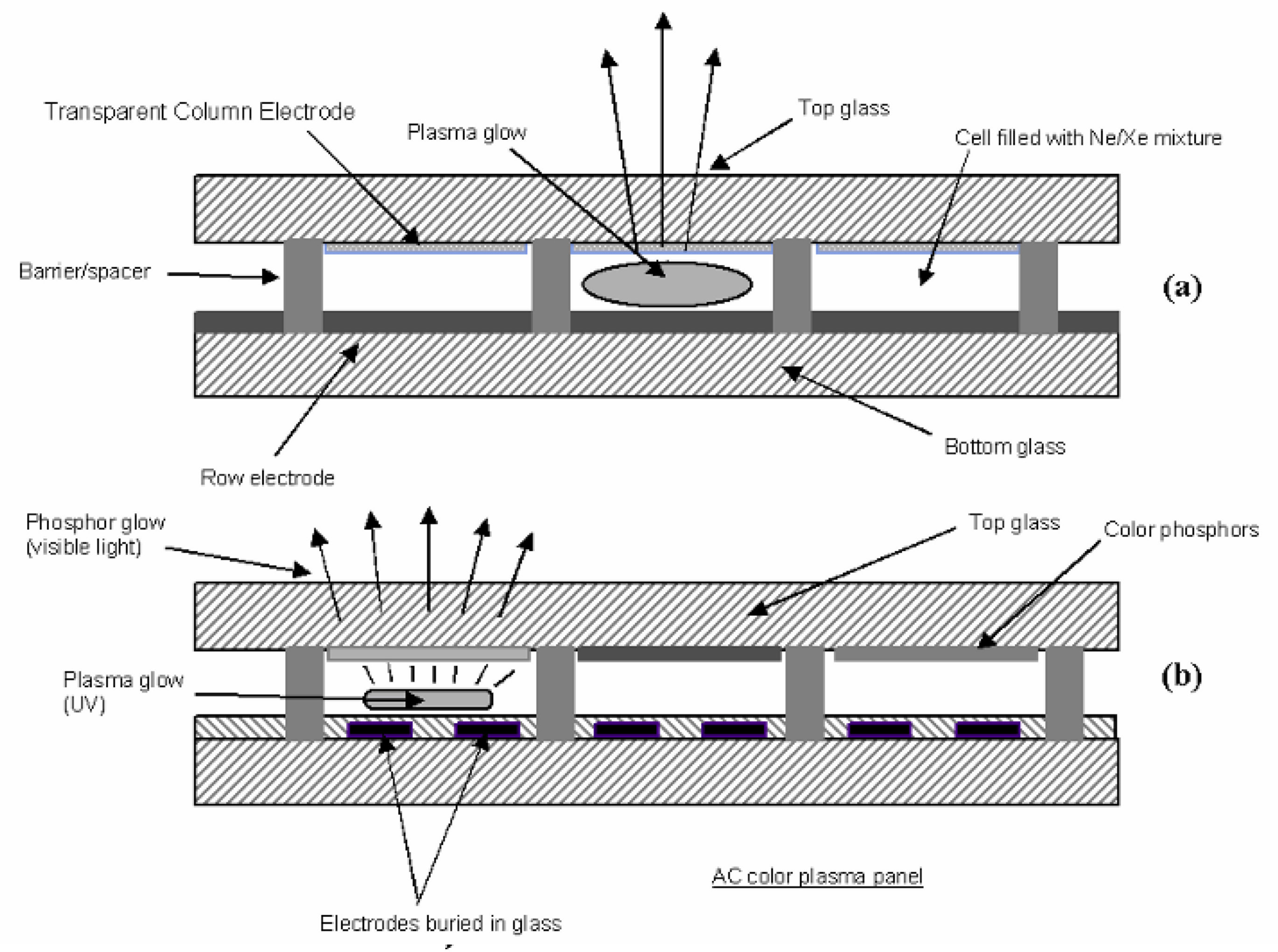

http://what-when-how.com/display-interfaces/display-technologies-and-applications-display-interfaces-part-3/

A lower breakdown voltages can be obtained with very small amounts of added gas

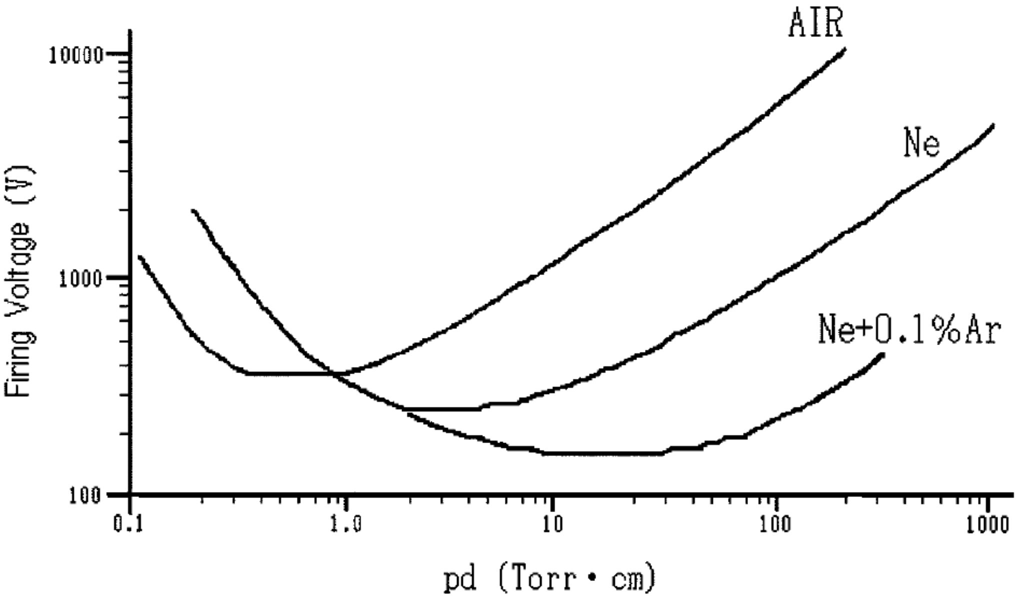

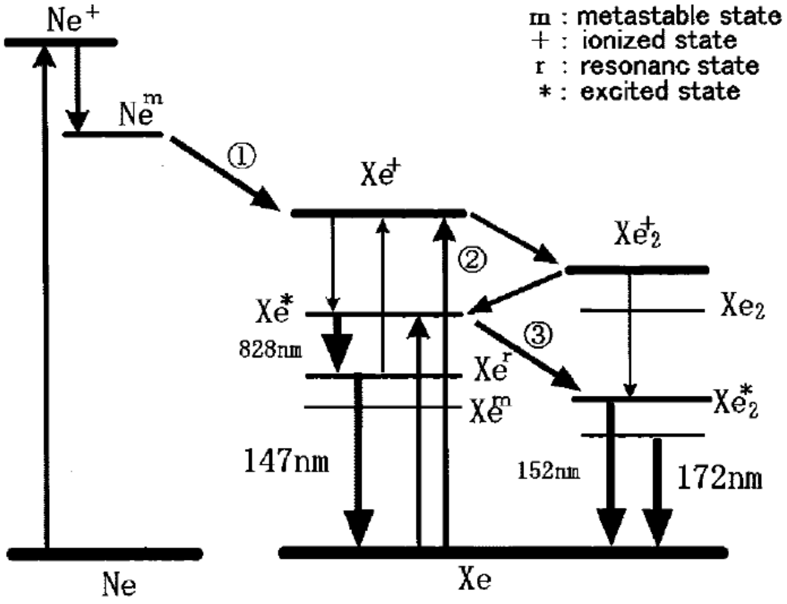

AT&T three-electrode patent

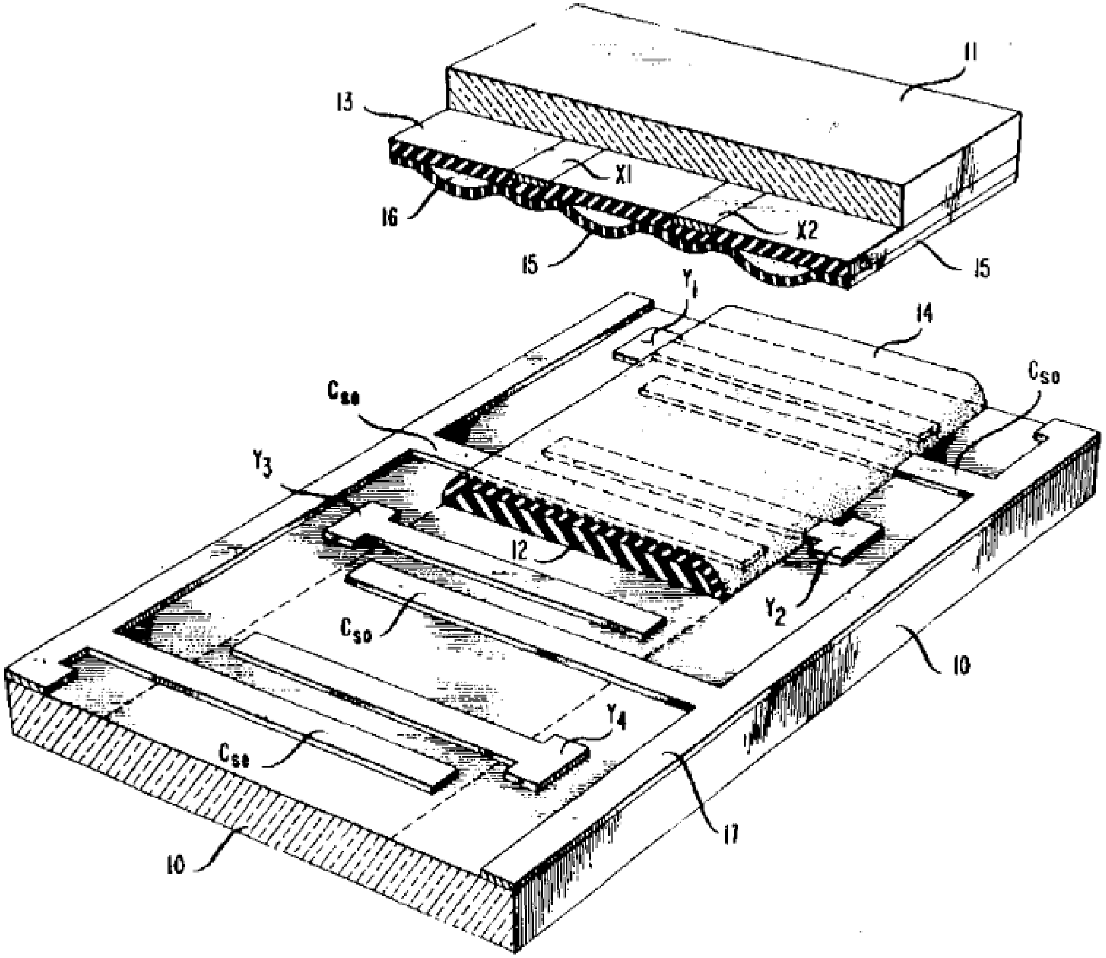

L. F. Weber, IEEE Trans. Plas. Scien., *34*, 268, 2006

Reflective phosphor geometry is used in most of today's plasma TVs

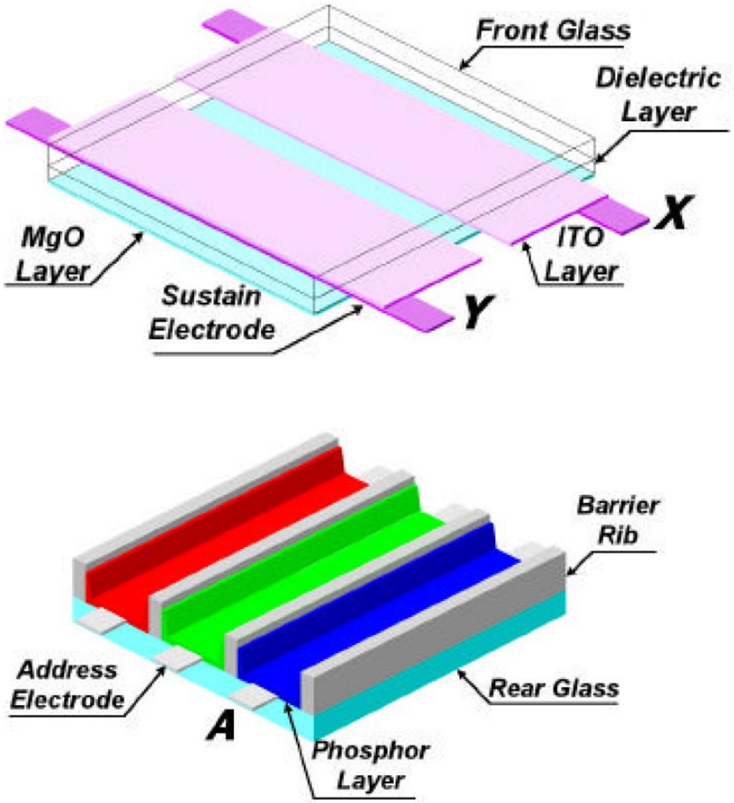

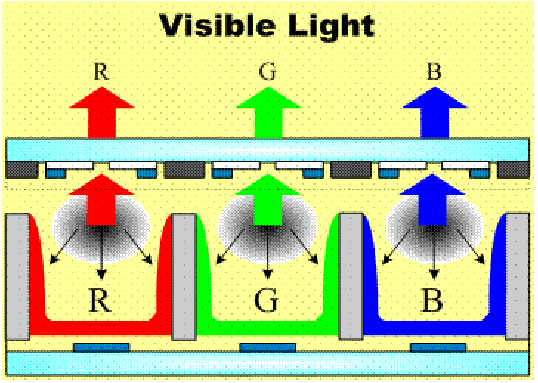

Spectrum of the different phosphors

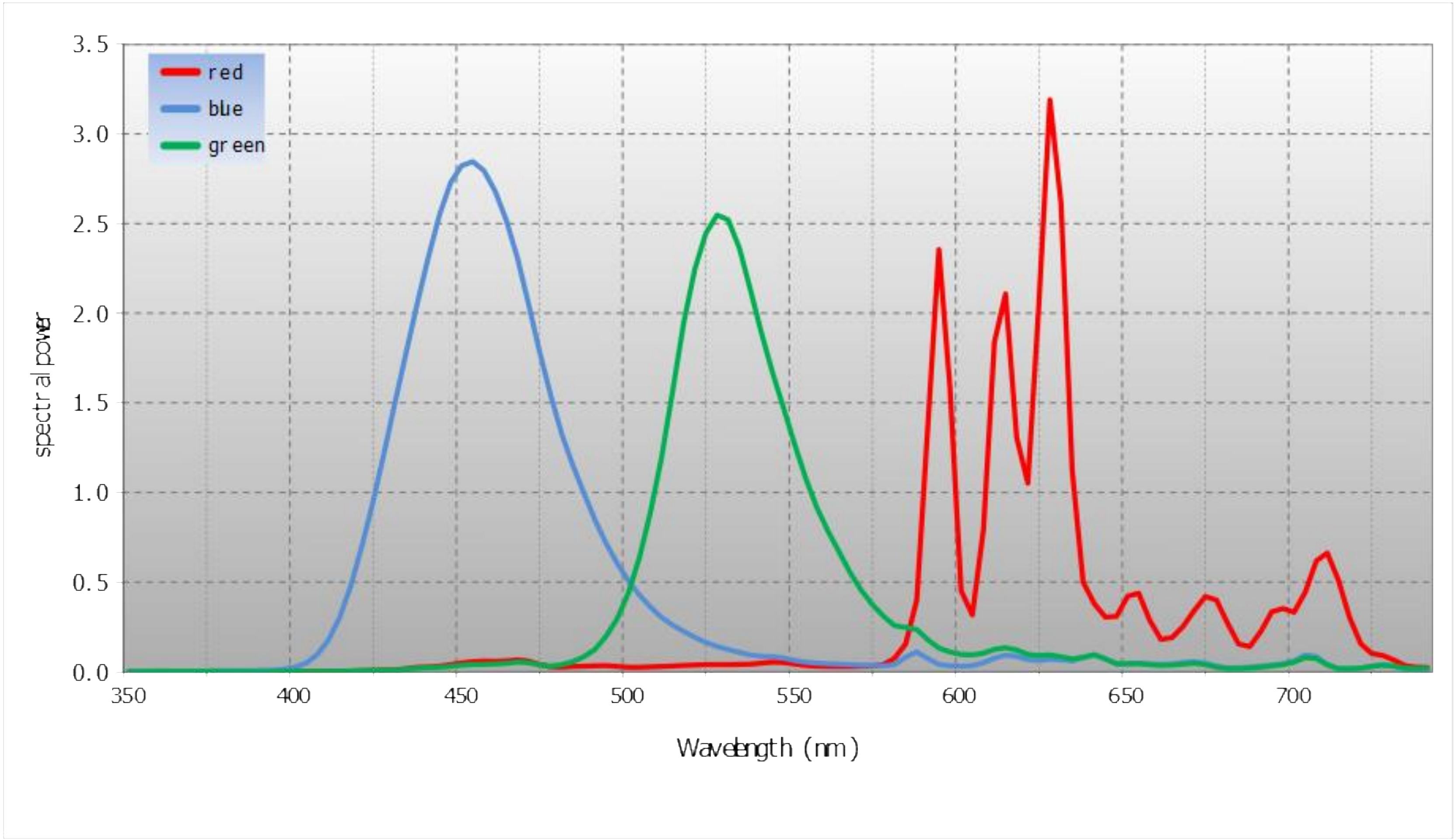

The foundation of AC discharge

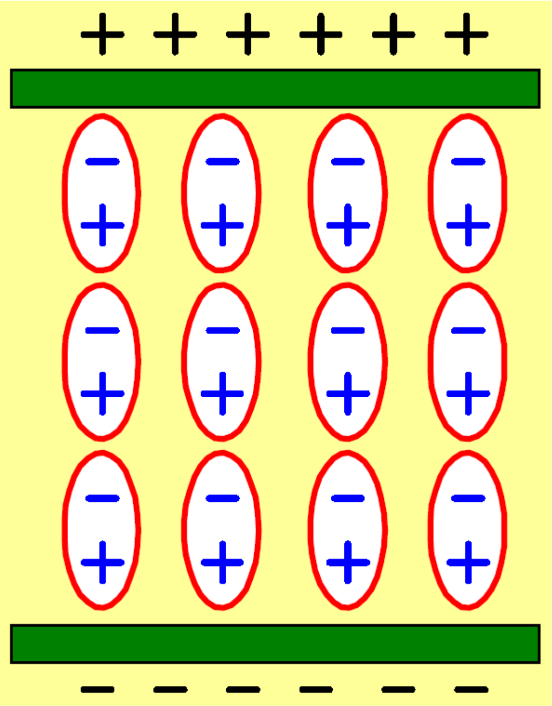

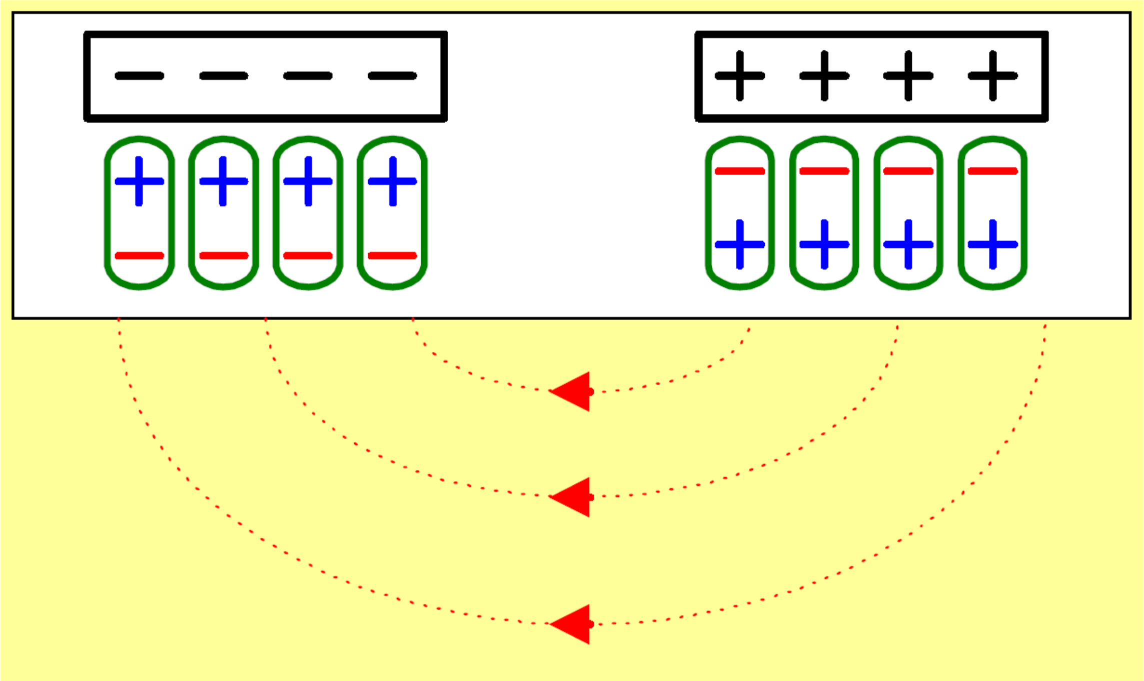

Slides from Prof. Heung-Sik Tae, School of Electronic and Electrical Engineering, Kyungpook National University

The plasma can be sustained using ac discharged

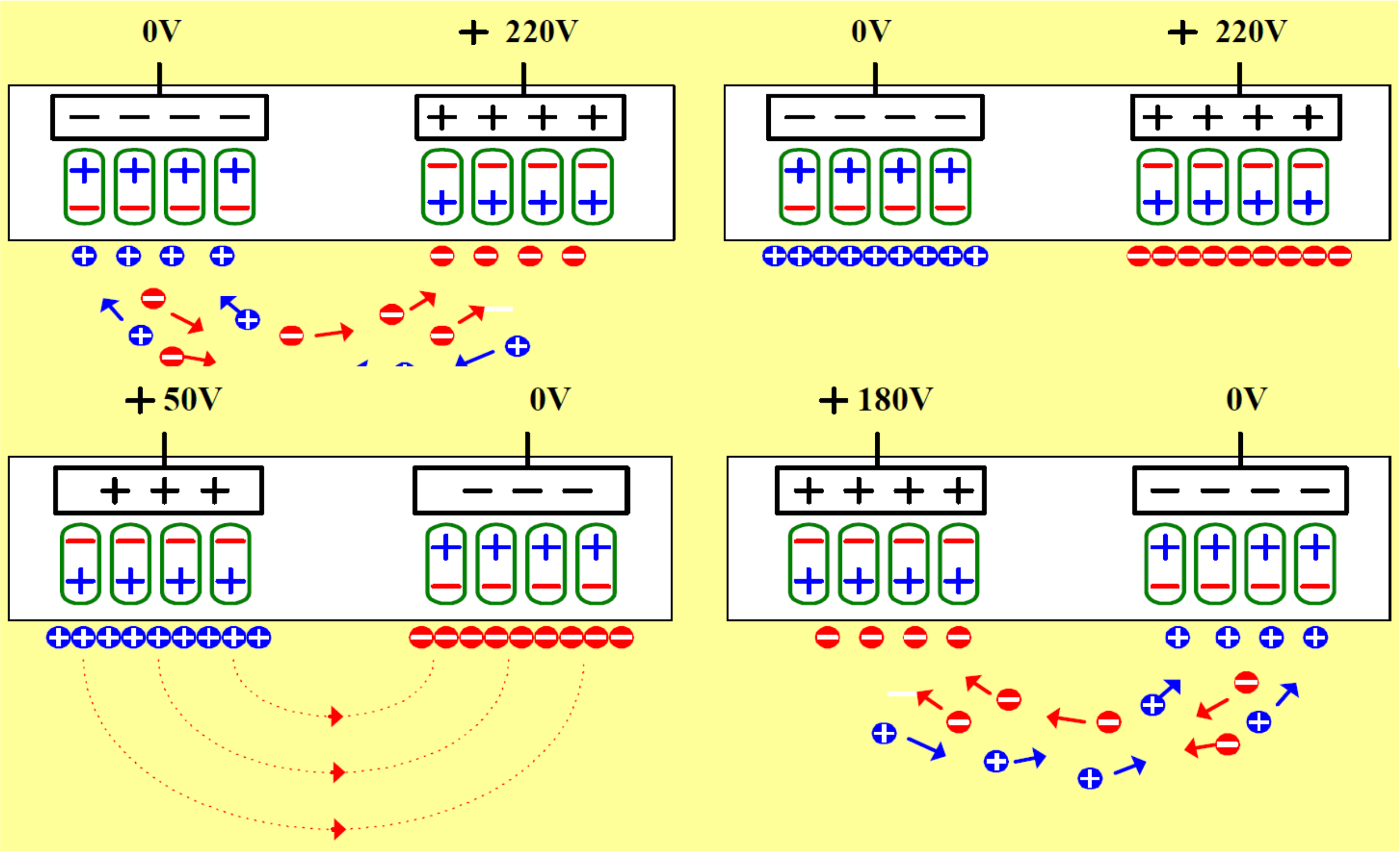

- **Wall discharge reduced the required discharge voltage**

Slides from Prof. Heung-Sik Tae, School of Electronic and Electrical Engineering, Kyungpook National University

Wall discharge reduced the required discharge voltage

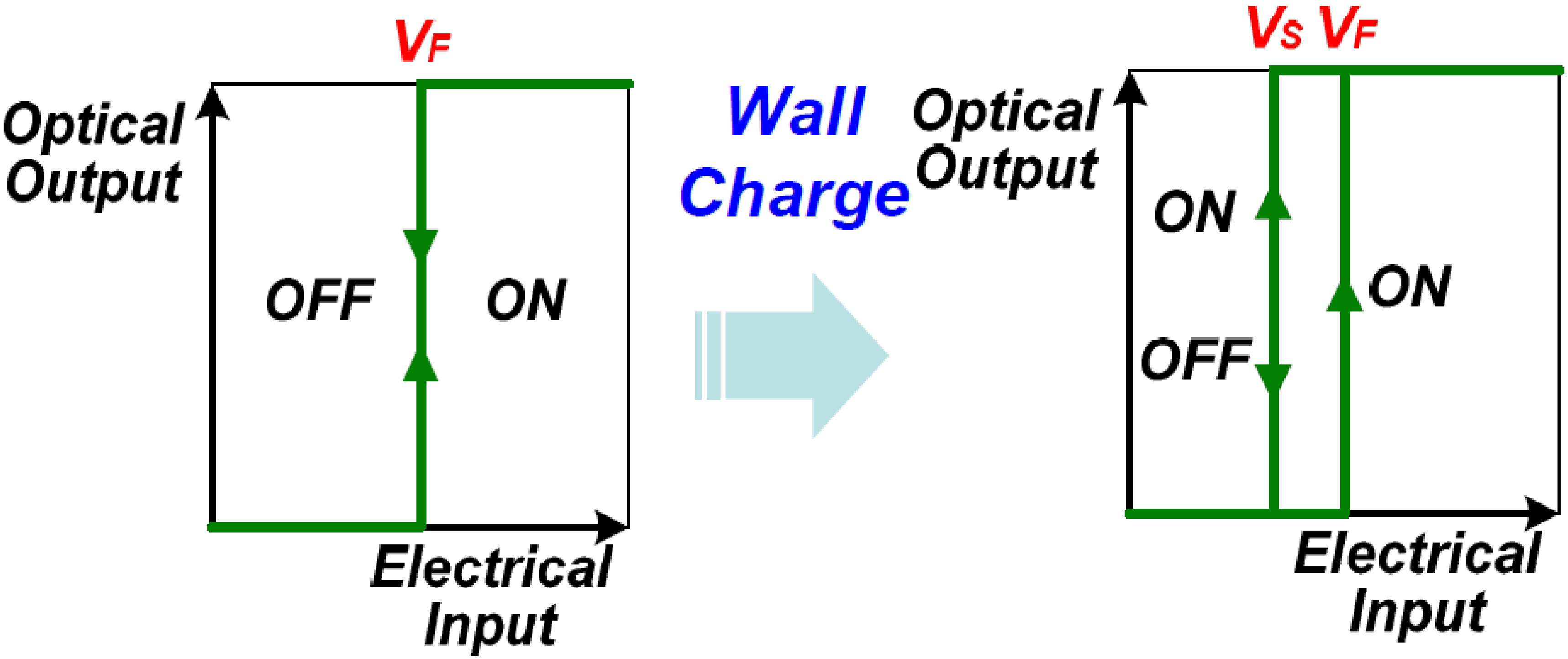

Slides from Prof. Heung-Sik Tae, School of Electronic and Electrical Engineering, Kyungpook National University

ON/OFF State Selection

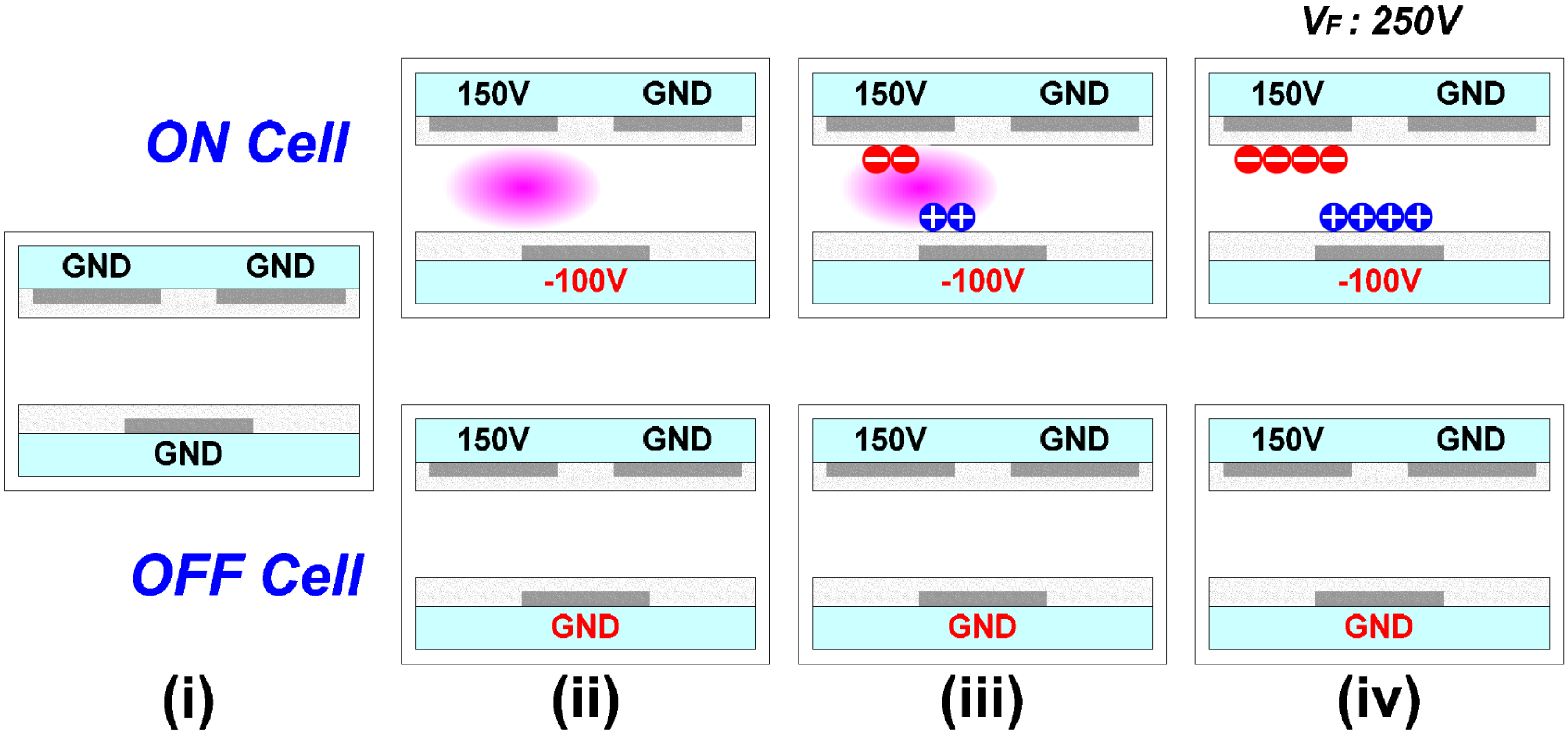

Slides from Prof. Heung-Sik Tae, School of Electronic and Electrical Engineering, Kyungpook National University

Sustain discharge

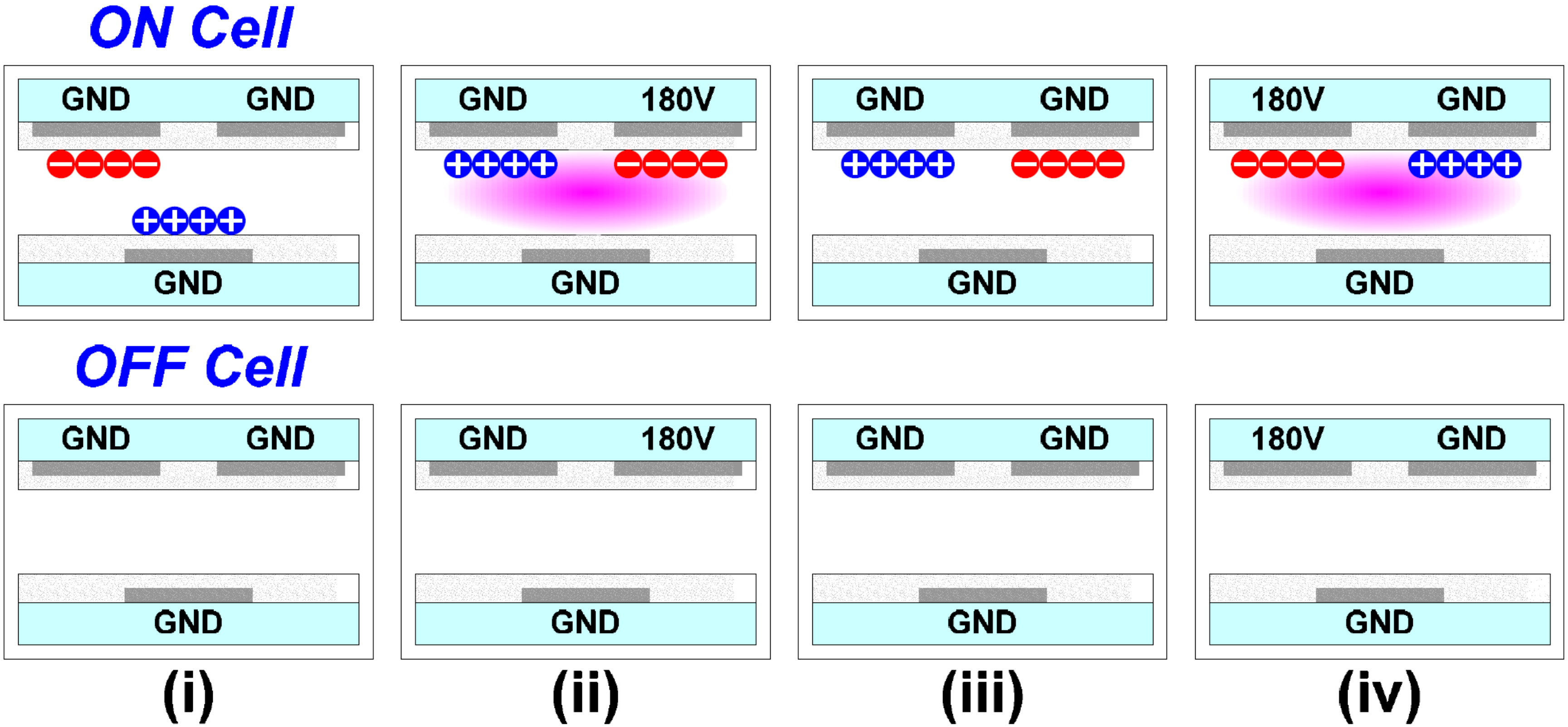

Slides from Prof. Heung-Sik Tae, School of Electronic and Electrical Engineering, Kyungpook National University

Address and sustain electrodes are connected to different drivers

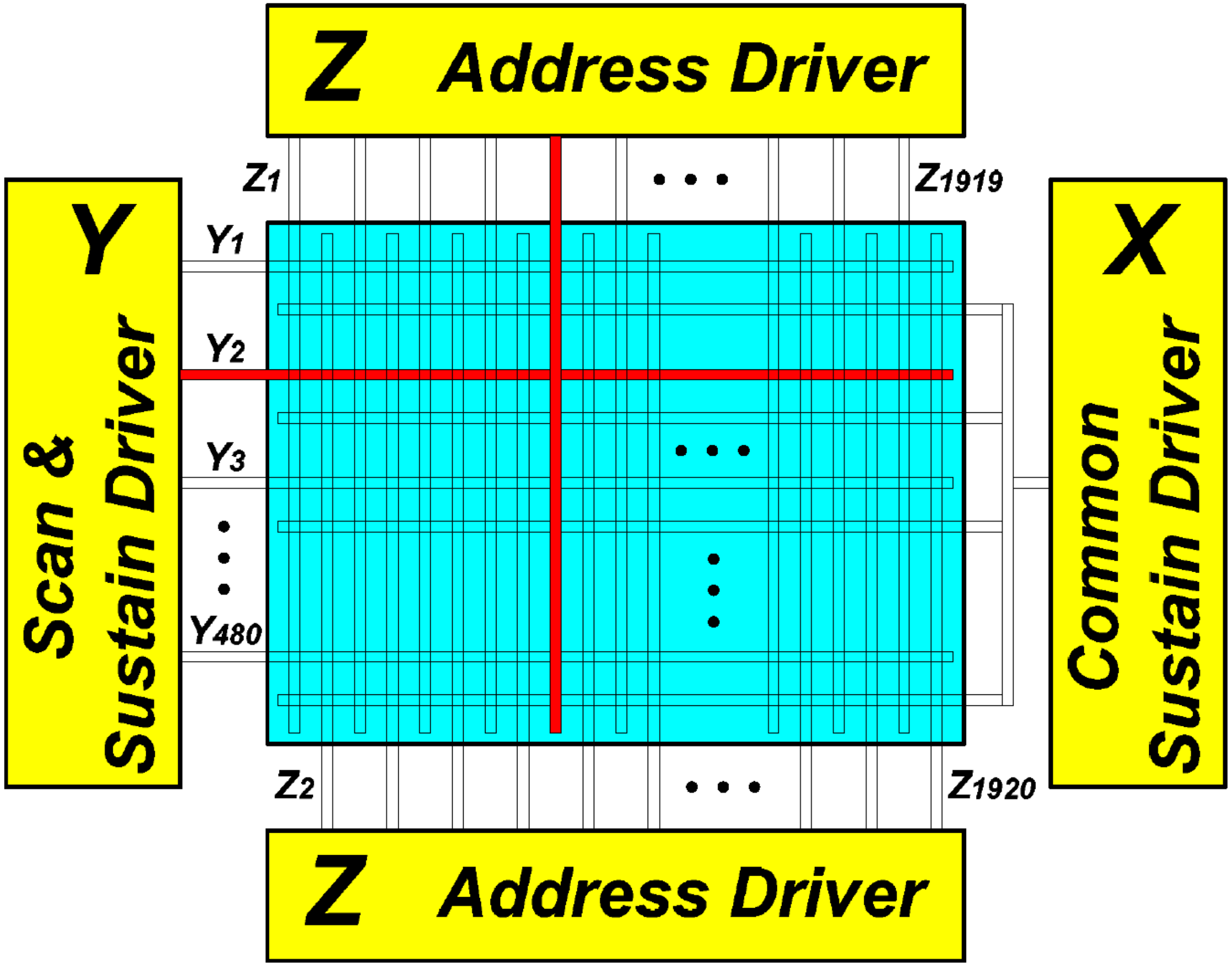

Slides from Prof. Heung-Sik Tae, School of Electronic and Electrical Engineering, Kyungpook National University

PDP pixel can only be either ON or OFF

- Cathode Ray Tube :

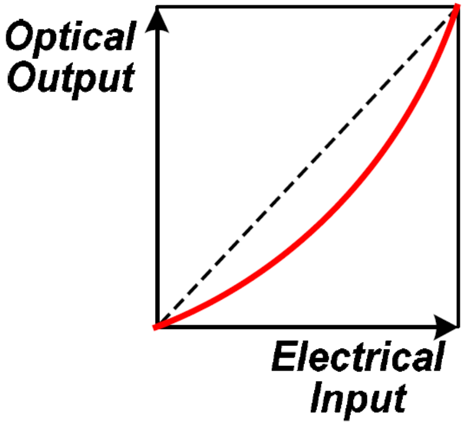

- Plasma Display Panel :

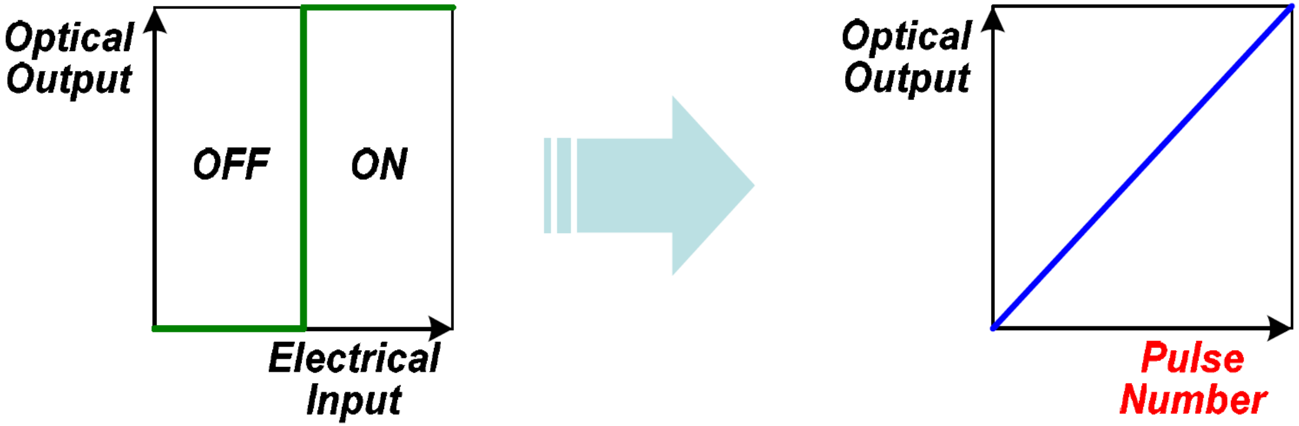

Slides from Prof. Heung-Sik Tae, School of Electronic and Electrical Engineering, Kyungpook National University

PDP luminance is controlled by using number of light pulses

- CRT : Control the Luminance using Electron Beam Intensity

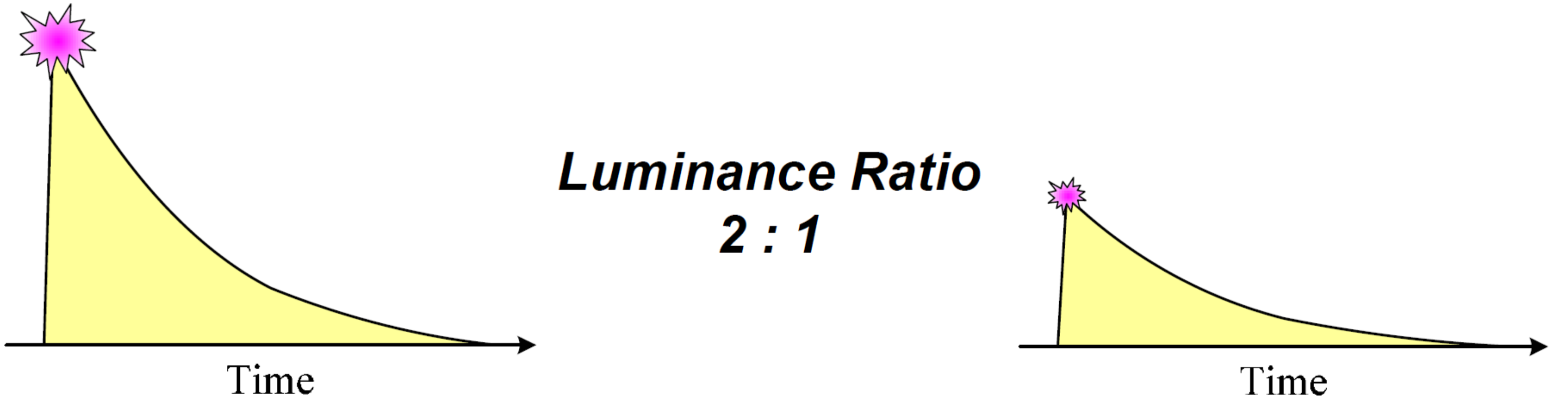

Luminance Ratio
2 : 1

- PDP : Control the Luminance using Number of Light Pulses

Luminance Ratio
2 : 1

Slides from Prof. Heung-Sik Tae, School of Electronic and Electrical Engineering, Kyungpook National University

A single field is divided into 8 subfield

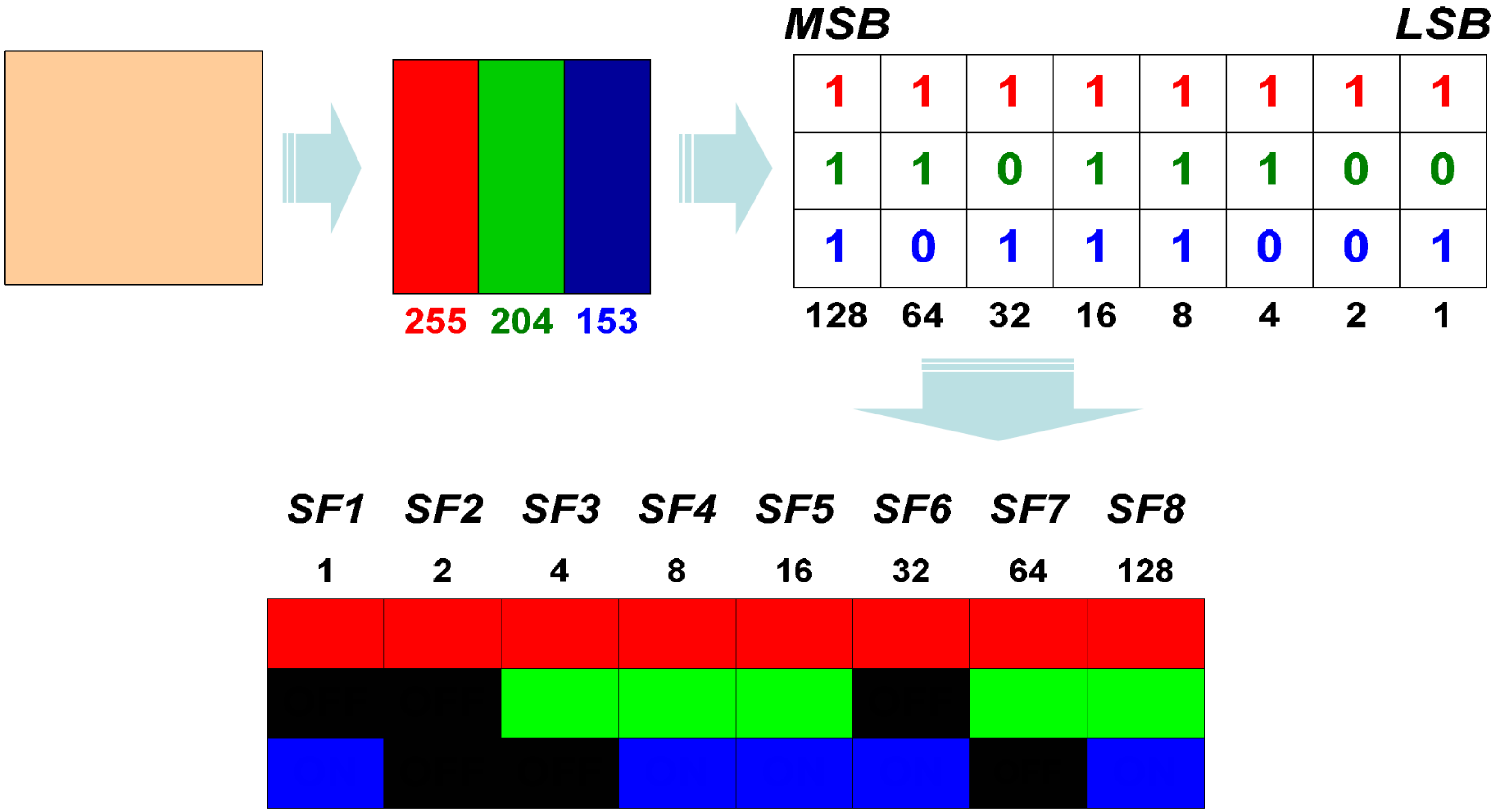

1	1	1	1	1	1	1	1
1	1	0	1	1	1	0	0
1	0	1	1	1	0	0	1
128	64	32	16	8	4	2	1

SF1	*SF2*	*SF3*	*SF4*	*SF5*	*SF6*	*SF7*	*SF8*
1	2	4	8	16	32	64	128
🟥	🟥	🟥	🟥	🟥	🟥	🟥	🟥
⬛	⬛	🟩	🟩	🟩	⬛	🟩	🟩
🟦	⬛	⬛	🟦	🟦	🟦	⬛	🟦

Slides from Prof. Heung-Sik Tae, School of Electronic and Electrical Engineering, Kyungpook National University

Composition of each subfield

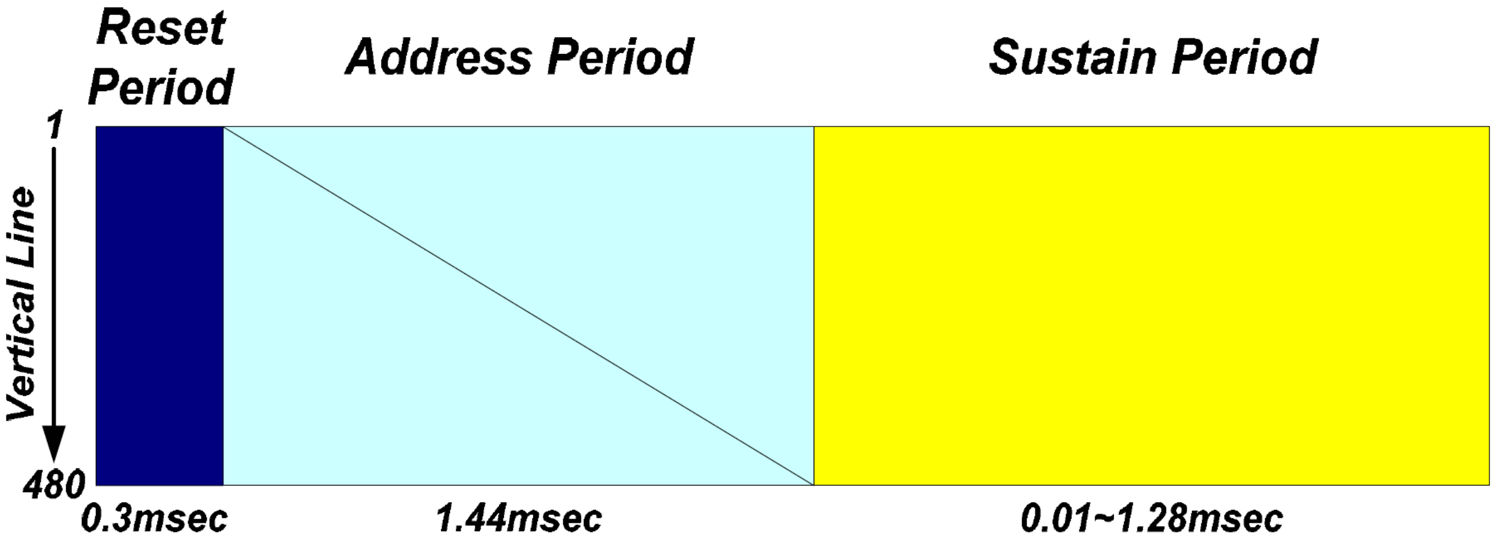

Reset Period

Address Period

Sustain Period

1

Vertical Line

480

0.3msec

1.44msec

0.01~1.28msec

*Spec : VGA (640*480)*
8 Subfield
0.03msec Address Pulse
100KHz Sustain Freq.

Slides from Prof. Heung-Sik Tae, School of Electronic and Electrical Engineering, Kyungpook National University

8 subfield in one TV-Field (ADS)

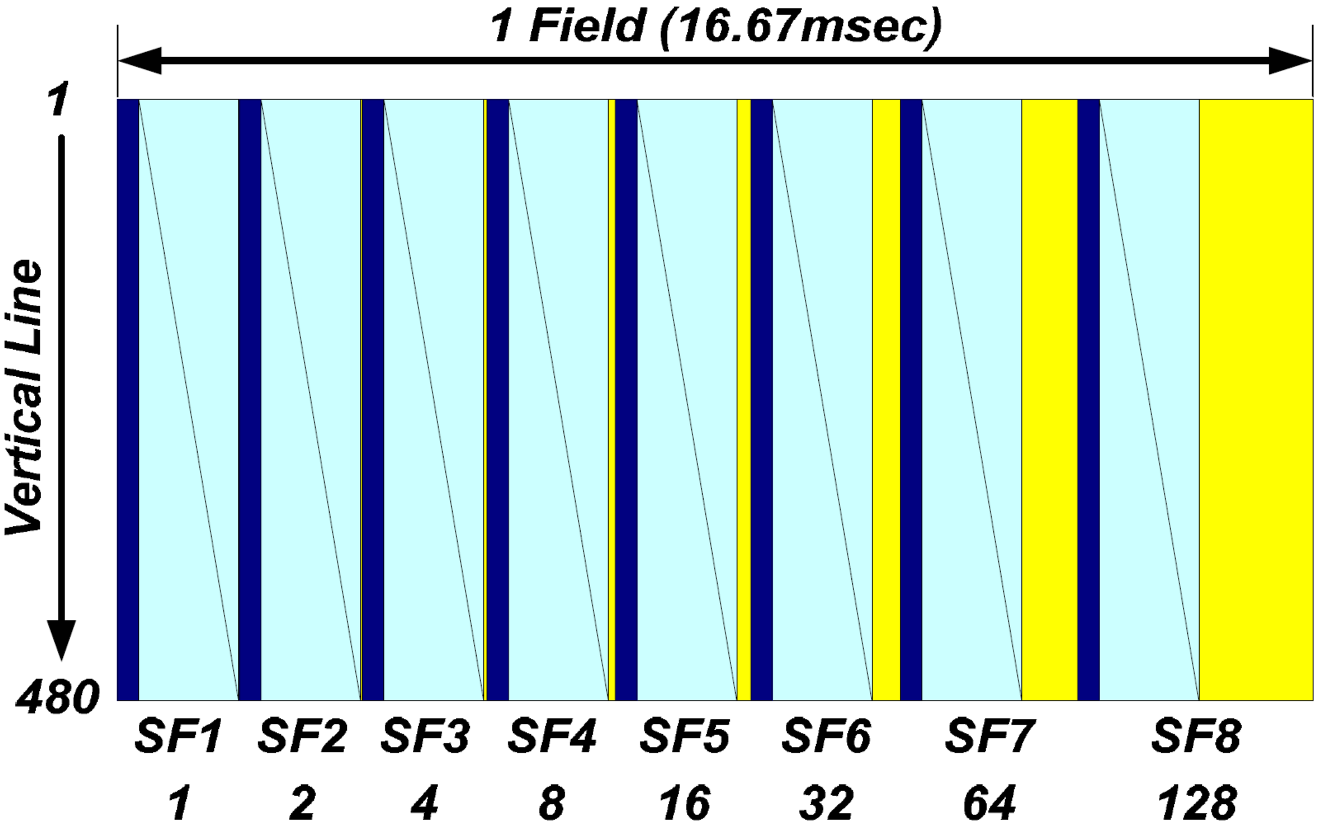

PDP uses line-by-line scanning

- Cathode Ray Tube : Cell-by-Cell Scanning

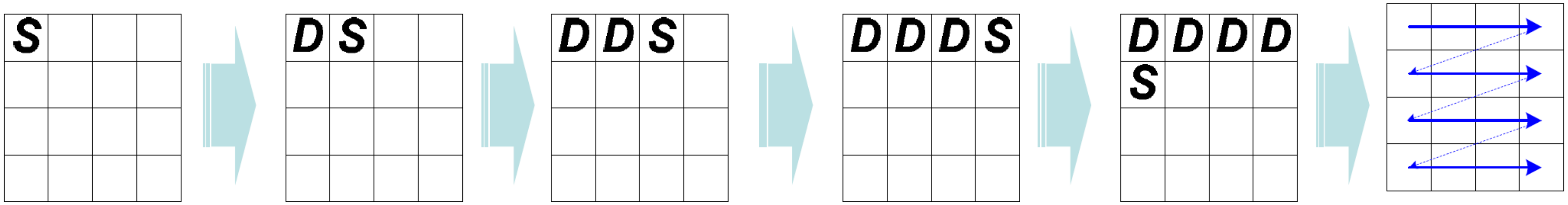

- PDP : Line-by-Line Scanning

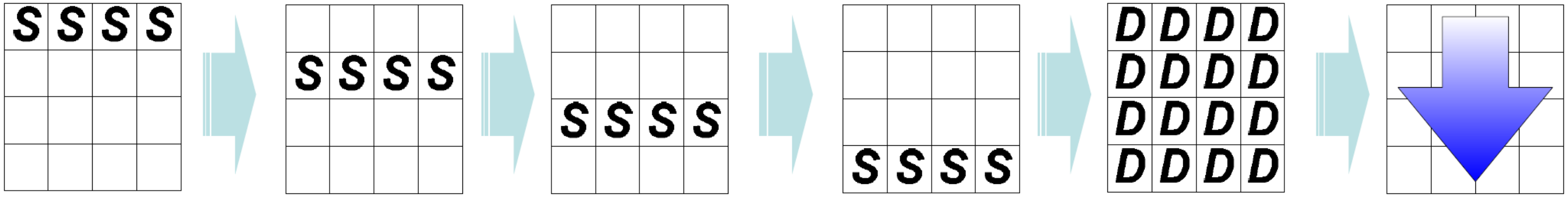

Slides from Prof. Heung-Sik Tae, School of Electronic and Electrical Engineering, Kyungpook National University

Video signal processing

- Analog Video Signal ⇨ Digital Pulse Signal

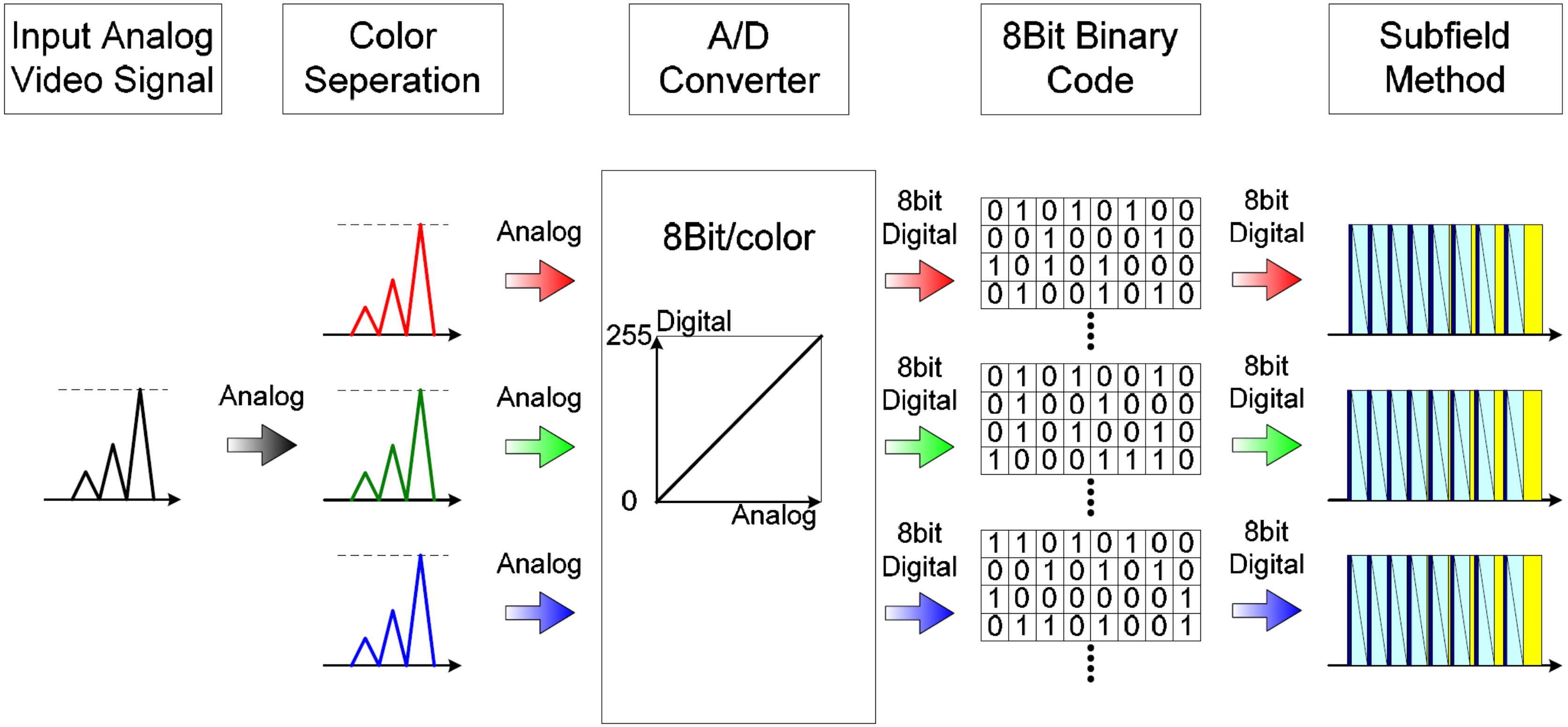

Input Analog Video Signal

Color Seperation

A/D Converter

8Bit Binary Code

Subfield Method

0	1	0	1	0	1	0	0
0	0	1	0	0	0	1	0
1	0	1	0	1	0	0	0
0	1	0	0	1	0	1	0

⋮

0	1	0	1	0	0	1	0
0	1	0	0	1	0	0	0
0	1	0	1	0	0	1	0
1	0	0	0	1	1	1	0

⋮

1	1	0	1	0	1	0	0
0	0	1	0	1	0	1	0
1	0	0	0	0	0	0	1
0	1	1	0	1	0	0	1

⋮

Slides from Prof. Heung-Sik Tae, School of Electronic and Electrical Engineering, Kyungpook National University

Addressing period


Original Image


SF1


SF2


SF3


SF4


SF5


SF6


SF7


SF8

Slides from Prof. Heung-Sik Tae, School of Electronic and Electrical Engineering, Kyungpook National University

Displaying period

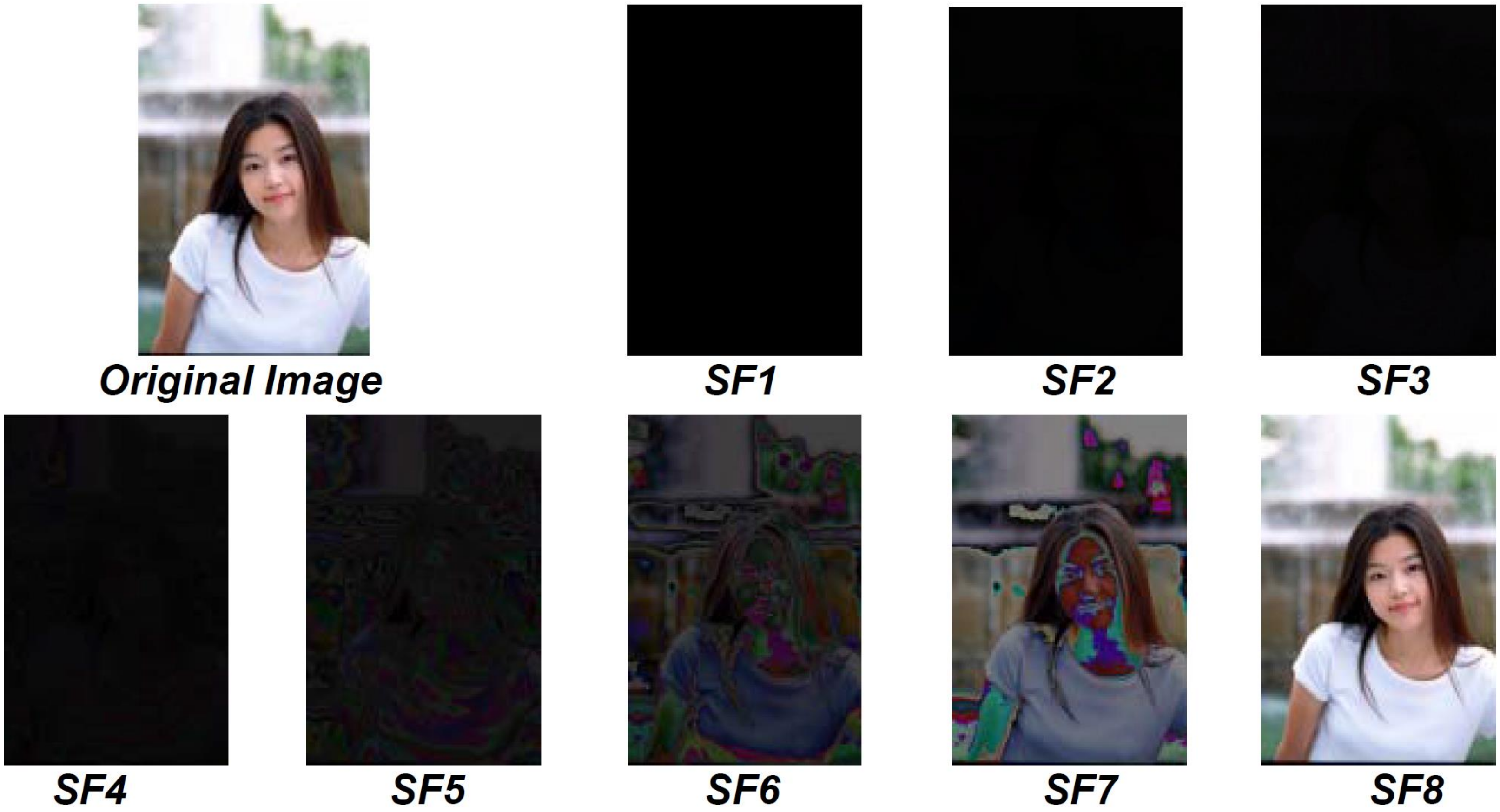

Slides from Prof. Heung-Sik Tae, School of Electronic and Electrical Engineering, Kyungpook National University

Liquid crystal are a special state of matter between liquid and crystal

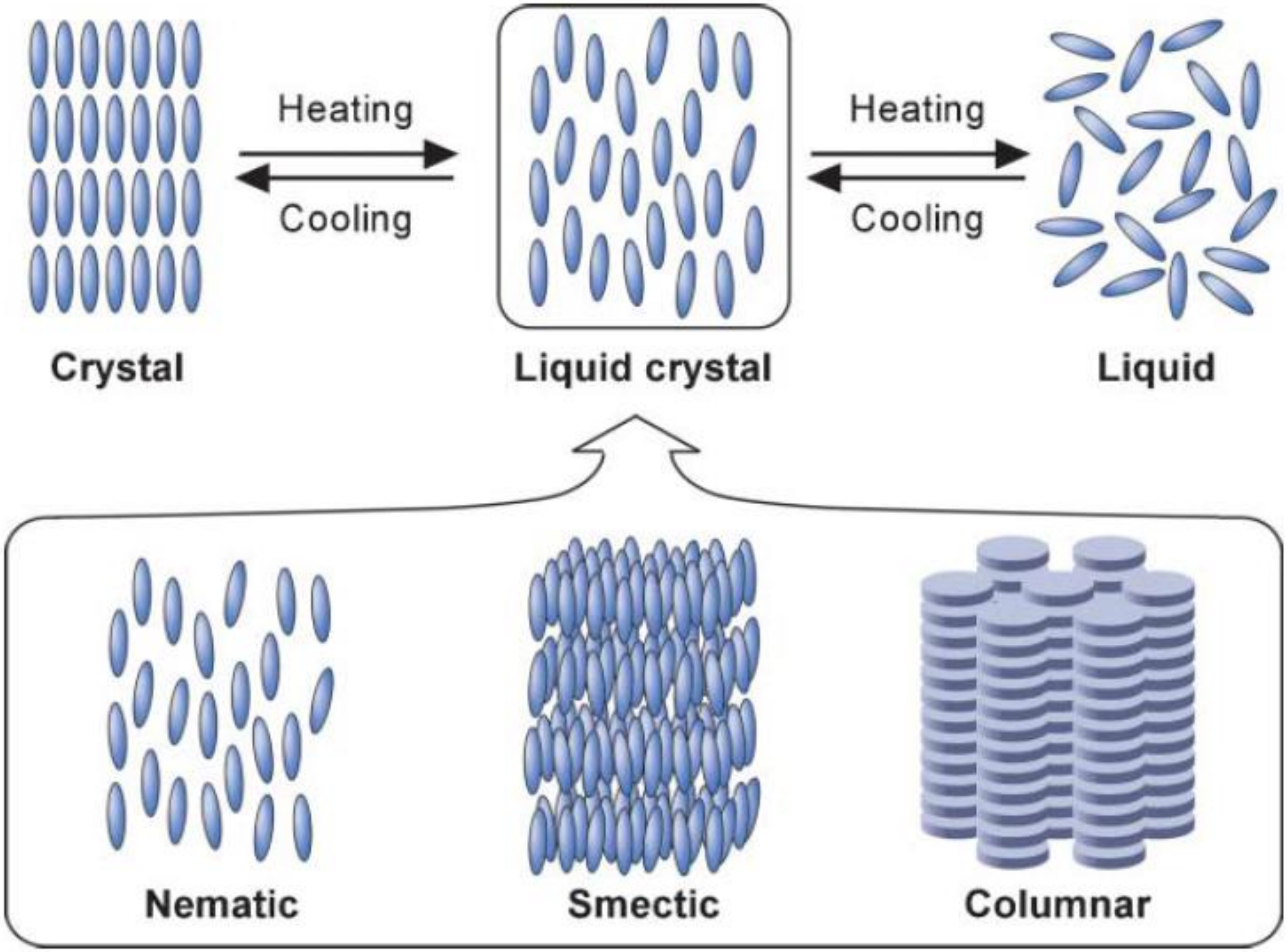

T. Kato, *et. al.*, Chem. Soc. Rev., *36*, 1845, 2007

Linear polarization of a light can be rotated by miss aligned liquid crystal

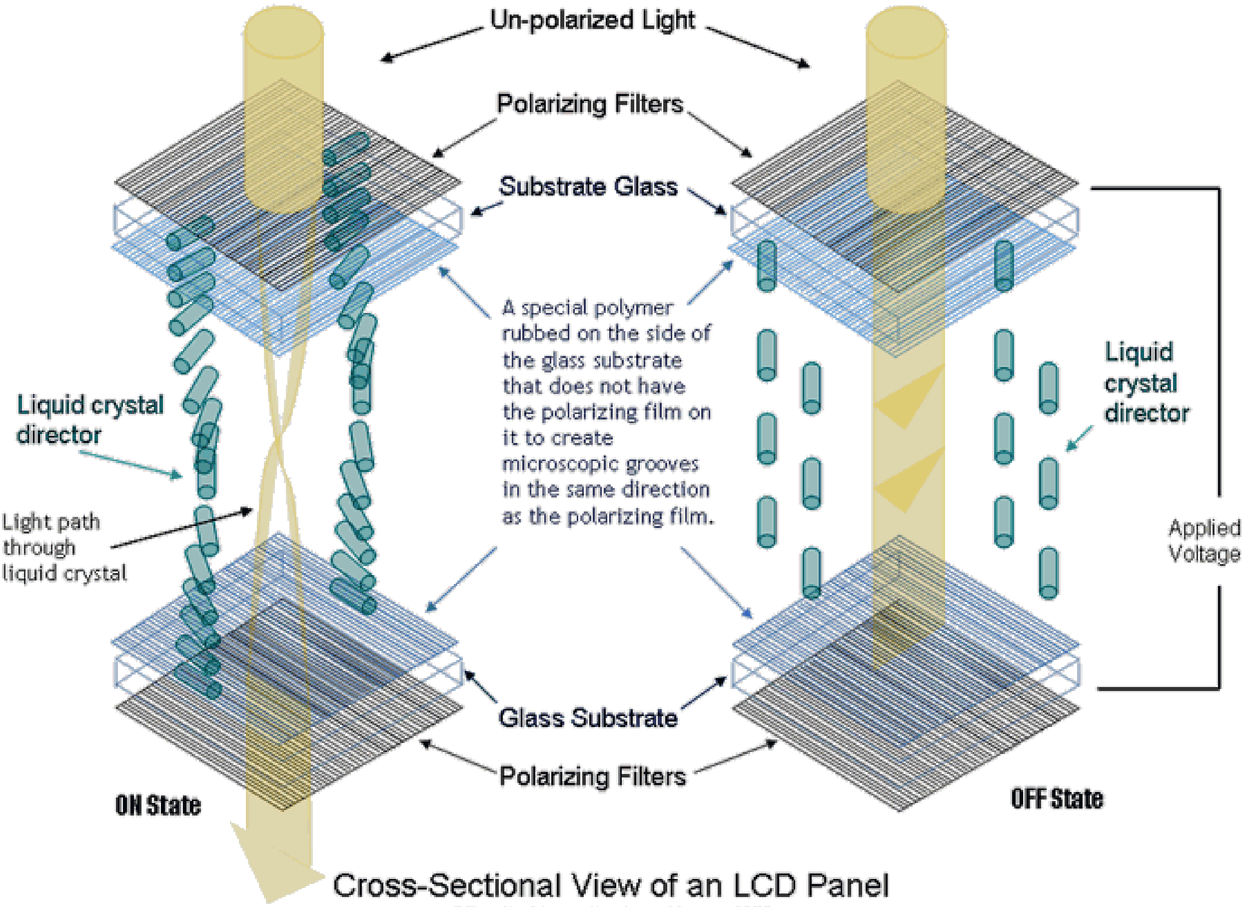

Cross-Sectional View of an LCD Panel

©Practical-home-theater-guide.com 2006

http://www.practical-home-theater-guide.com/lcd-display.html

Structure of Liquid crystal display (LCD)

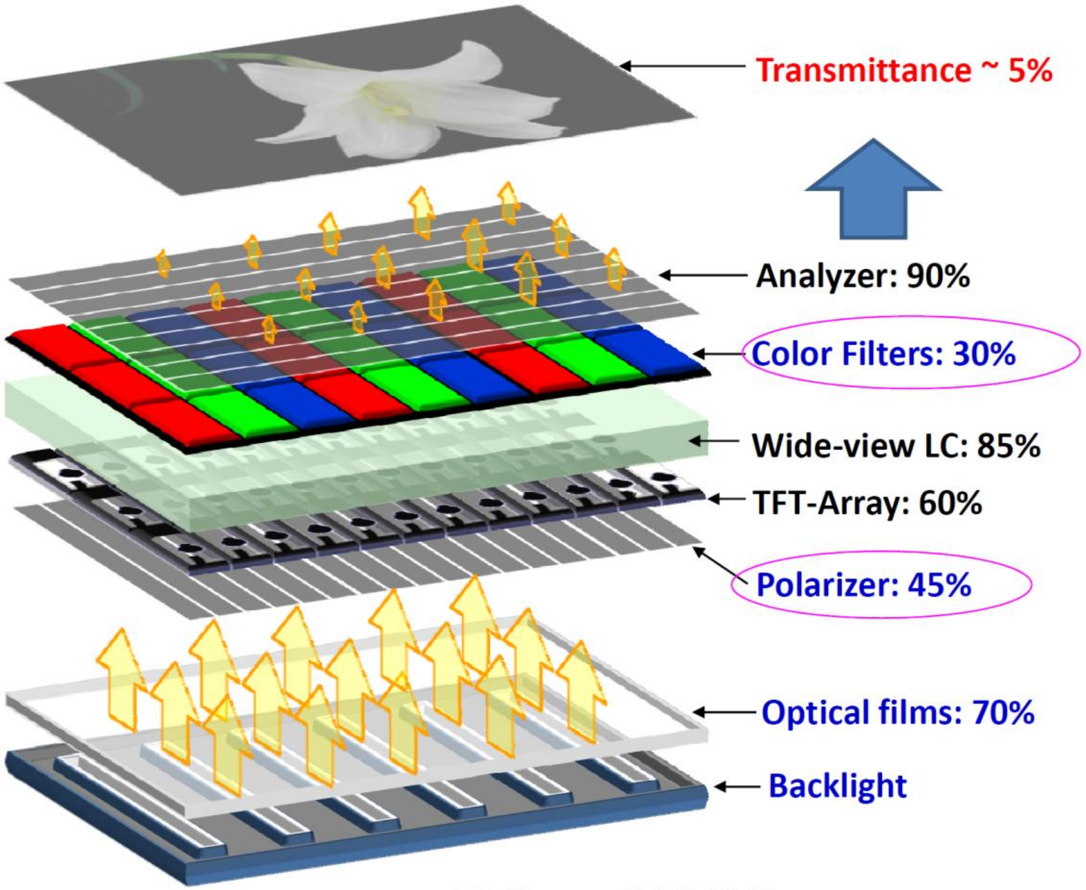

YB Huang, IDRC 2008

Notes from ST Wu, UCF

http://www6.cityu.edu.hk/cityu25/events/engineering/pdf/proftang.pdf

Optimistic projection of PDP market

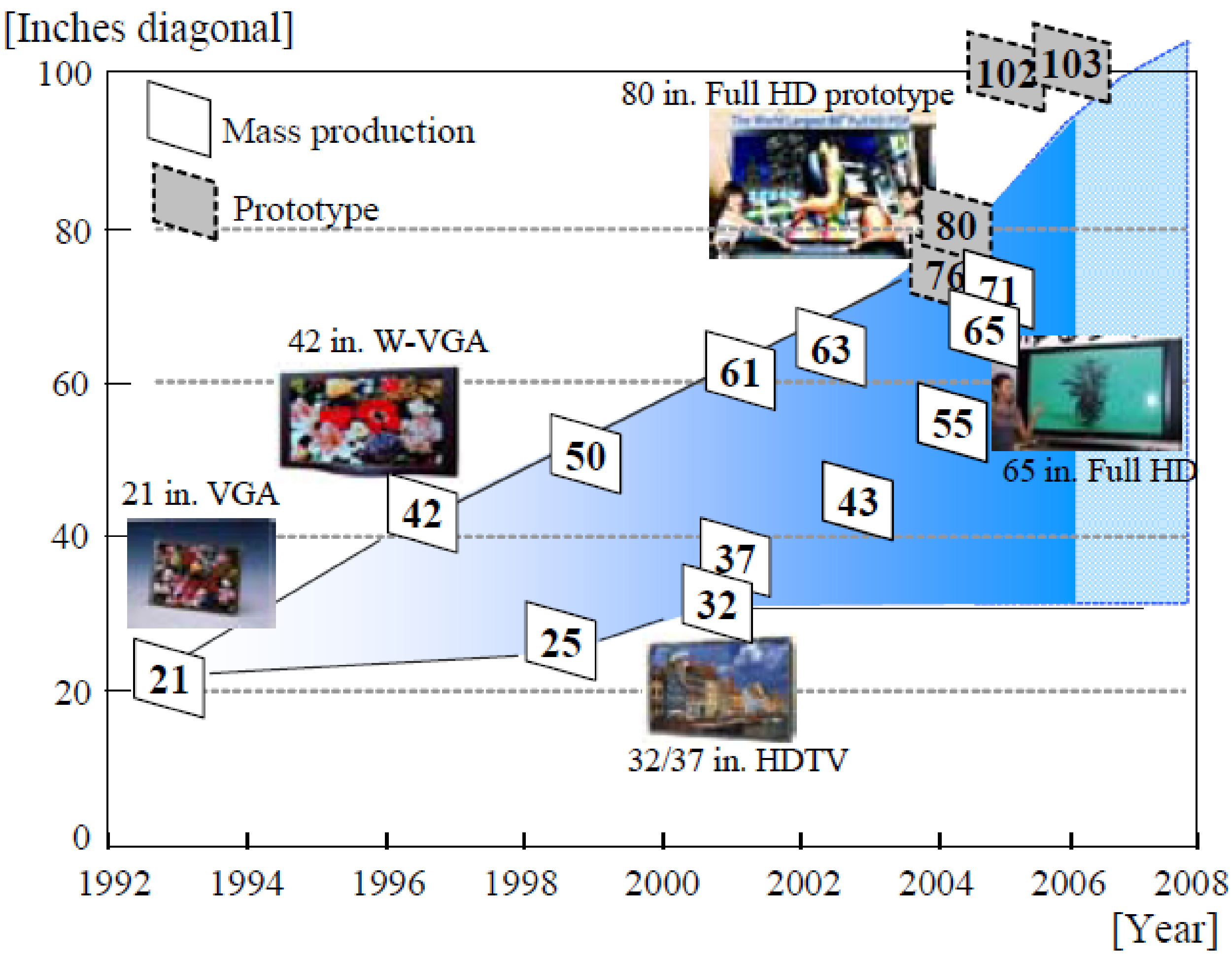

Reality

TV Shipment Growth by Technology

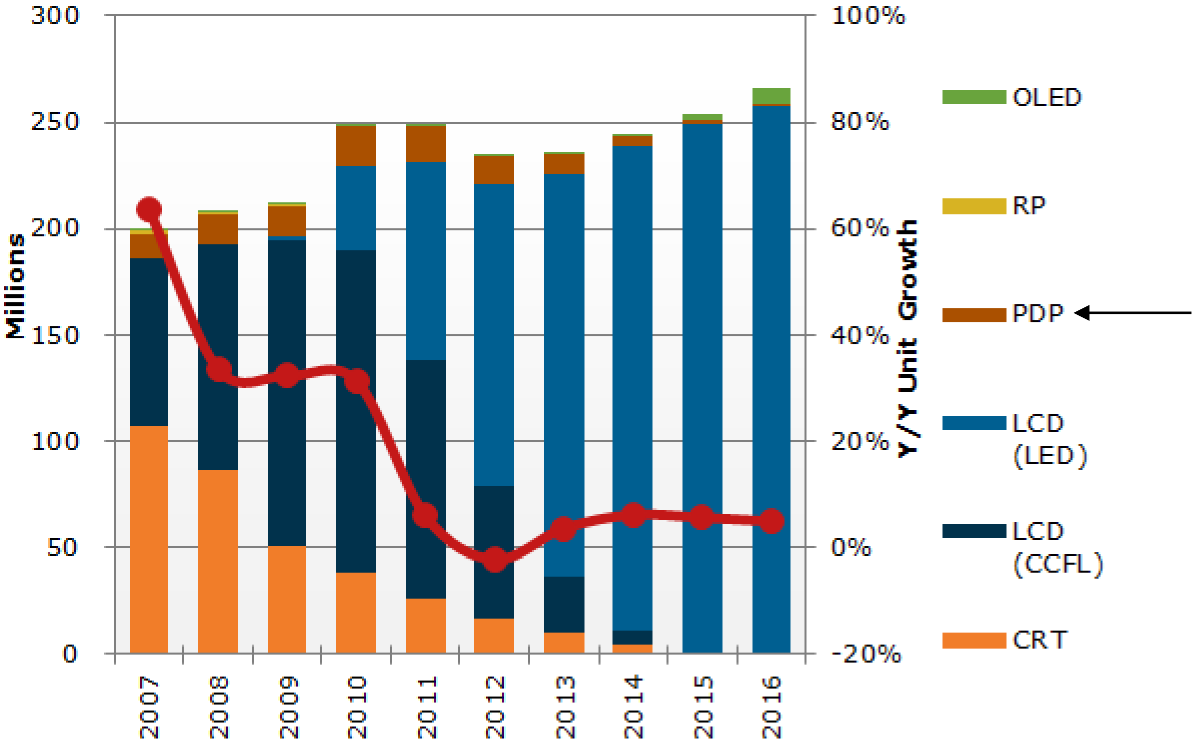

http://www.digitaltvnews.net/?p=22108

Too many reasons that PDP died!

- **Bright showroom conditions put plasmas at a distinct disadvantage versus LED-lit LCDs**
- **Aesthetics may have played a role in hastening plasma's demise**
- **UHD/4K caught on quickly**
- **Screen-size limitations also played a part in plasmas plight**
- **You can't bend a plasma**
- **Plasmas were harder to deal with than LCDs**
- **While OLED is still in the early stages of development, there's no question it offers greater potential than plasma**
- **Energy efficiency may have played a part in putting plasma out to pasture**
- **Plasma was the original flat-panel technology, People just thought of it as old technology.**
- **Projectors improved in quality and prices dropped**

http://www.avsforum.com/forum/40-oled-technology-flat-panels-general/2080650-10-reasons-plasma-died.html

Let’s stand up and do exercise!!

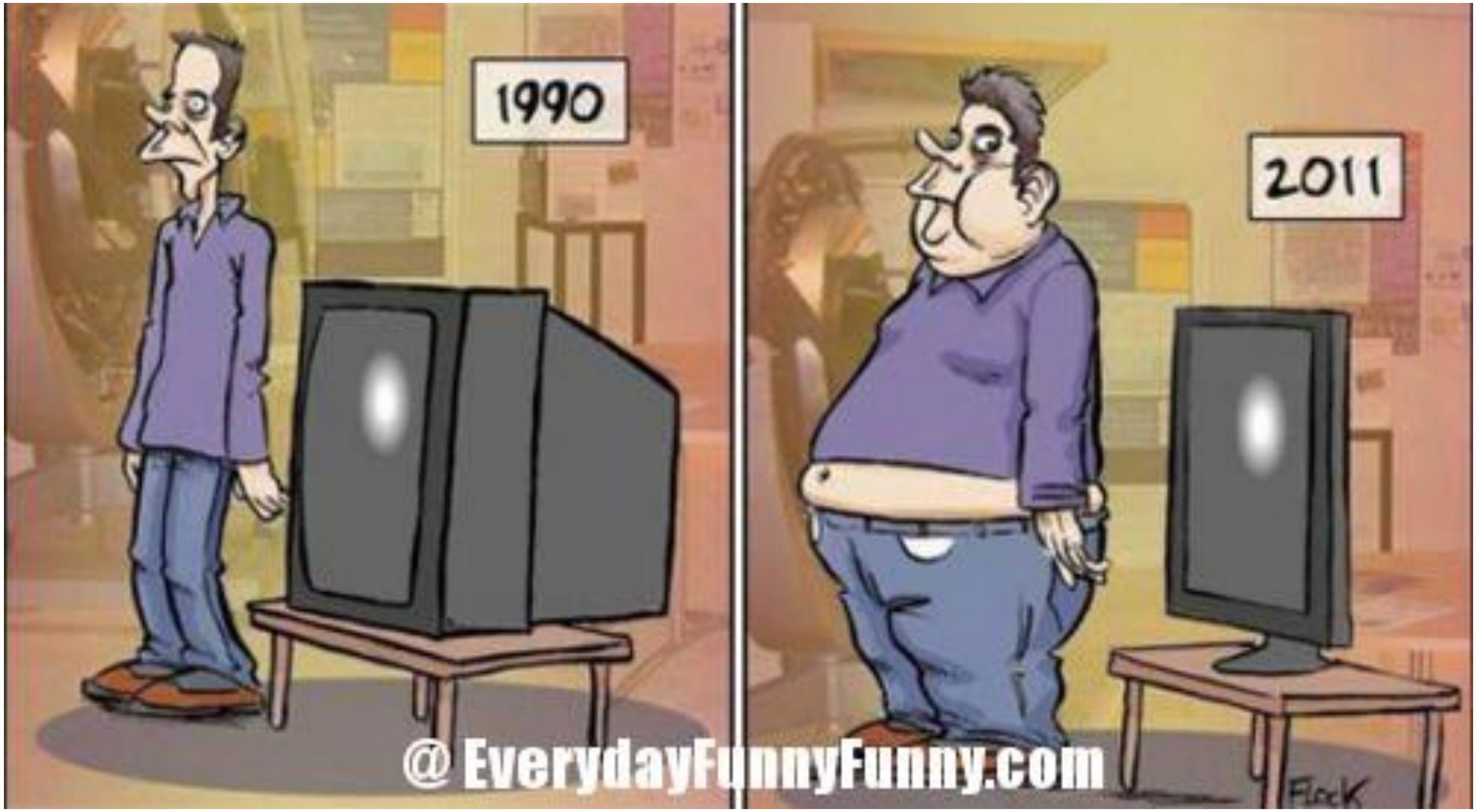

The hydrogen bomb

The “iron group” of isotopes are the most tightly bound

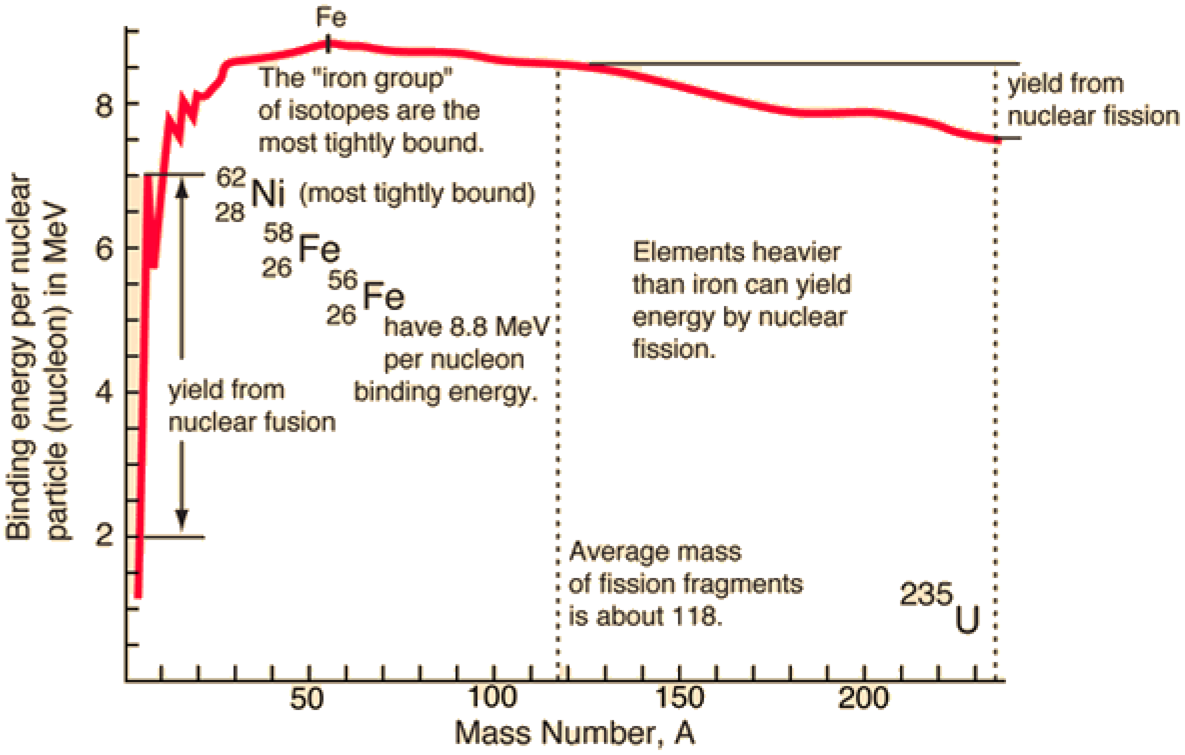

http://hyperphysics.phy-astr.gsu.edu/hbase/nucene/nucbin.html

Chain reaction can happen in U^{235} fission reaction

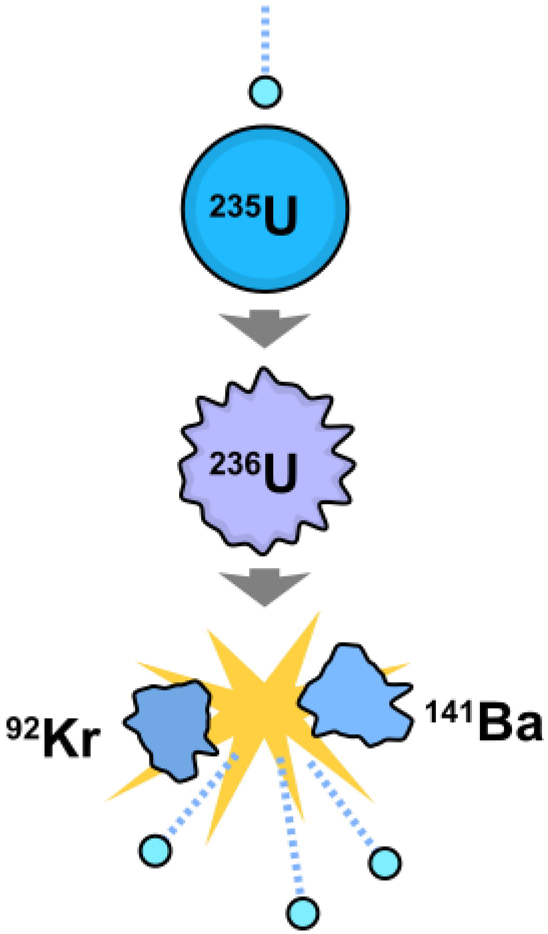

- ~ 200 million electron volts (MeV)/fission, ~million times more than chemical reactions
- Energy for bombs, or for civilian power can generate huge amounts of energy (and toxicity) in a small space with a modest amount of material
- Source of safety, security issues for nuclear power

https://en.wikipedia.org/wiki/Uranium-235
Talk given by Matthew Bunn, IGA-232: Controlling the World's Most Dangerous Weapons, Harvard Kennedy School, 2013

The neutrons are leaking out and stopping the chain reaction in a sub-critical mass

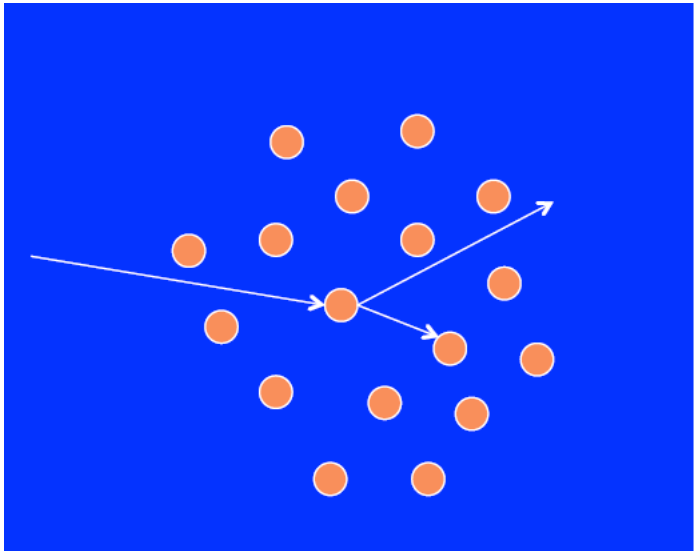

Solution 1: add more material

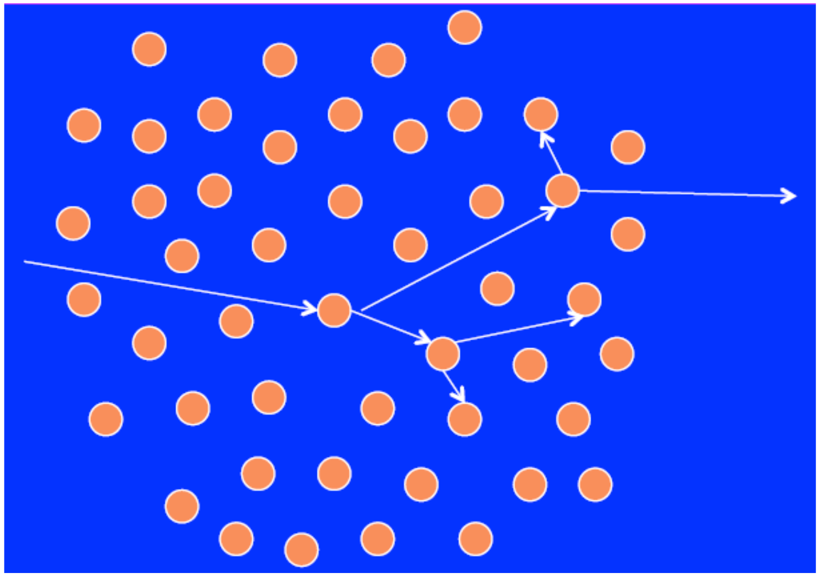

Solution2: reflect the neutron back in

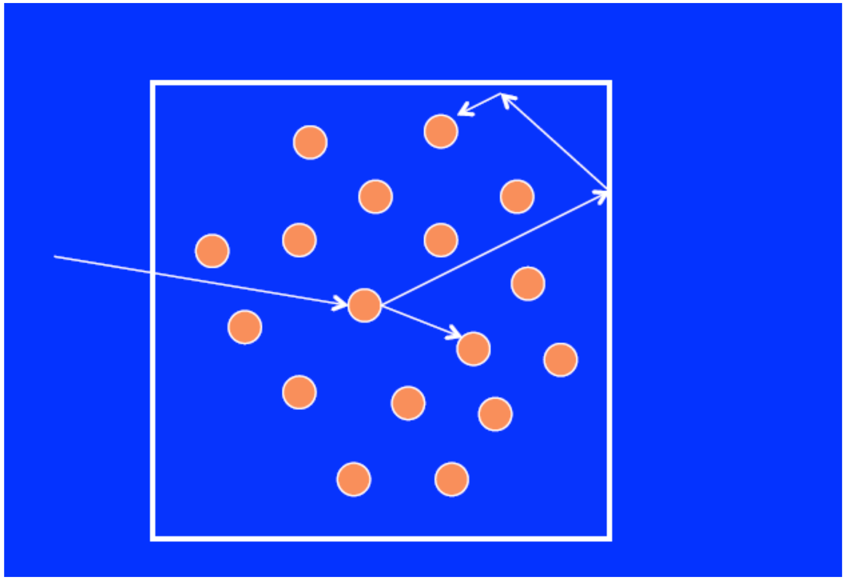

Talk given by Matthew Bunn, IGA-232: Controlling the World’s Most Dangerous Weapons, Harvard Kennedy School, 2013

Solution 3: increase the density

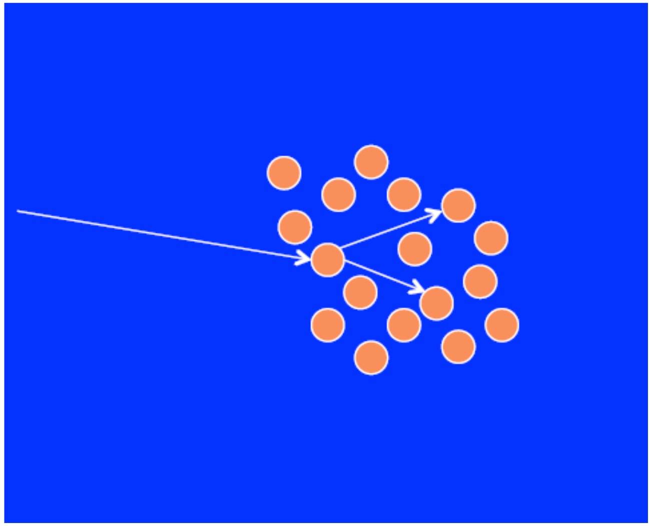

How to get the material together before it blows apart?

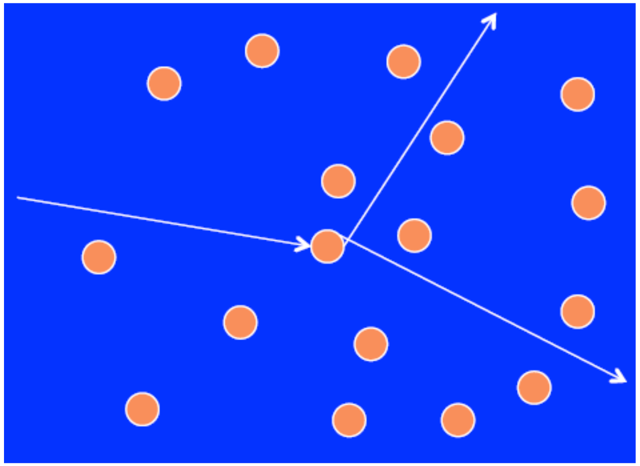

- There are always neutrons around
- Once chain reaction starts, material will heat up, expand, stop reaction
- How to get enough material together fast enough?

Talk given by Matthew Bunn, IGA-232: Controlling the World's Most Dangerous Weapons, Harvard Kennedy School, 2013

Gun-type bomb

- Simple, reliable – can be built without testing
- Highly inefficient – require lots of nuclear material (50-60 kg of 90% enriched HEU)
- Can only get high yield with HEU, not plutonium
- Hiroshima bomb: cannon that fired HEU projectile into HEU target

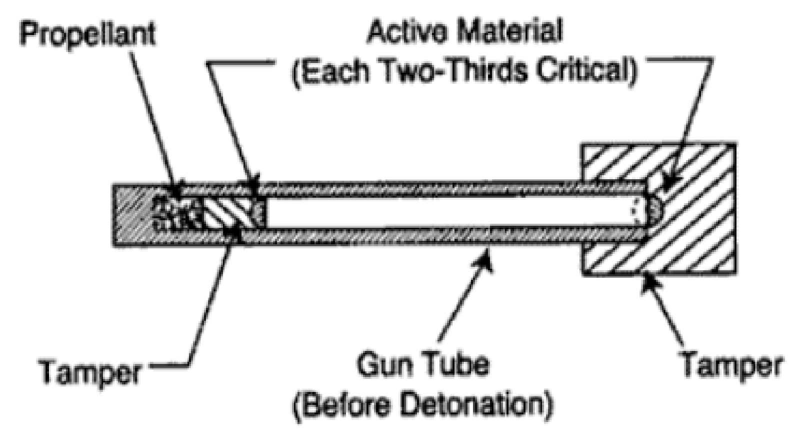

Source: NATO

Implosion design

- **A schematic diagram of an implosion bomb**

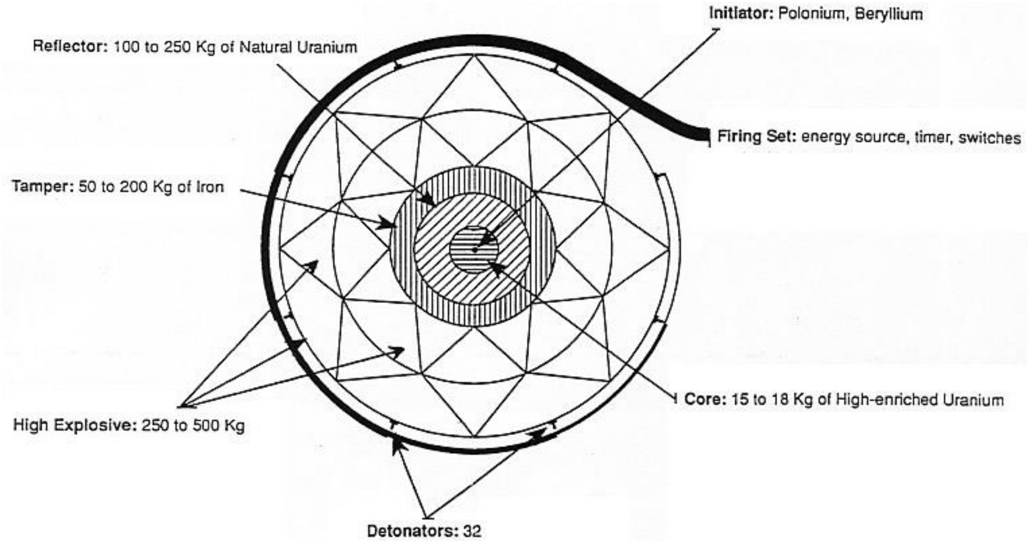

- **Small-scale slow-motion cross-section of a shaped charge implosion design**

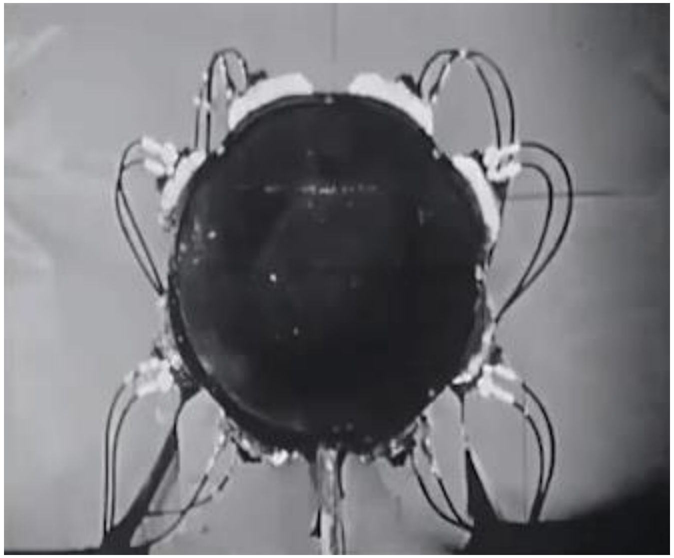

https://www.wisconsinproject.org/nuclear-weapons/
https://en.wikipedia.org/wiki/Trinity_%28nuclear_test%29

The 1st nuclear bomb: Trinity (Bradbury Science Museum)

- **Model of the Trinity Gadget**

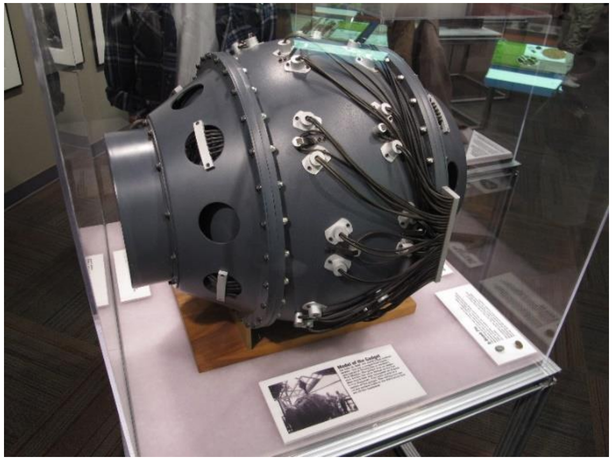

- **Project Y Atomic Bomb Detonator System**

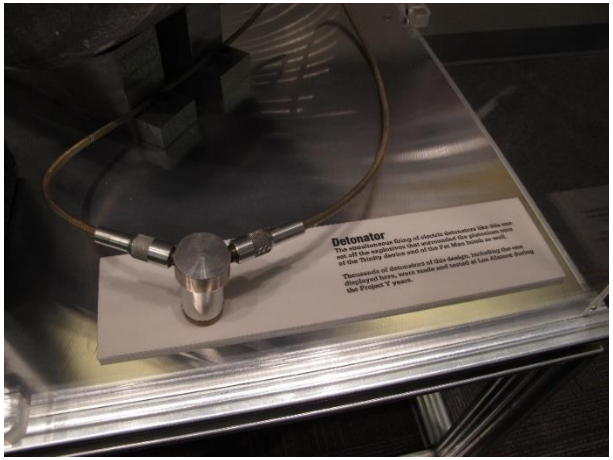

The simultaneous firing of electric detonators like this one set off the explosives that surrounded the plutonium core of the Trinity device and of the Fat Man bomb as well.

Thousands of detonators of this design, including the one displayed here, were made and tested at Los Alamos during the Project Y years.

- **Project Y Atomic Bomb Detonator System**

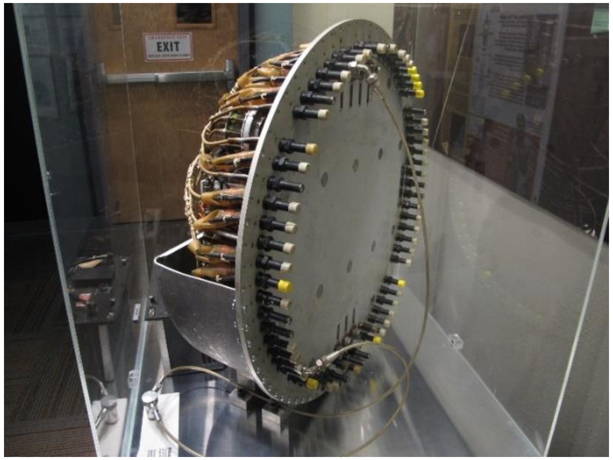

- **Project Y Atomic Bomb Detonator System Spark Gap Switch**

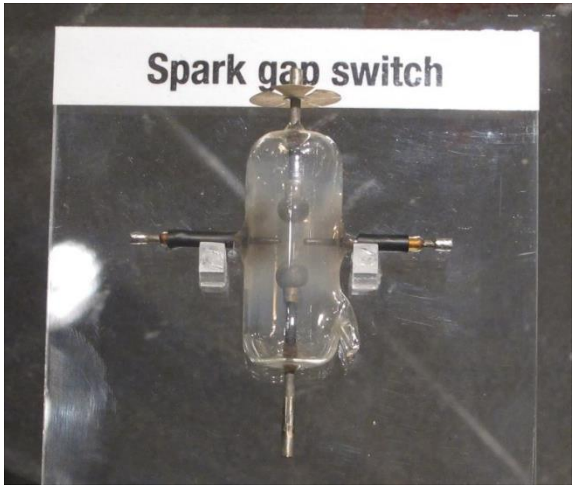

https://www.flickr.com/photos/rocbolt/with/8061684482

The 1st nuclear bomb: Trinity

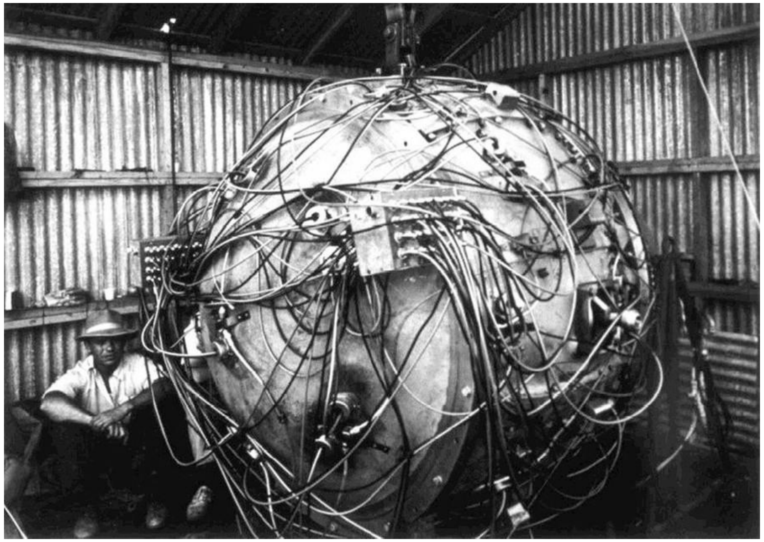

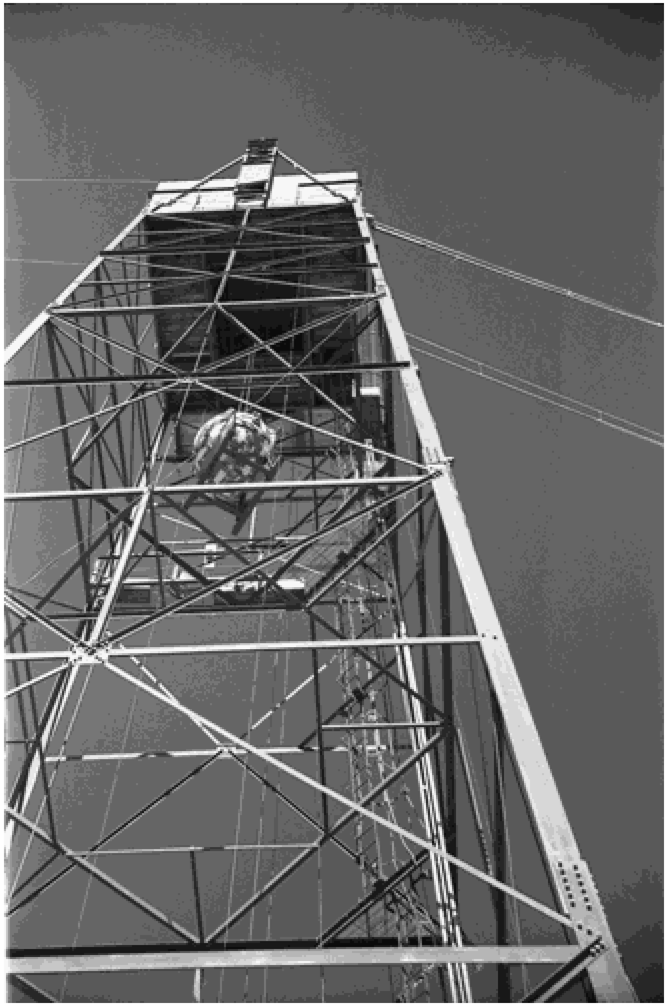

https://www.theatlantic.com/photo/2015/07/70-years-since-trinity-when-we-tested-nuclear-bombs/398735/
https://saddlebagnotes.com/arts-and-leisure/tucson-seismographs-detected-first-nuclear-test-at-trinity-n-m/article_b01c5b20-f6fb-11eb-a221-6327df2feaeb.html

Trinity explosion on July 16, 1945

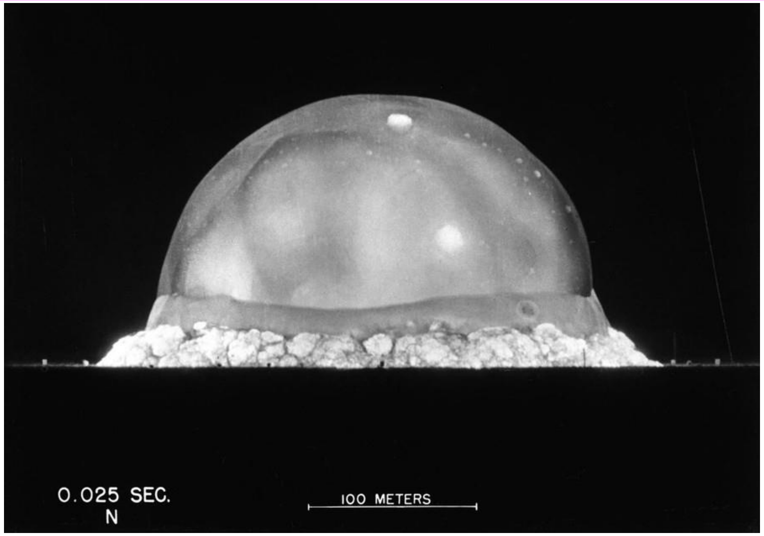

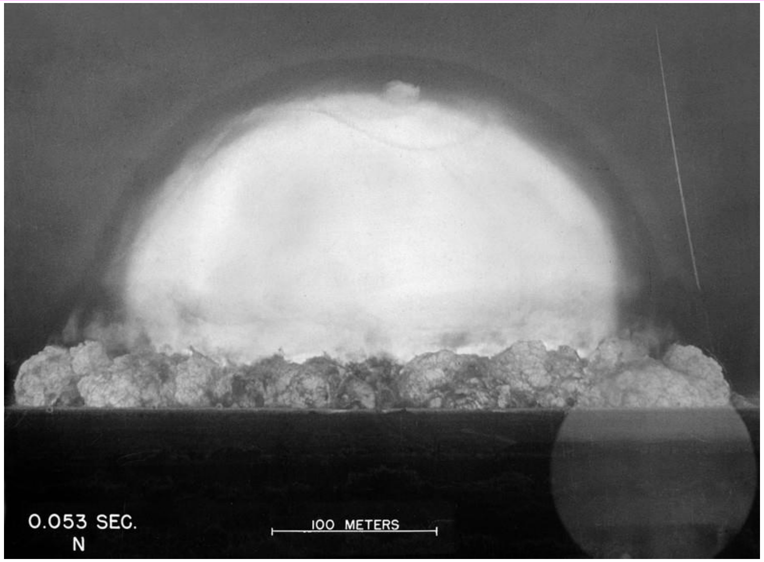

https://www.theatlantic.com/photo/2015/07/70-years-since-trinity-when-we-tested-nuclear-bombs/398735/
https://en.wikipedia.org/wiki/Trinity_%28nuclear_test%29

Hiroshima Bomb – “Little Boy”

Gun Type – Easiest to design and build (Hiroshima bomb was never tested)

About 13 kiloton explosive yield

Talk given by Dr. Charles D. Ferguson, President, Federation of American Scientists, Department of Physics, Colloquium, American University, 2012

Atomic bomb is very destructive

Hiroshima: August 6, 1945

Nagasaki: August 9, 1945

Talk given by Dr. Charles D. Ferguson, President, Federation of American Scientists, Department of Physics, Colloquium, American University, 2012

The fusion process

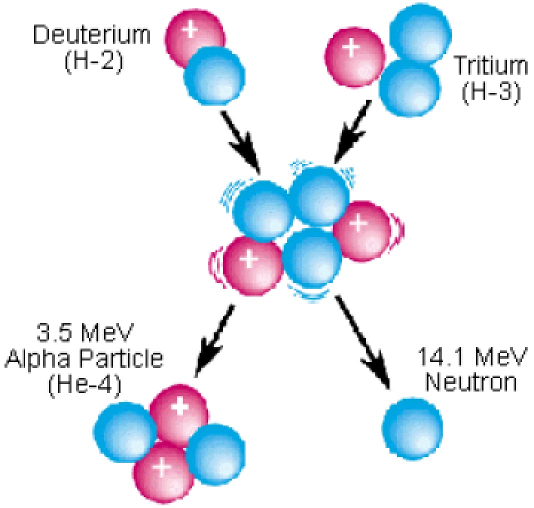

Deuterium-Tritium Fusion Reaction

$^{2}H+^{3}H \Rightarrow {}^{4}He+n+Q \equiv 17.6$ MeV

Energy release Q=17.6 MeV

In comparison

$^{2}H+^{2}H \Rightarrow {}^{1}H+^{3}H +Q \equiv 4.0$ MeV

$^{2}H+^{2}H \Rightarrow {}^{3}He+n +Q \equiv 3.2$ MeV

$^{3}H+^{3}H \Rightarrow {}^{4}He+2n+Q \equiv 11.3$ MeV

$^{235}U+n \Rightarrow X_A+X_B+3n +Q \approx 200$ MeV

Fusionable Material, deuterium ^{2}H (D) and tritium ^{3}H (t):

Deuterium: natural occurrence (heavy water) (0.015%).

Tritium: natural occurrence in atmosphere through cosmic ray bombardment; radioactive with $T_{1/2}$=12.3 y.

https://isnap.nd.edu/Lectures/phys20061/pdf/10.pdf

“Advantages” of hydrogen bomb

Fusion of ^{2}H+^{3}H: $$\frac{Q}{A}=\frac{17.6\ MeV}{(3+2)\,amu}=3.5\,\frac{MeV}{amu}$$

Fission of ^{235}U: $$\frac{Q}{A}=\frac{200\ MeV}{236\ amu}=0.85\,\frac{MeV}{amu}$$

Fusion is 4 times more powerful than fission and generates 24 times more neutrons!

Neutron production:

$$^{2}H+{}^{3}H:\quad \frac{n}{A}=\frac{1}{5}=0.2$$

$$^{235}U+n:\quad \frac{n}{A}=\frac{2}{236}=0.0085$$

https://isnap.nd.edu/Lectures/phys20061/pdf/10.pdf

Hydrogen bomb uses a fission bomb to initiate the fusion reaction

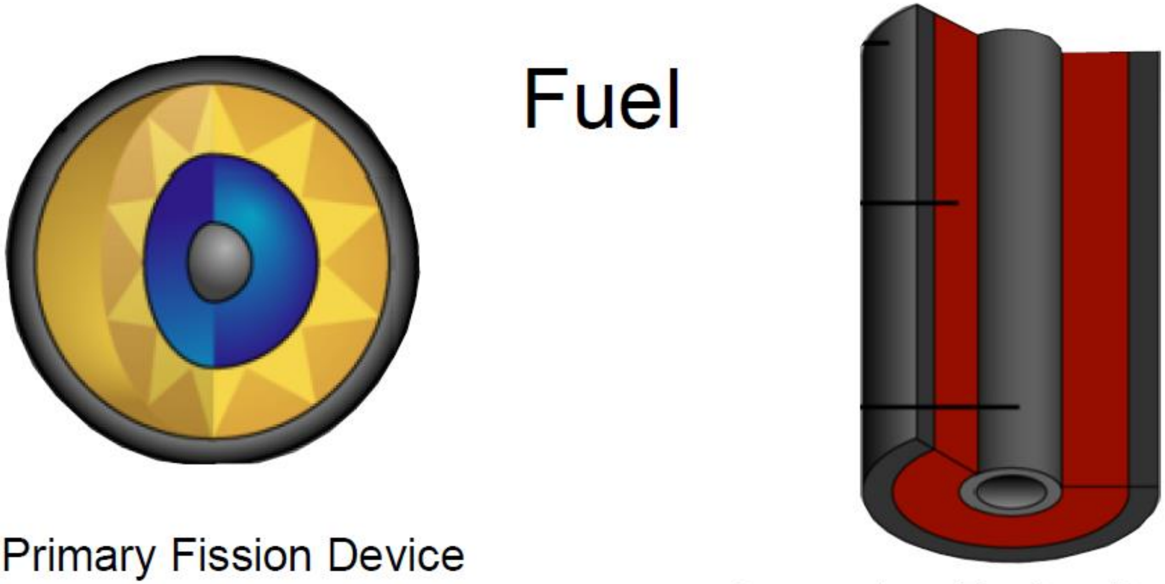

Primary Fission Device

Core: ^{239}Pu, ^{235}U,
plus ^{2}H+^{3}H booster

Shell: ^{238}U tamper

High explosive lenses

Secondary Fusion Device

Radiation channel

^{239}Pu sparkplug

^{6}Li, ^{2}H, ^{3}H fusion cell

^{238}U tamper

https://isnap.nd.edu/Lectures/phys20061/pdf/10.pdf

Event sequence

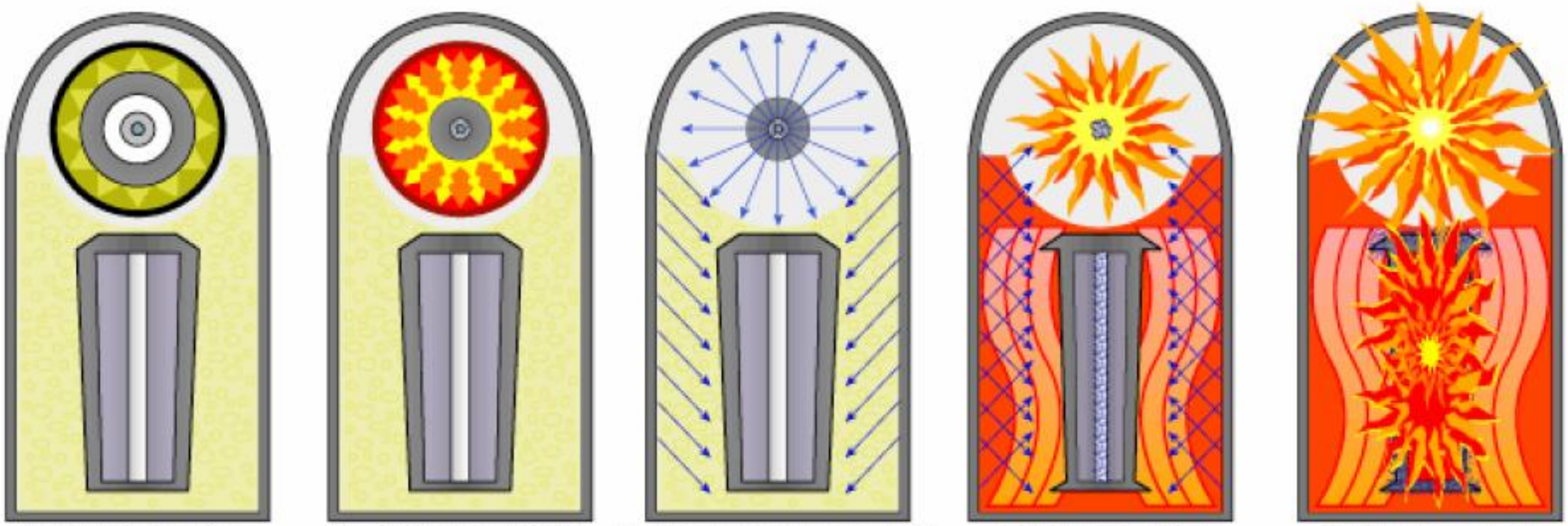

1. Warhead before firing; primary (fission bomb) at top, secondary (fusion fuel) at bottom, all suspended in polystyrene foam.

2. HE fires in primary, compressing plutonium core into supercriticality and beginning a fission reaction.

3. Fissioning primary emits X-rays which reflect along the inside of the casing, irradiating the polystyrene foam.

4. Polystyrene foam becomes plasma, compressing secondary, and plutonium sparkplug begins to fission.

5. Compressed and heated, lithium-6 deuteride fuel begins fusion reaction, neutron flux causes tamper to fission. A fireball is starting to form...

Additional pressure from recoil of exploding shell (ablation)!

https://isnap.nd.edu/Lectures/phys20061/pdf/10.pdf

You don’t want to build a hydrogen bomb!

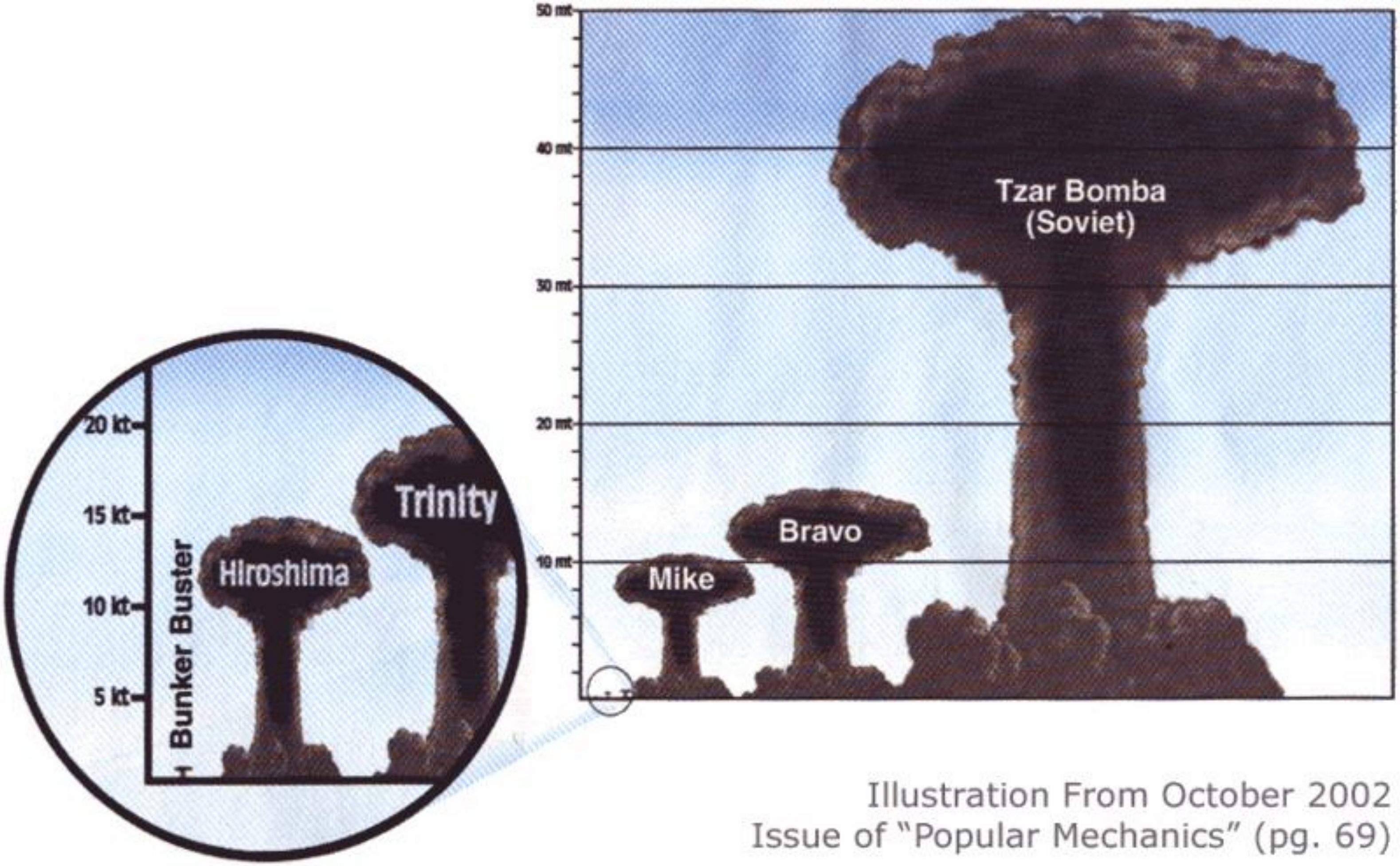

Illustration From October 2002
Issue of “Popular Mechanics” (pg. 69)